Πανεπιστημιο Ιωαννινων
Σχολη Θετικων Επιστημων
Τμημα Φυσικης

Μελέτη Ισορροπίας και Ευστάθειας Ελικοειδώς Συμμετρικού Μαγνητισμένου Πλάσματος

Αχιλλέας Ευαγγελιάς

Διδακτορική Διατριβή

ΙΩΑΝΝΙΝΑ 2020

UNIVERSITY OF IOANNINA
SCHOOL OF NATURAL SCIENCES
DEPARTMENT OF PHYSICS

DISSERTATION

Equilibrium and Stability of Helically Symmetric Magnetized Plasmas

SUBMITTED IN PARTIAL FULFILLMENT OF THE REQUIREMENTS FOR THE DEGREE OF:

DOCTOR OF PHILOSOPHY IN PHYSICS

BY

Achilleas Evangelias

IOANNINA 2020

Three-member advisory committee:

- George Throumoulopoulos (Supervisor)

  Professor, Section of Astrogeophysics, Physics Department, University of Ioannina

- George Leontaris

  Professor, Section of Theoretical Physics, Physics Department, University of Ioannina

- Alexander Nindos

  Associate Professor, Section of Astrogeophysics, Physics Department, University of Ioannina

Seven-member examination committee:

1. George Throumoulopoulos

   Professor, Section of Astrogeophysics, Physics Department, University of Ioannina

2. George Leontaris

   Professor, Section of Theoretical Physics, Physics Department, University of Ioannina

3. Alexander Nindos

   Associate Professor, Section of Astrogeophysics, Physics Department, University of Ioannina

4. Kyriakos Hizanidis

   Emeritus Professor, Division of Electromagnetics, Electrooptics and Electronic Materials, School of Electrical and Computer Engineering, National Technical University of Athens

5. Spiros Patsourakos

   Associate Professor, Section of Astrogeophysics, Physics Department, University of Ioannina

6. Nikolaos Bakas

   Assistant Professor, Section of Astrogeophysics, Physics Department, University of Ioannina

7. Ioannis Kominis

   Assistant Professor, Department of Mechanics, School of Applied Mathematical and Physical Sciences, National Technical University of Athens

ΠΡΑΚΤΙΚΟ ΔΗΜΟΣΙΑΣ ΠΑΡΟΥΣΙΑΣΗΣ ΕΞΕΤΑΣΗΣ ΚΑΙ ΑΞΙΟΛΟΓΗΣΗΣ ΔΙΔΑΚΤΟΡΙΚΗΣ ΔΙΑΤΡΙΒΗΣ

Σήμερα **Τετάρτη, 10 Ιουνίου 2020 και ώρα 9 π.μ.** στην αίθουσα σεμιναρίων του Τμήματος Φυσικής του Πανεπιστημίου Ιωαννίνων (κτίριο Φ2, 3ος όροφος, Αναγνωστήριο), πραγματοποιήθηκε η διαδικασία της δημόσιας παρουσίασης, εξέτασης και αξιολόγησης, ενώπιον της Επταμελούς Εξεταστικής Επιτροπής, της Διδακτορικής Διατριβής που εκπόνησε ο υποψήφιος διδάκτορας **κ. Αχιλλέας Ευαγγελιάς**.

Την Επταμελή Εξεταστική Επιτροπή, που όρισε με σχετική απόφασή της η Συνέλευση του Τμήματος Φυσικής (συν. αριθ. 1544/18/05/2020) αποτελούν οι:

1. **Γ. Θρουμουλόπουλος, Καθηγητής, Τμήμα Φυσικής, Π.Ι. (επιβλέπων)**
2. **Γ. Λεοντάρης, Καθηγητής, Τμήμα Φυσικής, Π.Ι.**
3. **Α. Νίντος, Αν. Καθηγητής, Τμήμα Φυσικής, Π.Ι.**
4. **Κ. Χιτζανίδης Ομότιμος, Καθηγητής, Σχολή Ηλεκτρολόγων Μηχανικών και Μηχανικών Υπολογιστών, Ε.Μ.Π.**
5. **Σ. Πατσουράκος, Αν. Καθηγητής, Τμήμα Φυσικής, Π.Ι.**
6. **Ν. Μπάκας, Επικ. Καθηγητής, Τμήμα Φυσικής, Π.Ι.**
7. **Ι. Κομίνης, Επικ. Καθηγητής, ΣΕΜΦΕ, Ε.Μ.Π.**

Από τα μέλη της Εξεταστικής Επιτροπής παρόντα ήταν πέντε (5), οι κ.κ. Γ. Θρουμουλόπουλος, Γ. Λεοντάρης, Α. Νίντος, Σ. Πατσουράκος και Ν. Μπάκας με φυσική παρουσία και οι κ.κ. Κ. Χιτζανίδης και Ι. Κομίνης μέσω τηλεδιάσκεψης.

Ο τίτλος της διδακτορικής διατριβής που εκπόνησε ο κ. Ευαγγελιάς και που παρουσίασε σήμερα είναι: «**Μελέτη ισορροπίας και ευστάθειας ελικοειδώς συμμετρικού μαγνητισμένου πλάσματος**».

Ο υποψήφιος παρουσίασε και ανέπτυξε το θέμα και απάντησε σε σχετικές ερωτήσεις των μελών της Εξεταστικής Επιτροπής.

Στη συνέχεια η Εξεταστική Επιτροπή αποσύρθηκε και μετά από συζήτηση κατέληξε στα ακόλουθα:

1. Η παρουσίαση και ανάπτυξη του θέματος της διατριβής ήταν κατανοητή, εμπεριστατωμένη και έδειχνε πλήρη γνώση των σχετικών μεθόδων που χρησιμοποιήθηκαν.
2. Η επιστημονική κατάρτιση του υποψηφίου σε γενικότερα θέματα Φυσικής Πλάσματος σχετικά με το αντικείμενο της διατριβής είναι υψηλού επιπέδου.
3. Η συγγραφή του κειμένου της διατριβής έγινε με σαφή τρόπο και μεθοδικότητα.
4. Τα αποτελέσματα της διατριβής είναι πρωτότυπα και συμβάλλουν στην περεταίρω κατανόηση φαινομένων ισορροπίας και ευστάθειας μαγνητικά περιορισμένου πλάσματος.

5. Μέρος των αποτελεσμάτων αποτελούν αντικείμενο 5 δημοσιεύσεων σε έγκριτα διεθνή περιοδικά και 5 ανακοινώσεων σε διεθνή συνέδρια και σχολεία.

Με βάση τα ανωτέρω τα μέλη της Εξεταστικής Επιτροπής εγκρίνουν ομόφωνα τη διδακτορική διατριβή του κ. Αχιλλέα Ευαγγελιά και εισηγούνται ανεπιφύλακτα και ομόφωνα την απονομή του τίτλου του διδάκτορα με βαθμό **«ΑΡΙΣΤΑ».**

Τα μέλη της Εξεταστικής Επιτροπής

1. Γ. Θρουμουλόπουλος, Καθηγητής, Τμήμα Φυσικής, Π.Ι. (επιβλέπων)

Γ. Θρουμουλόπουλος

2. Γ. Λεοντάρης, Καθηγητής, Τμήμα Φυσικής, Π.Ι.

3. Α. Νίντος, Αν. Καθηγητής, Τμήμα Φυσικής, Π.Ι.

4. Κ. Χιτζανίδης Ομότιμος, Καθηγητής, Σχολή Ηλεκτρολόγων Μηχανικών και Μηχανικών Υπολογιστών, Ε.Μ.Π.

5. Σ. Πατσουράκος, Αν. Καθηγητής, Τμήμα Φυσικής, Π.Ι.

6. Ν. Μπάκας, Επικ. Καθηγητής, Τμήμα Φυσικής, Π.Ι.

7. Ι. Κομίνης, Επικ. Καθηγητής, ΣΕΜΦΕ, Ε.Μ.Π.

"I know that what you call 'God' really exists, but not in the form you think; God is primal cosmic energy, the love in your body, your integrity, and your perception of the nature in you and outside of you."

Wilhelm Reich, Listen, Little Man!

Acknowledgements

First of all, I would like to express my deep gratitude to my supervisor, Professor George Throumoulopoulos for his continuous academic, moral and financial support and all the aspiring guidance and motivation he has given me during my graduate studies. I am thankful for his invaluably constructive criticism, friendly advice and patience whilst allowing me the room to work in my own way. I attribute the level of my PhD to his encouragement and effort and without him this thesis, too, would not have been completed or written. One simply could not wish for a better or friendlier supervisor. Also, I thank all the members of the examination committee for dedicating time in this thesis and for their valuable comments.

Furthermore, I would like to refer to the postdoctoral researchers in the local group of Plasma Physics, Dimitris Kaltsas, George Poulipoulis and Apostolis Kuiroukidis, for the stimulating discussions and our collaboration.

To all my family, specially my parents Rania and Nestoras, my sister Charoula and my grandmother Ypatia - thank you for your continuous moral and financial support and for always being there for me. Without your encouragement I could not have reached this stage.

I am indebted to all my childhood friends and all those I have met in Ioannina, who are too many to be named individually, for all the fun we have had together, keeping me sane.

At the end, a special thank to my Samira for coming into my life and making me believe in a better tommorow.

Parts of the research presented in this thesis were performed within the framework of the EUROfusion Consortium and have received funding from the Euratom research and training programme 2014-2018 and 2019-2020 under grant agreement No 633053 as well as the National Program for the Controlled Thermonuclear Fusion, Hellenic Republic. Also, they have been financially supported by the General Secretariat for Research and Technology (GSRT) and the Hellenic Foundation for Research and Innovation (HFRI) (scholarship code: 2119). The views and opinions expressed herein do not necessarily reflect those of the European Commission.

List of Publications

Within the context of my PhD studies, four publications in peer-reviewed journals and one publication in conference proceedings have been produced. They are listed here in descending chronological order.

1. A. Evangelias, A. Kuiroukidis and G. N. Throumoulopoulos "Helically symmetric equilibria with pressure anisotropy and incompressible plasma flow" *Plasma Physics and Controlled Fusion* **60** (2018) 025005.

2. G. N. Throumoulopoulos, D. A. Kaltsas, A. Evangelias and A. Kuiroukidis "Special ideal MHD equilibria with incompressible flow" *Physics Letters A* **382** (2018) 321.

3. A. Evangelias *et al.* "Certain developments on the equilibrium of magnetized plasmas" *45th EPS Conference on Plasma Physics, Prague, 2-6 July 2018; ECA,* Vol **42A** (2018) P1.1048.

4. A. Evangelias and G. N. Throumoulopoulos "Symmetry transformations for magnetohydrodynamics and Chew-Goldberger-Low equilibria revisited" *Plasma Science and Technology* **21** (2019) 095102.

5. A. Evangelias and G. N. Throumoulopoulos "On the linear stability of anisotropic pressure equilibria with field-aligned flow" *Journal of Plasma Physics* **86** (2020) 905860312.

Abstract

In this thesis the equilibrium and stability properties of a helically symmetric magnetized plasma with pressure anisotropy and incompressible flow are investigated. Helical symmetry consists of the most generic case of continuous geometrical symmetry including both the translational and axial symmetry as special cases. The main novel contribution is the derivation of a generalized Grad-Shafranov equation governing pertinent equilibria with flow of arbitrary direction, in connection with the steady states of two-dimensional 'straight stellarators' as well as of helically symmetric astrophysical jets. This equation includes six free surface functions and recovers known Grad-Shafranov-like equations in the literature as well as the usual static, isotropic one. In addition, a new class of analytical solutions of the aforementioned equation is obtained and specific equilibria are constructed for a plasma surrounded by a fixed boundary, and the impact of both pressure anisotropy and mass flow on their physical properties is examined. Also specific families of incompressible magnetohydrodynamic equilibria in which two out of the magnetic field, velocity, current density and vorticity vectors are specially related, including the 'force-free' and Beltrami cases, are studied. Furthermore, the symmetry transformations for magnetohydrodynamic equilibria with isotropic pressure and incompressible flow with collinear velocity and magnetic fields introduced by Bogoyavlenskij are generalized in the case of the respective Chew-Goldberger-Low equilibria with anisotropic pressure. It is proved that the geometrical symmetry of an initial equilibrium can be violated by those transformations only when the magnetic and velocity fields are purely poloidal. In this case three-dimensional equilibria from given axisymmetric ones are constructed. Regarding stability, a sufficient condition for the linear stability of plasma equilibria with incompressible flow parallel to the magnetic field, constant mass density and anisotropic pressure such that the ratio of the difference between the scalar pressures in the directions parallel and perpendicular to the magnetic field over the magnetic pressure remains constant, is derived. This condition is applicable to any steady state without geometrical restriction and involves physically interpretable terms related to the magnetic shear, the flow shear and the variation of total pressure perpendicular to the magnetic surfaces. On the basis of this condition the impact of pressure anisotropy, flow, and torsion of a helical magnetic axis on the stability properties of a specific class of analytic equilibria is examined.

Εκτεταμενη Περιληψη

(Extended Summary in Greek)

Είναι γεγονός πως η παγκόσμια ενεργειακή ζήτηση έχει αυξηθεί σημαντικά τα τελευταία χρόνια, ενώ προβλέπεται πως θα συνεχίσει να αυξάνεται με ραγδαίους ρυθμούς κύρια λόγω του ολοένα αυξανόμενου πληθυσμού του πλανήτη μας, της συνεχούς τεχνολογικής προόδου, αλλά και της κλιματικής αλλαγής. Έτσι διαφαίνεται ότι μια από τις μεγαλύτερες μελλοντικές προκλήσεις για την ανθρωπότητα είναι η ενεργειακή επάρκεια και μάλιστα με τρόπο φιλικό προς το περιβάλλον. Όλα τα παραπάνω κάνουν την ελεγχόμενη θερμοπυρηνική σύντηξη μια ελκυστική πηγή ενέργειας, η αξιοποίηση της οποίας θα τροφοδοτήσει την ανθρωπότητα με φθηνή, πρακτικά απεριόριστη και καθαρή ενέργεια.

Η έρευνα στην ελεγχόμενη πυρηνική σύντηξη έχει ξεκινήσει εδώ και περισσότερες από έξι δεκαετίες όμως ακόμη δεν έχει επιτευχθεί παραγωγή ενέργειας σε μεγάλη κλίμακα. Αυτό συμβαίνει διότι παραμένουν ακόμη πολλά άλυτα προβλήματα, όπως ο επιτυχής περιορισμός του πλάσματος ταυτόχρονα με τη θέρμανση και η επίτευξη της ανάφλεξης. Μια από τις κύριες μεθόδους στην οποία εστιάζεται η έρευνα για τον περιορισμό του πλάσματος είναι η συγκράτηση του με μαγνητικά πεδία σε κλειστά τοροειδή συστήματα, τα πιο διαδεδομένα εκ των οποίων είναι το Tokamak και το Stellarator. Το πλάσμα είναι δύσκολο να παραμείνει απόλυτα ευσταθές καθώς μεγάλα ποσά ενέργειας παγιδεύονται στον περιορισμένο χώρο των διατάξεων αυτών ικανά να διεγείρουν μια ποικιλία ασταθειών. Ο μαγνητικός περιορισμός του πλάσματος βασίζεται στην κατασκευή καλά ορισμένων ισορροπιών, οι οποίες θα πρέπει να είναι μακροσκοπικά ευσταθείς, καθώς και στον περιορισμό των φαινομένων μεταφοράς.

Η μελέτη της ευστάθειας ή αστάθειας του πλάσματος αρχίζει με τον προσδιορισμό των καταστάσεων ισορροπίας του. Στις περισσότερες μελέτες κατά το παρελθόν το πλάσμα θεωρούνταν ώς στατικό και με ισότροπη πίεση. Η περιγραφή τέτοιων ισορροπιών πλάσματος, στα πλαίσια του μοντέλου της Μαγνητοϋδροδυναμικής (ΜΥΔ) σε αξονική συμμετρία, διέπεται από την γνωστή εξίσωση Grad-Shafranov, μια ελλειπτική μερική διαφορική εξίσωση (ΜΔΕ) η οποία περιλαμβάνει δύο ελεύθερες συναρτήσεις. Όμως οι σύγχρονες μέθοδοι που χρησιμοποιούνται για την θέρμανση του πλάσματος, όπως για παράδειγμα η μέθοδος εμβολής δεσμών ουδέτερων σωματιδίων, δημιουργούν σημαντικές ροές μάζας και ανισοτροπία πίεσης, ανάλογα με την διεύθυνση της εμβαλλόμενης ροής.

Στη παρούσα διατριβή γίνεται μελέτη της ισορροπίας και της ευστάθειας μαγνητικά περιορισμένου πλάσματος, ελικοειδώς συμμετρικού, παρουσία ανισότροπης πίεσης και ροής μάζας. Η ελικοειδής συμμετρία αποτελεί μια γενική περίπτωση γεωμετρικής συμμετρίας η οποία περιλαμβάνει την μεταφορική και την αξονική συμμετρία ως ειδικές περιπτώσεις.

Μία από τις κύριες συνεισφορές της μελέτης αυτής αποτελεί η παραγωγή μιας γενικευμένης εξίσωσης Grad-Shafranov που διέπει την ισορροπία ελικοειδώς συμμετρικού πλάσματος με ανισότροπη πίεση και ασυμπίεστη ροή τυχαίας διεύθυνσης. Αυτή είναι μια ελλειπτική ΜΔΕ για την συνάρτηση πολοειδούς μαγνητικής ροής ψ η οποία περιλαμβάνει έξι ποσότητες επιφάνειας, δηλαδή συναρτήσεις των ολοκληρωμάτων του συστήματος. Η εξίσωση αυτή αποτελεί γενίκευση τόσο των εξισώσεων ισορροπίας ελικοειδώς συμμετρικού πλάσματος με ισότροπη πίεση, ή στατικού είτε παρουσία ροής, όσο και των εξισώσεων που διέπουν την ισορροπία αξονικά και μεταφορικά συμμετρικού πλάσματος παρουσία τόσο ισότροπης/ανισότροπης πίεσης ή/και ροής. Στα πλαίσια της παραγωγής αυτής η ισότροπη πίεση στα πλαίσια του μοντέλου ΜΥΔ αντικαθίσταται από τον τανυστή πίεσης Chew-Goldberger-Low (CGL). Ο τανυστής CGL είναι διαγώνιος με στοιχεία τις βαθμωτές πιέσεις στις διευθύνσεις της κίνησης παράλληλα, $P_{\|}$, και κάθετα, $P_{\perp}$, στο μαγνητικό πεδίο.

Ως μέτρο της ανισοτροπίας πίεσης ορίζεται η συνάρτηση $\sigma_d = \mu_0(P_\parallel - P_\perp)/\mathbf{B}^2$, η οποία θεωρείται πως μεταβάλλεται ομοιόμορφα πάνω στις μαγνητικές επιφάνειες ($\sigma_d = \sigma_d(\psi)$). Παράλληλα παράγεται και μια εξίσωση τύπου Bernoulli για την ενεργό πίεση $\mathcal{P}$, η οποία ορίζεται ως το ημιάθροισμα των βαθμωτών πιέσεων παράλληλα και κάθετα στο μαγνητικό πεδίο.

Στη συνέχεια, με τη μέθοδο γενικευμένων δυναμοσειρών παράγονται αναλυτικά λύσεις της γενικευμένης εξίσωσης Grad-Shafranov, με βάση τις οποίες κατασκευάζονται ισορροπίες πλάσματος σε σχέση με τον μαγνητικό σχηματισμό 'ευθύ stellarator'. Το 'ευθύ stellarator' αποτελείται από καλά ορισμένες, ένθετες, ελικοειδώς συμμετρικές μαγνητικές επιφάνειες με αυθαιρέτο σχήμα πολοειδούς διατομής, οι οποίες περιβάλλονται από σταθερό σύνορο. Οι σχηματισμοί αυτοί έχουν μη-μηδενική στρέψη και περιγράφουν προσεγγιστικά στο όριο πολύ μεγάλου λόγου όψεων το σύστημα μαγνητικού περιορισμού Stellarator. Οι νέες αναλυτικές λύσεις με κατάλληλη επιλογή συγκεκριμένων παραμέτρων μεταπίπτουν σε γνωστές στη βιβλιογραφία λύσεις εκφρασμένες μέσω κλασικών συναρτήσεων.

Κατόπιν μελετάται η επίδραση τόσο της ροής όσο και της ανισοτροπίας της πίεσης στα χαρακτηριστικά των νέων ισορροπιών μέσω φυσικών ποσοτήτων. Όσον αφορά τις μαγνητικές ιδιότητες του πλάσματος διαπιστώνεται ότι η ανισοτροπία της πίεσης δρα είτε παραμαγνητικά όταν $P_\parallel > P_\perp$, είτε διαμαγνητικά όταν $P_\parallel < P_\perp$, ανεξάρτητα από την παρουσία ροής ή μη. Απουσία ηλεκτρικού πεδίου η παράλληλη συνιστώσα της ροής δρα παραμαγνητικά και αθροιστικά με την ανισοτροπία πίεσης για $\sigma_d > 0$. Ωστόσο, για ροή τυχαίας διεύθυνσης η μη παράλληλη συνιστώσα της ροής, η οποία σχετίζεται με το ηλεκτρικό πεδίο, δρα διαμαγνητικά, με την παράλληλη ροή να ενισχύει την διαμαγνητική αυτή επίδραση. Επίσης, τόσο η ροή όσο και η ανισοτροπία πίεσης έχουν σημαντική επίδραση τόσο στην πυκνότητα ρεύματος όσο και στην ταχύτητα, στην παράμετρο β και στον παράγοντα ασφάλειας.

Επίπρόσθετα μελετώνται ειδικές περιπτώσεις ισορροπιών στις οποίες το μαγνητικό πεδίο, η ταχύτητα, η πυκνότητα ρεύματος και η στροβιλότητα ικανοποιούν ανά δύο ειδικές σχέσεις μεταξύ τους, ενώ εξετάζονται οι αντίστοιχες ελικοειδώς συμμετρικές ισορροπίες με βάση την ειδική μορφή της γενικευμένης εξίσωσης Grad-Shafranov σε κάθε περίπτωση.

Στο δεύτερο κύριο μέρος της διατριβής στα πλαίσια των μοντέλων ιδανικής MΥΔ και CGL μελετώνται οι μετασχηματισμοί συμμετρίας Bogoyavlenskij. Συγκεκριμένα, γενικεύονται οι μετασχηματισμοί που εφαρμόζονται σε αρχική MΥΔ ισορροπία με ασυμπίεστη ροή παράλληλη στο μαγνητικό πεδίο και παράγουν νέα MΥΔ ισορροπία με εν γένει συμπιεστή ροή, στην περίπτωση ανισότροπης πίεσης. Οι νέοι μετασχηματισμοί εφαρμόζονται σε αρχική ισορροπία CGL με ασυμπίεστη παράλληλη ροή στην οποία η συνάρτηση ανισοτροπίας σ_d μεταβάλλεται με σταθερό τρόπο πάνω στις μαγνητικές γραμμές και δημιουργούν επαναληπτικά νέες κλάσεις ισορροπιών CGL στις οποίες τόσο η συνάρτηση πυκνότητας μάζας όσο και η συνάρτηση ανισοτροπίας μπορούν να μεταβάλλονται πάνω στις μαγνητικές γραμμές. Ώστόσο, η ροή των μετασχηματισμένων ισορροπιών παραμένει ασυμπίεστη. Οι μετασχηματισμοί αυτοί μπορούν να εφαρμοστούν σε αρχικά στατική ισορροπία και να δημιουργήσουν νέες ισορροπίες με ροή, διατηρώντας την τοπολογία των μαγνητικών γραμμών της αρχικής ισορροπίας.

Ακολούθως, εξετάζεται η δομή των αυθαίρετων βαθμωτών συναρτήσεων οι οποίες εμπλέκονται στους μετασχηματισμούς, σε σχέση με την τοπολογία του μαγνητικού πεδίου της αρχικής ισορροπίας και την ύπαρξη μαγνητικών επιφανειών. Αποδεικνύεται ότι σε όλες τις περιπτώσεις μετασχηματισμών, η γεωμετρική συμμετρία μιας γνωστής ισορροπίας μπορεί να παραβιαστεί μέσω αυτών αν και μόνο αν αυτή έχει παράλληλη ροή και αμιγώς πολοειδές μαγνητικό πεδίο, ενώ σε κάθε άλλη περίπτωση οι μετασχηματισμένες ισορροπίες διατηρούν την αρχική συμμετρία. Στην περίπτωση αυτή κατασκευάζεται τρισδιάστατη ισορροπία από γνωστή, αξονικά συμμετρική αρχική ισορροπία.

Όσον αφορά στην ευστάθεια, μελετάται η γραμμική ευστάθεια ισορροπιών με ροή μάζας και ανισότροπη πίεση σε σχέση με τις μακροσκοπικές αστάθειες που εξελίσσονται στην ταχεία κλίμακα χρόνου της ιδανικής ΜΥΔ και είναι πολύ επικίνδυνες για τον περιορισμό του πλάσματος. Κύρια συνεισφορά της μελέτης αυτής είναι η παραγωγή μιας σχετικής ικανής συνθήκης ευστάθειας με εφαρμογή μιας Ενεργειακής Αρχής. Η συνθήκη αυτή είναι άμεσα εφαρμόσιμη σε οποιαδήποτε ισορροπία με ασυμπίεστη ροή παράλληλη στο μαγνητικό πεδίο, σταθερή πυκνότητα μάζας και σταθερή συνάρτηση ανισοτροπίας, χωρίς γεωμετρικό περιορισμό. Για την εξέταση της γραμμικής ευστάθειας τέτοιων ισορροπιών είναι ικανή η μελέτη του προσήμου μιας ποσότητας $\mathcal{A}$ η οποία είναι συνάρτηση φυσικά ερμηνεύσιμων όρων σχετιζόμενων με την μαγνητική διάτμηση, την ροή και την διάτμηση αυτής, καθώς και με την μεταβολή της ολικής πίεσης κάθετα στις μαγνητικές επιφάνειες.

Με βάση την συνθηκή αυτή αποδεικνύεται ότι εάν μια αρχική ισορροπία με παράλληλη ροή, είτε ισότροπη είτε ανισότροπη, είναι γραμμικά ευσταθής, τότε θα είναι επίσης και όλες οι νέες ισορροπίες που προκύπτουν από την εφαρμογή των μετασχηματισμών συμμετρίας στην αρχική ισορροπία όταν μια εμπλεκόμενη παράμετρος είναι θετική. Τέλος, η προαναφερθείσα συνθήκη εφαρμόζεται σε γνωστή κλάση ελικοειδώς συμμετρικών ισορροπιών και μελετάται η επίδραση της ροής, της ανισοτροπίας πίεσης και της στρέψης ενός ελικοειδούς μαγνητικού άξονα στην γραμμική ευστάθεια αυτών των ισορροπιών. Αποδεικνύεται ότι τόσο η ροή όσο και η ανισοτροπία πίεσης έχουν είτε σταθεροποιητική είτε αποσταθεροποιητική επίδραση στην ισορροπία, ενώ επίσης ότι ελικοειδώς συμμετρικοί σχηματισμοί με μικρότερη στρέψη και μεγαλύτερα μήκη κλίσης (pitch lengths) παρουσιάζουν βελτιωμένα χαρακτηριστικά ευστάθειας.

Contents

1 Introduction **1**
- 1.1 Plasma, the fourth state . . . 1
- 1.2 Thermonuclear fusion and magnetic confinement . . . 3
- 1.3 Plasma modeling . . . 5
  - 1.3.1 Kinetic description . . . 6
  - 1.3.2 Fluidistic description . . . 7
  - 1.3.3 Ideal MHD and CGL frameworks . . . 10
- 1.4 MHD equilibrium and stability elements . . . 15
  - 1.4.1 Equilibrium . . . 16
  - 1.4.2 Linear stability . . . 18
- 1.5 Helical symmetry . . . 20
- 1.6 Thesis objectives and outline . . . 23

2 Helically Symmetric Equilibria: Generalized Grad-Shafranov Equation **27**
- 2.1 Derivation of generalized Grad-Shafranov equation in the presence of pressure anisotropy and plasma flow . . . 27
  - 2.1.1 Divergence-free fields . . . 27
  - 2.1.2 Integrals of the system . . . 31
  - 2.1.3 GGS-Bernoulli system . . . 32
  - 2.1.4 GGS equation for incompressible flows and uniform anisotropy . . . 33
- 2.2 Special ideal incompressible MHD equilibria with anisotropic pressure . . . 36
  - 2.2.1 Parallel flows ($\mathbf{V} \parallel \mathbf{B}$) . . . 37
  - 2.2.2 Flows parallel to the current density ($\mathbf{V} \parallel \mathbf{J}$) . . . 37
  - 2.2.3 Beltrami flows ($\boldsymbol{\Omega} \parallel \mathbf{V}$) . . . 39
  - 2.2.4 "Force-free" equilibria ($\mathbf{J} \parallel \mathbf{B}$) . . . 39
  - 2.2.5 Equilibria with $\boldsymbol{\Omega} \parallel \mathbf{B}$ ($\boldsymbol{\Omega} \parallel \mathbf{J}$) . . . 40
  - 2.2.6 Special helically symmetric equilibria . . . 40

3 An Analytic Class of Helically Symmetric Equilibria **45**
- 3.1 Construction of analytic equilibrium solutions . . . 45
  - 3.1.1 Construction of straight helically symmetric equilibrium configurations 51
  - 3.1.2 Reduction to close form analytical solutions . . . 56
- 3.2 Impact of flow and pressure anisotropy . . . 59

4 Symmetry Transformations for Ideal MHD and CGL Equilibria **71**
- 4.1 Brief introduction to the symmetry transformations . . . 71
- 4.2 Transformations for ideal MHD equilibria with field-aligned flows . . . 72
- 4.3 Generalized symmetry transformations for anisotropic pressure . . . 72
- 4.4 Construction of 3D CGL equilibria with field-aligned flows . . . 77
- 4.5 Transformations for flow of arbitrary direction . . . 83
  - 4.5.1 Review of transformations between MHD-MHD and CGL-CGL equilibria 83

4.5.2 Transformations between MHD-CGL equilibria 87

5 Stability of Anisotropic Incompressible Equilibria 89
5.1 Energy principle and perturbation potential energy 89
5.2 Sufficient condition for linear stability of field-aligned equilibria 92
5.3 Stability under symmetry transformations 95
5.4 Linear stability of helically symmetric equilibria 96

6 Conclusions and potential future work 107
6.1 Summary and main conclusions 107
6.2 Future directions 110

Appendix A General curvilinear coordinates for magnetic confinement geometries 115
A.1 Covariant and contravariant basis vectors 115
A.2 Integration in general curvilinear coordinates 117
A.3 Vector operators in curvilinear coordinates 117
A.4 Physical components of a vector 118

Appendix B Helical coordinate system 119
B.1 Vector representation and differential operators 119
B.2 Helix parametrization 121
B.2.1 Frenet-Serret Formulas 122
B.3 Intrinsic coordinates - Poloidal cross-section modeling 123
B.3.1 Circular cross-section 124

Appendix C Solution of ODE (3.18) in the neighborhood of a regular singular point 129
C.1 n>0 130
C.2 n<0 132
C.3 n=0 133

Appendix D Proof of the relations (5.30)-(5.33) 135

Bibliography 139

List of Figures

1.1 The combination of toroidal, $\mathbf{B}_t$, and poloidal, $\mathbf{B}_p$, magnetic fields results in a twisted, helical magnetic field which is essential for confinement in toroidal geometry. 4

1.2 The coordinate surfaces of the helical system (r, u, ζ) defined in (1.71). The blue and green-colored surfaces $\zeta =$ constant and $r =$ constant respectively, are the same with the usual cylindrical surfaces. The red colored surface $u =$ constant is a helicoid, at every point of which there is a helix lying on the helicoid which passes through that point. 21

1.3 A helically symmetric tube composed of nested helicoidal surfaces of arbitrary cross-sectional shape. The innermost of these surfaces degenerates to a helical magnetic axis (red colored helix). The shape of the cross-section remains invariant along the helical direction. 22

3.1 The straight helically symmetric equilibrium configuration of circular cross-section obtained as a solution of the GGS equation (2.46) with W7-X parameters as described in the text. 53

3.2 Poloidal cut of the nested helicoidal magnetic surfaces of up-down symmetric circular cross-section of the equilibrium configuration obtained with W7-X characteristics as prescribed in the text, on (a) the plane (r, u) and (b) the poloidal plane $(\mathbf{n}, \mathbf{b})$. The boundary represented by the thick-blue line was prescribed analytically. 54

3.3 The flux function $U(r, u = u_a)$ on the (r, u)-plane for the equilibrium of figure 3.2. . 54

3.4 Up-down symmetric equilibrium of (a) banana- and (b) triangular- like cross-section-shape with W7-X geometrical characteristics, on the plane (r, u). The boundaries represented by the thick-blue lines were prescribed analytically. 55

3.5 (a) The magnetic field magnitude, $B(r, u_a)$, and (b) the function $I(r, u_a)$ related to the helical component of the magnetic field, as functions of the anisotropy parameter σ_{d_a}, for $M_{p_a} = \varphi_{11} = \varphi_{22} = 0$. 61

3.6 The profile of the static effective pressure, $\mathcal{P}_s(U(r, u_a))$, for the equilibrium of figure 3.2(a), in consistence with that of the flux function U shown in figure 3.3. 61

3.7 The impact of pressure anisotropy on $P_{\|}(r, u_a)$ for (a) $\sigma_{d_a} > 0$ and (b) $\sigma_{d_a} < 0$, for $M_{p_a} = \varphi_{11} = \varphi_{22} = 0$. 62

3.8 The impact of pressure anisotropy on $P_{\perp}(r, u_a)$ for (a) $\sigma_{d_a} > 0$ and (b) $\sigma_{d_a} < 0$, for $M_{p_a} = \varphi_{11} = \varphi_{22} = 0$. 62

3.9 Poloidal cut of the helicoidal surfaces $P_{\perp} =$ const. for (a) $\sigma_{d_a} = 0.003$ and (b) $\sigma_{d_a} = 0.006$, in constistence with the respective curves of graph 3.8(a). 63

3.10 The impact of the parallel flow in connection with the parameter $M_{p_a}^2$ on (a) $P_{\|}(r, u_a)$ and (b) $P_{\perp}(r, u_a)$, for $\varphi_{11} = \varphi_{22} = 0$, corresponding to the cases of figures 3.7(a) and 3.8(a). 63

3.11 (a) The impact of $M^2_{p_a}$ on the function $I(r, u_a)$ associated with the helicoidal component of the magnetic field, for $\sigma_{d_a} = 0.003$, $\varphi_{11} = \varphi_{22} = 0$. (b) the cumulative paramagnetic impact of the pressure anisotropy and the parallel flow in the absence of the electric field term; the displayed curves correspond to the following values: Isostatic (black straight curve): $\sigma_{d_a} = M^2_{p_a} = 0$; Anisostatic (blue dashed curve): $\sigma_{d_a} = 3 \times 10^{-3}$, $M^2_{p_a} = 0$; Isoflow (red dotted curve): $\sigma_{d_a} = 0$, $M^2_{p_a} = 10^{-4}$; Anisoflow (green dotdashed curve): $\sigma_{d_a} = 3 \times 10^{-3}$, $M^2_{p_a} = 10^{-4}$. 64
3.12 The impact of the parameter φ_{11} on (a) $P_\perp(r, u_a)$ and (b) $P_\parallel(r, u_a)$, for purely helicoidal flows: $M^2_p = 0$, $\varphi_{22} = -0.08$ and $\sigma_{d_a} = 0.003$. 65
3.13 The helicoidal component of the magnetic field for the equilibrium of figure 3.2(a) for different values of the non-parallel flow parameter φ_{11}, for $\varphi_{22} = -0.08$, $M^2_{p_a} = 10^{-4}$ and $\sigma_{d_a} = 3 \times 10^{-3}$. 65
3.14 The implicit diamagnetic action of parallel flow in the presence of non-parallel one through the second term in (3.70) for $\varphi_{11} = 0.5$ and $\varphi_{22} = -0.08$. The displayed graphs correspond to $\sigma_{d_a} = 0$; however the impact of M^2_p is similar for any $\sigma_{d_a} \neq 0$. 66
3.15 The pressure anisotropy strengthens the diamagnetic impact of the non-parallel flow for $P_\parallel < P_\perp$ and encounters that impact for $P_\parallel > P_\perp$. This figure corresponds to flows of arbitrary direction: $M^2_{p_a} = 5 \times 10^{-5}$, $\varphi_{11} = 0.5$, $\varphi_{22} = -0.08$. 66
3.16 The overall impact of pressure anisotropy and flow on the local beta on the magnetic axis. The displayed curves correspond to the values: Static: $M^2_{p_a} = \varphi_{11} = \varphi_{22} = 0$; Parallel flow: $M^2_{p_a} = 10^{-4}$, $\varphi_{11} = \varphi_{22} = 0$; Helicoidal flow: $M^2_{p_a} = 0$, $\varphi_{11} = 0.5$, $\varphi_{22} = -0.08$; Arbitrary flow: $M^2_{p_a} = 10^{-4}$, $\varphi_{11} = 0.5$, $\varphi_{22} = -0.08$. 67
3.17 (a) The impact of pressure anisotropy on $J_{\bar\zeta}$ in the absence of the flow ($M^2_{p_a} = \varphi_{11} = \varphi_{22} = 0$). (b) The impact of the non-parallel flow on $J_{\bar\zeta}$ through the parameter φ_{11}, for $\sigma_{d_a} = 3 \times 10^{-3}$, $M^2_{p_a} = 10^{-4}$ and $\varphi_{22} = -0.08$. 68
3.18 The impact on $V_{\bar\zeta}$ of : (a) M^2_p for field-aligned flows and isotropic pressure, $\sigma_{d_a} = \varphi_{11} = \varphi_{22} = 0$, (b) the non-parallel flow in connection with the parameter φ_{11}, for $\sigma_{d_a} = 3 \times 10^{-3}$, $M^2_{p_a} = 5 \times 10^{-5}$, $\varphi_{22} = -0.08$, (c) the parallel flow in the presence of the electric field term associated with non-parallel flow, for $\sigma_{d_a} = 0$, $\varphi_{11} = 0.5$, $\varphi_{22} = -0.08$. 69
3.19 (a) The influence of the parallel flow through $M^2_{p_a}$ on the safety factor, for $\varphi_{11} = 0.5$. (b) The impact of non-parallel flow on $\mathcal{Q}$ in connection with the parameter φ_{11}, for $M^2_{p_a} = 5 \times 10^{-5}$; Both figures correspond to the values $\varphi_{22} = -0.08$ and $\sigma_{d_a} = 0$. 69

4.1 Poloidal cut of nested toiroidal magnetic surfaces $U(\rho, z)$ =const. for the axisymmetric equilibria (4.22). 78
4.2 Topology of the purely poloidal magnetic field lines (left) and velocity streamlines (right) for the constructed axisymmetric equilibria (4.22). 78
4.3 Both the pressure anisotropy function, σ_d, (left) and density, ϱ, (right) of the original equilibria peak on the magnetic axis, where $\sigma_{d_a} = 0.3$ and $\varrho_a = 5 \times 10^{-7}$ Kg/m^3, and vanish on the bounding surface $U = 0$ for any toroidal angle ϕ. 78
4.4 The magnetic field magnitude vanishes on the magnetic axis and varies from the high field-side ($B = 0.68$ T) to the low field-side ($B = 0.47$ T) uniformly for every any angle ϕ. 79
4.5 (left) The magnitude of the transformed magnetic field, B_1, does change periodically along the toroidal direction. (right) Variation of B_1 along the radial direction on the plane $z = z_a$ for different values of the toroidal angle ϕ. 80
4.6 While the original B at a poloidal point (chosen as the point ($\rho = 1.8, z = z_a$ in the figure) is ϕ-independent, the respective transformed B_1 varies along the toroidal direction. The magnitude of the transformed field is in general higher than the respective original one except from some specific narrow toroidal regions. 80

4.7 (left) The transformed density $\varrho_1(U,\phi)$ on the plane $z=z_a$ does not remain uniform on the magnetic surfaces as the toroidal angle ϕ varies. (right) The value of ϱ_1 on the magnetic axis varies along ϕ and is higher than the respective value of the original ϱ, which is constant and maximum thereon. 81

4.8 (left) The variation of the anisotropy function, σ_{d_1}, of the transformed equilibria is not uniform along the toroidal direction. (right) The perpendicular pressure of the transformed equilibria is higher than the respective parallel one, except from the toroidal angles $\pi/2$ and $3\pi/2$ for which $P_{\parallel_1}=P_{\perp_1}$, in contrast with the original σ_d which is always peaked on-axis and positive for every ϕ. 81

4.9 The ϕ-derivative of the function g_1 changes periodically sign with respect to ϕ at a period $\pi/2$, thus vanishing for $\phi=\delta\frac{\pi}{2}$, $\delta=0,1,2,\ldots,$. This results in a similar variation of the poloidal current density component from negative to positive values. 82

4.10 The topology of the transformed poloidal -current-density lines for the toroidal angles $\phi=\frac{\pi}{4}$ (left), and $\phi=\frac{3\pi}{4}$ (right) 82

5.1 Poloidal cut of helicoidal magnetic surfaces $U(x,y,z=0)$ =const. for the helically symmetric equilibrium solution (5.56). 97

5.2 Profile of the function $U(x,y=0,z=0)$ =const. for the helically symmetric equilibrium solution (5.56). 97

5.3 The profiles of the scalar pressures (a) $P_\perp(x,y=0,z=0)$ and (b) $P_\parallel(x,y=0,z=0)$ for the constructed stationary equilibria, for $M_{p_0}^2=10^{-3}$. The blue dashed curve correspond to $\sigma_d=0.1$, while the red dotted one to $\sigma_d=-0.1$. 98

5.4 Variation of (a) $|\mathbf{B}(x,y=0,z=0)|$ and (b) $J_h(x,y=0,z=0)$, for the stationary equilibria constructed here, for $M_{p_0}^2=10^{-3}$ and the impact of pressure anisotropy on them for positive and negative values of σ_d. 99

5.5 Profiles of (a) the helicoidal velocity component for $M_{p_0}^2=0.06$, and the impact of pressure anisotropy through σ_d, and (b) the Mach function along the x-axis for different values of the flow parameter $M_{p_0}^2$. 99

5.6 (a): For the static anisotropic helically symmetric equilibrium ($\sigma_d=M_{p_0}^2=0$) the stability condition $\mathcal{A}\geq 0$ is satisfied in the orange coloured regions. (b): The term A_2 has a stabilizing effect (red-dotted curve) which counteracts the destabilizing one of A_1 (blue-dashed curve), so that the quantity $\mathcal{A}=A_1+A_2$ indicated by the black-straight curve becomes positive in the aforementioned orange coloured regions. 100

5.7 The impact of pressure anisotropy on the quantities (a) $\mathcal{A}$, (b) A_1 and (c) A_2 in the absence of flow ($M_{p_0}=0$) for $\sigma_d=0.2$ (blue-dashed curves) and $\sigma_d=-0.2$ (red-dotted curve). For comparison are also given the respective isotropic black continuous curves. In the regions where $\mathcal{A}\geq 0$ this impact is stabilizing for $\sigma_d>0$ and destabilizing for $\sigma_d<0$. 101

5.8 Impact of the flow through $M_{p_0}^2$ in the central orange colored region where the stability condition $\mathcal{A}\geq 0$ is satisfied in comparison with the respective static isotropic equilibrium. The maximum used value of the parameter M_{p_0} for which all the pressures remain positive is 0.08. 102

5.9 The impact of the flow parameter $M_{p_0}^2$ on the terms: (a) A_1, (b) A_2, and (c) A_3, for $\sigma_d=0$. 103

5.10 The overall stabilizing impact of pressure anisotropy in combination with flow on the stability of the constructed helically symmetric equilibria. The pertinent parametric values employed are as follows: (straight black curve) $\sigma_d=M_{p_0}^2=0$, (blue dashed curve) $\sigma_d=0$, $M_{p_0}^2=0.07$, (red dotted curve) $\sigma_d=0.07$, $M_{p_0}^2=0$, and (green dot-dashed curve) $\sigma_d=M_{p_0}^2=0.07$. 104

5.11 The impact of the torsion of the magnetic axis and of the picth on the linear stability of helically symmetric equilibria. Each pair of figures illustrate configurations that have same torsion, but different pitch values as explained in the text. 105

B.1 The coordinates of any point M on the poloidal plane: ρ^*, θ coordinates refer to the natural axes $\mathbf{n}, \mathbf{b}$; ρ^*, ω coordinates refer to the rotated axes $\mathbf{n}_R, \mathbf{b}_R$. 126

1 | Introduction

"*Plasma seems to have the kinds of properties one would like for life. It is somewhat like liquid water -unpredictable and thus able to behave in an enormously complex fashion. It could probably carry as much information as DNA does. It has at least the potential for organizing itself in interesting ways.*"

Friemann Dyson

1.1 Plasma, the fourth state

Upon the primary stages of mankind, man was already familiar with matter in its two first states, solids and liquids, to very later discover the gases. It was only in the early 20^{th} century to realize that matter exists in an additional form arrising as the next natural step from solid to liquid to gas, and with significantly different properties than these states. When a gas is heated up to the degree that the kinetic energy of its atoms becomes so high that when they collide with each other their electrons can be stripped away in the process, matter is formed as a collection of electrons and positive ions, as well as neutral particles. Plasma constitutes the fourth fundamental state of matter defined as an ionized gas, which is globally neutral and displays collective behavior. It is the most abundant form of ordinary matter in the cosmos, as it is estimated that more than 99% of baryonic matter in the visible Universe is in plasma state, including the Sun and all the stars, as well as the interplanetary, interstellar and intergalactic medium. On Earth plasmas can be found in a series of natural phenomena, like the lightning strikes, the electric sparks and the aurora borealis, as well as in numerous technological applications, including neon lights, plasma displays and thermonuclear fusion devices. In practice, however, the transition point between the gas and the plasma phase is not unique, but it is considered that 0.1% degree of ionization gives clear plasma properties, while 1% degree of ionization means approximately perfect conductivity. In fact, plasma is typically a good electrical conductor. The degree of ionization for a gas is given by the well known Saha's equation [1, 2], which implies that it increases rapidly with the temperature, while it is inversely proportional to the density of the ionized atoms in connection with the recombination effect. This explains the fact that the plasma state is less common in the lower atmospheric levels of our planet.

Plasma consists of a mixture of free oppositively charged particles and strongly interacts with electromagnetic fields, either applied externally or created by the plasma itself, i.e. charge separation between ions and electrons give rise to electric fields and charged particle flows give rise to currents and magnetic fields. A fundamental characteristic of a plasma is its ability to shield out applied electric fields. Despite the existence of localized charge concentrations, there are approximately equal numbers of positive and negative charges distributed, so that overall plasma is quasi-neutral. However, the distribution of these different kinds of particles are not

necessarily uniform in space and so charge density gradients and fields can still exist within the plasma. In fact, quasi-neutrality is plausible in large scale lengths, while deviations from charge neutrality can develop in shorter scales. The limiting distance over which significant charge separations can occur is the Debye length, which is the smallest macroscopic scale in the plasma with respect to the dimensions of the system. Whenever external potentials are introduced, they are shielded out in the Debye scale, so that the plasma is neutral enough but not to the rate that all the electromagnetic forces vanish. Although in some domains the Debye length is estimated to be in the order of less than millimeter, i.e. in solar corona and tokamak discharge, in others, like the solar wind, it can have macroscopic values, and in order for it to be a statistically valid concept there must be a large number of particles inside the sheath region.

Plasmas are characterized by a large spectrum of density and temperature values. Indeed, in the plasma state one can find densities similar to those in all different states of ordinary matter. However, a fundamental property of the plasma, that distinguishes it from them, concerns the way in which particles interact with each other. The particles of a neutral medium mainly interact with direct binary collisions and in a short distance. In contrast, the charged particles in a plasma predominantly interact through long-range Coulomb collisions, due to electrostatic interaction. Each particle is simultaneously influenced by a large number of surrounding particles, and therefore its trajectory is governed by a collective field. When an electric field is applied to a plasma charged particles will start to move responding to this field; however, their motion will be slowed down after a transient because of the presence of collisions, leading to a steady state. This overall dynamics can be represented as an effective resistivity of the plasma. In a relatively short time scale electrons, which are highly mobile, will collide with ions as well as with other electrons, therefore leading to an isotropization of their distribution function, which tends to a Maxwellian. In addition, collisions between the heavy ions tend to a thermalization of their distribution function in larger timescales, leading to a momentum exchange. Furthermore, on a much longer timescale, the electrons and the ions that have thermalized with each other will exchange energy and tend to reach the same temperature. According to Spitzer's law [3,4] the resistivity of a plasma is proportional to the effective electron-ion collision frequency, which in turn decreases with the electron temperature. Although fully ionized gases are mainly dominated by Coulomb collisions, in weakly ionized ones collisions with the neutral particles should also be taken into account. However, in order for an ionized gas to be chacterized as plasma collisions between charged and neutral particles must not be too frequent.

The earliest studies in plasma physics date back to the 1920's when few isolated scientists, among which Irving Langmuir, were performing research both on ionospheric plasmas, because these were affecting radio transmission, and on gaseous electron discharge tubes at the same time. Some years later, another pioneer working on plasma physics, Hannes Alfvén, discovered the fundamental magnetohydronamic waves and proposed that these have an impact on the dynamics of astrophysical plasmas. Since then, plasma physics has been expanded to the key physics for the study of several astrophysical phenomena, such as the behavior of the aurora, the Van Allen radiation belts, the effects of magnetic storms, the formation of astrophysical jets, the accretion discs of black holes and numerous other. However, the largest development of plasma physics came after the second world war as an offshoot of the nuclear weapons programme, when it was proposed that the nuclear fusion reaction that occurs in the stars could be controlled to make an effective reactor on our planet. Therefore, the strongest drive to the study of plasma physics has been the production of a clean and sustainable energy source that could cover the needs of a growing world population.

1.2 Thermonuclear fusion and magnetic confinement

The global demand for energy and especially electricity, has been increasing and will continue to increase rapidly, due to the development of civilization, due to population expansion, as well as due to climate change. As a consequence, the demand for fossil fuels, especially petroleum and gas, is everyday growing, and it is estimated that after it reaches a peak in the near future, their world reserves are going to be depleted within a century. At the same time, the renewable sources of energy, towards which an enegy shift is taking place, are not expected to have practically the potential of completely covering the fastly growing energy needs. On account on these facts, it seems that nuclear energy has a key role to play in our energy future as a stable and always available source, even when the wind is not blowing and the sun is not shining. Fission reactors are already being exploited and have an important contribution to the world energy reserves. However, the waste produced in vast amounts from such nuclear power stations are radioactive and their safe disposal is very difficult and expensive. Although experts are working on designing safer and more efficient fission reactors, the quantities of the related fuels would still not be enough, if a time span of several centuries is considered. A possible alternative, into which the scientific- and not only- community is vast devoting, is nuclear fusion.

Nuclear fusion is the same process that powers the sun and every other star in the universe, which can be viewed as 'natural fusion reactors'. In a fusion reaction, two light atoms fuse together to make a heavier one. To make the nuclei come close enough to each other and overcome the electrical repulsive forces they need to collide at a very high speed. This means that the plasma needs to have a very high temperature. Once the nuclei fuse, the process releases a large amount of energy which is potentially inexhaustible because it uses the most abundant element in the universe, hydrogen. In the sun 600 million tons of hydrogen is fused into helium each second due to the huge gravitational pressures and high tempreratures that exist there, and it is the energy from this process that sustains life on our planet. Since scientists first figured out what was causing the sun to shine they were inspired of harnessing this energy as a clean source, by achieving thermonuclear fusion in a controlled manner on Earth. However, in laboratory the hydrogen-hydrogen reaction would be impractical since it would require too much energy, and thus, lighter isotopes, such as Deuterium (D) and Tritium (T), are used. The D-T reaction, ${}^{2}_{1}D + {}^{2}_{1}T \rightarrow {}^{4}_{2}He\,(3.5\,MeV) + {}^{1}_{0}n\,(14.1\,MeV)$, has the highest cross-section and is the one to be undertaken in the first stages of development; this process needs a temperature of 100 to 150 million degrees Centigrade, which are higher than the temperatures in the core of the sun, and in which temperature matter is in plasma state. Despite the important advantages of nuclear fusion such as the abundance of fuel (Deuterium and Tritium are extracted and generated by sea water and lithium), the absence of greenhouse gas emissions, and the absence of hazards such as dangerous accidents in power plants and long-lasting radioactive waste products, achieving controlled thermonuclear fusion still remains an open issue.

The efficiency and self-sustainment of a nuclear fusion reaction relies on the simultaneous achievement of very high plasma temperature, T, at which the charged particles can overcome their repulsive forces, of sufficiently large density of fuel ions, n, as well as of sufficient energy confinement time, τ_c, which can be interpreted as the time of the retainment of energy before being lost. Maintenance of these conditions relies on the ratio of the thermal energy per unit volume, nT, which decreases by heat conduction and by particle losses, as well as on the power input. The Lawson criterion [5] states that in order for a fusion reaction to be energetically favourable the rate of the produced energy must be higher than the energy loss, and has to be satisfied for a successful operation of a fusion reactor. The fusion energy is three orders of magnitude higher than the mean thermal energy, and thus, τ_c has to be not

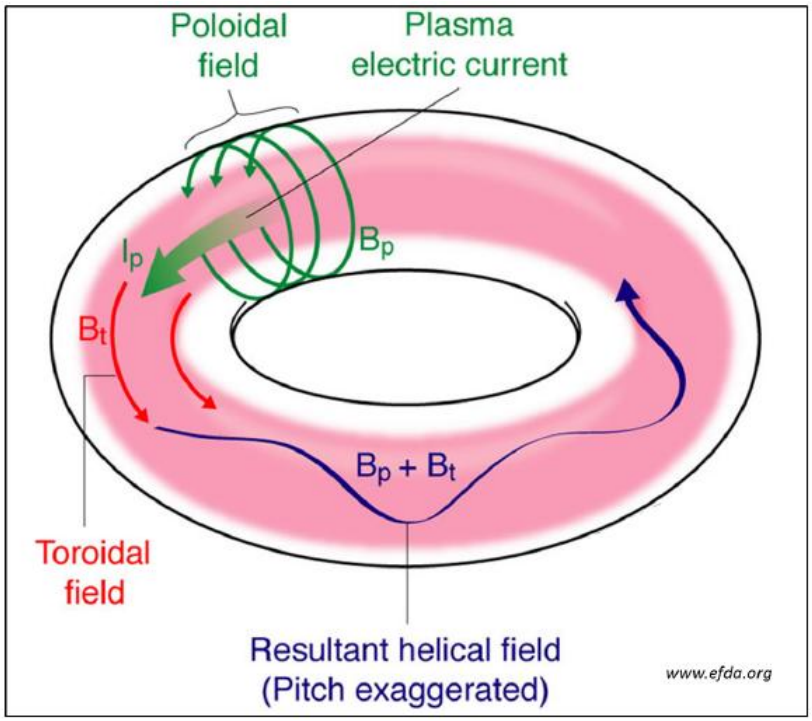

Figure 1.1: The combination of toroidal, $\mathbf{B}_t$, and poloidal, $\mathbf{B}_p$, magnetic fields results in a twisted, helical magnetic field which is essential for confinement in toroidal geometry.

less than 10^{-3} of complete burn time. As a result, for the D-T self-sustained reaction, and for a temperature of $T \sim 10\,keV$, the necessary condition $n\tau_c \geq 10^{20}\,m^{-3}s$ has to be satisfied. The reduction of energy and of particle losses, and the achievement of sufficiently high energy confinement times, indicate that the plasma should be heated and confined in a bounded volume. However, no known material enclosing the plasma volume can withstand the huge temperatures into which the plasma is heated.

At present, the major research effort in the area of controlled thermonuclear fusion is focused on the magnetic confinement fusion (MCF) technique, in which strong magnetic fields are used to confine the hot plasma, isolating it from the cold vessel walls. The MCF devices most actively studied are the toroidal configurations not having an open end. Toroidal geometry came as a replacement of the first studied linear (cylindrical) devices, which suffered from plasma leaking out at their ends. In the simple toroidal field, ions and electrons drift in opposite directions due to the gradient of the magnetic field, $\mathbf{B}^*$. This drift causes charge separation that induces an electric field, $\mathbf{E}^*$, directed parallel to the major axis of the torus. If the magnetic field is purely toroidal, then a drift velocity perpendicular to the resulting subsequent $\mathbf{E}^* \times \mathbf{B}^*$ field will result, which will point horizontally. So the plasma will very quickly drift straight to the outer walls of the device. In order to mitigate this tendency, it is necessary to connect the upper and lower parts of the plasma by lines of magnetic force thus leading to a short circuit of the separated charges along these field lines. Therefore, the combination of poloidal and toroidal fields tends to reduce the tendency of the plasma to drift to the walls, that would exist due to the non-uniform toroidal field, and the geometry enables longer confinement times for the plasma. Consequently, a twisted, helical magnetic field as that shown in figure 1.1 is essential to the equilibrium of toroidal plasmas. Such a field is characterized by the so called rotational transform, which can be roughly defined as the poloidal twist of the field lines round the short direction of the torus, while revolving round the long way around it. Toroidal devices may be classified according to the methods used to generate this rotational transform.

The most promising devices, into which the major scientific research is focused, are the

Tokamak and the Stellarator, both of these concepts being studied for almost half of a century. In a Tokamak device the twist of the magnetic field is produced by a toroidal plasma current driven inductively by an external coil. Although this fact leads to a simplified geometry, since the Tokamak is axisymmetric, the generation of the toroidal current by a transformer action makes it difficult to operate in steady state, as well as vulnerable to current driven instabilities. On the other hand, in a Stellarator the rotational transform is produced by external non-axisymmetric coils. Every Stellarator has its own symmetry, consisting of a different number of identical parts that are connected together, denoting the number of field periods, and of a non-planar magnetic axis. Each of the external helical windings has to be designed and positioned properly in every one of these field periods. Despite its complex geometry, a Stellarator is inherently current free, and thus, able to operate in steady state. A general comparison between Tokamak and Stellarator devices can be found in [6, 7]. The largest Tokamak device, ITER, is now being under construction in Cadarache, France, and is expected to start operating within the next decade, while the largest fusion device of the Stellarator type is the Wendelstein 7-X (W7-X), being already in operation in Greifswald, Germany. Both of these devices are characterized as experimental fusion reactors and not as functioning power plants, but their possible success is expected to bring humanity a step closer to achieving the dream of controlled thermonuclear fusion.

1.3 Plasma modeling

A plasma consists of charged particles which move under the effects of the electric and magnetic fields that they have themselves generated, as well as under the effects of externally applied fields, so that in general the equations of motion together with the Maxwell equations determine its dynamics. The Maxwell equations in SI units are the following

$$\nabla \cdot \mathbf{E}^* = \frac{\varpi}{\varepsilon_0}, \tag{1.1}$$

$$\nabla \cdot \mathbf{B}^* = 0, \tag{1.2}$$

$$\nabla \times \mathbf{E}^* = -\frac{\partial \mathbf{B}^*}{\partial t}, \tag{1.3}$$

$$\nabla \times \mathbf{B}^* = \mu_0 \mathbf{J}^* + \varepsilon_0 \mu_0 \frac{\partial \mathbf{E}^*}{\partial t}, \tag{1.4}$$

where $\mathbf{E}^*(\mathbf{r}, t)$ and $\mathbf{B}^*(\mathbf{r}, t)$ are the electric and the magnetic field, while $\varpi(\mathbf{r}, t)$ and $\mathbf{J}^*(\mathbf{r}, t)$ are the charge and the current density in terms of position and time; ε_0, μ_0 are the electric and magnetic constant permeabilities, satisfying the relation $c^2 = (\varepsilon_0 \mu_0)^{-1}$. In order for such a system to be closed the sources (ϖ, $\mathbf{J}^*$) have to be specified in terms of the fields ($\mathbf{E}^*$, $\mathbf{B}^*$). According to the Newton's law, once the forces, $\mathbf{F}_j$, that act on each plasma particle, $j = 1, 2, ..., N$, are known, then the velocity, $\boldsymbol{v}_j$, and the position, $\mathbf{r}_j$, of all the particles are also known; therefore the charge density and the current density of the plasma can be evaluated

$$\varpi = \sum_{j=1}^{N} q_j \delta(\mathbf{r} - \mathbf{r}_j), \qquad \mathbf{J}^* = \sum_{j=1}^{N} q_j \boldsymbol{v}_j \delta(\mathbf{r} - \mathbf{r}_j). \tag{1.5}$$

In fact, solving self-consistently the kinetic equation together with equations (1.1)-(1.4) is much more tougher because the spatial dependence of the fields appearing in the Lorenz force is not known from the outset. One could expect that this description would be able to represent the evolution and the motion of all the charged particles consisting the system in the most complete way, once a given set of initial conditions are given. However, such a

description is non practical, since it is impossible to determine the position and the velocity of the huge number of particles being present in a fusion experiment, even by using advanced supercomputers. In fact the self-consistent solution of equations (1.1)-(1.5) is much more complicated because the magnetic force depends on the particle velocity, $\boldsymbol{v}_j$. Also, such a description lacks rigorous treatment of various atomic processes, i.e. radiation emittions, as well as of phenomena for which quantum description is required. For this reason approximation schemes based on the application of different self-consistent or less self-consistent models, valid for different time and length scales, are employed to describe plasma dynamics.

1.3.1 Kinetic description

Kinetic theory provides a statistical description of the very large number of interacting particles constituting the plasma by the means of smooth distribution functions. From a microscopic viewpoint the description of the collective behavior of the plasma accounts on the treatment of the particles in the continuum limit as a whole, called also microfluid by averaging over all possible microstates, and not individually. The distribution function $f_\alpha(\mathbf{r}, \boldsymbol{v}, t)$ determines how the particles of each species-α, $\alpha = i, e$, for an ion - electron plasma, are distributed in the six-dimensional phase space $(\mathbf{r}, \boldsymbol{v})$ at an instant in time. Note that in general, there may exist different species of ions, with different charges and different masses in a plasma. The evolution of the distribution function is described by the Boltzmann's equation

$$\frac{\partial f_\alpha}{\partial t} + \boldsymbol{v} \cdot \nabla_{\mathbf{r}} f_\alpha + \frac{\mathrm{q}_\alpha}{m_\alpha}(\mathbf{E}^* + \boldsymbol{v} \times \mathbf{B}^*) \cdot \nabla_{\boldsymbol{v}} f_\alpha = \mathcal{C}[f_\alpha], \tag{1.6}$$

where q_α and m_α denote the charge and the mass for each species, while $\mathcal{C}[f_\alpha]$ is the so-called collision operator that is associated with the evolution of the distibution function due to the particle collisions. The Boltzmann equation (1.6) states that the derivative, with respect to time, of the distribution function, depends on the streaming of particles in configuration space, on the streaming in velocity space due the long-range electromagnetic forces, and on the short-range forces that are associated with collisions. Therefore, kinetic theory provides a distinction between the effects of long-range and short-range interactions. As concerns the collision operator, it is usually constructed by taking into account that particles of one species interact with particles of the same as well as of different species, but its form is not unique. It is an objective of kinetic theory to specify $\mathcal{C}[f_\alpha]$ in order for the respective effects to be taken into account in collisional plasmas. Examples of exact expressions of the collision operator are the Landau [8], the Lenard-Balescu [9, 10], and the Bhatnagar-Gross-Krook (BGK) [11] operators. As already mentioned, while in some plasmas as the low density, weakly ionized ones, collisions may play an important role, in highly ionized ones they can become negligible. Also, recall that the Spitzer law implies that the collision frequency decreases with the plasma temperature, specifically as $T^{-3/2}$, and thus, in high temperature plasmas as the ones in nuclear fusion, collisions can be neglected. In such applications the collision term of equation (1.6) can be approximated with zero, and the evolution of the distribution function for each species can be accurately described by the Vlasov equation

$$\frac{\partial f_\alpha}{\partial t} + \boldsymbol{v} \cdot \nabla_{\mathbf{r}} f_\alpha + \frac{\mathrm{q}_\alpha}{m_\alpha}(\mathbf{E}^* + \boldsymbol{v} \times \mathbf{B}^*) \cdot \nabla_{\boldsymbol{v}} f_\alpha = 0. \tag{1.7}$$

Equation (1.7) does not imply the absence of interactions; it implies that the charged particles interact through the dominant long-range Coulomb collisions.

Either for a collisional or a collisionless plasma, the solution of the Boltzmann (1.6) or the Vlasov (1.7) kinetic equations for the distribution function is not sufficient to completely describe the dynamics of the system. In order to complete the equations the following closures

for the sources are necessary

$$\varpi = \sum_{\alpha} \mathrm{q}_{\alpha} n_{\alpha}, \quad \mathbf{J}^{*} = \sum_{\alpha} \mathrm{q}_{\alpha} n_{\alpha} \mathbf{v}_{\alpha}, \tag{1.8}$$

where n_α and $\mathbf{v}_\alpha$ are the particle density and average velocity for each species, and which have to be expressed in terms of f_α. Therefore, equations (1.1)-(1.4) and (1.8) together with either (1.6) or (1.7) complete the kinetic theory equations. The kinetic description is very detailed and captures effectively most of the physical phenomena in a plasma. However, solving the kinetic equation self-consistently with the Maxwell ones is a tough, complicated task which even numerically becomes extremely expensive (in time). As a result, there is the need to come up with simpler models, such as fluid-like models, in order to describe the dynamics of a plasma.

1.3.2 Fluidistic description

In a fluid description the plasma is treated as a continuous medium and is described by well-defined macroscopic quantities, such as density, pressure, mean velocity and temperature, which are indeed measurable in related experiments. Different models employed in such an approach are the multi-fluid model, upon which the plasma is considered to consist of two or more co-existing fluids for each different particle species, and the magnetohydrodynamics model, in the framework of which the plasma is treated as a single electrically conducting fluid.

The multi-fluid equations are derived by taking the moments of the Boltzmann equation and are obtained upon properly chosen velocity dependent functions, weighted by the distribution function, and integrated over the velocity space. These equations include a number of fluid variables for each species α, as the particle number density, n_α, the average velocity, $\mathbf{v}_\alpha$, the thermal pressure tensor, P^{*}_{α}, and the heat flux tensor, T_α, defined as follows

$$\begin{aligned} n_\alpha(\mathbf{r},t) &= \int f_\alpha(\mathbf{r},\boldsymbol{v},t)d\boldsymbol{v}, \\ \mathbf{v}_\alpha(\mathbf{r},t) &= \frac{1}{n_\alpha}\int \boldsymbol{v} f_\alpha(\mathbf{r},\boldsymbol{v},t)d\boldsymbol{v}, \\ \mathsf{P}^{*}_{\alpha} &= m_\alpha \int (\boldsymbol{v}-\mathbf{v}_\alpha)(\boldsymbol{v}-\mathbf{v}_\alpha) f_\alpha(\mathbf{r},\boldsymbol{v},t)d\boldsymbol{v}, \\ \mathsf{T}_\alpha &= m_\alpha \int (\boldsymbol{v}-\mathbf{v}_\alpha)(\boldsymbol{v}-\mathbf{v}_\alpha)(\boldsymbol{v}-\mathbf{v}_\alpha) f_\alpha(\mathbf{r},\boldsymbol{v},t)d\boldsymbol{v}. \end{aligned} \tag{1.9}$$

By taking the zeroth, first and second order velocity moments of the Boltzmann equation, we come up with a continuity, a momentum, and an energy equation for each species, respectively. These are of the form:

$$\frac{\partial n_\alpha}{\partial t} + \nabla\cdot(n_\alpha \mathbf{v}_\alpha) = 0, \tag{1.10}$$

$$m_\alpha n_\alpha \frac{D\mathbf{v}_\alpha}{Dt} - \mathrm{q}_\alpha n_\alpha(\mathbf{E}^{*} + \mathbf{v}_\alpha \times \mathbf{B}^{*}) + \nabla\cdot\mathsf{P}^{*}_{\alpha} = m_\alpha \int (\boldsymbol{v}-\mathbf{v}_\alpha)\mathcal{C}[f_\alpha]d\boldsymbol{v}, \tag{1.11}$$

$$\frac{3}{2} n_\alpha \frac{DK_\alpha}{Dt} + \mathsf{P}^{*}_{\alpha} : \nabla\mathbf{v}_\alpha + \nabla\cdot\mathsf{Q}_\alpha = \frac{1}{2} m_\alpha \int |\boldsymbol{v}-\mathbf{v}_\alpha|^2 \mathcal{C}[f_\alpha]d\boldsymbol{v}, \tag{1.12}$$

where

$$\mathsf{Q}_\alpha = \frac{1}{2} m_\alpha \int |\boldsymbol{v}-\mathbf{v}_\alpha|^2 (\boldsymbol{v}-\mathbf{v}_\alpha) f_\alpha(\mathbf{r},\boldsymbol{v},t)d\boldsymbol{v}, \tag{1.13}$$

is the heat flux vector, defined through contracting with the third-rank tensor T_α, which represents the energy flux as observed in a frame moving with velocity $\boldsymbol{v}$, and $K_\alpha = \frac{m_\alpha}{3n_\alpha}\int |\boldsymbol{v}-$

$\mathbf{v}_\alpha|^2 f_\alpha(\mathbf{r},\boldsymbol{\upsilon},t)d\boldsymbol{\upsilon}$ is the kinetic energy due to the spreading around fluid velocity, properly normalized; $D/Dt = \partial/\partial t + \mathbf{v}_\alpha \cdot \nabla$ is the convective derivative. The terms on the right-hand side (RHS) of equations (1.11)-(1.12), involving $\mathcal{C}[f_\alpha]$, represent the viscous forces due to the collisions and the heat generated by such forces, therefore implying that the collision operator has yet to be determined. However, the contribution of the related integrals are usually thought to be negligible based on general conservation laws involving the collision term, i.e that the collisions characterized by $\mathcal{C}[f_\alpha]$ are purely elastic Coulomb collisions such that the energy and the momentum between both like and unlike particles are conserved; also, inelastic collisions related with phenomena such as ionization, alpha production, recombination etc., are not as dominant as Coulomb collisions in fusion plasmas. The continuity equation (1.10) was derived upon the assumption that the number of the total particles is conserved; however, this may not be the case when fusion reactions take place.

The above multi-fluid equations were evaluated under the assumptions that the Boltzmann equation is valid, and that the acting forces are the electromagnetic ones, such that the Maxwell equations are also valid; however, gravitational forces may also be included in related plasmas. In such a multi-fluid model some microscopic properties, arising from the separate treatment between the different species, are accurately described, i.e. ion/electron skin depth.

The simplest model to describe the dynamics of plasmas interacting with an electromagnetic field is the one-fluid magnetohydrodynamics (MHD) in the framework of which the plasma is treated as a continuous single conducting fluid, by the means of a single mass density, ϱ^*, a single mean fluid velocity, $\mathbf{V}^*$, a charge density, ϖ and a current density, $\mathbf{J}^*$. These single-fluid macroscopic variables are defined from the respective quantities of the two-fluid model, which can be thought as the degenerate multi-fluid model when the plasma consists, among with the electron fluid, of only one-kind ion fluid, such that $\alpha = i,\, e$; they are of the form

$$\begin{aligned} \varrho^* &= \sum_{\alpha=i,\,e} n_\alpha m_\alpha, \qquad & \mathbf{V}^* &= \frac{\sum_{\alpha=i,\,e} n_\alpha m_\alpha \mathbf{v}_\alpha}{\sum_{\alpha=i,\,e} n_\alpha m_\alpha}, \\ \varpi &= e(n_e - n_i), \qquad & \mathbf{J}^* &= e(n_e \mathbf{v}_e^* - n_i \mathbf{v}_i^*). \end{aligned} \tag{1.14}$$

The derivation of the single-fluid equations that describe the dynamics of magnetized plasmas is based on the key assumptions that MHD involves low-frequency and large spatial scale phenomena. In fact, the MHD length scales, L, are much larger than the Debye length, $\lambda_D/L \ll 1$, and as described earlier the plasma is quasi-neutral in such macroscopic length scales. Owing to quasineutrality, for a fully-ionized plasma the electron and the ion number densities are assumed to be approximately equal, i.e. for a hydrogen plasma it holds $n_e \approx n_i = n$, where n is defined as the common plasma density. As a result the charge density of equation (1.14) vanishes, $\varpi \approx 0$, and the quasineutrality condition accurately substitutes the Poisson's law (1.1), which is no more considered for an MHD description. Also, the MHD related frequencies are much less than the plasma frequency and the electron cyclotron frequency. On account of this assumption the electrons respond very fast to acting forces, such that the heavy ions dominate the fluid quantities (1.14), $m_e/m_i \ll 1$, which therefore can be written to a good approximation as: $\varrho^* \approx m_i n$, $\mathbf{V}^* \approx \mathbf{v}_i^*$, and $\mathbf{J}^* \approx ne(\mathbf{V}^* - \mathbf{v}_e^*)$. Equivalently, the electrons are asymptotically assumed to be massless, and thus, their inertia can be neglected and the displacement current can be dropped from the Amprere's law (1.4), which therefore reduces to

$$\nabla \times \mathbf{B}^* = \mu_0 \mathbf{J}^*. \tag{1.15}$$

By combining the continuity equations (1.10) of the two-fluid model, under the above described assumptions, we obtain the following continuity equation for the single fluid

$$\frac{\partial \varrho^*}{\partial t} + \nabla \cdot (\varrho^* \mathbf{V}^*) = 0, \tag{1.16}$$

together with the equation

$$\nabla \cdot \mathbf{J}^* = 0, \tag{1.17}$$

which implies that the single-fluid current density is divergence-free. Furthermore, by combining the respective two-fluid momentum equations for the two species we obtain the following momentum equation for the single-fluid

$$\varrho^* \frac{D\mathbf{V}^*}{Dt} = \mathbf{J}^* \times \mathbf{B}^* - \nabla \cdot \mathsf{P}^*, \tag{1.18}$$

where $D/Dt \equiv \partial/\partial t + \mathbf{V}^* \cdot \nabla$, and $\mathsf{P}^* \equiv \mathsf{P}_i^* + \mathsf{P}_e^*$, can be interpreted as a single-fluid pressure tensor, which in general is not diagonal; in fact, the respective pressure tensors for each particle species can be written in the form $\mathsf{P}_{i,e}^* = P_{i,e}^* \mathbf{I} + \mathbf{\Pi}_{i,e}$, where $\mathbf{I}$ is the unit tensor, while the scalars $P_{i,e}^*$ denote the diagonal elements of $\mathsf{P}_{i,e}^*$ and the tensors $\mathbf{\Pi}_{i,e}$ consist of the non-diagonal parts of $\mathsf{P}_{i,e}^*$, involving quantities such as the fluid viscocity. In addition, from the two-fluid momentum equations we obtain the following generalized Ohm's law for the single-fluid

$$\mathbf{E}^* + \mathbf{V}^* \times \mathbf{B}^* = \frac{1}{en} \left(\mathbf{J}^* \times \mathbf{B}^* - \nabla \cdot \mathsf{P}_e^* \right) + \widetilde{\eta} \mathbf{J}^*, \tag{1.19}$$

where $\widetilde{\eta}$ is defined as the resistivity of the fluid. Whenever the terms consisting the RHS of equation (1.19) are not negligible, the dynamics of the related plasma is described by different versions of the ordinary MHD model, namely, the resistive MHD (RMHD), the Hall MHD (HMHD), and the Extended MHD (XMHD) models, depending on which of these different terms is being considered important. Finally, as concerns the energy equations of the two-fluid theory, under the MHD basic assumptions employed above, these can be cast into the following forms

$$\frac{3\varrho^{*\gamma}}{2} \frac{D}{Dt} \left(\frac{P_i^*}{\varrho^{*\gamma}} \right) + \nabla \cdot \mathsf{Q}_i + \mathbf{\Pi}_i : \nabla \mathbf{V}^* = 0, \tag{1.20}$$

$$\frac{3\varrho^{*\gamma}}{2} \frac{D}{Dt} \left(\frac{P_e^*}{\varrho^{*\gamma}} \right) + \nabla \cdot \mathsf{Q}_e + \mathbf{\Pi}_e : \nabla \left(\mathbf{V}^* - \frac{\mathbf{J}^*}{en} \right) - \frac{1}{en} \mathbf{J}^* \cdot \nabla \left(\frac{P_e^*}{\varrho^{*\gamma}} \right) = 0, \tag{1.21}$$

containing both the single-fluid variables and two-fluid effects, but can be properly manipulated in an one-fluid form. Note that we have neglected all integrals including the collision operator.

From the above analysis it follows that both the multi-fluid and the MHD models are not complete since the pertinent equations consisting each of these models do not form a closed system of equations. In this respect, either the multi-fluid equations (1.9)-(1.12) or the MHD ones (1.14)-(1.20) should properly be called moment equations rather than fluid equations.

Closure of the fluid equations

Every fluid model suffers from an "autoimmune" problem known as the closure problem, since any fluid equation obtained from the N^{th} moment of the Boltzmann equation also contains a quantity of its $(N+1)^{th}$ moment, so that each time an additional equation for the evolution of this moment is required to close the system. Specifically, in deriving the multi-fluid equations the 0^{th} moment yields the continuity equation (1.10) which contains the species velocity, $\mathbf{v}_\alpha$; the 1^{st} moment gives the momentum equation (1.11) in which the second rank pressure tensor, P_α^*, appears, while the 2^{nd} moment yields the energy equation (1.12), containing the heat flux vector Q_α related with the third rank tensor T_α, which can be thought as an unknown. Obviously, taking further moments of the kinetic equation does not cure the problem since each time a higher rank tensor will appear, thus, making calculations more and more complicated and only delaying the problem.

Two main closure schemes are usually employed to close the fluid equations; these are either an asympotic approach, which involves the kinetic equation itself in some degree by

expanding the distribution function with respect to a small parameter of interest, i.e. [12], or a truncation scheme in which higher order moments are expressed in terms of lower ones or simply are assumed to vanish. In the framework of the single-fluid description of plasmas, a truncation up to the second moment is being considered, such that the pertinent equations are closed up to an energy equation, i.e. by assuming either adiabatic, isothermal, or incompressible flows. In this respect, specific equations of state describing the evolution of the pressure tensor have to be employed. Along the lines of the present thesis special emphasis will be given to the Ideal MHD [13] and the Chew-Goldberge-Low (CGL) [14] models, which were established within different assumptions for plasma collisionality. In the framework of these models the plasma is treated as a perfectly conducting fluid completely described through single-fluid variables, i.e. information concerning the different species pressure tensors $\mathsf{P}^*_{i,e}$ is lost from the coupled energy equations (1.20)-(1.21), and the respective equations are closed under the imposure of the adiabatic or the double-adiabatic equations of state.

1.3.3 Ideal MHD and CGL frameworks

Ideal MHD is the simplest model than can describe the plasma as a conducting fluid and is valid under specific length and timescales. The key assumtpion made to close the MHD equations is that both the ions and the electrons are collision-dominated. More presicely, this means that the mean free path of both the ions and the electrons is small relative to the chacteristic scale length of the system, L, as well as that the collision time for the ions and the electrons is short compared to the characteristic timescales of MHD which equals to the inverse of the characteristic MHD frequency, $\widetilde{\omega}$. In fact, the ions that are heavy and moving slowly are dominated by collisions with other ions, in timescales τ_{ii}, while for the electrons that are higly mobile collisions with both ions and with other electrons are important, for the timescales of which it is estimated that $\tau_{ei} \sim \tau_{ee} \sim (m_i/m_e)^{-1/2}\tau_{ii}$. Therefore, the high collisionality assumption can be described by the relation

$$\left(\frac{m_i}{m_e}\right)^{1/2} \widetilde{\omega}\tau_{ii} \ll 1, \tag{1.22}$$

which justifies the accuracy of the assumption that the energy transfer terms involving the collision operators are neglected from equations (1.20)-(1.21). Owing to the high collisionality the plasma tends to have an isotropic velocity distribution. This is because the collisions between the particles lead to a randomization of their respective distribution functions which tend to be Maxwellians. As a consequence the off-diagonal elements of the pertinent pressure tensors are negligible, $\mathbf{\Pi}_{i,e} = 0$, such that the total pressure tensors can be replaced by respective scalar pressures, and the plasma can be accurately described by a single-fluid MHD scalar pressure P^*:

$$\mathsf{P}^*_i \to P^*_i, \qquad \mathsf{P}^*_e \to P^*_e, \qquad P^* = P^*_i + P^*_e. \tag{1.23}$$

With the use of (1.23) it is straightforward that the momentum equation (1.18) in the ideal MHD limit reduces into the form

$$\varrho^* \frac{D\mathbf{V}^*}{Dt} = \mathbf{J}^* \times \mathbf{B}^* - \nabla P^*. \tag{1.24}$$

In addition to the assumption of high collisionality, two more conditions, related with the ion gyroradius, r_{L_i}, and the resistivity, $\widetilde{\eta}$, have to be satisfied in order for the ideal MHD model to be valid. Recall that the MHD is characterized as a low-frequency theory because its characteristic frequencies are slow relative to the ion cyclotron frequency. This is equivalent to the requirement that the ion gyroradius is small compared to the characteristic length scales in plasma

$$\frac{r_{L_i}}{L} \ll 1, \tag{1.25}$$

which is well satisfied in fusion related experiments. Furthermore, within the ideal MHD framework, the conductivity of the plasma is considered very high, or equivalently the resistive diffusion is thought to be negligible:

$$\frac{|\widetilde{\eta}\mathbf{J}^*|}{|\mathbf{V}^* \times \mathbf{B}^*|} \ll 1. \tag{1.26}$$

As a consequence, the magnetic field lines are frozen into the plasma and do not diffuse due to the resistivity, which is very low. Such a condition is well satisfied for high temperature fusion plasmas owing to Spitzer's law, but this condition puts a further restriction on the smalness of the collision time related with the high collisionality assumption (1.22). However, the resistivity term may be important in some astrophysical plasmas in which magnetic reconnection occurs.

On account of the above conditions, the terms in equations (1.19)-(1.21) related with the resistivity, the Hall term, the electron inertia and the viscosity terms, are negligible, and thus, the ideal Ohm's law has the following form:

$$\mathbf{E}^* + \mathbf{V}^* \times \mathbf{B}^* = 0. \tag{1.27}$$

The above equation implies that the electric field, $\mathbf{E}^*$, can be calculated from the velocity and the magnetic field. Also, recall that due to the quasineutrality assumption the Poisson's equation (1.1) is not included in the MHD equations. Therefore, the electric field can be entirely eliminated once the ideal Ohm's law (1.27) and the Faraday's law (1.3) are simplified to one single equation

$$\nabla \times (\mathbf{V}^* \times \mathbf{B}^*) = \frac{\partial \mathbf{B}^*}{\partial t}. \tag{1.28}$$

That is $\mathbf{E}^*$ in ideal MHD is not considered a dynamical variable, and as a result its component parallel to $\mathbf{B}^*$ is always zero.

Finally, as concerns equations (1.20) and (1.21), under the conditions (1.23)-(1.26) these can be simplified to a single energy equation in terms of one fluid variables of the form

$$\frac{D}{Dt}\left(\frac{P^*}{\varrho^{*\gamma}}\right) + \frac{2}{3\varrho^{*\gamma}}(\nabla \cdot \mathsf{Q}) = 0, \tag{1.29}$$

where the single fluid heat flux related variable is defined as, $\mathsf{Q} \equiv \mathsf{Q}_i + \mathsf{Q}_e$, and is proportional to the existing temperature gradients [15]. In fact, the heat flux is stronger in the direction parallel to the local magnetic field since the particles stream freely in this direction. The closure usually adopted in the framework of the ideal MHD model is that of adiabaticity, $\mathsf{Q} = 0$. That is, there is no heat conduction between the system and the environment as well as between the elements consisting the system. In this case the plasma is governed by the ideal gas equation of state

$$\frac{P^*}{\varrho^{*\gamma}} = \text{const.}, \tag{1.30}$$

where γ is the constant ratio of specific heats, and which equation completes the set of ideal MHD equations. An alternative to the adiabatic equation of state, is the assumption of incompressible fluid motion

$$\nabla \cdot \mathbf{V}^* = 0, \tag{1.31}$$

implying that the fluid elements do not suffer any compression due to the external pressure forces, and the plasma density remains homogeneous. In fact, the incompressibility condition (1.31) corresponds to a singular limit of the adiabatic equation of state for $\gamma \to \infty$, and can not be formally considered as an equation of state since the pressure is no longer an independent dynamic variable. In general, the dynamics of the plasma can be assumed incompressible once the velocity and the frequency are also small compared to that of the propagating compressional

waves [16, 17]. Incompressibility is a reasonable assumption for the motion perpendicular to the magnetic field and will be considered as the key closure along the lines of the present thesis.

Fluidistic description of a system near to thermodynamic equilibrium requires a certain degree of collisions, and in this respect the collision-dominated ideal MHD model should properly describe plasmas as fluids. However, the region of validity of ideal MHD is limited since for many important hot plasmas, as that related to fusion experiments, the mean free path and the collision time is so long, that the high collisionality assumption (1.22) is never satisfied. Such plasmas should be better described as collisionless rather than collisional, and in general are anisotropic owing to the presence of a strong magnetic field.

Collisionless fluid modeling

A plasma can be considered as collisionless whenever length scales shorter than the mean free path and timescales smaller than the collision time become not important, such that collisions between charged particles can be completely ignored. Comprehesively, collisionless plasmas are described by the Vlasov equation (1.7), which comes from the respective Boltzmann equation (1.6) once the collision operator vanishes. It would appear that for such plasmas a fluid description would not be appropriate. However, in the direction perpendicular to the magnetic field the gyroradius, which is usually very small, plays the role of the effective mean free path, restricting particle motion, and thus, the magnetic field itself plays the role of collisions [18]. Also, even in the absence of Coulomb collisions turbulence can result to dissipation such that in general the related distribution functions do not relax to Maxwelians, while it turns out that gradients of the distribution function in the direction parallel to the magnetic field are much weaker than in the perpendicular direction [17]. Therefore, for large-scale motions of collisionless plasmas the possibility of a fluid description is restored.

The establishment of a collisionless fluidistic description is based on pertinent fluid equations obtained upon taking the velocity moments of the Vlasov equation (1.7) in a procedure analogous to that of deriving the respective MHD equations. Note that the MHD equations were derived from the Boltzmann equation (1.6) without a specific prescription of the collision related term, which later was neglected due to the ideal approximation. Therefore, it follows that the MHD equations can also be derived from the Vlasov equation in a straightforward way. However, both the multi-fluid models as well as the single fluid MHD (ideal or not) are implicitly highly-collisional once a scalar pressure, corresponding to a Maxwellian distribution function, is forced. However, in magnetized collisionless (or weakly collisional) plasmas the distribution functions depart from Maxwellians and become anisotropic, and thus, cannot be accurately described by a single scalar pressure. In this case, pressure fluctuations in the directions along and across the magnetic field are different even if no mean temperature anisotropy exists in these directions. In this respect, a collisionless fluid model is one derived from the moments of the Vlasov equation (1.7) and for which two different pressure evolution equations, parallel and perpendicular to the magnetic field, hold.

Macroscopic, single fluid, equations for a collisionless plasma in the presence of a strong magnetic field, with the Lorentz force playing a role analogous to that of the collision term, were derived in [14]. Such a derivation is formally based upon an asymptotic expansion of the distribution function in powers of the Larmor radius (or gyroradius), $r_{L_\alpha} = m_\alpha c \mathbf{v}_\alpha / \mathrm{q}_\alpha \mathbf{B}^*$, which is very small relative to the macroscopic physical length scales, i.e. $f_\alpha(\mathbf{r}, \boldsymbol{v}, t) = f_{\alpha 0} + \mathcal{O}(r_{L_\alpha})$; in fact, that derivation is based upon considering the lowest order approximation, $f_\alpha \sim f_{\alpha 0}$, also called gyrotropic approximation. By taking the first-order moment of the Vlasov equation, with respect to the definitions (1.9), we obtain a momentum equation for each species analogous to (1.11) but with zero right hand side. Such an equation contains the anisotropic pressure tensor, P^*_α, an equation for the evolution of which is obtained from

the second velocity moment of (1.7) of the form:

$$\frac{\partial \mathsf{P}^*_\alpha}{\partial t} + \nabla \cdot (\mathbf{v}_\alpha \mathsf{P}^*_\alpha + \mathsf{Q}_\alpha) + \mathsf{P}^*_\alpha \cdot \nabla \mathbf{v}_\alpha + (\mathsf{P}^*_\alpha \cdot \nabla \mathbf{v}_\alpha)^T + \frac{\mathrm{q}_\alpha}{m_\alpha c} (\mathbf{B}^* \times \mathsf{P}^*_\alpha - \mathsf{P}^*_\alpha \times \mathbf{B}^*) = 0, \tag{1.32}$$

where the superscript T indicates the transpose of the respective tensor. On account of the smallness of the gyroradius the last term of equation (1.32) is dominant to the lowest order, such that it reduces to the form

$$\mathbf{B}^* \times \mathsf{P}^*_{\alpha_0} = \mathsf{P}^*_{\alpha_0} \times \mathbf{B}^*. \tag{1.33}$$

The most general solution satisfying equation (1.33) is the following

$$\mathsf{P}^*_{\alpha_0} = P^*_{\perp_\alpha} (\mathsf{I} - \mathbf{b}^* \mathbf{b}^*) + P^*_{\parallel_\alpha} \mathbf{b}^* \mathbf{b}^*, \tag{1.34}$$

where I is the unit tensor; $\mathbf{b}^* = \mathbf{B}^*/|\mathbf{B}^*|$ is a unit vector pointing in the direction of the local magnetic field, while $P^*_{\parallel_\alpha}(\mathbf{r}, t)$ and $P^*_{\perp_\alpha}(\mathbf{r}, t)$ are the scalar pressure tensor elements for each species along and across this direction, defined as

$$\begin{aligned} P^*_{\parallel_\alpha} &= m_\alpha \int (v_\parallel - \mathbf{v}_\alpha \cdot \mathbf{b}^*)^2 f_{\alpha_0} d\boldsymbol{v}, \\ P^*_{\perp_\alpha} &= \frac{m_\alpha}{2} \int |\boldsymbol{v}_\perp - \mathbf{v}_{\alpha_\perp}|^2 f_{\alpha_0} d\boldsymbol{v}, \end{aligned} \tag{1.35}$$

with respect to a velocity decomposition in the directions parallel and perpendicular to $\mathbf{b}^*$. It readily follows that, to the lowest order, the pressure tensor is diagonal in a local rectangular system one of whose axes points along $\mathbf{B}^*$:

$$[\mathsf{P}^*_{\alpha_0}]_{ij} = \begin{pmatrix} P^*_{\perp_\alpha} & 0 & 0 \\ 0 & P^*_{\perp_\alpha} & 0 \\ 0 & 0 & P^*_{\parallel_\alpha} \end{pmatrix}. \tag{1.36}$$

We recall that this approximation is acceptable only at spatial scales very long compared to the gyroradius and frequencies very low relative to the gyrofrequency. However, at length scales comparable to the gyroradius, higher order corrections to the pressure tensor may become significant and must be taken into account. In this case the entire pressure tensor is of the form

$$\mathsf{P}^*_\alpha = \mathsf{P}^*_{\alpha_0} + \Pi_\alpha, \tag{1.37}$$

where, Π_α is called the gyroviscous stress tensor or Finite Larmor Radius (FLR) tensor, containing all non-gyrotropic corrections to $\mathsf{P}^*_{\alpha_0}$ [for a detailed review see [19]]. For the purposes of the present study the FLR corrections described by Π_α will be assumed negligible. In this respect, from now on the subscript 0 will be dropped, and henceforth P^*_α will be referred to the gyrotropic part of the entire pressure tensor, also called as CGL pressure tensor.

Introducing the variables, $P^*_\parallel(\mathbf{r}, t) = \sum_{\alpha=i,e} P^*_{\parallel_\alpha}$, $P^*_\perp(\mathbf{r}, t) = \sum_{\alpha=i,e} P^*_{\perp_\alpha}$, and on account of the definitions (1.14), we come up with a single fluid description of the pertinent collisionless plasmas. Thus, a momentum equation of the form (1.18) holds, in which the CGL pressure tensor is defined as

$$\mathsf{P}^*(\mathbf{r}, t) = P^*_\perp (\mathsf{I} - \mathbf{b}^* \mathbf{b}^*) + P^*_\parallel \mathbf{b}^* \mathbf{b}^*. \tag{1.38}$$

It is clear that $P_\perp^*$ represents the thermal energy associated with gyration, while $P_\parallel^*$ measures the thermal motion along the magnetic field. A more convenient form for equation (1.38) is

$$\mathsf{P}^* = P_\perp^* \mathsf{I} + \frac{\sigma_d^*}{\mu_0}\mathbf{B}^*\mathbf{B}^*, \tag{1.39}$$

where the dimensionless function

$$\sigma_d^* := \frac{\mu_0(P_\parallel^* - P_\perp^*)}{|\mathbf{B}^*|^2} \tag{1.40}$$

is a measure of the pressure anisotropy between the parallel and perpendicular motion. It is clear that particle collisions equilibrating parallel and perpendicular energies lower the value of σ_d^*, and therefore a highly collisional plasma is described accurately by a single scalar pressure, P^*. In view of this fact, when pressure anisotropy is present it is useful to introduce an effective isotropic pressure,

$$\mathcal{P}^*(\mathbf{r},t) := \frac{P_\parallel^* + P_\perp^*}{2}, \tag{1.41}$$

that reduces to P^* in the absence of anisotropy.

In addition, in the ideal approximation, in which the resistivity and the Hall term are negligible, the ideal Ohm law of the form (1.27) is valid, while two evolution equations are obtained for the scalar pressures parallel and perpendicular to the magnetic field, of the form

$$\begin{aligned}
\frac{D}{Dt}\left(\frac{P_\parallel^*|\mathbf{B}^*|^2}{\varrho^{*3}}\right) &= -\frac{|\mathbf{B}^*|^2}{\varrho^{*3}}\left[\nabla\cdot(Q_\parallel\mathbf{b}^*) - 2Q_\perp\nabla\cdot\mathbf{b}^*\right], \\
\frac{D}{Dt}\left(\frac{P_\perp^*}{\varrho^*|\mathbf{B}^*|}\right) &= -\frac{1}{\varrho^*|\mathbf{B}^*|}\left[\nabla\cdot(Q_\perp\mathbf{b}^*) + Q_\perp\nabla\cdot\mathbf{b}^*\right].
\end{aligned} \tag{1.42}$$

The above equations are derived by combining the respective equations (1.32) for each species in a form containing only one-fluid variables, and decomposing the gyrotropic pressure tensor and the gyrotropic part of the heat flux vector into the parallel and perpendicular directions. In this respect, $Q_\parallel$ and $Q_\perp$ are defined as the elements of the gyrotropic part of the one fluid heat flux variable, i.e. $\mathsf{Q}_0 = \sum_{\alpha=i,\,e}\mathsf{Q}_{\alpha_0}$ (all non-gyrotropic FLR effects having been neglected). Equations (1.42) were first derived in [14] [see equations (31) and (32) therein], their exact form (1.42) being recovered by the substitutions $q_n = Q_\parallel - 3Q_\perp$, $q_s = Q_\perp$, therein [see [19]]. Therefore, the dynamics of an ideal collisionless anisotropic plasma are described macroscopically by the equation of continuity (1.16), the equation of momentum (1.18), the Ohm's law (1.27), and the energy equations (1.42), along with the Maxwell equations (1.2), (1.15) and (1.28). However, this system of equations still remains incomplete since two additional equations (for the heat flux vector components) are required in order to be closed. Two such equations are the double adiabatic equations of state, associated with the CGL fluid model [14], which are recovered from equations (1.42) under the assumption that there is no heat conduction in neither of the directions parallel and perpendicular to $\mathbf{B}^*$, $Q_\parallel = Q_\perp = 0$; they are of the form

$$\begin{aligned}
\frac{D}{Dt}\left(\frac{P_\parallel^*|\mathbf{B}^*|^2}{\varrho^{*3}}\right) &= 0, \\
\frac{D}{Dt}\left(\frac{P_\perp^*}{\varrho^*|\mathbf{B}^*|}\right) &= 0,
\end{aligned} \tag{1.43}$$

implying that the first and second adiabatic invariants are conserved. In connection with the present study, however, we will assume incompressible flows (see equation (1.31)) together

with the condition

$$\mathbf{B}^* \cdot \nabla \sigma_d^* = 0, \tag{1.44}$$

in order to close the fluid equations. Equation (1.44) implies that the anisotropy function is constant on the magnetic field lines. The motivation for this choice will be explained later.

To summarize, we present below together all the equations derived above, which describe the motion of an ideal collisionless plasma:

$$\frac{\partial \varrho^*}{\partial t} + \nabla \cdot (\varrho^* \mathbf{V}^*) = 0, \tag{1.45}$$

$$\varrho^* \frac{D\mathbf{V}^*}{Dt} = \mathbf{J}^* \times \mathbf{B}^* - \nabla \cdot \mathsf{P}^*, \tag{1.46}$$

$$\nabla \times (\mathbf{V}^* \times \mathbf{B}^*) = \frac{\partial \mathbf{B}^*}{\partial t}, \tag{1.47}$$

$$\nabla \cdot \mathbf{B}^* = 0, \tag{1.48}$$

$$\nabla \times \mathbf{B}^* = \mu_0 \mathbf{J}^*, \tag{1.49}$$

where P^* is defined through equations (1.39)-(1.40). Recall that in the limit $\sigma_d^* = 0$, the scalar pressures parallel and perpendicular to $\mathbf{B}^*$ equilibrate. Therefore in this case the pressure tensor becomes isotropic $[\mathsf{P}^*]_{ij} = P^* \mathsf{I}$, such that the plasma state in the presence of many collisions can be accurately described by a scalar pressure, $P^* (= \mathcal{P}^* = P_\parallel^* = P_\perp^*)$. In this respect, the ideal MHD model equations are recovered from the respective equations (1.45)-(1.49) by setting $\sigma_d^* = 0$. In fact this substitution takes effect only into the momentum equation (1.46), since the rest of them are not dependent on the anisotropy function. Therefore, we will further refer to an isotropic plasma as one described by the set of equations (1.45)-(1.49) for $\sigma_d^* = 0$. We note that although the CGL collisionless model and the ideal MHD model are established through different physical assumptions for the particle collisions, the form of the equations they consist of are identical, such that passing from the one set of equations to the other is mathematically convenient.

1.4 MHD equilibrium and stability elements

Plasmas are, in general, found to be unstable once large amounts of energy are concenrated in a limited volume of a laboraty device. For favorable confinement a potential magnetic configuration must meet the following criteria: (i) it must operate in steady state and thus, the plasma should be in equilibrium state, (ii) once established, an equilibrium must be macroscopically stable, and (iii) the loss of plasma energy to the surrounding walls, arising from heat and particle transport, must be reduced. In principle, the examination of the problem of stability or instability of a physical system is based upon the establishment of a background equilibrium, so that the construction of such an equilibrium is the basis of stability and transport studies. Such low entropy states are susceptible to numerous instabilities as strong ideal pressure and current driven modes, resistive instabilities often associated with magnetic reconnection, and kinetic micro-instabilities which occur when the distribution functions depart from Mawxellians. Also, certain instabilities are a source of turbulence, which can drive transport. Investigation of macro-instabilities is usually performed within the framework of MHD, since this model is a good approximation in describing the plasma as a macroscopic fluid and capturing most of the physics of the force balance. Although microscopic instabilities -the study of which requires kinetic theory- may sometimes become important, it is the MHD instabilities that are more dangerous for a successful confinement [20].

1.4.1 Equilibrium

The ideal MHD equilibrium states of a plasma with flow and anisotropic pressure are governed by the following counterpart to the set (1.45)-(1.49) time-independent equations:

$$\nabla \cdot (\varrho \mathbf{V}) = 0, \tag{1.50}$$
$$\varrho(\mathbf{V} \cdot \nabla)\mathbf{V} = \mathbf{J} \times \mathbf{B} - \nabla \cdot \mathsf{P}, \tag{1.51}$$
$$\nabla \times (\mathbf{V} \times \mathbf{B}) = 0, \tag{1.52}$$
$$\nabla \cdot \mathbf{B} = 0, \tag{1.53}$$
$$\nabla \times \mathbf{B} = \mu_0 \mathbf{J}, \tag{1.54}$$

where the absence of the superscript $*$ denotes equilibrium and therefore not dependence on time. In this sense, the equilibrium variables, $\mathbf{B}(\mathbf{r})$, $\mathbf{V}(\mathbf{r})$, $\mathbf{J}(\mathbf{r})$, $\varrho(\mathbf{r})$, as well as all quantities related with the pressure, are functions only of the spatial variables. In this respect, the equilibrium related pressure tensor of equation (1.51) is

$$\mathsf{P}(\mathbf{r}) = P_\perp \mathsf{I} + \frac{\sigma_d}{\mu_0}\mathbf{B}\mathbf{B}, \qquad \sigma_d(\mathbf{r}) = \frac{\mu_0[P_\parallel(\mathbf{r}) - P_\perp(\mathbf{r})]}{|\mathbf{B}|^2}. \tag{1.55}$$

In particular, the so called force-balance equation (1.51) describes the balance of the forces associated with the anisotropic pressure tensor, $\nabla \cdot \mathsf{P}$, the convective flow term, $\varrho(\mathbf{V} \cdot \nabla)\mathbf{V}$, and the magnetic one, $\mathbf{J} \times \mathbf{B}$. We recall that an important physical property of ideal MHD is the magnetic flux conservation associated with the frozen of the magnetic field lines in the fluid elements. Despite its simplicity, MHD is very accurate in examining configurations of complex geometries, with emphasis on the magnetic-field shaping which is essential for confinement.

A magnetic field line before closing to itself may either cover a surface, if such a surface exists, or fill a volume. Any surface that is traced out by a number of magnetic field lines is called magnetic surface. In plasmas of fusion devices, however, the name is usually reserved for nested toroidal surfaces. The generic structure of the magnetic field can be either "open", in the sense that it closes to itself through infinity, as for example in magnetic mirror, screw pinch and earth's magnetosphere, or closed if it remains in a spatially finite region, as for example in the central region of tokamak and stellarator. It can be proved that if the magnetic field lines lie on some closed surfaces contained in a bounded region and do not have any singularities, then they must be toroids (topological tori) [21–23].

The lines of force lying on nested toroidal magnetic surfaces encircle the magnetic axis. This encirclement is characterized by the rotational transform which is defined as the ratio of the number of poloidal transits (the short way around the toroid) to the number of toroidal transits (the long way around it) of a field line. If the rotational transform is a rational number then the magnetic field lines close upon themselves on surfaces that are called rational surfaces, leaving finite parts of them with vanishing magnetic field. If not, the surfaces are ergodic (or irrational) and the field lines cover them densely everywhere. In systems without geometrical symmetry there might exist stochastic regions in which the magnetic field lines do not lie on any surfaces but are chaotic, e.g. near a separatrix. Such regions are undesirable for MHD equilibrium and stability. If the symmetry of the field is violated, for example by superimposing a perturbation, then magnetic surfaces may no longer be uniquely defined or be defined at all [24].

The form of the Ohm-Faraday law (1.52) implies that

$$\mathbf{V} \times \mathbf{B} = \nabla\Phi(\mathbf{r}) \Rightarrow \Phi(\mathbf{r}) = \int_{\mathbf{r}_0}^{\mathbf{r}} (\mathbf{V} \times \mathbf{B}) \cdot d\mathbf{s}, \tag{1.56}$$

where the scalar function Φ is the electrostatic potential. Therefore, it follows that in the ideal MHD framework, the plasma velocity and the magnetic field share common surfaces, i.e. the

electrostatic potential is a flux label, $\Phi = \Phi(\psi)$, whenever magnetic surfaces $\psi =$ const. can be defined. Also, for static isotropic plasmas the momentum equation (1.51) reduces into the form

$$\mathbf{J} \times \mathbf{B} = \nabla P \Rightarrow \mathbf{B} \cdot \nabla P = \mathbf{J} \cdot \nabla P = 0, \tag{1.57}$$

implying that the total kinetic pressure is a flux label, or equivalently P is constant on the magnetic surfaces $\psi =$ const., i.e. $P = P(\psi)$. However, this is not the case in the presence of flow and/or pressure anisotropy, because of the respective additional terms in the force-balance equation (1.51), which can be cast into the useful form:

$$\varrho \nabla \left(\frac{V^2}{2} \right) - \varrho \mathbf{V} \times \mathbf{\Omega} = (1 - \sigma_d) \mathbf{J} \times \mathbf{B} - \nabla \mathcal{P} - \frac{\mathbf{B}}{\mu_0} (\mathbf{B} \cdot \nabla \sigma_d) + \frac{|\mathbf{B}|^2}{2\mu_0} \nabla \sigma_d, \tag{1.58}$$

where, $\mathbf{\Omega}$ is the vorticity, defined as

$$\mathbf{\Omega} = \nabla \times \mathbf{V}, \tag{1.59}$$

and $\mathcal{P}$ is the equilibrium effective pressure given by

$$\mathcal{P} = \frac{P_{\parallel} + P_{\perp}}{2}. \tag{1.60}$$

To derive equation (1.58) we employed the relations (1.55) together with the identities:

$$\nabla \cdot (f \mathbf{G} \mathbf{G}) \equiv [\nabla \cdot (f \mathbf{G})] \mathbf{G} + [(f \mathbf{G}) \cdot \nabla] \mathbf{G},$$

$$\nabla (\mathbf{F} \cdot \mathbf{G}) \equiv (\mathbf{G} \cdot \nabla) \mathbf{F} + (\mathbf{F} \cdot \nabla) \mathbf{G} + \mathbf{F} \times (\nabla \times \mathbf{G}) + \mathbf{G} \times (\nabla \times \mathbf{F}).$$

In [25] it was proved that all smooth steady MHD equilibria with field-aligned incompressible flows possess (open) magnetic surfaces, with possible exception the force-free or Beltrami equilibria. Also, in [26] it was proved the existence of (open) magnetic surfaces of three-dimensional (3D) equilibria with field-aligned flows.

A fundamental quantity that measures the efficiency of plasma confinement by the magnetic field is the plasma beta, $\bar{\beta}$. There is no unique definition of $\bar{\beta}$ in the literature and various definitions are distinguished by different geometric factors in connection with the aspect ratio and cross sectional shape of a given configuration. The plasma beta is locally defined as the ratio of the thermal pressure to the magnetic pressure, i.e. for isotropic plasmas this corresponds to $\bar{\beta} = P/(B^2/2\mu_0)$. Recall that in the presence of pressure anisotropy we represent the plasma pressure by the effective pressure, so that the plasma beta can be defined in this case as $\bar{\beta} = \mathcal{P}/(B^2/2\mu_0)$, where $\mathcal{P}(\mathbf{r})$ is the equilibrium effective isotropic pressure (1.60). Using the relations (1.55) and (1.60), the equilibrium scalar pressures parallel and perpendicular to $\mathbf{B}$ are given by

$$\begin{aligned} P_{\parallel}(\mathbf{r}) &= \mathcal{P} + \sigma_d \frac{|\mathbf{B}|^2}{2\mu_0}, \\ P_{\perp}(\mathbf{r}) &= \mathcal{P} - \sigma_d \frac{|\mathbf{B}|^2}{2\mu_0}. \end{aligned} \tag{1.61}$$

A more practically useful equilibrium figure of merit is the average beta, defined as the ratio of the average plasma energy to the average magnetic energy

$$\bar{\beta}_{av} := \frac{\bar{P}}{< B_t^2 + B_p^2 > /2\mu_0}, \tag{1.62}$$

where B_t and B_p correspond to the toroidal and poloidal components of the magnetic field, the presence of both of each is essential for toroidal confinement, and $\bar{P}(\mathbf{r})$ is the average plasma pressure, defined as

$$\bar{P} := \frac{1}{3}Tr(\mathsf{P}) = \frac{P_{\parallel} + 2P_{\perp}}{3} = \mathcal{P} - \sigma_d \frac{|\mathbf{B}|^2}{6\mu_0}. \tag{1.63}$$

In general, high values of plasma beta are desirable for fusion reactor economics and technology. However, there is a maximum allowable value of $\bar{\beta}$ set by MHD related instabilities driven by the pressure gradients.

1.4.2 Linear stability

In order to investigate the stability of a hydromagnetic system being initially in an equilibrium, one must examine the system's reaction to displacements from that equilibium. In general, if those displacements shortly burn out, such that the system returns to its initial state, then the system is said to be stable; on the other hand, if the displacements evolve in time, such that the system deviates more and more from the background equilibrium state, then it is said to be unstable. There are two main methods for studying ideal MHD stability: first, for small perturbations from the equilibrium, linear stability is examined by the normal mode analysis which can calculate the perturbation growth rate and second, the use of variational principles, involving perturbations of arbitrary amplitude and therefore covering the nonlinear regime, in connection with the sign of the perturbation potential energy. Both methods are briefly presented below.

The method of normal mode analysis examines stability as an initial value problem within a linear framework as follows. Assume that the initial equilibrium state of interest, originated in a position $\mathbf{r}$, is perturbed to a position $\mathbf{r}^*(\mathbf{r}, t)$ through the Lagrangian displacement vector $\boldsymbol{\xi}(\mathbf{r}, t)$, defined as

$$\boldsymbol{\xi} := \mathbf{r}^* - \mathbf{r}, \tag{1.64}$$

such that all physical quantities at the new position $\mathbf{r}^*$, denoted by $\mathfrak{N}^*(\mathbf{r}, t)$, are given by

$$\mathfrak{N}^* = \mathfrak{N}(\mathbf{r}) + \mathfrak{N}^{\ddagger}(\mathbf{r}, t), \tag{1.65}$$

where $\mathfrak{N}(\mathbf{r})$ correspond to the respective equilibrium physical quantity, and $\mathfrak{N}^{\ddagger}(\mathbf{r}, t)$ is the small initial perturbation, in the sense that $|\mathfrak{N}^{\ddagger}/\mathfrak{N}| \ll 1$. Upon substituting (1.65) for all physical quantities into the dynamical MHD equations (1.45)-(1.49) and by keeping only first-order terms involving the perturbations, a linearized system of the respective equations is obtained in which all quantities $\mathfrak{N}^{\ddagger}$ are then expressed in terms of $\boldsymbol{\xi}$. The resulting linearized equation of motion is of the form

$$\mathsf{L}\boldsymbol{\xi} = \hat{\mathcal{F}}[\boldsymbol{\xi}], \tag{1.66}$$

where L is a differential operator involving derivatives with respect to time, e.g. for static initial equilibrium ($\mathbf{V} = 0$) it has the form $\mathsf{L} = \varrho(\partial^2/\partial t^2)$, and $\hat{\mathcal{F}}$ is the so-called force operator, which is self-adjoint [27]. Furthermore, by adopting in connection with the linearization a time evolution for the displacement vector of the form $\boldsymbol{\xi}(\mathbf{r}, t) = \widetilde{\boldsymbol{\xi}}(\mathbf{r})e^{i\omega t}$ the problem of linear stability reduces to an eigenvalue problem which has to be solved together with appropriate boundary conditions. That is, stability is determined from the independent solutions (eigenvectors), $\widetilde{\boldsymbol{\xi}}_i(\mathbf{r})$, so-called normal modes, each of them corresponding to a respective normal frequency (eigenvalue), ω_i. It follows that if for every ω_i it holds $\omega_i^2 > 0$, then $|\boldsymbol{\xi}|$ is bounded, and the system is stable, thus oscillating around the equilibrium position. In contrast, if there exists at least one ω_i for which it holds, $\omega_i^2 < 0$, then the respective normal mode $\widetilde{\boldsymbol{\xi}}_i$ grows exponentially, and therefore the equilibrium is characterized unstable. In general, the determination of the eigenvalues of equation (1.66) is a difficult task.

The Energy Principle offers a more direct approach to the investigation of the stability of an ideal MHD equilibrium configuration, based upon a variational formulation. Such method relies on the fact that in the ideal framework the total energy of the perturbation is conserved, $E = K + W =$ constant. Here, K is the kinetic energy of the perturbation, given by

$$K = \frac{1}{2}\int \varrho \left(\frac{\partial^2 \boldsymbol{\xi}}{\partial t^2}\right) d^3\mathbf{r}, \tag{1.67}$$

and W is the perturbation's potential energy,

$$W = -\frac{1}{2}\int \boldsymbol{\xi}\cdot\hat{\mathcal{F}}[\boldsymbol{\xi}]d^3\mathbf{r}, \tag{1.68}$$

where integrations are perfomed throughout the system's volume. Suppose that W_0 is a total maximum of the potential energy, such that when the equilibrium is perturbed into a neighboring position it happens that $\delta W = W - W_0 < 0$. Owing to the energy conservation, $K + W = K_0 + W_0$, where K_0 is the initial kinetic energy originated by a small perturbation, one finds that $\delta K = K - K_0 > 0$, implying that the system has a tendency to further depart from its equilibrium state, and therefore is unstable. On the other hand, if W_0 consists of a total minimum, then $\delta K < 0$, so that the system remains localized around equilibrium position and can be characterized stable. Since K is quadratic in velocity, and therefore non-negative, stability is related to the sign of W. That is, for stability the relation $W \geq 0$ must be satisfied or equivalently

$$\int \boldsymbol{\xi}\cdot\hat{\mathcal{F}}[\boldsymbol{\xi}]d^3\mathbf{r} < 0, \tag{1.69}$$

for all possible displacements $\boldsymbol{\xi}$. When the background equilibrium is a static one, $\mathbf{V} = 0$, if there exists a displacement $\boldsymbol{\xi}$ for which the integral of equation (1.69) is positive, then the system is unstable. However, this is not the case in the presence of equilibrium flows, in which situation the above condition is only sufficient. Although the Energy Principle is not suitable in establishing the existence of an instability, since the exact form of the kinetic energy is not known, it is a powerful technique capable of answering the important question of stability of a given equilibrium, and which can in general be applied to more complex and realistic configurations.

The safety factor

A key parameter for plasma confinement in toroidal devices is the safety factor $\mathcal{Q}$, which plays an important role in determining stability and is also involved in transport theory. The safety factor is defined as the ratio of the times a magnetic field line travels around the toroidal direction (the long way around the torus) to the respective times around the poloidal direction (the short way around the torus), and is a measure of the helical twist of the field lines. An alternative expression for $\mathcal{Q}$ is obtained in terms of the magnetic fluxes when nested toroidal surfaces, i.e. $\psi =$ const., are defined. In such case the safety factor can be defined as the rate of change of the toroidal magnetic flux, ψ_t, with respect to the poloidal magnetic flux, ψ_p, as

$$\mathcal{Q} := \frac{d\psi_t(\mathbf{r})}{d\psi_p(\mathbf{r})}. \tag{1.70}$$

Note that the safety factor is usually employed in tokamak devices, while in stellarators the rotational transform, defined as the inverse of the safety factor: $\iota := 2\pi/\mathcal{Q}$, is commonly used for analogous considerations. Plasmas that rotate equal number of times along both toroidally and poloidally are susceptible to certain instabilities and, in general, higher values of $\mathcal{Q}$ are desirable for an equilibrium to be stable. In order for a tokamak equilibrium to be

stable with respect to current driven modes there exists a necessary condition known as the Kruskal-Shafranov criterion, which implies that $\mathcal{Q}$ must be higher than the unit: $\mathcal{Q} > 1$. A clarification on the Kruscal-Shafranov limit is given in [28] [see paragraph 2.4.3(b) therein].

1.5 Helical symmetry

The establishment of a specific equilibrium within the framework of ideal MHD relies on the solution of the pertinent system of equations (1.50)-(1.54) together with appropriate boundary conditions. In practice, however, this consists of a 3D and fully nonlinear problem, the solution of which is not guaranteed in the most general case, in connection of the existence of well defined toroidal magnetic surfaces. Also, although 3D codes offer an efficient tool in performing numerical equilibrium calculations, their success is often limited because of the current computers efficiency, particularly when highly complicated geometries are considered; also, from a physical point of view, there is usually no self-consistent treatment of the equilibrium problem within a totally computational framework. However, when the system under consideration is invariant under a specific group of uniparametric transformations its dimensionality can be reduced. That is the case when the geometry of a magnetic configuration possesses a continuous symmetry in which an ignorable coordinate exists, and thus the system is described as two-dimensional (2D).

The most general known kind of continuous geometrical symmetry is the concept of helical symmetry, which can be visualized as the motion along a helical (or screw) axis as a result of the combination of a rotation around a fixed axis and a simultaneous translation along this same axis. If the ratio of the values of the speeds of the respective rotational and translational motions is constant, then the resulting helical motion is called ordinary and the pertinent surfaces formed by the respective helical curves are called ordinary helical surfaces. There is a number of phenomena for the description of which helical geometry is employed. More spefically, helical geometry is used to model flows arising behind propellers and wind turbines [29, 30] and general fluid flows [31, 32], particularly, inside helically symmetric pipes [33–43], related with engineering applications of fluid mechanics. Also, blood flow inside the aorta [44, 45] and helical configurations of chain molecules of polymers, i.e. of proteins, nucleic acids etc. [46–48], are studied within such a framework. In addition, helical symmetry is widely employed in astrophysics for the modelling of the structure of astrophysical jets [49–52]. As concerns space physics, according to recent observations, the emitted plasma outflow from stellar and galactic jets is described as helically symmetric [53, 54].

In connection with magnetic confinement fusion, helical symmetry is used towards a first step understanding of the Physics of stellarators, since it can approximately describe a 'straight stellarator' configuration without toroidal curvature [55–57]. The geometry of a stellarator is inherently 3D, and such a complex geometry makes the theoretical analysis of MHD equilibria and stability complicated. Stellarator equilibrium configurations may be divided into two classes based on the magnetic axis formation: first, conventional stallarators in which the magnetic surfaces surround a central planar axis, and second, stellarators with a non-planar axis following large helical excursions from the center. The 'straight stellarator' configuration is acquired in the limit of very-large-aspect-ratio expansion of a non-planar axis stellarator, which is well approximated as helical invariant. Therefore, helical symmetry corresponds to 2D configurations with constant torsion and without toroidicity. The free-boundary equilibrium problem for such systems was studied in a number of papers, e.g. [58–60].

For both analytical and numerical computations of equilibrium, stability and transport of toroidal plasmas, the use of appropriate curvilinear coordinates is important. The basic elements of such general systems of coordinates are presented in Appendix A. For the description of a helical system we introduce the non-orthogonal system of helical coordinates $\mathbf{r} = (r, u, \zeta)$,

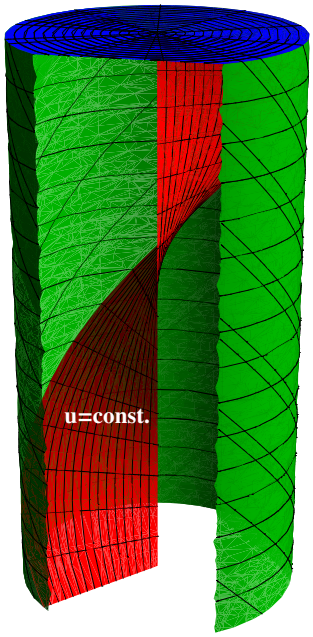

Figure 1.2: The coordinate surfaces of the helical system (r, u, ζ) defined in (1.71). The blue and green-colored surfaces ζ = constant and r = constant respectively, are the same with the usual cylindrical surfaces. The red colored surface u = constant is a helicoid, at every point of which there is a helix lying on the helicoid which passes through that point.

given in terms of the usual cylindrical coordinates (ρ, ϕ, z), as

$$\begin{aligned} r &= \rho, \\ u &= m\phi - kz, \\ \zeta &= z, \end{aligned} \tag{1.71}$$

where m, k are real constants, and u can be interpreted as a 'helical angle'. It may be seen that these coordinates are not well defined on the z-axis (since neither the cylindrical coordinates are well defined therein). However, helical coordinates are convenient since in this system a helix is a straight line parallel to the ζ-axis, simply defined by the parametric equations: r = constant, u = constant. Therefore, a helical scalar function is a function which has invariance along a helix, or equivalently: *a scalar function* $f : \mathbb{R}^3 \to \mathbb{R}$ *is helically symmetric if and only if it is independent of* ζ*:* $\partial f/\partial\zeta = 0 \Rightarrow f = f(r, u)$. In this respect, a vector field is helically symmetric if and only if all its components in basis of the helical coordinates defined in Appendix B.1 are helically symmetric scalar functions [61]. The characteristic coordinate surfaces of the helical system are illustrated in figure 1.2. We note that each helix described by the equations ($r = r_0 =$ const., $u = u_0 =$ const.) has a pitch length $\eta_0 = 2\pi(|m/k|)$, and a constant torsion, $\tau_0 = km/(k^2 r_0^2 + m^2)$. Certain details are given in Appendix B.2. The effect of the torsion on helical pipe flows were studied in a series of papers [62–66].

At this point we define the vector

$$\mathbf{h} := mq\mathbf{g}_\zeta = q(rk\hat{\boldsymbol{\phi}} + m\hat{\mathbf{z}}), \tag{1.72}$$

where $\mathbf{g}_\zeta$ is the ζ-covariant basis vector, and

$$q := (k^2 r^2 + m^2)^{-1}. \tag{1.73}$$

It follows that the helical vector $\mathbf{h}$ is tangent to the helix ($r =$ const., $u =$ const.) and points along the direction resulting from a rotation around the z axis and a parallel translation along

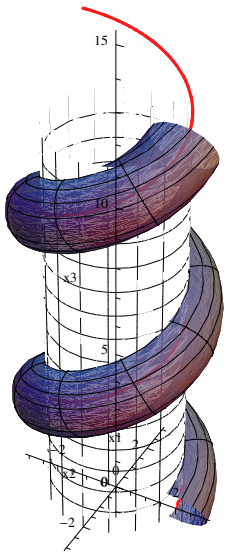

Figure 1.3: A helically symmetric tube composed of nested helicoidal surfaces of arbitrary cross-sectional shape. The innermost of these surfaces degenerates to a helical magnetic axis (red colored helix). The shape of the cross-section remains invariant along the helical direction.

the same axis. Also, the helical vector satisfies the relations

$$\nabla \cdot \mathbf{h} = 0, \tag{1.74}$$

$$\nabla \times \mathbf{h} = 2kmq\mathbf{h}, \tag{1.75}$$

$$\mathbf{h} \cdot \nabla f = 0 \qquad \forall f = f(r, u), \tag{1.76}$$

which imply that $\mathbf{h}$ is a divergent-free, Beltrami vector.

Helical symmetry consists of the most general case of continuous geometric symmetry and includes axisymmetry, which describes an ideal tokamak, and translational symmetry, in which the system is unbounded along the symmetry direction, as limiting cases. We note that the latter category can represent a 'straight tokamak' when the magnetic field is periodic along the direction of symmetry and therefore can be considered as a toroidal field, since a single period of such a field is topologically equivalent to a torus. In specific, in the limit $(k = -1, m = 0)$ it follows that the condition of axisymmetry is recoved, i.e. $\partial f/\partial\phi = 0\,\forall f(r, z)$, since in this case $u \to z$ and $\mathbf{h} \to -\nabla\phi$, while in the limit $(k = 0, m = 1)$ we obtain, $u \to \phi$ and $\mathbf{h} \to \hat{\boldsymbol{z}}$, and hence the system is translationally symmetric, i.e. $\partial f/\partial z = 0\,\forall f(r, \phi)$. For this reason, although a helix can be characterized by just one parameter, for instance k/m, it is convenient to keep both m and k in order to discuss these limiting cases.

Hamiltonian theory assures the existence of magnetic surfaces in all three kinds of continuous geometrical symmetry [67], namely: helical symmetry, axisymmetry, and translational symmetry. For such systems the magnetic surfaces are nested and well defined by the level sets of a function $\psi(x^1, x^2)$, with the third spatial coordinate, x^3, being ignorable because of the symmetry condition. Such a nested helical surface of circular cross-sectional shape is shown in Figure 1.3. In general, however, the shape of the tube's cross-section is arbitrary, and remains invariant along the helical direction. The innermost of these nested surfaces degenerates to single curve defining the configuration's magnetic axis, which in the helically symmetric case is a helix, e.g. $(r = r_a, u = u_a)$ cf Appendix B.2. Recall that two important directions are defined in closed toroidal systems; these are the toroidal direction (the long way round the torus), and the poloidal direction (the short way around). For example, in axisymmetric

systems, a toroidal field is the one pointing in the symmetry direction, $\hat{\phi}$, while a poloidal field is the one that lies on the plane (r, z). In this respect, for the helical configurations of interest we shall refer to a helicoidal field as a field pointing along the direction of symmetry, $\mathbf{h}$, and to a poloidal field as that lying on the plane transverse to this direction. To this end, the cross-section of a helicoidal surface shall be refered as poloidal cross-section.

1.6 Thesis objectives and outline

Understanding the equilibrium properties of magnetically confined plasmas in one of the most important tasks of fusion research, since such steady states can be starting points of stability and transport studies. Within the framework of ideal MHD the equilibrium states of general 2D plasmas are governed by a pertinent equilibrium equation for the poloidal flux function, obtained from the reduction of the 3D and fully non linear MHD equations, owing to the existing continuous geometrical symmetry. In specific, the MHD steady states of static axisymmetric plasmas are governed by the well known Grad-Shafranov (GS) equation [68, 69]. The most widely employed analytic solutions of this equation are the Solovev solution [70] and the Hernegger-Maschke solution [71, 72], the former corresponding to toroidal current density non vanishing on the plasma boundary and the latter to toroidal current density vanishing thereon. Also, exact global solutions of the Grad-Shafranov equation were obtained in [73, 74] which model static, axisymmetric astrophysical jets and solar prominences. In addition, the ideal steady states of static helically symmetric plasmas are governed by a respective GS-type equation, also called helical GS equation or Johnson-Frieman-Kulsrud-Oberman (JFKO) equation [75]. Different families of closed form analytic solutions of the JFKO equation were obtained in [51, 52, 76–79]. Both the GS and the JFKO equations contain two scalar functions associated with the pressure and the toroidal/helicoidal current, and which functions in the static case, i.e when the convective flow terms is neglected in equation (1.51), depend only on the poloidal flux and therefore are flux labels. However, this is not the case in the presence of equilibrium flows.

In the last thirty years there has been an increasing interest in equilibria with mass flows which are created in plasmas of various fusion devices mainly as a result of auxiliary heating. More specifically, mass flows can be driven externally with either electromagnetic waves or neutral beam injection for plasma heating and current drive, or can be created spontaneously (zonal flows). For example, plasma flows as a result of heating with neutral beams have been observed in stellarators [80]. These flows are usually associated with radial electric fields which play a significant role in the transitions to improved confinement regimes such as the L-H transition [81] and the formation of internal transport barriers [82–85]. An additional effect of external heating, depending on the direction of the injected momentum, is pressure anisotropy. For tokamaks and stellarators the MHD pressure is usually considered isotropic. However, plasma heating by the neutral beam injection, ion resonance waves and electron cyclotron waves can produce strong plasma anisotropy [86–90]. Thus, pressure anisotropy is present in strongly magnetized plasmas and may play a role in some astrophysical ones [91–100] as well as in several magnetic fusion related problems [101–113].

In a series of papers (e.g. [51, 85, 105, 114–138]) ideal MHD equilibria both static with pressure anisotropy and with mass flow, either isotropic or anisotropic, were investigated under various symmetries. In connection with the present thesis, we particularly mention [114] on axisymmetric equilibria with incompressible flow and pressure anisotropy and [115] regarding helically symmetric equilibria with incompressible flow and isotropic pressure. In the presence of mass flow the equilibrium satisfies a generalized Grad-Shafranov (GGS) equation together with a Bernoulli equation involving the pressure (see for example [117, 139, 140]). For compressible flow the GGS equation can be either elliptic or hyperbolic, depending on the value of a Mach

function associated with the poloidal velocity, and is coupled with the Bernoulli equation through the density which is not uniform on magnetic surfaces. Note that the toroidal velocity is inherently incompressible because of the existing continuous geometrical symmetry. For incompressible flow the density becomes a surface quantity and the GGS equation becomes elliptic and decouples from the Bernoulli equation; consequently one has to solve an easier and well posed elliptic boundary value problem. In particular for fixed boundaries, convergence to the solution is guaranteed under mild requirements of monotonicity fot the free functions involved in the GGS equation [141]. In contrast to the static isotropic GS equation, in the presence of flow and/or anisotropic pressure the free functions involved in the GGS equation are more than two. For plasmas with anisotropic pressure the equilibrium equations involve the function σ_d associated with this anisotropy [equation (1.55)], such that in this situation the pertinent GGS and Bernoulli equations are coupled through the anisotropy function (together with the density for stationary anisotropic equilibria). Therefore, to get a closed set of reduced equilibrium equations an assumption on the functional dependence of this function is required (cf. [102, 106, 124, 125, 129, 142, 143] for static equilibria and [103–105, 107, 114, 116, 128, 130, 133] for stationary ones).

In [115] a GGS equation governing helically symmetric equilibria with incompressible flow, generalizing the static JFKO equation, was derived. Furthermore, in [114] a GGS equation governing axisymmetric plasma equilibria with incompressible flow and anisotropic pressure, under the assumption that the anisotropy function is constant on the magnetic surfaces, was derived. The latter equation reduces to the original GS equation [68, 69] in the absence of anisotropy and mass flow. Both of the above equations were obtained upon the reduction of the 3D MHD equations in a self-consistent way.

The main motivation of the present work was the extension of the results of [114] to the more generic case of helical symmetry, or alternatively the exention of the results of [115] to the case of anisotropic pressure. In other words, it was the derivation of a GGS equation which would govern the equilibrium states of stationary, anisotropic plasmas, with potential generalization of the respective GS or GS-type ones governing all kinds of geometrically symmetric equilibria, either static, and/or with flow and pressure anisotropy or not. Since as already mentioned in nowadays and future experiments in toroidal devices the external momentum sources employed for heating and current drive usually induce both plasma flow and pressure anisotropy, understanding their combined effects is of practical importance. To this end, once a pertinent helically symmetric equilibrium is constructed in connection with a 'straight stellarator', then one can examine the impact of anisotropy on its characteristics and compare with that of the flow.

Another important motive of the thesis is the investigation of the stability properties of such kind of equilibria, particularly in the presence of anisotropic pressure.

The well known Energy Principle [27] is a powerful tool for deriving necessary and sufficient conditions for the linear stability of static MHD equilibria, e.g. for such a stability criterion for symmetric equilibria see [144]. In the presence of flow, however, the problem of stability becomes much tougher because of the anti-Hermitian convective flow term in the momentum equation. As a result, only sufficient conditions for the linear stability of stationary equilibria were previously obtained [145–149]. Particularly, in connection with the present study, the derivation of a sufficient condition for the linear stability of ideal MHD equilibria and plasmas of constant density, isotropic pressure and incompressible flow parallel to the magnetic field, was initiated in [147, 148] and completed in [149]. A key element to obtain this condition is that the pressure perturbation remains arbitrary, that is, there is no need to express that perturbation in terms of the Lagrangian displacement vector. Also, pressure anisotropy is usually responsible for various instabilities, such as the fire-hose and the mirror instability [150–155]. Therefore, investigation of the stability properties of anisotropic plasmas, either static or stationary, is

also a significant objective. Thus, a further incentive was the potential generalization of the sufficient stability condition derived in [149] for the case of anisotropic pressure and its application to the constructed helically symmetric equilibria in order to investigate their stability properties as well as the impact of the flow and pressure anisotropy on them.

Before proceeding to the outline of this thesis, we note in passing that equilibrium solvers have also been developed to model helically symmetric systems [156,157] as well as 3D configurations in connection with stellarators [112,158–162]. In these studies equilibrium construction is based, among others, on the widely applied 3D MHD, free boundary codes VMEC [163] for isotropic pressure and its extension ANIMEC for anisotropic pressure [164]. These codes use a variational principle to minimize the plasma energy functional. In the presence of pressure anisotropy this functional consists of the magnetic energy and the parallel pressure energy. The parallel pressure consists of a thermal-particle part and a hot-particle contribution calculated by means of a bi-Mawxellian distribution function. The perpendicular pressure is not determined as a moment of the distribution function but by employing the MHD force-balance parallel to the equilibrium magnetic field; in this respect the code is based on a hybrid (kinetic-MHD) model. In this respect, it should be understood that although 3D equilibrium codes provide a more realistic description, they may lack self-consistency.

The derivations and main results of this thesis are presented in four leading chapters, namely

- Helically Symmetric Equilibria: Generalized Grad-Shafranov Equation (Chapter 2).
- An Analytic Class of Helically Symmetric Equilibria (Chapter 3).
- Symmetry Transformations for Ideal MHD and CGL Equilibria (Chapter 4).
- Stability of Anisotropic Incompressible Equilibria (Chapter 5).

In more detail, in Chapter 2 a GGS equation with pressure anisotropy and non-parallel flow governing helically symmetric equilibria is derived by employing helical coordinates described in Section 1.5. This equation involves six arbitrary surface quantities and recovers known equations as particular cases. Together we obtain a Bernoulli equation for the effective isotropic pressure. For the derivation we assume that the function of pressure anisotropy is uniform on the magnetic surfaces. Also, under the assumption of well defined 3D toroidal magnetic surfaces we examine the properties of special ideal MHD equilibria with incompressible flow and pressure anisotropy, such that any two of the velocity, magnetic field, current density and vorticity vectors are parallel one another, including the cases of magnetic-field aligned flows, force-free, in the sense that the magnetic force vanishes, Beltrami, and complex-lamellar equilibria. In each of these cases we employ specific forms of the GSS equation governing respective helically symmetric equilibria. In Chapter 3 adopting the most generic linearizing ansatz for the free functions involved in the derived GGS equation we obtain a new class of exact analytical solutions describing a '2D straight stellarator'. Moreover, on the basis of the constructed solutions we examine the impact of flow and pressure anisotropy on the equilibrium characteristics. Parts of the results presented in Chapters 2 and 3 were published in [165,166]. Also, the results presented in Section 2.2 consist of a generalization of that published in [167]. Chapter 4 deals with the important sets of equilibrium transformations, known as Bogoyavlenskij transformations, previously introduced in the literature, and which are proven very useful in constructing new families of MHD equilibria. Specifically, we introduce a set of transformations that can be applied to any known anisotropic CGL equilibria with field-aligned incompressible flows (or static equilibria) and anisotropy function constant on magnetic field lines, and produce an infinite family of anisotropic equilibria with collinear velocity and magnetic fields, but density and anisotropy functions that may remain arbitrary; these transformations

consist of a generalization of the respective Bogoyavlenskij transformations concerning field-aligned MHD equilibria with isotropic pressure. In addition, we prove that all these sets of transformations can break the geometrical symmetries of a known given equilibrium, static or with field-aligned flow, if and only if its magnetic field is purely poloidal. Then we construct 3D equilibria by applying the introduced transformations to a known class of axisymmetric equilibria. The results presented in Chapter 4 were published in [168]. In Chapter 5 we derive a sufficient condition for the linear stability of plasma equilibria with incompressible flow parallel to the magnetic field, constant mass density and pressure anisotropy, such that the pertinent anisotropy function remains constant. This condition is applicable to any steady state without geometrical restriction and generalizes the respective condition for MHD equilibria with isotropic pressure and constant density previously derived in [149]. On the basis of this condition we prove that if a given equilibrium is linearly stable, then the ones resulting from the application of Bogoyavlenskij symmetry transformations are linearly stable too, provided that a parameter involved in those transformations is positive. In addition, we examine the impact of pressure anisotropy, flow, and torsion of a helical magnetic axis, for a specific class of analytic equilibria. The results presented in Chapter 5 were published in [169]. Finally, in Chapter 6 the main results of the aforementioned chapters are summarized and the overall conclusions are presented. Also, potential projects for future research are briefly outlined.

2 | Helically Symmetric Equilibria: Generalized Grad-Shafranov Equation

"*In order to understand the phenomena in a certain plasma region, it is necessary to map not only the magnetic but also the electric field and the electric currents. Space is filled with a network of currents which transfer energy and momentum over large or very large distances. The currents often pinch to filamentary or surface currents. The latter are likely to give space, as also interstellar and intergalactic space, a cellular structure.*"

Hannes Alfvén

2.1 Derivation of generalized Grad-Shafranov equation in the presence of pressure anisotropy and plasma flow

The ideal MHD states of plasma flows and anisotropic pressure are governed by the set of equations (1.50)-(1.54) and (1.55) presented in Section 1.4. From the reduction of these equations we obtain a GGS equation under the condition of helical symmetry, by using helical coordinates presented in Section 1.5. The derivation of the GGS equation has been organized as follows: first, we express the divergence-free fields, the magnetic field, the current density and the mass flow in terms of helical scalar functions. Second, we identify some integrals of the system in the form of surface quantities, and third, by using these integrals we derive a GGS equation together with a Bernoulli equation for the effective pressure, under specific assumptions for the density and the anisotropy function. This derivation procedure is presented below in detail.

2.1.1 Divergence-free fields

Owing to equations (1.50), (1.53) and to the equilibrium counterpart of equation (1.17), $\nabla \cdot \mathbf{J} = 0$, it is obvious that each of the magnetic field, $\mathbf{B}$, the momentum density field, $\varrho\mathbf{V}$, and the current density, $\mathbf{J}$, can be expressed as the 'vorticity' of a pertinent vector field, or in other words, each of $\mathbf{B}$, $\varrho\mathbf{V}$, $\mathbf{J}$, can be expressed as the curl of a respective vector field. In specific, as concerns the magnetic field, with respect to equation (1.53) it can be expressed in terms of a magnetic vector potential, denoted by $\mathbf{A}$, as

$$\mathbf{B} = \nabla \times \mathbf{A}. \tag{2.1}$$

Under the assumption of helical symmetry, the above equation yields

$$\mathbf{B} = \frac{m}{r}\left[\frac{\partial A_\zeta}{\partial u}\mathbf{g}_r - \frac{\partial A_\zeta}{\partial r}\mathbf{g}_u + \left(\frac{\partial A_u}{\partial r} - \frac{\partial A_r}{\partial u}\right)\mathbf{g}_\zeta\right], \tag{2.2}$$

where A_i, $i = (r, u, \zeta)$, are the covariant components of the magnetic potential and which are helical scalar functions. Furthermore, by expanding $\mathbf{B}$ in the covariant base, as

$$\mathbf{B} = B^r\mathbf{g}_r + B^u\mathbf{g}_u + B^\zeta\mathbf{g}_\zeta, \tag{2.3}$$

and substituting this form into equation (1.53) we obtain

$$\frac{1}{r}\frac{\partial}{\partial r}(rB^r) + \frac{\partial B^u}{\partial u} = 0. \tag{2.4}$$

At this point it is useful to introduce the stream function ψ, defined through the ζ-covariant component of the magnetic potential as

$$\psi(r, u) := -mA_\zeta(r, u). \tag{2.5}$$

On account of the definition (2.5), by comparing equations (2.2) and (2.3) it readily follows that

$$B^r = -\frac{1}{r}\frac{\partial\psi}{\partial u}, \qquad B^u = \frac{1}{r}\frac{\partial\psi}{\partial r}, \tag{2.6}$$

under which equation (2.4) is trivially satisfied. Then, on account of the equations (2.6) the magnetic field in equation (2.3) can be re-written in the form

$$\mathbf{B} = B^\zeta\mathbf{g}_\zeta + \mathbf{B}_p, \tag{2.7}$$

where $\mathbf{B}_p$ is the poloidal magnetic field defined as

$$\mathbf{B}_p := m^{-1}\mathbf{g}^\zeta \times \nabla\psi. \tag{2.8}$$

Therefore, the stream function ψ is related to the poloidal magnetic field through the poloidal magnetic field components (B^r, B^u). However, the expression (2.7) for the magnetic field involves both the covariant and the contravariant basis vectors $\mathbf{g}_\zeta$ anb $\mathbf{g}^\zeta$. This in fact dictated us to make use of the helical vector $\mathbf{h}$, which also points along the symmetry direction $\mathbf{g}_\zeta$ (see equation (1.72)), and show that the field on the plane normal to $\mathbf{h}$ is related to the poloidal magnetic field as

$$\mathbf{h} \times \nabla\psi = \mathbf{B}_p - kqr\frac{\partial\psi}{\partial r}\mathbf{g}_\zeta. \tag{2.9}$$

As a result, by the substitution of equation (2.9) into (2.7) we obtain the following compact expression for $\mathbf{B}$ in terms of helical scalar functions

$$\mathbf{B} = I\mathbf{h} + \mathbf{h} \times \nabla\psi, \tag{2.10}$$

where $I(r, u)$ relates to the helicoidal magnetic field and is defined as

$$I := \frac{B^\zeta}{mq} + \frac{kr}{m}\frac{\partial\psi}{\partial r} = \frac{\mathbf{B}\cdot\mathbf{h}}{q}. \tag{2.11}$$

Note that from equation (2.10) it also follows that

$$\nabla\psi = \frac{\mathbf{B}\times\mathbf{h}}{q}. \tag{2.12}$$

Along the same lines, on the basis of the continuity equation (1.50) the momentum density field is expressed in terms of helical scalar functions as

$$\varrho\mathbf{V} = \Theta\mathbf{h} + \mathbf{h}\times\nabla F, \tag{2.13}$$

where the function $\Theta(r,u)$ is defined as

$$\Theta := \frac{\varrho V^{\zeta}}{mq} + \frac{kr}{m}\frac{\partial F}{\partial r} = \frac{\varrho\mathbf{V}\cdot\mathbf{h}}{q}, \tag{2.14}$$

while $F(r,u)$ is a stream function for the field $\varrho\mathbf{V}$, in analogy with ψ, for which it holds

$$\nabla F = \frac{\varrho\mathbf{V}\times\mathbf{h}}{q}. \tag{2.15}$$

In addition, upon the substitution of equation (2.10) into the Ampere law (1.54) we derive in a straightforward way the following expression for the current density, involving the scalar functions ψ and I

$$\mathbf{J} = \frac{1}{\mu_0}(\mathcal{L}\psi + 2kmqI)\mathbf{h} - \frac{1}{\mu_0}\mathbf{h}\times\nabla I, \tag{2.16}$$

where the operator $\mathcal{L}$ is defined as

$$\mathcal{L} := \frac{1}{q}\vec{\nabla}\cdot(q\vec{\nabla}) = \frac{1}{r}\frac{\partial}{\partial r}\left(r\frac{\partial}{\partial r}\right) + \frac{1}{qr^2}\frac{\partial^2}{\partial u^2} - 2k^2rq\frac{\partial}{\partial r}. \tag{2.17}$$

That is, we have expressed the divergence-free helical fields, $\mathbf{B}$, $\varrho\mathbf{V}$, and $\mathbf{J}$, in terms of the helical scalar functions ψ, I, Θ, and F, as indicated by equations (2.10), (2.13) and (2.16). We have to note that the force balance equation (1.58) involves another divergence-free field, and that is the vorticity, $\boldsymbol{\Omega} = \nabla\times\mathbf{V}$, having the following form in helical geometry

$$\boldsymbol{\Omega} = \left[\frac{F'}{\varrho}\mathcal{L}\psi + \left(\frac{F'}{\varrho}\right)'|\nabla\psi|^2 + \frac{2kmq\Theta}{\varrho}\right]\mathbf{h} - \mathbf{h}\times\nabla\left(\frac{\Theta}{\varrho}\right), \tag{2.18}$$

where the prime implies differentiation with respect to ψ, $' := d/d\psi$. However, the use of this vector is not necessary in deriving the GGS equilibrium equation.

Physical interpretation of ψ and I

Owing to the helical symmetry and on account of the relations (1.74)-(1.76) the following important equation arises from (2.10):

$$\mathbf{B}\cdot\nabla\psi = 0, \tag{2.19}$$

which indicates that the magnetic field lies on well defined nested helicoidal surfaces, $\psi(r,u) =$ const., henceforth called magnetic surfaces. Note that a representation for the magnetic field (and as a result for all the divergence-free fields) as that in equation (2.10) is possible in all kinds of continuous geometrical symmetry, including axisymmetry and translational symmetry, which consist of reductions of the general case of helical symmetry employed here. For example, under invariance with respect to the cylindrical coordinate ϕ, the axisymmetric magnetic field is usually expressed in terms of the scalar functions $\psi_{ax}(\rho,z) = -\rho A_{\phi}(\rho,z)$ and $I_{ax}(\rho,z) = \rho B_{\phi}(\rho,z)$, as

$$\mathbf{B}_{ax} = \frac{1}{\rho}\left(I_{ax}\hat{\mathbf{e}}_{\phi} + \hat{\mathbf{e}}_{\phi}\times\nabla\psi_{ax}\right), \tag{2.20}$$

where B_ϕ and A_ϕ denote the toroidal components of the axisymmetric magnetic field and magnetic potential with respect to cylindrical coordinates. In addition, under the condition of translational symmetry, the magnetic field is usually expressed in the form

$$\mathbf{B}_{tr} = B_z(\rho,\phi)\hat{\mathbf{e}}_z + \hat{\mathbf{e}}_z \times \nabla\psi_{tr}(\rho,\phi), \tag{2.21}$$

where $\psi_{tr}(\rho,\phi) = -A_z(\rho,\phi)$, $B_z(\rho,\phi)$, are respective translationally symmetric functions. It can be shown from equation (2.20) that in axisymmetric equilibria the magnetic field lies on nested toroidal surfaces $\psi_{ax}(\rho,z) = \text{const.}$ $(\mathbf{B}_{ax}\cdot\nabla\psi_{ax} = 0)$, and that the function ψ_{ax} relates to the poloidal magnetic flux, $\psi_{p_{ax}}$, through a disk lying on the plane $z = \text{const.}$, as $\psi_{p_{ax}} = -2\pi\psi_{ax}$. Respectively, in the case of translationally symmetric equilibria, there exist well defned nested cylindrical surfaces $\psi_{tr}(\rho,\phi) = \text{const.}$ in which the magnetic field lie on $(\mathbf{B}_{tr}\cdot\nabla\psi_{tr} = 0)$, the function ψ_{tr} in this situation being related to the poloidal magnetic flux $\psi_{p_{tr}}$ passing through a section $\phi = \text{const.}$ of a cylindrical surface of height L, as $\psi_{p_{tr}} = L\psi_{tr}$.

Considering equations (B.11), (B.14) and (B.24) it follows that the ζ-covariant helical component of the magnetic potential is expressed through its respective components in the cylindrical base as $A_\zeta = (rk/m)A_\phi + A_z$, and as a result equation (2.5) yields

$$\psi(r,u) = k\psi_{ax} + m\psi_{tr}. \tag{2.22}$$

Therefore, the helical stream function ψ is decomposed into two parts each of them recovering the respective axisymmetric and translationally symmetric stream functions as limiting cases. Recall that the stream function ψ is related with the poloidal magnetic field as indicated by equation (2.8). In order to calculate the poloidal magnetic flux consider the coordinate transformation $(r,u,\zeta) \to (\psi(r,u),u,\zeta)$ with Jacobian, $\mathcal{J} = (r/m)/(\partial\psi/\partial r)$. Then the magnetic flux through a helical surface of height $L = N\eta$, $\eta = (2\pi m)/k$ being the pitch and N is an integer, and of surface area $d\mathbf{s} = \mathcal{J}d\psi d\zeta\mathbf{g}^u$, is calculated:

$$\psi_p = \int \mathbf{B}_p\cdot d\mathbf{s} = \frac{1}{m}\int_0^\psi d\psi\int_0^L d\zeta \Rightarrow \psi_p = \frac{2\pi N}{k}\psi. \tag{2.23}$$

Thus, the helical function ψ is indeed the poloidal flux per radian, and which reduces to the respective axisymmetric and translationally symmetric poloidal fluxes, owing to the decomposition

$$\psi_p = -N\psi_{p_{ax}} + \psi_{p_{tr}}. \tag{2.24}$$

In addition, from equation (2.16) it readily follows that

$$\mathbf{J}\cdot\nabla I = 0, \tag{2.25}$$

and therefore the current density lies on nested helical surfaces $I = \text{const.}$, which need no coincide with the magnetic surfaces. Note that, additional kinds of pressure surfaces, on which $\mathcal{P}$, $P_\parallel$, $P_\perp$ take constant values, can be defined; although for static isotropic equilibria these sets of surfaces are identical (e.g. see equation (1.57)), in the presence of flow and anisotropic pressure, in general, they do not coincide. In an analogous way, it can be shown that the function I, which is related to the magnetic field component in the direction of symmetry, can be decomposed into the respective functions employed in the limiting cases of axisymmetric and translationally symmetric equilibria, $I_{ax}(\rho,z) = \rho B_\phi$ and $I_{tr}(\rho,\phi) = B_z$, as

$$I = kI_{ax} + mI_{tr}, \tag{2.26}$$

and its physical interpretation is indeed the net poloidal current per radian

$$I_p = \int \mathbf{J}_p\cdot d\mathbf{s} = -\frac{2\pi NI}{k\mu_0}, \tag{2.27}$$

which can be further decomposed as $I_p = -NI_{p_{ax}} + I_{p_{tr}}$; here the specific relations for the axisymmetric and translationally symmetric poloidal currents are given by $I_{p_{ax}} = (2\pi I_{ax})/\mu_0$ and $I_{p_{tr}} = -(LB_z)/\mu_0$. Finally, as concerns the function F, it turns out that it is related to the poloidal flux of the momentum density field.

2.1.2 Integrals of the system

Equations (1.50)-(1.54) can be reduced by the means of certain integrals of the system, which are shown to be surface quantities. These integrals are obtained by the projection of the Ohm's law in the directions $\mathbf{h}$, $\mathbf{B}$, $\nabla\psi$, and of the momentum equation along $\mathbf{h}$, using the relations (2.10), (2.13) and (2.16). In particular, expressing the time independent electric field in terms of the electrostatic potential, $\mathbf{E} = -\nabla\Phi$, with Φ being a helical scalar function, and projecting the Ohm's law, in the form (1.56), along the helical direction, $\mathbf{h}$, yields

$$\mathbf{h}\cdot(\nabla\psi\times\nabla F) = 0 \Rightarrow F = F(\psi), \tag{2.28}$$

implying that the function F is a surface quantity. This is reasonable since in the absence of resistivity $\mathbf{V}$ and $\mathbf{B}$ share common surfaces; therefore, the velocity field lies on the magnetic surfaces $\psi = \text{const.}$. Furthermore, projection of the Ohm's law along the direction of the magnetic field implies that the electrostatic potential is also a surface quantity

$$\mathbf{B}\cdot\nabla\Phi = 0 \Rightarrow \Phi = \Phi(\psi). \tag{2.29}$$

An additional integral is found from the component of the Ohm's law perpendicular to a magnetic surface; i.e. the derivative of the electrostatic potential with respect to ψ is a surface quantity

$$\Phi' = \frac{q}{\varrho}(IF' - \Theta). \tag{2.30}$$

In addition, by substituting the above equation into (2.13) leads to the following useful relation for the velocity

$$\mathbf{V} = \frac{M_p}{\sqrt{\mu_0\varrho}}\mathbf{B} - \frac{\Phi'}{q}\mathbf{h}, \tag{2.31}$$

where $M_p(\mathbf{r})$ denotes the poloidal Mach function, defined as

$$M_p := \frac{|\mathbf{V}_p|}{V_{A_p}} = \sqrt{\frac{\mu_0(F')^2}{\varrho}}, \tag{2.32}$$

with $V_{A_p} = |\mathbf{B}_p|/(\sqrt{\mu_0\varrho})$ being the Alfvén velocity associated with the poloidal magnetic field. Equation (2.31) implies that $\mathbf{V}$ is decomposed into a component parallel to $\mathbf{B}$ and a non-parallel one associated with the electric field in consistence with the Ohm's law. Therefore, in the absence of the electric field, $\Phi' = 0$, the velocity is aligned with the magnetic field, $\mathbf{V} \parallel \mathbf{B}$ (field-aligned flows).

To identify another integral of the system, we project the momentum equation, in the form (1.58), along the direction of $\mathbf{h}$; this yields the following surface quantity

$$X(\psi) := (1 - \sigma_d - M_p^2)I + \frac{\mu_0\Phi' F'}{q}. \tag{2.33}$$

From equation (2.33) it follows that, in general, in the presence of mass flow and anisotropic pressure I is not a surface quantity, since it holds

$$I(\psi, r) = \frac{X - \frac{\mu_0\Phi' F'}{q}}{1 - \sigma_d - M_p^2}. \tag{2.34}$$

The condition that for static, isotropic equilibria the current surfaces coincide with the magnetic surfaces is recovered from (2.34), since for $\Theta = F = M_p = \sigma_d = 0$ it reduces to $I = X(\psi)$. Furthermore, by combining equations (2.30) and (2.33) the following expression for the function Θ arises

$$\Theta(\psi, r) = \frac{XF' - \frac{(1-\sigma_d)\varrho\Phi'}{q}}{1 - \sigma_d - M_p^2}. \tag{2.35}$$

We note that from equations (2.33) and (2.35) it follows that helically symmetric equilibria with purely poloidal flow, non-parallel to the magnetic field ($\Theta = 0, F' \neq 0, \Phi' \neq 0$) cannot exist because of the following contradiction: from equation (2.35) it follows that $X = \frac{(1-\sigma_d)\varrho\Phi'}{q(r)F'}$, implying that X has an explicit dependence on r, while it has been shown earlier in equation (2.33) that X is a surface quantity.

2.1.3 GGS-Bernoulli system

In order to obtain a reduced set of equilibrium equations we project the momentum equation (1.58) along the direction of the magnetic field as well as along $\nabla\psi$. In particular, the component of (1.58) along $\mathbf{B}$ yields the following equation:

$$\mathbf{B} \cdot \left[\nabla \left(\frac{V^2}{2} + \frac{\Theta\Phi'}{\varrho} \right) + \frac{\nabla \mathcal{P}}{\varrho} + \frac{B^2}{2\mu_0} \frac{\nabla \sigma_d}{\varrho} \right] = 0, \tag{2.36}$$

which may be interpreted as a Bernoulli equation for $\mathcal{P}$. Before proceeding to the next step, we first put the terms $-\varrho\mathbf{V} \times \mathbf{\Omega}$ and $\mathbf{J} \times \mathbf{B}$, involved in equation (1.58), in a more useful form. On account of equations (2.10), (2.13) and (2.16), these terms are calculated as

$$\begin{aligned} -\varrho\mathbf{V} \times \mathbf{\Omega} &= \left[-\nabla \cdot \left(\frac{q(F')^2}{\varrho} \nabla\psi \right) + \frac{qF'F''}{\varrho} |\nabla\psi|^2 - 2kmq^2 \frac{\Theta F'}{\varrho} \right] \nabla\psi \\ &+ \left[(\mathbf{h} \times \nabla\psi) \cdot \nabla \left(\frac{\Theta F'}{\varrho} \right) \right] \mathbf{h} - \frac{1}{2} q\varrho \nabla \left(\frac{\Theta}{\varrho} \right)^2, \\ \mathbf{J} \times \mathbf{B} &= -\frac{q}{\mu_0} \left(\mathcal{L}\psi + 2kmqI \right) \nabla\psi - \nabla\psi \cdot (\mathbf{h} \times \nabla I)\mathbf{h} - \frac{q}{2\mu_0} \nabla I^2. \end{aligned} \tag{2.37}$$

Subsequently, projection of the momentum conservation equation (1.58) perpendicular to the magnetic surfaces, together with the use of the relations (2.37), yields the following GGS equilibrium equation

$$\begin{aligned} &\left\{ \nabla \cdot \left[(1 - \sigma_d - M_p^2) q \nabla\psi \right] + q \left[\mu_0 \frac{F'F''}{\varrho} |\nabla\psi|^2 + \nabla\psi \cdot \nabla\sigma_d \right] + 2kmq^2 X \right\} |\nabla\psi|^2 \\ &+ \mu_0 \left\{ \varrho \nabla \left(\frac{V^2}{2} \right) - \frac{q}{2} \left[\varrho \nabla \left(\frac{\Theta}{\varrho} \right)^2 - (1 - \sigma_d) \frac{\nabla I^2}{\mu_0} \right] + \nabla \mathcal{P} - \left(\frac{B^2}{2\mu_0} \right) \nabla\sigma_d \right\} \cdot \nabla\psi \\ &= 0. \end{aligned} \tag{2.38}$$

Therefore, the equilibrium of helically symmetric plasmas with flow and anisotropic pressure is governed by the equations (2.36) and (2.38) which are valid for generic (compressible flows), being coupled through the density $\varrho(\mathbf{r})$ and the anisotropy function $\sigma_d(\mathbf{r})$. For compressible flow these equations remain coupled and the pertinent differential equation can be either elliptic or hyperbolic in connection with specific transition points of the poloidal Mach function M_p^2 [103, 104, 170]. Also, equation (2.38) has a singularity when $\sigma_d + M_p^2 = 1$ and so we must assume that $\sigma_d + M_p^2 \neq 1$. For isotropic pressure this corresponds to the Alfvénic value of the poloidal Mach function ($M_p^2 = 1$). In [171] it was found that sub-Alfvénic and super-Alfvénic regions separated by this Alfvén singularity can be smoothly connected by the Hall-effect.

2.1.4 GGS equation for incompressible flows and uniform anisotropy

To reduce further the equilibrium equations two assumptions for the arbitrary functions ϱ and σ_d must be made in connection with the closure problem of the MHD equations. At first, an equation of state is required such as isentropic or isothermal magnetic surfaces, associated inherently with compressible flow, or alternatively incompressibility. Since experimental poloidal velocities lie within the first elliptic regime incompressibility associated with ellipticity is a reasonable approximation [172]. Indeed incompressible flow, $\nabla \cdot \mathbf{V} = 0$ (see equation (1.31)), which we henceforth consider, implies that the mass density is a surface quantity

$$\varrho = \varrho(\psi), \tag{2.39}$$

as it follows from the mass conservation equation (1.50). Therefore, from equations (2.28), (2.32) and (2.39) it also follows that the Mach function is a surface quantity

$$M_p = M_p(\psi). \tag{2.40}$$

However, it should be clarified that compressible equilibrium flows permitting variations of ϱ and M_p on magnetic surfaces represent better the actual experimental situation. In addition, following [51,114,124,125,128] we adopt the condition (1.44) which implies that the anisotropy function is uniform on the magnetic surfaces

$$\sigma_d = \sigma_d(\psi). \tag{2.41}$$

For static equilibria this follows from equation (2.33), which becomes $X(\psi) = (1-\sigma_d)I$, if in the presence of anisotropy the current density remains on the magnetic surfaces ($I = I(\psi)$), i.e. for low-pressure plasmas ($P_{\parallel,\perp}/B^2 \ll 1$) and/or weakly anisotropic ones ($P_\parallel - P_\perp \ll B^2$) [173]. Since $M_p = M_p(\psi)$, the same implication holds for parallel incompressible flow ($\Phi^{'} = 0$) as well as for purely helical flow ($F = 0$, $\Theta \neq 0$). Also, the hypothesis $\sigma_d = \sigma_d(\psi)$, according to [124], may be the only suitable for satisfying the boundary conditions on a rigid, perfectly conducting wall.

Owing to the assumptions (2.39)-(2.41), equations (2.36), (2.38) decouple one another as follows; first equation (2.36) can be put in the form

$$\mathbf{B}\cdot\nabla\left[\underbrace{\varrho\frac{V^2}{2}+\frac{XF^{'}\Phi^{'}}{1-\sigma_d-M_p^2}-\frac{(1-\sigma_d)\varrho(\Phi^{'})^2}{q(1-\sigma_d-M_p^2)}+\mathcal{P}}_{:=f}\right]=0, \tag{2.42}$$

which implies that the scalar function, under the above gradient term is a surface quantity, $f = f(\psi)$. As a result, we obtain in a straightforward way a Bernoulli equation for the effective pressure in the following form

$$\mathcal{P} = \mathcal{P}_s(\psi) - \varrho\left[\frac{V^2}{2}-\frac{(1-\sigma_d)(\Phi^{'})^2}{q(1-\sigma_d-M_p^2)}\right], \tag{2.43}$$

where $\mathcal{P}_s := f(\psi) - \frac{XF^{'}\Phi^{'}}{1-\sigma_d-M_p^2}$. Therefore, in the presence of flow the magnetic surfaces in general do not coincide with surfaces on which $\mathcal{P}$, and as a result $P_\parallel$, $P_\perp$, lie on[1]. In this respect, the term containing $\mathcal{P}_s(\psi)$ is the static part of the effective pressure which does not

[1] In fact it will be shown that the $P_\parallel$ and $P_\perp$ surfaces do not coincide with the magnetic surfaces irrespective of the flow.

vanish when $\mathbf{V} = 0$. Then by substituting the expression (2.43) into (2.38), the later reduces to the following elliptic differential equation

$$(1-\sigma_d-M_p^2)\mathcal{L}\psi \;+\; \frac{1}{2}(1-\sigma_d-M_p^2)'|\nabla\psi|^2+\frac{1}{2}\left[\frac{X^2}{1-\sigma_d-M_p^2}\right]'+ \\ +\;\frac{\mu_0}{q}\mathcal{P}_s'+\frac{\mu_0}{2q^2}\left[\frac{(1-\sigma_d)\varrho(\Phi')^2}{(1-\sigma_d-M_p^2)}\right]'+2kmqX=0. \tag{2.44}$$

Equation (2.44) is the GGS equation that governs the equilibrium of helically symmetric plasmas with pressure anisotropy and incompressible flow. It contains six arbitrarily specified surface quantities, i.e. the poloidal Alfvén Mach function, $M_p(\psi)$, the pressure anisotropy function, $\sigma_d(\psi)$, the density, $\varrho(\psi)$, the electrostatic potential, $\Phi(\psi)$, the static part of the effective pressure, $\mathcal{P}_s(\psi)$, and the function $X(\psi)$ associated with the helicoidal magnetic field. Note that this equation contains a term involving the quantity $|\nabla\psi|^2$. It is also noted that while in numerical studies, e.g. [156, 157], $P_\perp$ and $P_\parallel$ are prescribed as functions of ψ and B, here, since the anisotropy function is uniform on the magnetic surfaces because of incompressibility, we only have to prescribe the pressure $\mathcal{P}_s(\psi)$ which explicitly appears in (2.44). Then $P_\perp$ and $P_\parallel$ can be calculated from the relations (1.61).

Under the transformation

$$U(\psi)=\int_0^\psi\sqrt{1-\sigma_d(g)-M_p^2(g)}dg,\;\; |M_p^2+\sigma_d|<1, \tag{2.45}$$

the GGS equation (2.44) reduces to the simpler and more compact form

$$\mathcal{L}U+2kmq\mathcal{I}+\frac{1}{2}\frac{d\mathcal{I}^2}{dU}+\frac{\mu_0}{q}\frac{d\mathcal{P}_s}{dU}+\frac{\mu_0}{2q^2}\frac{d\mathcal{F}}{dU}=0, \tag{2.46}$$

where the surface functions $\mathcal{I}$ and $\mathcal{F}$ are defined as follows

$$\mathcal{I}(U):=\frac{X}{\sqrt{1-\sigma_d-M_p^2}}, \tag{2.47}$$

$$\mathcal{F}(U):=(1-\sigma_d)\varrho\left(\frac{d\Phi}{dU}\right)^2. \tag{2.48}$$

Transformation (2.45) does not affect the magnetic surfaces, it just relabels them by the flux function U, and is a generalization of that introduced in [174] for isotropic equilibria with incompressible flow ($\sigma_d = 0$) and that introduced in [125] for static anisotropic equilibria ($M_p^2 = 0$). Note that no quadratic term as $|\nabla U|^2$ appears anymore in (2.46). Also, note that transformation (2.45) involves the square root of $1-\sigma_d-M_p^2$, and therefore our study is restricted to the sub-Alfvénic region ($|M_p^2+\sigma_d|<1$), this constraint however being practically insignificant because it is well satisfied in laboratory fusion plasmas. The GGS equation (2.46) is the most general equation governing the ideal steady plasma states of equilibrium configurations processing a continuous geometrical symmetry, either helical, axial or translational, since all these equations, static or stationary and/or isotropic/anisotropic, consist of limiting cases of (2.46) as presented below.

- *Helical Symmetry*

  - In the absence of pressure anisotropy ($\sigma_d = 0$) equation (2.46) reduces to the respective equation governing helically symmetric equilibria with incompressible flow and isotropic pressure derived in [115] [see equation (27) therein].

- In the static isotropic limit ($\sigma_d = M_p^2 = 0$) it reduces to the JFKO equation [75] [see equation (30) therein].

- *Axisymmetry*

  - In the limit ($k = -1, m = 0$) the respective equation governing axisymmetric equilibria with pressure anisotropy and incompressible flow derived in [114] is recovered [see equation (34) therein].

  - For vanishing flow ($M_p^2 = 0$) it reduces to the respective equation governing static anisotropic axisymmetric equilibria derived in [124] [see equation (9) therein].

  - In the absence of anisotropy ($\sigma_d = 0$) it reduces to the respective equation governing axisymmetric equilibria with incompressible flow and isotropic pressure introduced in [174] [see equation (17) therein].

  - In the absence of both flow and pressure anisotropy ($\sigma_d = M_p^2 = 0$) equation (2.46) reduces to the well-known GS equation [68, 69].

- *Translational Symmetry*

  - In the limit ($k = 0, m = 1$) equation (2.46) in the absence of pressure anisotropy, $\sigma_d = 0$, reduces to the respective equation governing cylindrically symmetric incompressible equilibria derived in [174, 175] [see equation (8) in [174]].

Once a solution of the GGS equation (2.46) is found, the equilibrium can be completely constructed in the U-space by using (2.45) and the inverse transformation

$$\psi(U) = \int_0^U (1 - \sigma_d(g) - M_p^2(g))^{-1/2} dg. \tag{2.49}$$

Thus, the equilibrium quantities of interest, presented above, are written in the following forms in U-space:

$$\mathcal{P} = \mathcal{P}_s(U) - \varrho \left[\frac{V^2}{2} - \frac{(1-\sigma_d)}{q} \left(\frac{d\Phi}{dU} \right)^2 \right], \tag{2.50}$$

$$X(U) = (1 - \sigma_d - M_p^2)^{1/2} \left[(1 - \sigma_d - M_p^2)^{1/2} I + \frac{\mu_0}{q} \left(\frac{M_p^2 \varrho}{\mu_0} \right)^{1/2} \left(\frac{d\Phi}{dU} \right) \right], \tag{2.51}$$

$$\mathbf{B} = I\mathbf{h} + (1 - \sigma_d - M_p^2)^{-1/2} \mathbf{h} \times \nabla U, \tag{2.52}$$

$$\mathbf{V} = \frac{M_p}{\sqrt{\mu_0 \varrho}} \mathbf{B} - (1 - \sigma_d - M_p^2)^{1/2} \left(\frac{d\Phi}{dU} \right) \frac{\mathbf{h}}{q}, \tag{2.53}$$

$$\mu_0 \mathbf{J} = \left[\frac{\mathcal{L}U}{1 - \sigma_d - M_p^2} + \frac{(1 - \sigma_d - M_p^2)^{-3/2}}{2} \times \frac{d(\sigma_d + M_p^2)}{dU} |\nabla U|^2 + 2kmqI \right] \mathbf{h} - \mathbf{h} \times \nabla I, \tag{2.54}$$

$$\mathbf{\Omega} = \left\{ \frac{M_p}{\sqrt{\mu_0 \varrho}} (1 - \sigma_d - M_p^2)^{-1/2} \mathcal{L}U + \frac{d}{dU} \left[\frac{M_p}{\sqrt{\mu_0 \varrho}} (1 - \sigma_d - M_p^2)^{-1/2} \right] |\nabla U|^2 + \frac{2kmq\Theta}{\varrho} \right\} \mathbf{h} - \mathbf{h} \times \nabla \left(\frac{\Theta}{\varrho} \right). \tag{2.55}$$

The safety factor in helical coordinates

Consider an infinitesimal annulus between two flux surfaces; with the use of the relations (2.7) and (2.23) for the helically symmetric magnetic field, the expression (1.70) for the safety factor yields

$$\mathcal{Q} = \frac{k}{2\pi N}\frac{d\int B^{\zeta} d\mathbf{s}}{d\psi}. \tag{2.56}$$

We apply the coordinate transformation $(r, u, \zeta) \longrightarrow (\psi(r,u), l_p(r,u), \zeta)$ with Jacobian

$$\mathcal{J} = \left[(\nabla\psi_p \times \nabla l_p)\cdot \mathbf{g}^{\zeta}\right]^{-1} = \left[\frac{m}{r}\left(\frac{\partial\psi}{\partial r}\frac{\partial l_p}{\partial u} - \frac{\partial\psi}{\partial u}\frac{\partial l_p}{\partial r}\right)\right]^{-1}, \tag{2.57}$$

where ψ is the usual poloidal flux function and l_p denotes the length element along the poloidal direction. Then equation (2.56) assumes the form

$$\mathcal{Q} = \frac{k}{2\pi N}\oint \mathcal{J} B^{\zeta} dl_p, \tag{2.58}$$

where we have used $d\mathbf{s} = \mathcal{J} d\psi dl_p \mathbf{g}^{\zeta}$; here $\oint dl_p$ is the line integral along the intersection curve of the helicoidal flux surface with the poloidal plane. Moreover, we calculate the quantity $\mathbf{B}_p \cdot \nabla l_p$ and find

$$\mathbf{B}_p \cdot \nabla l_p = \frac{1}{r}\left(\frac{\partial\psi}{\partial r}\frac{\partial l_p}{\partial u} - \frac{\partial\psi}{\partial u}\frac{\partial l_p}{\partial r}\right) = (m\mathcal{J})^{-1}. \tag{2.59}$$

Furthermore, we represent l_p as $\nabla l_p = \mathbf{B}_p/B_p$ and obtain the following expression from which the safety factor can be numerically calculated in terms of equilibrium quantities

$$\mathcal{Q} = \frac{1}{\eta N}\oint \frac{B^{\zeta}(r,u)}{B_p(r,u)} dl_p. \tag{2.60}$$

2.2 Special ideal incompressible MHD equilibria with anisotropic pressure

The GGS equation (2.38), valid for generic flow and anisotropy function, as well as its reduced form (2.44), governing incompressible equilibria with anisotropy function uniform on magnetic surfaces, were obtained from a reduction of the ideal MHD equilibrium equations (1.50)-(1.54) under the condition of helical symmetry, in which the existence of well-defined magnetic surfaces is assured. However, it is known that well-defined magnetic surfaces for 3D toroidal equilibria in general do not exist [24, 176]; the existence of such 3D equilibrium states are important for finite-beta stellarators. The aforementioned 3D equilibrium equations contain the vectors $\mathbf{V}$, $\mathbf{\Omega}$, $\mathbf{B}$ and $\mathbf{J}$, which in general are arbitrary. However, steady states involving special relative orientations between two of these vectors have drawn particular attention. An example of such special steady states are the force-free ones in which the magnetic force, $\mathbf{J}\times\mathbf{B}$, vanishes [177–183]; in this case the convective flow term is usually neglected in the force-balance equation and therefore the plasma pressure is constant. Also, steady states with Beltrami flows, in which the velocity $\mathbf{V}$ is parallel to the vorticity $\mathbf{\Omega}$ are of particular interest [182–186]. We will examine the properties of such kind of special 3D equilibria by assuming the existence of well defined magnetic surfaces labelled by a smooth function $\psi(\mathbf{r})$, on which surfaces both the fluid element velocity and the magnetic field lie on (see equation (1.56)), as follows.

2.2.1 Parallel flows ($\mathbf{V} \parallel \mathbf{B}$)

In the special case of collinear velocity and magnetic fields related through

$$\mathbf{V} = \frac{\lambda(\mathbf{r})}{\sqrt{\mu_0 \varrho}}\mathbf{B}, \tag{2.61}$$

with λ an arbitrary dimensionless scalar function, the continuity equation (1.50) yields

$$\frac{1}{\varrho}(\mathbf{B}\cdot\nabla\varrho) = -\frac{2}{\lambda}(\mathbf{B}\cdot\nabla\lambda). \tag{2.62}$$

Then with the use of the relations (2.61) and (2.62) the momentum equation (1.58) for field-aligned flows reads

$$(1-\sigma_d-\lambda^2)\mathbf{J}\times\mathbf{B} = \nabla\left(\mathcal{P}+\lambda^2\frac{B^2}{2\mu_0}\right) + \frac{B^2}{2\mu_0}\nabla(1-\sigma_d-\lambda^2) - \frac{\mathbf{B}}{\mu_0}\left[\mathbf{B}\cdot\nabla(1-\sigma_d-\lambda^2)\right], \tag{2.63}$$

being valid for arbitrary functions ϱ and σ_d, and therefore for compressible flows. We further assume that the anisotropy function is uniform on magnetic surfaces, $\sigma_d = \sigma_d(\psi)$, together with incompressible flows, $\varrho = \varrho(\psi)$. In this case equation (2.62), implies that the function λ is also a surface quantity, $\lambda = \lambda(\psi)$, and equation (2.63) reduces to

$$(1-\sigma_d-\lambda^2)\mathbf{J}\times\mathbf{B} = \nabla\left(\mathcal{P}+\lambda^2\frac{B^2}{2\mu_0}\right) - (\sigma_d+\lambda^2)'\frac{B^2}{2\mu_0}\nabla\psi. \tag{2.64}$$

The component of (2.64) parallel to $\mathbf{B}$ implies that $\mathcal{P}+\lambda^2B^2/(2\mu_0)$ is a magnetic-surface quantity, to be called $\mathcal{P}_s(\psi)$, in consistency with (2.43) for field-aligned flows given by (2.61); consequently, (2.64) yields

$$\mathbf{J}\times\mathbf{B} = g(\psi, B^2)\nabla\psi, \tag{2.65}$$

where

$$g(\psi,B^2) := (1-\sigma_d-\lambda^2)^{-1}\left[\mathcal{P}_s' - (\sigma_d+\lambda^2)'\frac{B^2}{2\mu_0}\right]. \tag{2.66}$$

Equation (2.65) implies that $\mathbf{J}$ lies on the magnetic surfaces, a property which was very useful in obtaining the sufficient condition for linear stability in [149].

At this point let us mention the special class of isodynamic equilibria introduced by Palumbo [187] in which by definition the magnetic field modulus is uniform on magnetic surfaces. Thus, they may have favourable confinement properties because the ∇B drift vanishes. The latter equilibria are degenerate in the sense that irrespective of the choice of the functional dependence of the free functions in the GGS equation the equilibrium configuration is unique [188]. In this configuration the magnetic surfaces in the vicinity of the magnetic axis have circular cross-sections and the outermost magnetic surface reaches the axis of symmetry through a corner; this will be called Palumbo equilibrium. When the magnetic field magnitude is a surface quantity, $B^2 = B^2(\psi)$, equation (2.65) can be put in the form $\mathbf{J}\times\mathbf{B} = \nabla G(\psi)$, which in the isotropic limit is formally equivalent to the well known static ideal MHD equation. Consequently, the only isodynamic equilibrium with parallel incompressible flow is the axisymmetric Palumbo one, as it was proved for static equilibria in [189]. This also holds for anisotropic equilibria with $\sigma_d = \sigma_d(\psi)$ as noted in [114].

2.2.2 Flows parallel to the current density ($\mathbf{V} \parallel \mathbf{J}$)

Assume that the velocity and the current density vectors are collinear, related through

$$\mathbf{V} = \lambda(\mathbf{r})\mathbf{J}, \tag{2.67}$$

with λ being an arbitrary scalar function. This is physically plausible case too because certain species of charged fluid elements should be in motion in order to create the current. For static equilibria $\mathbf{J}$ is created by the electrons; for stationary ones the ions may also contribute. In this case $\mathbf{V}$, $\mathbf{B}$ and $\mathbf{J}$ have common surfaces by the Ohm's law, which reads

$$\mathbf{J}\times\mathbf{B}=\lambda^{-1}\nabla\Phi. \tag{2.68}$$

Also, under relation (2.67) the continuity equation takes the form

$$\varrho(\mathbf{J}\cdot\nabla\lambda)=-\lambda(\mathbf{J}\cdot\nabla\varrho). \tag{2.69}$$

Let us discuss here the physical meaning of λ. Recall that the MHD momentum equation is derived by adding the two-fluid momentum equations and using the relations for $\mathbf{V}^*$, $\mathbf{J}^*$ given in (1.14). Since $\mathbf{V}^*=\lambda\mathbf{J}^*$ then we can compute the electron velocity in terms of the ion velocity, i.e.

$$\mathbf{v}_e^*=\frac{ne(m_i+m_e)\lambda-m_i}{ne(m_i+m_e)\lambda+m_e}\mathbf{v}_i^*=\mu(\lambda,n)\mathbf{v}_i^*. \tag{2.70}$$

Therefore $\mathbf{v}_e^*\parallel\mathbf{v}_i^*$ as it was expected and in addition we conclude that λ determines the relative velocity of electrons and ions for a given particle density n. In particular, for $|\lambda|\gg 1$ (i.e. for velocity magnitudes much more greater than the current density) the electrons are moving nearly with the ion velocity (almost no current). For very small and reversed flow velocity compared to the current density, the electrons are moving in the same direction with the ions but much faster. Also, for small but positive (with respect to the direction of $\mathbf{J}$) flows the electron velocity reverses and the electrons move in the opposite direction with respect to the ions. This case is not desirable since it is generally known that opposing beams of charged particles drive the so called two stream instability. The threshold for electron flow reversal is $\lambda_c=m_i[en(m_i+m_e)]^{-1}$.

Assuming uniform pressure anisotropy, $\sigma_d=\sigma_d(\psi)$, together with incompressible flows, $\varrho=\varrho(\psi)$, in this case equation (2.69) implying $\lambda=\lambda(\psi)$ since $\mathbf{J}$, $\mathbf{B}$ share the same surfaces, the Ohm's law is written in the form

$$\mathbf{J}\times\mathbf{B}=\varsigma(\psi)\nabla\psi, \tag{2.71}$$

where $\varsigma:=\Phi'/\lambda$ is the charge density. Furthermore the momentum equation in this case takes the form

$$(1-\sigma_d)\mathbf{J}\times\mathbf{B}+\varrho\lambda^2\mathbf{J}\times(\nabla\times\mathbf{J})=\nabla\left(\mathcal{P}+\frac{\varrho\lambda^2J^2}{2}\right)-\left(\sigma_d'\frac{B^2}{2\mu_0}+(\varrho\lambda^2)'\frac{J^2}{2}\right)\nabla\psi. \tag{2.72}$$

The component of (2.72) parallel to $\mathbf{J}$ implies that $\mathcal{P}+(\varrho\lambda^2J^2)/2$ is a surface quantity to be called $\mathcal{P}_s(\psi)$, in consistency with (2.43) for flows parallel to the current density given by (2.67); consequently, (2.72) yields

$$\mathbf{J}\times(\nabla\times\mathbf{J})=g(\psi,B^2,J^2)\nabla\psi, \tag{2.73}$$

where

$$g(\psi,B^2,J^2):=\frac{1}{\varrho\lambda^2}\left[\mathcal{P}_s'-(\varrho\lambda^2)'\frac{J^2}{2}-\sigma_d'\frac{B^2}{2\mu_0}-(1-\sigma_d)\varsigma\right]. \tag{2.74}$$

From equation (2.73) it follows that the vector field $\nabla\times\mathbf{J}=-\nabla^2\mathbf{B}/\mu_0$ also lies on the magnetic surfaces.

2.2.3 Beltrami flows ($\boldsymbol{\Omega} \parallel \mathbf{V}$)

This kind of flows have been thoroughly investigated in the framework of hydrodynamics. The Beltrami condition, $\boldsymbol{\Omega} = \lambda(\mathbf{r})\mathbf{V}$, λ being an arbitrary scalar function, together with the condition of divergence-free vorticity, $\nabla \cdot \boldsymbol{\Omega}$, yield

$$\lambda(\nabla \cdot \mathbf{V}) = -\mathbf{V} \cdot \nabla\lambda, \tag{2.75}$$

which under the incompressibility condition implies that $\lambda = \lambda(\psi)$. By further assuming that $\sigma_d = \sigma_d(\psi)$ the momentum equation takes the form

$$(1-\sigma_d)\mathbf{J} \times \mathbf{B} = \nabla\left(\mathcal{P} + \varrho\frac{V^2}{2}\right) - \left(\varrho^{'}\frac{V^2}{2} + \sigma_d^{'}\frac{B^2}{2\mu_0}\right)\nabla\psi. \tag{2.76}$$

Then projection of equation (2.76) along $\mathbf{B}$ (or $\mathbf{J}$) implies that $\mathcal{P} + (\varrho V^2)/2 := \mathcal{P}_s(\psi)$ is a surface quantity, and consequently equation (2.76) assumes the form

$$\mathbf{J} \times \mathbf{B} = g(\psi, B^2, V^2)\nabla\psi, \tag{2.77}$$

with

$$g(\psi, B^2, V^2) := \frac{1}{1-\sigma_d}\left[\mathcal{P}_s^{'} - \varrho^{'}\frac{V^2}{2} - \sigma_d^{'}\frac{B^2}{2\mu_0}\right], \tag{2.78}$$

thus implying that all four vectors $\boldsymbol{\Omega}$, $\mathbf{V}$, $\mathbf{J}$, $\mathbf{B}$ lie on the magnetic surfaces.

2.2.4 "Force-free" equilibria ($\mathbf{J} \parallel \mathbf{B}$)

The force-free condition relates the current density with the magnetic field through

$$\mathbf{J} = \lambda(\mathbf{r})\mathbf{B}, \tag{2.79}$$

where λ is an arbitrary scalar function. This case has also been extensively investigated in the literature in connection with relaxed states of astrophysical and fusion magnetically confined plasmas. The most known example is associated with the Taylor conjecture [190, 191] according to which a slightly resistive plasma surrounded by a fixed perfectly conducting boundary relaxes to a state of minimum magnetic energy under the constraint of global magnetic helicity conservation, a state which is deduced to the force-free with $\lambda =$ constant. For static isotropic equilibria if the magnetic force is zero the pressure must be constant and therefore none force is exerted on the fluid element, which justifies the term force-free. A physical reason that many astrophysical plasmas relax to such a state is that if the current would not be parallel to the magnetic field the resulting magnetic force should be so large that it could not be balanced by pressure-gradient and gravitational forces. However, in the presence of plasma flow if the magnetic force vanishes the pressure can not be constant because a ∇P-force is required to balance the inertial flow one. This is the reason we use here quotation marks for the term "force-free".

Since both $\mathbf{J}$ and $\mathbf{B}$ are divergence-free the "force-free" condition implies that $\lambda = \lambda(\psi)$. Under the assumptions of incompressible flows and uniform anisotropy the momentum equation takes the form

$$\varrho\mathbf{V} \times \boldsymbol{\Omega} = \nabla\left(\mathcal{P} + \varrho\frac{V^2}{2}\right) - \left(\varrho^{'}\frac{V^2}{2} + \sigma_d^{'}\frac{B^2}{2\mu_0}\right)\nabla\psi. \tag{2.80}$$

Then projection of latter equation along $\mathbf{V}$ implies that $\mathcal{P} + (\varrho V^2)/2 := \mathcal{P}_s(\psi)$ is a surface quantity, and consequently equation (2.80) reduces into the form

$$\mathbf{V} \times \boldsymbol{\Omega} = g(\psi, B^2, V^2)\nabla\psi, \tag{2.81}$$

with

$$g(\psi, B^2, V^2) := \frac{1}{\varrho}\left[\mathcal{P}_s^{'} - \varrho^{'}\frac{V^2}{2} - \sigma_d^{'}\frac{B^2}{2\mu_0}\right], \tag{2.82}$$

thus implying that all four vectors $\boldsymbol{\Omega}$, $\mathbf{V}$, $\mathbf{J}$, $\mathbf{B}$ lie on the magnetic surfaces.

2.2.5 Equilibria with $\boldsymbol{\Omega} \parallel \mathbf{B}$ ($\boldsymbol{\Omega} \parallel \mathbf{J}$)

Assume that the vorticity is parallel to the magnetic field through, $\boldsymbol{\Omega} = \lambda(\mathbf{r})\mathbf{B}$; then owing to both $\boldsymbol{\Omega}$ and $\mathbf{B}$ being divergence-free, the scalar function λ is a surface function, $\lambda = \lambda(\psi)$. For incompressible flows and uniform pressure anisotropy function, the force balance equation takes the form

$$[(1-\sigma_d)\mathbf{J} + \varrho\lambda\mathbf{V}] \times \mathbf{B} = \nabla\left(\mathcal{P} + \varrho\frac{V^2}{2}\right) - \left(\varrho^{'}\frac{V^2}{2} + \sigma_d^{'}\frac{B^2}{2\mu_0}\right)\nabla\psi. \tag{2.83}$$

Then projection of the latter equation along $\mathbf{V}$ implies that $\mathcal{P}+(\varrho V^2)/2 := \mathcal{P}_s(\psi)$ is a surface quantity, and consequently equation (2.80) reduces to

$$[(1-\sigma_d)\mathbf{J} + \varrho\lambda\mathbf{V}] \times \mathbf{B} = g(\psi, B^2, V^2)\nabla\psi, \tag{2.84}$$

with

$$g(\psi, B^2, V^2) := \frac{1}{\varrho}\left[\mathcal{P}_s^{'} - \varrho^{'}\frac{V^2}{2} - \sigma_d^{'}\frac{B^2}{2\mu_0}\right]. \tag{2.85}$$

Also in this case the Ohm's law implies that

$$\mathbf{J} \times \mathbf{B} = \frac{(\varrho\lambda\Phi^{'})}{1-\sigma_d}\nabla\psi, \tag{2.86}$$

and thus, all four vectors $\boldsymbol{\Omega}$, $\mathbf{V}$, $\mathbf{J}$, $\mathbf{B}$ share the same surfaces.

Now consider a different kind of equilibria in which the vorticity is parallel to the current density, $\boldsymbol{\Omega} = \lambda(\mathbf{r})\mathbf{J}$; since both $\boldsymbol{\Omega}$ and $\mathbf{J}$ being divergence-free, it follows that the scalar function λ is uniform on the current surfaces, S = const., on which the current density lie on, $\lambda = \lambda(S)$, assuming that such surfaces are well-defined. Under the condition of incompressibility together with σ_d being uniform on the magnetic surfaces the momentum equation takes the form

$$[\varrho\lambda\mathbf{V} - (1-\sigma_d)\mathbf{B}] \times \mathbf{J} = \nabla\left(\mathcal{P} + \varrho\frac{V^2}{2}\right) - \left(\varrho^{'}\frac{V^2}{2} + \sigma_d^{'}\frac{B^2}{2\mu_0}\right)\nabla\psi. \tag{2.87}$$

In order to further reduce the above equation we assume that the magnetic surfaces coincide with the current surfaces, $\mathbf{J}\cdot\nabla\psi = 0$, in which case the projection of (2.87) along $\mathbf{J}$ yields that $\mathcal{P} + (\varrho V^2)/2 := \mathcal{P}_s(\psi)$ is a surface quantity, and consequently

$$[\varrho\lambda\mathbf{V} - (1-\sigma_d)\mathbf{B}] \times \mathbf{J} = g(\psi, B^2, V^2)\nabla\psi, \tag{2.88}$$

with

$$g(\psi, B^2, V^2) := \left[\mathcal{P}_s^{'} - \varrho^{'}\frac{V^2}{2} - \sigma_d^{'}\frac{B^2}{2\mu_0}\right]. \tag{2.89}$$

2.2.6 Special helically symmetric equilibria

Here we examine the special helically symmetric equilibria with incompressible flows ($\varrho = \varrho(\psi)$, $M_p = M_p(\psi)$) and pressure anisotropy function uniform on magnetic surfaces ($\sigma_d = \sigma_d(\psi)$) respective to those of subsections 2.2.1-2.2.5 together with the cases of equilibria with either complex lamellar $\mathbf{V}$ and complex lamellar $\mathbf{B}$, as follows.

Parallel flows

The poloidal component of relation (2.61) implies that $\lambda = M_p = \lambda(\psi)$, in consistency with (2.31). Also, equation (2.34) for $\Phi^{'} = 0$ implies that $I = X/(1-\sigma_d - M_p^2) = I(\psi)$ and thus, the current surfaces coincide with the magnetic surfaces. In addition, the helicoidal component of (2.61) yields $\Theta = (M_p I\sqrt{\varrho})/\sqrt{\mu_0}$ in consistency with (2.30) for $\Phi^{'} = 0$. Consequently, M_p, the helicoidal Alfvén Mach function, $M_t = V_h/(B_h/\sqrt{\mu_0\varrho})$, and the parallel Alfvén Mach function, $M = V/(B/\sqrt{\mu_0\varrho})$, are equal one another. Since the electric field vanishes the GGS equation (2.44) under the transformation (2.45) takes the following form in U space

$$\mathcal{L}U + 2kmqI + \frac{1}{2}\frac{dI^2}{dU} + \frac{\mu_0}{q}\frac{d\mathcal{P}_s}{dU} = 0, \tag{2.90}$$

which is identical with the static isotropic JFKO equilibrium equation. Furthermore, the Bernoulli equation (2.50) becomes $\mathcal{P} = \mathcal{P}_s - M_p^2(B^2/2\mu_0)$. Therefore non-negativeness of $\mathcal{P}$ sets a lower bound (approximately) for the plasma beta

$$\bar{\beta} \geq M_p^2. \tag{2.91}$$

Flows parallel to the current density

The helicoidal and poloidal components of relation (2.67) yield respectively

$$\mathcal{L}\psi = \frac{\mu_0\Theta}{\varrho\lambda} - 2kmqI, \tag{2.92}$$

and

$$\frac{\mu_0 F^{'}}{\varrho}\mathbf{h}\times\nabla\psi = -\mathbf{h}\times\nabla I. \tag{2.93}$$

From the projection of (2.93) along $\nabla\psi$ it follows that $I = I(\psi)$. Compatibility with the relation (2.34) implies that for the current density to stay on the magnetic surfaces the velocity should be either helicoidal $(M_p = 0)$ or parallel to the magnetic field $(\Phi^{'} = 0)$.

In the isotropic axisymmetric limit $(\sigma_d = 0,\ \mathcal{P}\to P,\ k\to -1,\ m\to 0,\ u\to z,\ q\to\rho^{-1})$ the pertinent equilibrium states are governed by the following equation

$$(1-M_p^2)\Delta^{\star}\psi - \frac{(M_p^2)^{'}}{2}|\nabla\psi|^2 + \frac{1}{2}\left(\frac{X^2}{1-M_p^2}\right)^{'} + \mu_0\rho^2 P_s^{'} + \frac{\rho^4}{2}\left[\frac{\varrho(\Phi^{'})^2}{1-M_p^2}\right]^{'} = 0, \tag{2.94}$$

while equation (2.92) takes the form

$$\Delta^{\star}\psi = \frac{\mu_0\Theta}{\varrho\lambda}. \tag{2.95}$$

Here, $\psi = \psi(\rho, z)$, $\Delta^{\star} = \rho^2\nabla\cdot(\nabla/\rho^2)$ and P_s is the static part of the isotropic axisymmetric pressure. In this case equations (2.94) and (2.95) imply that ψ should satisfy a couple of equations of the form

$$\Delta^{*}\psi = a_1(\psi) + \rho^2 a_2(\psi), \tag{2.96}$$

$$|\nabla\psi|^2 = a_3(\psi) + \rho^2 a_4(\psi) + \rho^4 a_5(\psi), \tag{2.97}$$

where the functions a_i, $i = 1, ...5$, can be expressed in terms of X, P_s, M_p, ϱ, Φ, and λ. The set of equations (2.96)-(2.97) describe a special class of isodynamic-like equilibria with non-parallel flow [192] associated with the so-called Mawxellian condition, $P + B^2(2\mu_0) = \text{const.}$, in connection with a hidden integrability of ideal MHD. It is also noted that alternative "side-conditions" imposed on axisymmetric incompressible equilibria, as $B^2 = B^2(\psi)$ or $P = P(\psi)$

[193], lead to more generic isodynamic-like equilibria in connection with an additional term on the RHS of (2.96) of the form $\rho^4 a_6(\psi)$. For parallel flows it holds $a_5 = 0$ and (2.96)-(2.97) lead to the Palumbo configuration. The presence of non-parallel flow ($\Phi^{'} \neq 0$) modifies this configuration, i.e. the magnetic surfaces in the vicinity of the magnetic axis can have elliptical cross-sections elongated either parallel or perpendicular to the axis of symmetry [193].

Beltrami flows

The poloidal component of the Beltrami condition, $\mathbf{\Omega} = \lambda(\psi)\mathbf{V}$, reads

$$\mathbf{h} \times \nabla\Theta = \left(\frac{\Theta \varrho^{'}}{\varrho} - \lambda F^{'} \right) \mathbf{h} \times \nabla\psi. \tag{2.98}$$

Then projection of this equation perpendicular to the magnetic surfaces implies that $\Theta = \Theta(\psi)$. To be this compatible with the integral (2.30) it follows that $\Phi^{'} = 0$ and therefore helically symmetric incompressible Beltrami flows must be parallel to $\mathbf{B}$. Also, from relation (2.34) it follows that in this case the current density remains on the magnetic surfaces, $I = I(\psi)$. The GGS equation governing such helically symmetric Beltrami equilibria has the following form under the transformation (2.45)

$$\mathcal{L}U + 2kmqI + \frac{1}{2}\frac{dI^2}{dU} + \frac{\mu_0}{q}\frac{d\mathcal{P}_s}{dU} = 0, \tag{2.99}$$

with $\mathcal{P} = \mathcal{P}_s - M^2B^2/(2\mu_0)$, the parallel Mach function being equal in this case to $M = \sqrt{\mu_0}\Theta/(\sqrt{\varrho}I)$.

"Force-free" equilibria

Since in this case, $\mathbf{\Omega}$, $\mathbf{V}$, $\mathbf{B}$ and $\mathbf{J}$ share the same surfaces it should hold $I = I(\psi)$ and $\Theta = \Theta(\psi)$. Consequently compatibility with (2.30) implies, as in the Beltrami case, that the flows should be parallel to $\mathbf{B}$. In this case the pertinent momentum equation describes the balance between the pressure tensor related force and the flow force, while the resulting GGS equation governing the equilibrium is identical with (2.99).

Vorticity parallel to the magnetic field/current density

Consider the case $\mathbf{\Omega} = \lambda\mathbf{B}$. Projection of the poloidal component of this relation,

$$\mathbf{h} \times \nabla\Theta = \left(\frac{\Theta \varrho^{'}}{\varrho} - \varrho\lambda \right) \mathbf{h} \times \nabla\psi, \tag{2.100}$$

onto the direction of $\nabla\psi$ implies that $\Theta = \Theta(\psi)$. Consequently, compatibility with (2.35) leads to flows parallel to $\mathbf{B}$.

Similarly, the ∇I-component of the relation $\mathbf{\Omega} = \lambda(\psi)\mathbf{J}$ implies that Θ is uniform on the current surfaces, which in this case coincide with the magnetic surfaces, $\Theta = \Theta(I) = \Theta(\psi)$. This restricts one more the flows to be parallel to $\mathbf{B}$.

Complex lamellar equilibria

Complex lamellar is a vector field, $\mathbf{a}$, which is orthogonal to its own curl, $\mathbf{c} = \nabla \times \mathbf{a}$. This is related to the orthogonal decomposition of $\mathbf{c}$ with respect to the direction of $\mathbf{a}$: $\mathbf{c} = \lambda_1\mathbf{a} + \mathbf{a} \times \mathbf{w}$. When $\mathbf{w} = 0$ the field $\mathbf{a}$ becomes Beltrami while for $\lambda_1 = 0$, $\mathbf{a}$ becomes complex lamellar ($\mathbf{a} \cdot \mathbf{c} = 0$). In hydrodynamics all the two-dimensional flows satifying the Navier-Stokes equation are complex-lamellar. The research of complex lamellar flow has been

of great help to understanding the complexity and generality of the flow, e.g. [194–197]. Also, in helically symmetric MHD equilibria with purely toroidal (helicoidal) flow, inherently incompressible because of symmetry, this flow is complex lamellar. Here we examine helically symmetric and axisymmetric equilibria with complex lamellar flow.

Employing equations (2.13), (2.18) and (2.35) the condition $\mathbf{V}\cdot\mathbf{\Omega}=0$ yields

$$\left(A(\psi)+\frac{C(\psi)}{q}\right)\left[D(\psi)\mathcal{L}\psi+2kmq\left(A(\psi)+\frac{C(\psi)}{q}\right)\right]-2k^2rC(\psi)D(\psi)\frac{\partial\psi}{\partial r}$$
$$+\left[\left(A(\psi)+\frac{C(\psi)}{q}\right)D^{'}(\psi)-D(\psi)\left(A^{'}(\psi)+\frac{C^{'}(\psi)}{q}\right)\right]|\nabla\psi|^2=0, \tag{2.101}$$

where $A:=(XM_p)/\sqrt{\mu_0\varrho}(1-\sigma_d-M_p^2)$, $C:=-(1-\sigma_d)\Phi^{'}/(1-\sigma_d-M_p^2)$ and $D:=M_p/\sqrt{\mu_0\varrho}$. Therefore the equilibrium is governed by the GGS equation (2.44) and (2.101). In the special case of axisymmetry the corresponding equations can be cast in the forms

$$(a_1(\psi)+\rho^2a_2(\psi))\Delta^{\star}\psi+a_3(\psi)\rho\frac{\partial\psi}{\partial\rho},$$
$$=A_1(\psi)+A_2(\psi)\rho^2+A_3(\psi)\rho^4+A_4(\psi)\rho^6, \tag{2.102}$$
$$(a_1(\psi)+\rho^2a_2(\psi))|\nabla\psi|^2+b_3(\psi)\rho\frac{\partial\psi}{\partial\rho},$$
$$=B_1(\psi)+B_2(\psi)\rho^2+B_3(\psi)\rho^4+B_4(\psi)\rho^6, \tag{2.103}$$

where a_i, A_i, B_i are known functions of the surface quantities of equilibrium. Consequently, the electric field gives rise to a class of non-isodynamic axisymmetric equilibria with complex lamellar flow governed by equations (2.102) and (2.103). The construction of specific equilibria can be pursued by a method introduced in [187] and employed in [193]. For parallel flow $(C=0)$ these equations reduce to

$$\Delta^{\star}\psi=d_1(\psi)+\rho^2d_2(\psi), \tag{2.104}$$
$$|\nabla\psi|^2=u_1(\psi)+\rho^2u_2(\psi), \tag{2.105}$$

and thus, in this case the equilibrium becomes isodynamic. We note that the same result holds for equilibria with complex lamellar magnetic field, $\mathbf{B}\cdot\mathbf{J}=0$.

3 | An Analytic Class of Helically Symmetric Equilibria

"There are endless planes of attention, endless realities and endless mind states. They're like collections of atoms and protons and neutrons, nuclei. They just go on forever. They're plasma, they're fluid ... they're alive."

Frederick Lenz

3.1 Construction of analytic equilibrium solutions

The equilibrium of a helically symmetric plasma with anisotropic pressure and incompressible flow of arbitrary direction is governed by the GGS equation (2.46), which is a non-linear, partial differential equation of second order. In order to solve analytically that equation we first have to linearize it for several choices of the free function terms $\mathcal{I}(U)$, $\mathcal{F}(U)$, and $\mathcal{P}_s(U)$. These choices should correspond to reasonable profiles of the equilibrium surface quantities $X(U)$, $\varrho(U)$, $\Phi(U)$, $M_p(U)$ and $\sigma_d(U)$, since both $\mathcal{I}(U)$ and $\mathcal{F}(U)$ depend on these quantities. In particular, to solve equation (2.46) we adopt the most generic linearizing ansatz for the free function terms as

$$\begin{aligned} \mathcal{I}(U) &:= \chi_{00} + \chi_{11}(U-U_b), \\ \mu_0\mathcal{F}(U) &:= \varphi_{00} + \varphi_{11}(U-U_b) + \varphi_{22}(U-U_b)^2, \\ \mu_0\mathcal{P}_s(U) &:= \pi_{00} + \pi_{11}(U-U_b) + \pi_{22}(U-U_b)^2, \end{aligned} \tag{3.1}$$

where χ_{00}, χ_{11}, π_{00}, π_{11}, π_{22}, φ_{00}, φ_{11}, φ_{22}, U_b are free parameters which will thereafter be specified. In particular, the parameter U_b refers to the outermost magnetic flux surface or equivalently is the value of U on the plasma boundary. We note that for plasmas of magnetic confinement fusion interest, both the mass flow and the pressure must vanish on the plasma boundary; otherwise a well defined equilibrium may not be maintained, potentially leading to catastrophic disruptions. In this sense, in connection with modeling of fusion related equilibrium configurations, we henceforth assume $\pi_{00} = (\pi_{11} - \pi_{22}U_b)U_b$ and $\varphi_{00} = (\varphi_{11} - \varphi_{22}U_b)U_b$, which imply that for $U = U_b$ the profiles of both the electric field term and of the static effective pressure vanish thereon[1]. It is also noted that the first two choices of the ansatz (3.1) specify the functional dependence of a couple out of the free functions $X^2(U)$, $\varrho(U)$, $\Phi'(U)^2$, $M_p(U)$ and $\sigma_d(U)$. In this respect we choose these functions to be X^2 and $(\Phi')^2$; therefore the solutions to be constructed are valid for any functions $\sigma_d(U)$, $M_p^2(U)$ and $\varrho(U)$. Then under the coordinate transformation

$$s := \frac{k^2 r^2}{m^2}, \tag{3.2}$$

[1] In the special case $U_b = 0$ one has to assume that $\pi_{00} = \varphi_{00} = 0$.

equation (2.46) takes the form

$$\frac{s^2}{1+s}\frac{\partial^2 U}{\partial s^2}+\frac{m^2}{4}\frac{\partial^2 U}{\partial u^2}+\frac{s}{(1+s)^2}\frac{\partial U}{\partial s}+\Upsilon(s)U=\Gamma(s), \tag{3.3}$$

in connection with the following definitions:

$$\Upsilon(s) := s\left[\lambda_{22}+\lambda_{33}(1+s)+\frac{\lambda_{11}}{(1+s)^2}+\frac{\lambda_{11}^2}{(1+s)}\right], \tag{3.4}$$

$$\lambda_{11} := \frac{m\chi_{11}}{2k},\ \lambda_{22}:=\frac{\pi_{22}m^4}{2k^2},\ \lambda_{33}:=\frac{\varphi_{22}m^6}{4k^2}, \tag{3.5}$$

$$\Gamma(s) := -s\left[\tau_{22}+\tau_{33}(1+s)+\frac{\tau_{11}}{(1+s)^2}+\frac{\tau_{11}\lambda_{11}}{(1+s)}\right], \tag{3.6}$$

$$\tau_{11} := \frac{m\widetilde{\chi}_{00}}{2k},\ \tau_{22}:=\frac{\widetilde{\pi}_{11}m^4}{2k^2},\ \tau_{33}:=\frac{\widetilde{\varphi}_{11}m^6}{4k^2}, \tag{3.7}$$

$$\widetilde{\chi}_{00} := \chi_{00}-\chi_{11}U_b,\ \widetilde{\pi}_{11}:=(\pi_{11}-2\pi_{22}U_b)/2,\ \widetilde{\varphi}_{11}:=(\varphi_{11}-2\varphi_{22}U_b)/2. \tag{3.8}$$

Thus, the problem reduces into solving the non-homogeneous, linear PDE (3.3). The general solution of (3.3) should be of the form

$$U(s,u)=U_h(s,u)+U_p(s), \tag{3.9}$$

where $U_h(s,u)$ is the general solution of the respective homogeneous equation

$$\frac{s^2}{1+s}\frac{\partial^2 U_h(s,u)}{\partial s^2}+\frac{m^2}{4}\frac{\partial^2 U_h(s,u)}{\partial u^2}+\frac{s}{(1+s)^2}\frac{\partial U_h(s,u)}{\partial s}+\Upsilon(s)U_h=0, \tag{3.10}$$

while $U_p(s)$ is any particular solution of (3.3) satisfying equation

$$\frac{s^2}{1+s}\frac{d^2 U_p(s)}{ds^2}+\frac{s}{(1+s)^2}\frac{dU_p(s)}{ds}+\Upsilon(s)U_p(s)=\Gamma(s). \tag{3.11}$$

In order to first solve the homogeneous PDE (3.10) we apply the method of separation of variables for $U_h(s,u)$:

$$U_h(s,u)=H(s)T(u). \tag{3.12}$$

Then substitution of the trial form (3.12) into (3.10) reduces the problem to a couple of linear ODEs of the second order, in connection with a separation constant, n. The first for the function $T(u)$ is

$$\frac{d^2T(u)}{du^2}+\left(\frac{2n}{m}\right)^2 T(u)=0, \tag{3.13}$$

having the periodic in u general solution

$$T(u;n)=l_1\cos\left(\frac{2nu}{m}\right)+l_2\sin\left(\frac{2nu}{m}\right), \tag{3.14}$$

where l_1, l_2 are arbitrary coefficients. The second ODE satisfied by the function $H(s)$ is

$$s^2(1+s)\frac{d^2H(s)}{ds^2}+s\frac{dH(s)}{ds}+\left(\sum_{i=0}^{4}\Upsilon_i s^i\right)H(s)=0, \tag{3.15}$$

where Υ_i, $i = 1, ..4$ are functions of the free parameters and n defined as follows

$$\begin{aligned} \Upsilon_0 &:= -n^2, \\ \Upsilon_1 &:= \lambda_{11} + \lambda_{11}^2 + \lambda_{22} + \lambda_{33} - 2n^2, \\ \Upsilon_2 &:= \lambda_{11}^2 + 2\lambda_{22} + 3\lambda_{33} - n^2, \\ \Upsilon_3 &:= \lambda_{22} + 3\lambda_{33}, \\ \Upsilon_4 &:= \lambda_{33}. \end{aligned} \tag{3.16}$$

Moreover, for the radial function $H(s)$ we apply the transformation

$$H(s) = s^n e^{-\varkappa s} R(s), \qquad \varkappa^2 := -\Upsilon_3, \tag{3.17}$$

under which ODE (3.15) reduces further into a more compact one for the function R(s)

$$s(1+s)\frac{d^2R(s)}{ds^2} + (\varepsilon_{00} + \varepsilon_{11}s + \varepsilon_{22}s^2)\frac{dR(s)}{ds} + (\varepsilon_{33} + \varepsilon_{44}s + \Upsilon_4 s^3)R(s) = 0. \tag{3.18}$$

Here the parameters appearing in the polynomial coefficients (which are analytic functions of s except for $s = 0$ and $s \to \infty$) are defined as follows

$$\begin{aligned} \varepsilon_{00} &:= 1 + 2n, \qquad \varepsilon_{11} = 2(n - \varkappa), \qquad \varepsilon_{22} := -2\varkappa, \\ \varepsilon_{33} &:= \Upsilon_1 - (n + \varkappa) - 2n\varkappa + n^2, \qquad \varepsilon_{44} := \Upsilon_2 + \varkappa^2 - 2n\varkappa. \end{aligned} \tag{3.19}$$

We note that the form of transformation (3.17) implies that one may consider different kinds of solutions depending on the specific relation between the parameters $\varkappa$ and Υ_3. In particular, if one assumes $\varkappa = i\sqrt{\Upsilon_3}$, $\Upsilon_3 > 0$, such that $\varkappa$ be imaginary, then the radial solution will possess an oscillatory part involving sines and cosines in terms of s. However, if one assumes $\Upsilon_3 < 0$ such that $\varkappa$ be real, then the solution will involve an exponential part either growing or decaying with s, depending on the sign of $\varkappa$. Here we consider the latter case:

$$(\Upsilon_3, \varkappa) \in \mathbb{R}, \qquad \Upsilon_3 < 0 < \varkappa. \tag{3.20}$$

In this situation, owing to the relations (3.5), (3.16) and (3.20) the following constraint for the values of the parameters π_{22} and φ_{22}, related with the non-linear with respect to U parts of the effective pressure and non-parallel flow ansatz (3.1), arises

$$\pi_{22} + \frac{3\varphi_{22}m^2}{2} < 0, \tag{3.21}$$

which in the absence of the electric field term becomes $\pi_{22} < 0$. Let us now find the general solution of (3.18) under the above assumptions. Note that for the variable s it holds that $s \geq 0$, since it is defined through the radial helical coordinate r by (3.2). Consequently, $s = 0$ is a regular singular point of (3.18) while $+\infty$ consists of an irregular singularity of this equation. In the present thesis we solve (3.18) analytically in the neighborhood of an ordinary point $\{s_0 \,|\, s_0 \in \mathbb{R}_+,\, s_0 \neq 0,\, +\infty\}$. In this case it is known that if s_0 is an ordinary point of ODE (3.18) and $\bar{\rho}$ denotes the finite distance between s_0 and the nearest zero of the polynomial coefficient $s(s+1)$ of $d^2R(s)/ds^2$, which is $s = 0$, then every solution of (3.18) can be represented by a Taylor series expansion around s_0 of the form

$$R(s) = \sum_{j=0}^{\infty} W_j \chi^j, \quad \chi := s - s_0, \tag{3.22}$$

that converges at least in the open interval $(s_0 - \bar{\rho},\, s_0 + \bar{\rho})$. Such kind of solutions are sufficient for describing helically symmetric plasma tubes of major radius $s_0 = (k^2 r_0^2)/m^2$,

corresponding to the configuration's geometric center, i.e. the helix $(r = r_0, u = u_0)$, and minor radius related with the poloidal cross-section $\bar{\rho} < r_0$, as that illustrated in figure 1.3, for which the origin $s = 0$ (or $r = 0$) lies outside of configurations of interest. In addition, in Appendix C we derive an alternative analytical solution of (3.18) in the neighborhood of the regular singular point $s = 0$ for completeness.

Substituting (3.22), together with its first and second s-derivatives, into the ODE (3.18) yields the following relations

$$\begin{aligned}
& 0 \cdot W_0\chi^{-2} \\
+\ & (0 \cdot W_0 + 0 \cdot W_1)\chi^{-1} \\
+\ & [2t_{00}W_2 + Y_0W_1 + Z_0W_0]\,\chi^0 \\
+\ & [6t_0W_3 + 2(t_{11} + Y_0)W_2 + (Y_1 + Z_0)W_1 + Z_1W_0]\,\chi^1 \\
+\ & [12t_{00}W_4 + 3(2t_{11} + Y_0)W_3 + (2 + 2Y_1 + Z_0)W_2 + (\varepsilon_{22} + Z_1)W_1 + Z_2W_0]\,\chi^2 \\
+\ & \sum_{j=5}^{\infty} \{j(j-1)t_{00}W_j + (j-1)\,[(j-2)t_{11} + Y_0]\,W_{j-1} + [(j-2)(j-3)+ \\
& (j-2)Y_1 + Z_0]\,W_{j-2} + [(j-3)\varepsilon_{22} + Z_1]\,W_{j-3} + Z_2W_{j-4} + \Upsilon_4W_{j-5}\}\,\chi^{j-2} \\
=\ & 0, \qquad (3.23)
\end{aligned}$$

where:

$$\begin{aligned}
t_{00} &:= s_0(1 + s_0), \qquad t_{11} := 1 + 2s_0, \\
Y_0 &:= \varepsilon_{00} + \varepsilon_{11}s_0 + \varepsilon_{22}s_0^2, \qquad Y_1 := \varepsilon_{11} + 2\varepsilon_{22}s_0, \qquad (3.24) \\
Z_0 &:= \varepsilon_{33} + \varepsilon_{44}s_0 + \Upsilon_4 s_0^3, \qquad Z_1 := \varepsilon_{44} + 3\Upsilon_4 s_0^2, \qquad Z_2 := 3\Upsilon_4 s_0.
\end{aligned}$$

In order for equation (3.23) to be satisfied all coefficients of χ^j must vanish; this evidently implies that both W_0 and W_1 remain arbitrary as well as that all coefficients W_j, with $j > 1$, can be expressed as a linear combination of W_0, W_1 of the form $W_j = W_0B_j + W_1C_j$. As a result, the general solution of the radial ODE (3.18) is written in the form

$$R(s) = W_0R_1(s;n) + W_1R_2(s;n), \qquad (3.25)$$

where R_1, R_2 are two linearly independent solutions of (3.18) given by

$$R_1(s;n) = 1 + \sum_{j=2}^{\infty} B_j(j;n)(s - s_0)^j, \qquad R_2(s;n) = \sum_{j=1}^{\infty} C_j(j;n)(s - s_0)^j. \qquad (3.26)$$

In the latter solutions the specific recurrence relations for the power series coefficients $B_j(j;n)$ and $C_j(j;n)$ were calculated as

$$\begin{aligned}
B_2 &= -\frac{Z_0}{2t_{00}}, \\
B_3 &= -\frac{1}{6t_{00}}\,[2(t_{11} + Y_0)B_2 + Z_1]\,, \\
B_4 &= -\frac{1}{12t_{00}}\,[3(2t_{11} + Y_0)B_3 + (2 + 2Y_1 + Z_0)B_2 + Z_2]\,, \\
B_5 &= -\frac{1}{20t_{00}}\,[4(3t_{11} + Y_0)B_4 + (6 + 3Y_1 + Z_0)B_3 + (2\varepsilon_{22} + Z_1)B_2 + \Upsilon_4]\,, \\
B_6 &= -\frac{1}{30t_{00}}\,[5(4t_{11} + Y_0)B_5 + (12 + 4Y_1 + Z_0)B_4 + (3\varepsilon_{22} + Z_1)B_3 + Z_2B_2]\,, \\
B_j &= -\frac{1}{t_{00}j(j-1)}\,\{(j-1)\,[t_{11}(j-2) + Y_0]\,B_{j-1}+ \\
&\quad + [(j-2)(j-3) + (j-2)Y_1 + Z_0]\,B_{j-2} + [(j-3)\varepsilon_{22} + Z_1]\,B_{j-3}+ \\
&\quad + Z_2B_{j-4} + \Upsilon_4B_{j-5}\}\,, \qquad j \geq 7, \qquad (3.27)
\end{aligned}$$

and

$$
\begin{aligned}
C_1 &= 1,\\
C_2 &= -\frac{Y_0}{2t_{00}},\\
C_3 &= -\frac{1}{6t_{00}}\left[2(t_{11}+Y_0)C_2 + Y_1 + Z_0\right],\\
C_4 &= -\frac{1}{12t_{00}}\left[3(2t_{11}+Y_0)C_3 + (2+2Y_1+Z_0)C_2 + \varepsilon_{22} + Z_1\right],\\
C_5 &= -\frac{1}{20t_{00}}\left[4(3t_{11}+Y_0)C_4 + (6+3Y_1+Z_0)C_3 + (2\varepsilon_{22}+Z_1)C_2 + Z_2\right],\\
C_6 &= -\frac{1}{30t_{00}}\left[5(4t_{11}+Y_0)C_5 + (12+4Y_1+Z_0)C_4 + (3\varepsilon_{22}+Z_1)C_3 + Z_2C_2 + \Upsilon_4\right],\\
C_j &= -\frac{1}{t_{00}j(j-1)}\left\{(j-1)\left[t_{11}(j-2)+Y_0\right]C_{j-1} + \right.\\
&\quad + \left[(j-2)(j-3)+(j-2)Y_1+Z_0\right]C_{j-2} + \left[(j-3)\varepsilon_{22}+Z_1\right]C_{j-3} +\\
&\quad \left. + Z_2C_{j-4} + \Upsilon_4 C_{j-5}\right\}, \qquad j \geq 7.
\end{aligned}
\tag{3.28}
$$

Therefore, we have found the general solution of the homogeneous equation (3.10), valid for arbitrary values of the separation constant n; this is

$$
U_h(s;u;n) = s^n e^{-\varkappa s}\left[W_0R_1(s;n) + W_1R_2(s;n)\right]\left[l_1b_1\cos\left(\frac{2nu}{m}\right) + l_2\sin\left(\frac{2nu}{m}\right)\right]. \tag{3.29}
$$

For further treatment it is convenient to restrict the separation constant n to positive integer values, $n \in \mathbb{Z}_+$. Therefore, by applying the linear superposition principle the general solution of (3.10), periodic in u, is given by

$$
\begin{aligned}
U_h(s,u) = \sum_{n=1}^{n_m} s^n &\left[a_nR_1(s;n)\cos\left(\frac{2nu}{m}\right) + b_nR_1(s;n)\sin\left(\frac{2nu}{m}\right) + \right.\\
&\left. + c_nR_2(s;n)\cos\left(\frac{2nu}{m}\right) + d_nR_2(s;n)\sin\left(\frac{2nu}{m}\right)\right]e^{-\varkappa s},
\end{aligned}
\tag{3.30}
$$

where n_m is an arbitrary upper bound on the linear superposition and a_n, b_n, c_n, d_n are arbitrary coefficients to be determined.

Then we proceed to find a special solution of the inhomogeneous equation (3.11). First we write this equation as

$$
s(s+1)\frac{d^2U_p(s)}{ds^2} + \frac{dU_p(s)}{ds} + \left(\sum_{i=0}^{3}K_is^i\right)U_p(s) = \left(\sum_{i=0}^{3}M_is^i\right), \tag{3.31}
$$

where

$$
\begin{aligned}
K_0 &:= \lambda_{11}^2 + \lambda_{11} + \lambda_{22} + \lambda_{33},\\
K_1 &:= \lambda_{11}^2 + 2\lambda_{22} + 3\lambda_{33},\\
K_2 &:= \lambda_{22} + 3\lambda_{33},\\
K_3 &:= \lambda_{33},\\
M_0 &:= -\left(\tau_{11} + \tau_{22} + \tau_{33} + \tau_{11}\lambda_{11}\right),\\
M_1 &:= -\left(2\tau_{22} + 3\tau_{33} + \tau_{11}\lambda_{11}\right),\\
M_2 &:= -\left(\tau_{22} + 3\tau_{33}\right),\\
M_4 &:= -\tau_{33}.
\end{aligned}
\tag{3.32}
$$

Following again a procedure as that of solving the respective homogeneous equation we assume a power series expansion for $U_s(s)$, around the regular point s_0, of the form

$$U_p(s) = \sum_{j=0}^{\infty} D_j \chi^j, \qquad \chi = s - s_0. \tag{3.33}$$

Upon substitution of (3.33) into (3.31) yields

$$\begin{aligned}
& 0 \cdot D_0 \chi^{-2} \\
+ \; & (0 \cdot D_0 + 0 \cdot D_1)\chi^{-1} \\
+ \; & (2t_{00}D_2 + D_1 + H_0 D_0 - L_0)\,\chi^0 \\
+ \; & [6t_{00}D_3 + 2(t_{11}+1)D_2 + H_0 D_1 + H_1 D_0 - L_1]\,\chi^1 \\
+ \; & [12t_{00}D_4 + 3(2t_{11}+1)D_3 + (2+H_0)D_2 + H_1 D_1 + H_2 D_0 - L_2]\,\chi^2 \\
+ \; & [20t_{00}D_5 + 4(3t_{11}+1)D_4 + (6+H_0)D_3 + H_1 D_2 + H_2 D_1 + H_3 D_0 - L_3]\,\chi^3 \\
+ \; & \sum_{j=0}^{\infty} \{(j+6)(j+5)t_{00}D_{j+6} + (j+5)\,[(j+4)t_{11}+1]\,D_{j+5} + [(j+4)(j+3)+ \\
& H_0]\,D_{j+4} + H_1 D_{j+3} + H_2 D_{j+2} + H_3 D_{j+1}\}\,\chi^{j+4} \\
= \; & 0,
\end{aligned} \tag{3.34}$$

where the parameters H_i and L_i, $i = 0, 1, 2, 3$, are defined as

$$\begin{aligned}
H_0 &:= K_0 + K_1 s_0 + K_2 s_0^2 + K_3 s_0^3, \\
H_1 &:= K_1 + 2K_2 s_0 + 3K_3 s_0^2, \\
H_2 &:= K_2 + 3s_0 K_3, \\
H_3 &:= K_3, \\
L_0 &:= M_0 + M_1 s_0 + M_2 s_0^2 + M_3 s_0^3, \\
L_1 &:= M_1 + 2M_2 s_0 + 3M_3 s_0^2, \\
L_2 &:= M_2 + 3s_0 M_3, \\
L_3 &:= M_3.
\end{aligned} \tag{3.35}$$

From equation (3.34) it follows that both D_0 and D_1 remain arbitrary and thus, without loss of genereality we choose: $D_0 = 0$, $D_1 = 1$. Thus, we find that

$$U_p(s) = \sum_{j=1}^{\infty} D_j (s - s_0)^j \tag{3.36}$$

consists of a special solution of the inhomogeneous ODE (3.11), with coefficients D_j satisfying the following recursion relations:

$$\begin{aligned}
D_1 &= 1, \\
D_2 &= -\frac{1}{2t_{00}}\,(1 - L_0)\,, \\
D_3 &= -\frac{1}{6t_{00}}\,[2(t_{11}+1)D_2 + H_0 - L_1]\,, \\
D_4 &= -\frac{1}{12t_{00}}\,[3(2t_{11}+1)D_3 + (2+H_0)D_2 + H_1 - L_2]\,, \\
D_5 &= -\frac{1}{20t_{00}}\,[4(3t_{11}+1)D_4 + (6+H_0)D_3 + H_1 D_2 + H_2 - L_3] \\
D_j &= -\frac{1}{t_{00}j(j-1)}\,\{(j-1)\,[t_{11}(j-2)+1]\,D_{j-1} + [(j-2)(j-3) + H_0]\,D_{j-2} \\
&\quad + H_1 D_{j-3} + H_2 D_{j-4} + H_3 D_{j-5}\}\,, \qquad j \geq 6.
\end{aligned} \tag{3.37}$$

To summarize, the general solution of the linearized GGS equation (3.3) for the flux function U with respect to the ansatz (3.1) has the form

$$U(r,u) = \sum_{n=1}^{n_m} s^n \left[a_n R_1(s;n) \cos\left(\frac{2nu}{m}\right) + b_n R_1(s;n) \sin\left(\frac{2nu}{m}\right) + \right.$$
$$\left. + c_n R_2(s;n) \cos\left(\frac{2nu}{m}\right) + d_n R_2(s;n) \sin\left(\frac{2nu}{m}\right) \right] e^{-\varkappa s} + U_p(s), \tag{3.38}$$

in which the explicit forms of the power series R_1, R_2, U_p are given by the relations (3.26)-(3.28) and (3.36)-(3.37), respectively. As concerns the free coefficients a_n, b_n, c_n and d_n, their values will be determined by imposing boundary (shaping) conditions, in connection with the construction of pertinent, helically symmetric, equilibrium configurations.

3.1.1 Construction of straight helically symmetric equilibrium configurations

The construction of a specific equilibrium relies on the values of the free coefficients a_n, b_n, c_n, d_n in the general solution (3.38). These values are specified by the imposure of appropriate boundary (shaping) conditions related with physical and/or geometrical characteristics of desirable configurations. In this work we are interested in "modeling" equilibria pertinent to stellarator devices. However, the flux function $U(r,u)$ is a helical scalar function, and as noted before, helical symmetry corresponds to 2D 'straight stellarators', of constant torsion without toroidicity, and not to the actual 3D devices. To this end we have to clarify that the term "modeling" here actually refers to using values of geometrical quantities, e.g. major and minor radius, in connection with specific stellarator-device characteristics.

Consider a spatial curve described by the vector

$$\mathbf{r}_0(\ell) = \mathbf{r}_0(r = r_0 = \text{const.}, u = u_0 = \text{const.}, \zeta(\ell) = m q_0^{1/2} \ell) \tag{3.39}$$

in helical coordinates, where ℓ is the differential arc-length along this helix of reference (see Appendix B.3). Employing the Frenet-Serret formulas we find that the tangent vector to this helix is defined by

$$\mathbf{t}(\ell) = \frac{\mathbf{h}_0(\ell)}{|\mathbf{h}_0|}, \tag{3.40}$$

where $\mathbf{h}_0 := \mathbf{h}_{|_{r_0,u_0}}$; also, we obtain the first and second normal vectors to the helical curve

$$\mathbf{n}(\ell) = -\mathbf{g}^r(\ell), \qquad \mathbf{b}(\ell) = -r_0\sqrt{q_0}\mathbf{g}^u(\ell), \tag{3.41}$$

where $q_0 := q(r = r_0)$. These vectors define the perpendicular plane $(\mathbf{n}, \mathbf{b})$ on each point of this helix, henceforth called poloidal plane [198]. Then, the position of each point of the poloidal plane, originated at a specific length ℓ, is described by the system of intrinsic coordinates (x_n, x_b, ℓ) as:

$$\mathbf{r}(x_n, x_b, \ell) \;:=\; \mathbf{r}_0(\ell) + \underbrace{x_n \mathbf{n}(\ell) + x_b \mathbf{b}(\ell)}_{\text{poloidal cross-section}}. \tag{3.42}$$

It is clear that x_n is the distance from the helix $(r = r_0 = \text{const.}, u = u_0 = \text{const.})$ in the direction $\mathbf{n}$ and x_b measures the distance from that helix in the direction $\mathbf{b}$; in this sense, the coordinates x_n, x_b define a "Cartesian" plane at each point $\ell = \ell_0$ (origin), and thus, moving along the helix. Intrinsic coordinates are useful when imposing a specific boundary and/or for considerations based on expansions near the magnetic axis [198]. We note that (x_n, x_b, ℓ) do not form an orthogonal coordinate system (see Appendix B.3), and although these

coordinates are useful when imposing rectangular boundaries, for circular or elliptical cross-sectional shapes one has to consider alternative sets of coordinates. For such considerations, following the arguments made in [62, 199, 200] we employ the "generalized intrinsic polar coordinates" (ρ^*, ω) defined by the transfomations

$$\begin{aligned} x_n &= \rho^* \cos(\omega - \tau_0 \ell), \\ x_b &= \rho^* \sin(\omega - \tau_0 \ell), \end{aligned} \tag{3.43}$$

where ρ^* is the distance of any point on the poloidal plane from the reference helix, $\mathbf{r}_0$, of torsion $\tau_0 = kmq_0$, and ω can be interpreted as a rotational angle in the poloidal plane which is related with the usual polar coordinate θ, measured from the principal normal $\mathbf{n}$, as

$$\omega = \theta + \int_0^\ell \tau_0 d\ell. \tag{3.44}$$

In contrast with the usual intrinsic polar coordinates (ρ^*, θ, ℓ) which are not orthogonal, the generalized intrinsic polar ones (ρ^*, ω, ℓ) form an orthonormal system of coordinates with metric [62, 199, 200]:

$$d\mathbf{r} \cdot d\mathbf{r} = d\rho^{*2} + \rho^{*2} d\omega^2 + [1 - \kappa\rho^* \cos(\omega - \tau_0 \ell)]^2 d\ell^2, \tag{3.45}$$

where κ is the curvature of the helix of reference; however, the two systems of intrinsic polar coordinates become identical at $\ell = 0$. The coordinates (ρ^*, ω, ℓ) are widely employed in hydrodynamics for investigations of the fluid flow through helically symmetric pipes of circular cross-sectional shape [33,35,41,44,62,65,66]. A detailed description of that coordinate system is given in Appendix B.3.1.

The transformation between the helical coordinates (r, u) and the intrinsic coordinates (ρ^*, ω, ℓ) is:

$$\begin{aligned} r &= \sqrt{[r_0 - \rho^* \cos(\omega - \tau_0 \ell)]^2 + \rho^{*2} \sin^2(\omega - \tau_0 \ell) m^2 q_0}, \\ u &= m \arccos\left[\frac{(r_0 - \rho^* \cos(\omega - \tau_0 \ell)) \cos(k\sqrt{q_0}\ell)}{r(\rho^*, \omega, \ell)} + \right. \\ &\quad \left. \frac{\rho^* \sin(\omega - \tau_0 \ell) m \sqrt{q_0} \sin(k\sqrt{q_0}\ell)}{r(\rho^*, \omega, \ell)} \right] - k\sqrt{q_0}(m\ell + k r_0 \rho^* \sin(\omega - \tau_0 \ell)). \end{aligned} \tag{3.46}$$

Based on the above transformation one can fully determine the solution (3.38) by imposing boundary conditions pertinent to fusion magnetic configurations, i.e. of the form $U(\rho_0^*, \omega, \ell) = U_b =$ const. in circular geometry, implying that the flux function takes a constant value on a circular boundary of radius $\rho^* = \rho_0^*$ as well as that the flow and the pressures vanish thereon. Such conditions involve the free parameters r_0, k, m and ρ_0^* the values of which may be assigned in connection with geometrical characteristics of specific stellarator devices. As noted earlier, every stellarator device consists of a specific number of field periods, denoted by N, with the shape of the cross-section being changed with the toroidal angle in each of these field periods composing the closed toroid. In fact, in several stellarators the configuration becomes poloidally symmetric only in toroidal angles π/N. However, for a 'straight stellarator' the equivalent N should satisfy the relation $2\pi R_0 = N\eta_0$, where $\eta_0 = 2\pi|m/k|$ is the straight helicoidal pitch length and R_0 corresponds to the major radius of the respective 3D device. Due to this analogy, we shall relate the parameters ρ_0^* and r_0 with the respective minor and major radius of a stellarator of interest; in this sense the helix of reference, $\mathbf{r}_0$, denotes the geometrical center of the corresponding 'straight stellarator' equilibrium to be constructed. In such a system

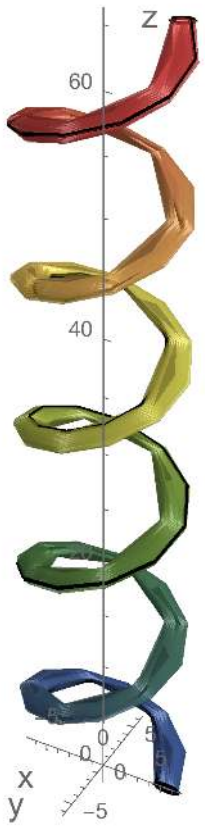

Figure 3.1: The straight helically symmetric equilibrium configuration of circular cross-section obtained as a solution of the GGS equation (2.46) with W7-X parameters as described in the text.

because of the helical symmetry the poloidal cross-section shaping remains invariant along the direction of symmetry (helical axis) unlike the toroidal variation of the respective poloidal shaping in 3D equilibria. Therefore, a cross-section obtained from the pertinent boundary conditions at a specific arc-length ℓ_0, based upon the transformation $r(\rho_0^*, \ell_0, \omega)$, $u(\rho_0^*, \ell_0, \omega)$ in (3.46), will remain ℓ-invariant moving in the helical direction[2].

In order to fully determine the function U we choose $n_m = 6$ in (3.38), and thus we need to solve a system of twenty four algebraic equations with equal number of unknown coefficients, a_1, a_2, ..., b_1, ..., b_6, c_1, ..., d_1, ..., d_6, arrising from the imposure of Dirichlet-type boundary conditions in circular geometry, of the form

$$U[r(\rho_0^*, \ell_0, \omega),\, u(\rho_0^*, \ell_0, \omega)] = U_b, \qquad \tau_0 \ell_0 \leq \omega \leq 2\pi + \tau_0 \ell_0. \tag{3.47}$$

Figure 3.1 shows an example of the straight helically symmetric configuration constructed having the following W7-X characteristics [201] (in pertinent SI units): $r_0 = 5.5$, $\rho_0^* = 0.53$ and $m = 0.1$, $k = 0.05$ such that $N = 5$, $\tau_0 = 0.0584$; also we have choosen to perform the calculations at $\ell_0 = \eta_0/2 = 6.283$. The constructed configuration is composed of nested helicoidal magnetic surfaces of circular cross-sectional shape and has a finite length (in the ζ-direction) equal to $L = 5\eta_0$. The up-down symmetric cross-section of the constructed equilibria are shown in figure 3.2 both on the plane (r, u) and on the poloidal plane $(\mathbf{n}, \mathbf{b})$. The values

[2]In general the coordinates ℓ, ρ^* can effectively desrcibe an unbounded region varying within the limits $-\infty < \ell < \infty$, $0 \leq \rho^* < \infty$. However, to describe a 'straight stellarator' bounded configuration extending radially up to a finite helicoidal surface (boundary) and of finite length, L, we choose $0 \leq \ell \leq L$ and $0 \leq \rho^* \leq \rho_0^* < r_0$.

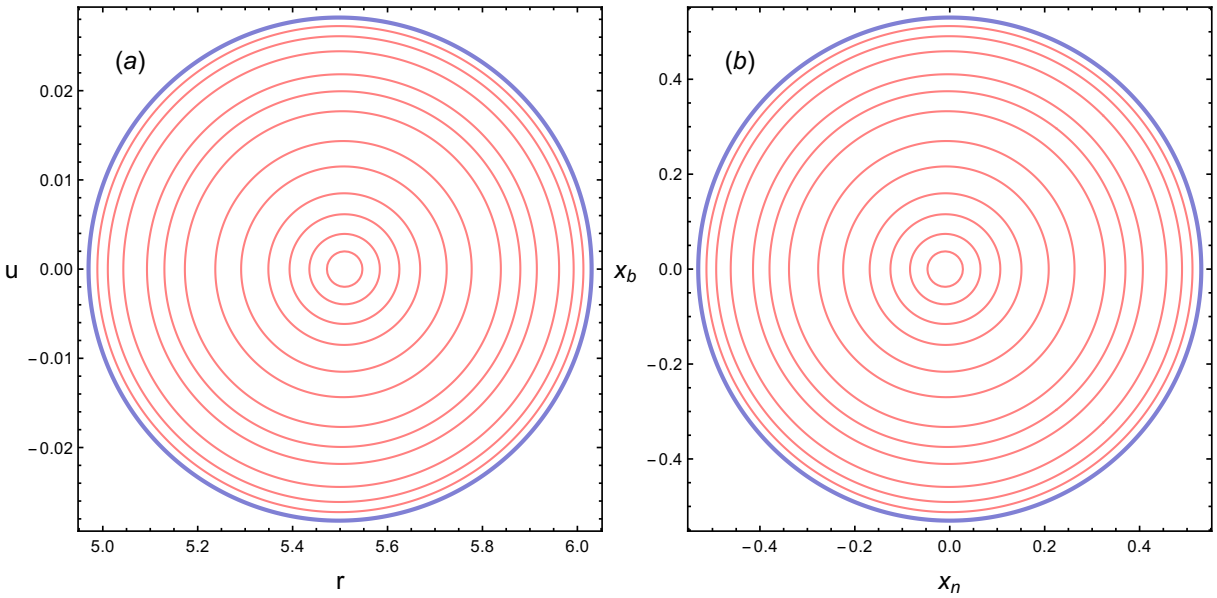

Figure 3.2: Poloidal cut of the nested helicoidal magnetic surfaces of up-down symmetric circular cross-section of the equilibrium configuration obtained with W7-X characteristics as prescribed in the text, on (a) the plane (r, u) and (b) the poloidal plane $(\mathbf{n}, \mathbf{b})$. The boundary represented by the thick-blue line was prescribed analytically.

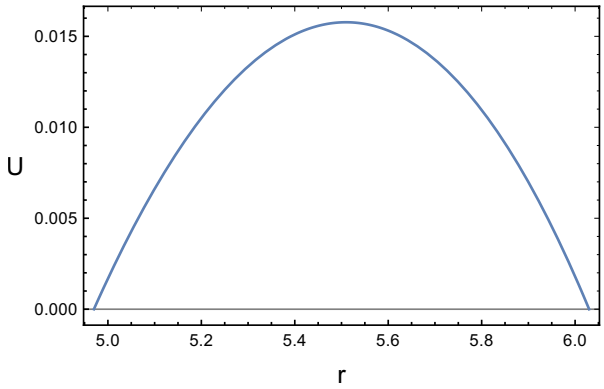

Figure 3.3: The flux function $U(r, u = u_a)$ on the (r, u)-plane for the equilibrium of figure 3.2.

of the other constants used are (in pertinent SI units): $\chi_{00} = 0.8, \chi_{11} = -0.002$, $\varphi_{11} = 0.5$, $\varphi_{22} = -0.08$, $\pi_{11} = 1.528$, $\pi_{22} = -0.103$ and $U_b = 0$. Therefore, the flux function U vanishes on the boundary while it peaks on the magnetic axis, where $U_a = 0.01577$. The magnetic axis on the $(\mathbf{n}, \mathbf{b})$ plane is at the position of $(x_{n_a} = -0.0097, x_{b_a} = -5.67 \times 10^{-7})$, while on the (r, u) plane it is at $(r_a = 5.5097, u_a = 3.02 \times 10^{-8})$. The variation of U with respect to the radial coordinate r, on the plane of magnetic axis, is shown in figure 3.3. We note that the convergence of the power series appearing in the general solution was checked by extensive numerical tests; for the construction of the specific equilibrium of figure 3.2 we have included up to fifty terms in each of those series.

The intrinsic polar coordinates ρ^*, ω (θ) are usually employed for investigating configurations the magnetic surfaces of which possess circular cross-sections; in toroidal geometry these coordinates are connected with the so-called Shafranov coordinates [202]. However, since elongation and triangularity play an important role on confinement both in tokamak [203, 204] and stellarator [205, 206] devices, one may resort to more general coordinate systems which permit the control of these geometrical parameters, and thus, greater shaping flexibility. Here we introduce such a system of intrinsic coordinates (ρ^*, ω, ℓ) related with the coordinates

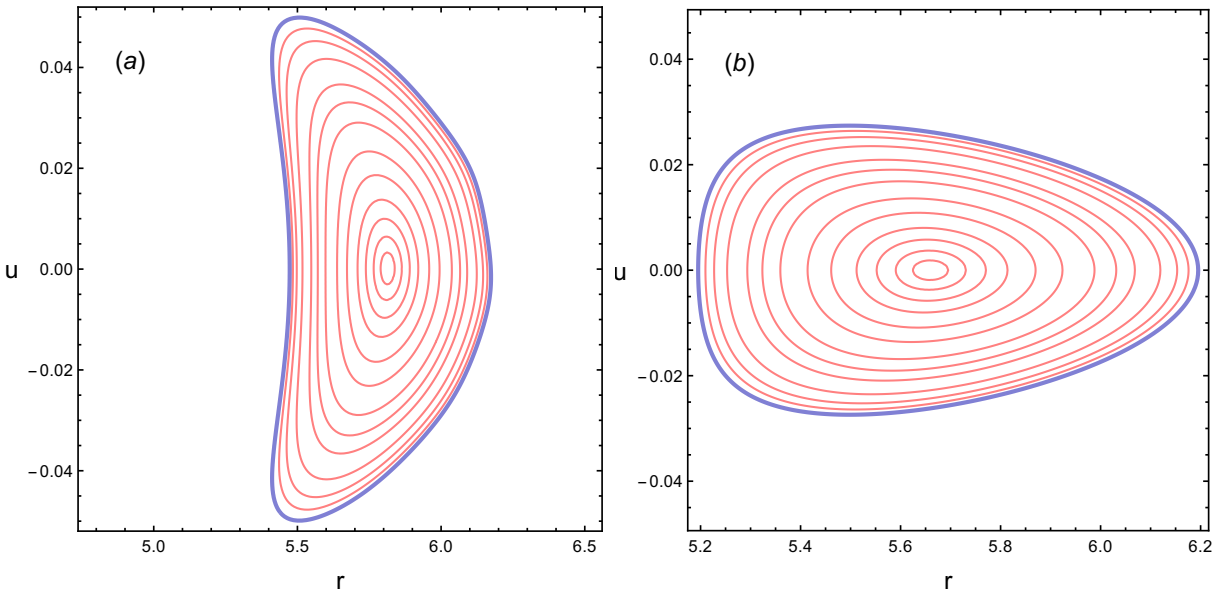

Figure 3.4: Up-down symmetric equilibrium of (a) banana- and (b) triangular- like cross-section-shape with W7-X geometrical characteristics, on the plane (r, u). The boundaries represented by the thick-blue lines were prescribed analytically.

(x_n, x_b) through the transformation

$$\begin{aligned} x_n &= \rho^*[1+\delta(\rho^*)\cos(\omega-\tau\ell)]\cos(\omega-\tau\ell), \\ x_b &= e_1\rho^*\sin(\omega-\tau\ell), \end{aligned} \tag{3.48}$$

where

$$\delta(\rho^*) := \gamma_1 + \gamma_2(\rho^*)^{\beta_1}, \tag{3.49}$$

and e_1, γ_1, γ_2 and β_1 are arbitrary parameters related with the elongation and triangularity of the magnetic surfaces. These coordinates do not form an orthogonal system; however, for $\gamma_1 = \gamma_2 = 0$ and $e_1 = 1$ they reduce to the orthogonal ones given in (3.43). The coordinate system (3.48) is simpler than others employed for similar considerations, i.e. in describing D-shaped magnetic surfaces [203, 204], because it does not involve highly non-linear composite trigonometric functions of the form $\cos(\sin(f(\varepsilon,\theta))$, where the parameter ε is connected with the triangularity. These coordinates consist of a more general form of the ones introduced in [207] to study the impact of the elongation and the triangularity on respective axisymmetric equilibria ($\tau = 0$), i.e. they reduce to the ones in [207] for $\gamma_2 = 0$, in which case the parameter γ_1 is indeed the triangularity. Note that in general alternative functional forms for $\delta(\rho^*)$ may be chosen.

Following the same procedure as above, we have constructed up-down symmetric equilibria of banana- and triangular-like cross sectional shape, with W7-X parameters, by employing the relations (3.48). The magnetic surfaces of these equilibria are shown in figure 3.4. For the configuration of banana-like cross-section presented in figure 3.4(a) we have used the following values: $\rho_0^* = 0.35$, $e_1 = 2.68$, $\gamma_1 = -0.45$, $\gamma_2 = -0.8$, $\beta_1 = 1/2$, while for the triangular-like equilibrium of figure 3.4(b) the values: $\rho_0^* = 0.53$, $e_1 = 1.03$, $\gamma_1 = -0.15$, $\gamma_2 = -0.34$ and $\beta_1 = 1/2$, respectively. We note that the analytical solutions obtained here permit the construction of equilibria with desirable poloidal cross-section-boundary shape by appropriately assigning the arbitrary constants in the general solution (3.38) as well as in the relations (3.43), (3.48) related with the applied boundary conditions. This shaping choice is as flexible as in

the numerical equilibrium construction; an indication is that the configurations of figure 3.4 remarkably resemble the symmetric ones of W7-X on the poloidal plane corresponding to zero and $\pi/5$ toroidal angles [162] (figures 2(a) and 2(c) therein obtained with consistent ANIMEC equilibrium), as it was also obtained by the VMEC code [208] (figure 6 therein). However, as already mentioned in the helically symmetric equilibria constructed in the framework of this thesis, pertinent to 'straight stellarators', the poloidal cross-section remains invariant along the direction of the symmetry, irrespective of its specific shape.

Finally, it may be noted that we can obtain a more instructive relation for $\mathcal{Q}$ than (2.60), in circular geometry with the use of the intrinsic coordinates (ρ^*, ω) given in (3.43). In this coordinate system the length element of the poloidal cross section at any point $\ell = \text{const.}$ is written in the form (see equation (3.45)):

$$d\mathbf{r}\cdot d\mathbf{r} := dl_p^2 = d\rho^{\star 2} + \rho^{\star 2} d\omega^2 \Rightarrow dl_p = d\omega \left[\rho^{\star 2} + \left(\frac{d\rho^\star}{d\omega}\right)^2\right]^{1/2}. \tag{3.50}$$

In particular, on a streamline $U(\rho^\star, \omega, \ell) = \text{const.}$ it holds

$$dU = \frac{\partial U}{\partial \rho^\star} d\rho^\star + \frac{\partial U}{\partial \omega} d\omega + \frac{\partial U}{\partial \ell} d\ell = 0, \tag{3.51}$$

and thus, for a specific poloidal cross section $\ell = \ell_0 = \text{const.}$ the above relation yields

$$\frac{d\rho^\star}{d\omega} = -\frac{U_\omega}{U_{\rho^\star}}, \tag{3.52}$$

where $U_\omega = \frac{\partial U}{\partial \omega}$ and $U_{\rho^\star} = \frac{\partial U}{\partial \rho^\star}$. As a result, one can calculate the profile of the safety factor by performing an integration in the angle ω around the poloidal cross-section, once first all equilibrium quantities are expressed in terms of intristic coordinates, by employing the following relationship:

$$\mathcal{Q} = \frac{1}{\eta N}\int_{\tau\ell_0}^{2\pi+\tau\ell_0} \frac{B^\zeta(\rho^\star,\omega)}{B_p(\rho^\star,\omega)}\left[\rho^{\star 2} + \left(\frac{U_\omega}{U_{\rho^\star}}\right)^2\right]^{1/2} d\omega. \tag{3.53}$$

3.1.2 Reduction to close form analytical solutions

Ansatz (3.1) consists of the most generic one under which the GGS equation (2.46) remains linear. Under those generic profiles for the free functions contained therein we have obtained a class of analytic solutions of the GGS equation in terms of generalized power series and constructed equilibria with pressure anisotropy and incompressible flow of arbitrary direction in general. However, when one or more of the free parameters in the ansatz (3.1) vanish the solution to the linearized GGS equations can be expressed in terms of well-known analytical mathematical functions. Such special cases are presented below.

Linear profiles ($\pi_{22} = \varphi_{22} = 0$)

This case corresponds to linear profiles for all surface functions $\mathcal{I}(U)$, $\mathcal{F}(U)$ and $\mathcal{P}_s(U)$. We shall also assume that $\pi_{00} = \pi_{11} U_b$ and $\varphi_{00} = \varphi_{11} U_b$, such that both the flow and the static pressure vanish on the plasma boundary. Under these profiles, the radial ODE (3.15) for the function $H(s)$ reduces to

$$s^2(1+s)\frac{d^2H(s)}{ds^2} + s\frac{dH(s)}{ds} + \left(\sum_{i=0}^{2} \Upsilon_i s^i\right) H(s) = 0, \tag{3.54}$$

where Υ_i, $i = 1, ..2$ are given by the respective forms (3.16) for $\lambda_{22} = \lambda_{33} = 0$. ODE (3.54) admits the exact general solution, in terms of the first order Bessel functions of the first and second kind J_{2n} and Y_{2n}, of the form

$$H(s;n) = \nu_1 H^1(s;n) + \nu_2 H^2(s;n), \tag{3.55}$$

$$H^1 = 2^{3n+2}(2n)!\frac{(\lambda_{11}^2 - n^2)^{-n/2}}{n+\lambda_{11}} s^{1-\lambda_{11}} \frac{d}{ds}\left[s^{\lambda_{11}} J_{2n}\left(\sqrt{4s(\lambda_{11}^2 - n^2)}\right)\right], \tag{3.56}$$

$$H^2 = \frac{n}{2^n|2n-1|!}\frac{(\lambda_{11}^2 - n^2)^{n/2}}{n-\lambda_{11}} s^{1-\lambda_{11}} \frac{d}{ds}\left[s^{\lambda_{11}} Y_{2n}\left(\sqrt{4s(\lambda_{11}^2 - n^2)}\right)\right], \tag{3.57}$$

valid for $\lambda_{11}^2 \neq n^2$. Thus, is this case the general solution of the GGS equation (2.46) is determined by the relations (3.9), (3.12), (3.14) and (3.55)-(3.57), where U_p is any solution satisfying the limiting form of ODE (3.31), (3.32) for $\lambda_{22} = \lambda_{33} = 0$. We note that the exact solution (3.55)-(3.57) was previously obtained in [76] upon solving the respective static, isotropic helically symmetric GGS (JFKO equation). However, we have succesfully showed that this solution is also valid for pressure anisotropic, stationary equilibria, and indeed for flow of arbitrary direction since in our case $\varphi_{11} \neq 0$. In the limit of parallel flows, $\varphi_{11} = 0$, implying that $\tau_{33} = 0$, an exact expression for the particular solution can be found of the form

$$U_p(s) = \frac{\tau_{22} - \lambda_{11}(\lambda_{11}\tau_{11} + \tau_{22}(1+s))}{\lambda_{11}^3}. \tag{3.58}$$

$\mathcal{I} = \text{constant}$ $(\chi_{11} = \varphi_{22} = 0)$

In this case, in the absence of pressure anisotropy and flow $(\sigma_d = M_p = 0)$ it follows that the quantity X related with the integral (2.33) is constant. In addition, the function $\mathcal{F}(U)$, related with the non-parallel component of the flow, becomes linear in U, while the static effective pressure has the explicit form given in (3.1). Again we assume that these quantities vanish on the plasma boundary, i.e. $\varphi_{00} = \varphi_{11}U_b$, $\pi_{00} = (\pi_{11} - \pi_{22}U_b)U_b$. On the basis of these profiles the radial ODE (3.15) for the function $H(s)$ reduces to

$$s^2(1+s)\frac{d^2H(s)}{ds^2} + s\frac{dH(s)}{ds} + (1+s)^2(\lambda_{22}s - n^2)H(s) = 0, \tag{3.59}$$

since it follows that $\lambda_{11} = \lambda_{33} = 0$. ODE (3.59) admits the exact general solution of the form

$$H(s;n) = \nu_1 H^1(s;n) + \nu_2 H^2(s;n), \tag{3.60}$$

$$H^1 = s^n e^{ns}\frac{d}{ds}\left[e^{-s(n+i\sqrt{\lambda_{22}})}{}_1F_1\left(\frac{(n+i\sqrt{\lambda_{22}})^2}{2i\sqrt{\lambda_{22}}}, 2n, i\sqrt{\lambda_{22}}s\right)\right], \tag{3.61}$$

$$H^2 = s^n e^{ns}\frac{d}{ds}\left[e^{-s(n+i\sqrt{\lambda_{22}})}\widetilde{U}\left(\frac{(n+i\sqrt{\lambda_{22}})^2}{2i\sqrt{\lambda_{22}}}, 2n, i\sqrt{\lambda_{22}}s\right)\right], \tag{3.62}$$

valid for $\lambda_{11}^2 \neq n^2$, where ${}_1F_1(\ell, n, s)$ is the confluent hypergeometric function and $\widetilde{U}(\ell, n, s)$ are two independent solutions of the Kummer's differential equation:

$$s\frac{d^2W(s)}{ds^2} + (n-s)\frac{dW(s)}{ds} - \ell W(s) = 0. \tag{3.63}$$

Thus, is this case the general solution of the GGS equation (2.46) is determined by the relations (3.9), (3.12), (3.14) and (3.60)-(3.62), where U_p is any solution satisfying the limiting form

of ODE (3.31), (3.32) for $\lambda_{11} = \lambda_{33} = 0$. Note that for $\pi_{22} = 0$, corresponding to linear dependence of $\mathcal{P}_s$ on U, the linearly independent radial homogeneous solutions (3.61), (3.62) reduce to

$$H^1(s;n) = s^n e^{ns}, \qquad H^2(s;n) = s^{-n} e^{-ns}. \tag{3.64}$$

The above exact solutions (3.60)-(3.64) was previously obtained in [76] upon solving the respective static, isotropic helically symmetric GGS (JFKO equation). However, we have again shown that this solution is also valid for anisotropic, stationary equilibria with flow of arbitrary direction, since in our case $\varphi_{11} \neq 0$.

A model for astrophysical jets ($\chi_{00} = \pi_{11} = \mathcal{F} = 0$, $\pi_{00} \neq 0$)

In this case the profiles for the free functions in (3.1) simply become[3]

$$\begin{aligned} \mathcal{I}(U) &:= \chi_{11} U, \\ \mu_0 \mathcal{P}_s(U) &:= \pi_{00} + \pi_{22} U^2, \end{aligned} \tag{3.65}$$

where the absence of the electric field term ($\mathcal{F} = 0$) implies equilibria with flow parallel to the magnetic field. Under the substitutions: $m \to -m$, $k = -1$ and $\pi_{22} = -2w^2$, where w is also a free parameter, on account of the ansatz (3.65) the helically symmetric GGS equation (2.46) reduces to the following linearized form:

$$\frac{1}{r^2}\frac{\partial^2 U}{\partial u^2} + \frac{1}{r}\frac{\partial}{\partial r}\left(\frac{r}{r^2+m^2}\frac{\partial U}{\partial r}\right) + \left(\frac{\chi_{11}^2}{r^2+m^2} + \frac{2\chi_{11} m}{(r^2+m^2)^2} - 4w^2\right) U = 0. \tag{3.66}$$

The above homogeneous PDE was solved analytically in [209] and the exact solution, polynomial in the variable r, obtained therein is

$$U_{\delta\mu\nu}(r, u = m\phi - z) = e^{-wr^2}\{f_\delta H_{0\delta}(\upsilon) + r^\mu H_{\mu\nu}(\upsilon)[c_{\mu\nu}\cos(\mu u/m) + d_{\mu\nu}\sin(\mu u/m)]\}, \tag{3.67}$$

where δ, μ, ν are arbitrary integers ≥ 0 satisfying the condition $2\delta > 2\nu + \mu$; f_δ, $c_{\mu\nu}$, $d_{\mu\nu}$ are arbitrary coefficients, and $\upsilon = 2wr^2$. The form of the polynomial functions $H_{\mu\nu}(\upsilon)$ involve derivatives of the Laguerre polynomials $L_{\mu+\nu}(\upsilon)$ as

$$\begin{aligned} H_{\mu\nu}(\upsilon) &= \frac{d^\mu}{d\upsilon^\mu} L_{\mu+\nu}(\upsilon) - R_{\mu\nu}\upsilon \frac{d^{\mu+1}}{d\upsilon^{\mu+1}} L_{\mu+\nu}(\upsilon), \\ \gamma_{\mu\nu} &= \frac{1}{2\mu\nu}[4(\delta-\nu) - \mu - \sqrt{(4\delta-\mu)^2 - 16\nu\delta}], \end{aligned} \tag{3.68}$$

e.g see equations (3.7)-(3.8) in [209], and $H_{0\delta}$ is the respective polynomial for $\mu \to 0$, $\nu = \delta \neq 0$. On account of solution (3.67), different classes of exact helically symmetric MHD equilibria describing astrophysical jets with isotropic pressure ($\sigma_d = 0$) were constructed in [209]. For such kind of equilibria both the magnetic field, the flow velocity and the current density fall rapidly to zero at $r \to \infty$, while the pertinent isotropic pressure takes a limiting constant value therein. As a result, the above solution is not pertinent in describing magnetically confined fusion related plasmas. We have to note that solution (3.67) can also accurately describe helically symmetric CGL anisotropic pressure equilibria, with σ_d being a surface quantity (or constant), and incompressible flow. This is due to the fact that although the MHD and CGL models are established through different physical assumptions for the particle collisions, the respective generalised GS equations governing them are identical in form.

[3] We have assumed $U_b = 0$ without loss of generality.

3.2 Impact of flow and pressure anisotropy

To completely determine the equilibria we have to properly assign the remaining, unspecified surface quantities appearing in the GGS equation (2.46) in terms of U; those are the plasma density, $\varrho(U)$, the Mach function, $M_p(U)$ and the anisotropy function, $\sigma_d(U)$. Here we choose the following functional forms, peaked on the magnetic axis and vanishing on the boundary,

$$\sigma_d = \sigma_{d_a}\left(\frac{U-U_b}{U_a-U_b}\right)^{\mu},\ M_p^2 = M_{p_a}^2\left(\frac{U-U_b}{U_a-U_b}\right)^{\nu},\ \varrho = \varrho_a\left(\frac{U-U_b}{U_a-U_b}\right)^{\lambda}, \tag{3.69}$$

where the parameters σ_{d_a}, $M_{p_a}^2$, ϱ_a denote the pertinent maximum values on the magnetic axis, while the parameters μ, ν, λ are related with the shaping of the respective profiles. We note that the above profiles are connected with on-axis heating sources. However, alternative functional dependence on the flux function U, i.e. connected with off-axis heating sources, can also be adopted for these profiles.

In the present Section we investigate the characteristics of the helically symmetric equilibrium of circular poloidal cross-section of figure 3.2, constructed with W7-X parameters, through physical quantities, on the basis of the obtained analytic solution (3.38) together with the relations (2.50)-(2.55) and (3.69)[4]. In particular, we examine the impact of pressure anisotropy and flow on the equilibrium through the variation of the parameters σ_{d_a}, associated with the anisotropy, $M_{p_a}^2$, associated with the parallel component of the flow, and φ_{11}, φ_{22}, associated with the non-parallel flow component. For the rest of the parameters in the profiles (3.69) we assign the following values: $\mu=\nu=2$, $\lambda=1/2$, $\varrho_a = 5\times10^{-7}\,Kg/m^3$. From the requirement of positiveness for all pressures within the whole plasma region, we find that for the free anisotropy parameter it must hold: $-6\times10^{-3}\le\sigma_{d_a}\le 6\times10^{-3}$, both for static as well as for stationary equilibria; here negative anisotropy implies that $P_\perp > P_\parallel$, and vise versa in the case $\sigma_d>0$. It is noted that both cases of anisotropy $(P_\parallel - P_\perp)$, either positive or negative, are of practical interest for magnetic confinement systems [133, 210, 211]. For field-aligned flow the same requirement for the above values of anisotropy parameter yields for the Mach number $0\le M_{p_a}^2\le 3\times10^{-4}$; however, in the presence of the electric field term, associated with the non-parallel flow, the maximum values for the poloidal Mach number can be almost one order of magnitude greater, $0\le M_{p_a}^2\le 10^{-3}$. Such values of $M_{p_a}^2$ imply rotation velocities of the order $10^4-10^6\,ms^{-1}$ which are good for large conventional tokamaks on account of experimental evidence [212, 213]. We note that the approximate maximum permissible values of the free parameter σ_{d_a} in connection with the non negativeness of the pressures, are, in general, larger than the respective ones for $M_{p_a}^2$.

To examine the impact of pressure anisotropy and flow on the equilibrium, employing equations (2.47), (2.48) and (2.50)-(2.53), we find for the function I, related to the helicoidal magnetic field, the magnetic field magnitude, $B\,(:=|\mathbf{B}|)$, and the effective pressure, $\mathcal{P}$, the following expressions in terms of σ_{d_a}, $M_{p_a}^2$ and $\mathcal{F}(\varphi_{11},\varphi_{22})$:

$$I(r,U) = \frac{\mathcal{I}}{(1-\sigma_d-M_p^2)^{1/2}} - \frac{\sqrt{\mu_0}}{q}\frac{M_p\mathcal{F}^{1/2}}{(1-\sigma_d-M_p^2)^{1/2}(1-\sigma_d)^{1/2}}, \tag{3.70}$$

$$B(r,U) = \left[\frac{q(\mathcal{I}^2+|\nabla U|^2)}{1-\sigma_d-M_p^2} + \frac{\mu_0 M_p^2\mathcal{F}}{q(1-\sigma_d-M_p^2)(1-\sigma_d)} - \frac{2\mathcal{I}\sqrt{\mu_0}M_p\mathcal{F}^{1/2}}{(1-\sigma_d-M_p^2)(1-\sigma_d)^{1/2}}\right]^{1/2}, \tag{3.71}$$

[4]Since the topology of the magnetic surfaces remains unchanged in both planes of figure 3.2 we may restrict our study on the (r,u)-plane (figure 3.2(a)).

$$\mathcal{P}(r,U) = \mathcal{P}_s - \frac{M_p^2}{(1-\sigma_d-M_p^2)}\frac{q(\mathcal{I}^2+|\nabla U|^2)}{2\mu_0} + \frac{M_p\mathcal{F}^{1/2}(1-\sigma_d)^{1/2}}{(1-\sigma_d-M_p^2)}\frac{\mathcal{I}}{\sqrt{\mu_0}} + \frac{\mathcal{F}}{2q}\left(1-\frac{M_p^2}{1-\sigma_d-M_p^2}\right). \tag{3.72}$$

Then, substituting (3.71) and (3.72) into equations (1.61), we come up with the following relations for the parallel and perpendicular pressures as functions of σ_{d_a}, $M_{p_a}^2$ and $\mathcal{F}(\varphi_{11},\varphi_{22})$:

$$P_\perp(r,U) = \mathcal{P}_s - \frac{(\sigma_d+M_p^2)}{(1-\sigma_d-M_p^2)}\frac{q(\mathcal{I}^2+|\nabla U|^2)}{2\mu_0} + \frac{M_p\mathcal{F}^{1/2}\mathcal{I}}{\sqrt{\mu_0}(1-\sigma_d-M_p^2)(1-\sigma_d)^{1/2}} + \frac{\mathcal{F}}{2q}\left[1-\frac{M_p^2}{(1-\sigma_d-M_p^2)(1-\sigma_d)}\right], \tag{3.73}$$

$$P_\parallel(r,U) = \mathcal{P}_s + \frac{(\sigma_d-M_p^2)}{(1-\sigma_d-M_p^2)}\frac{q(\mathcal{I}^2+|\nabla U|^2)}{2\mu_0} + \frac{(1-2\sigma_d)M_p\mathcal{F}^{1/2}\mathcal{I}}{\sqrt{\mu_0}(1-\sigma_d-M_p^2)(1-\sigma_d)^{1/2}} + \frac{\mathcal{F}}{2q}\left[1-\frac{(1-2\sigma_d)M_p^2}{(1-\sigma_d-M_p^2)(1-\sigma_d)}\right]. \tag{3.74}$$

To begin with, we consider static equilibria ($M_p=\varphi_{11}=\varphi_{22}=0$). In the absence of the flow equation (3.71) yields for the magnetic field magnitude

$$B(r,U) = \sqrt{\frac{q(\mathcal{I}^2+|\nabla U|^2)}{1-\sigma_d}}. \tag{3.75}$$

From the above equation it follows that pressure anisotropy acts paramagnetically for $P_\parallel > P_\perp$, since in that case the magnetic field increases from its isotropic values with $\sigma_{d_a}>0$, while it acts diamagnetically for $P_\parallel < P_\perp$, since B decreases with $\sigma_{d_a}<0$, as shown in figure 3.5(a). Observe that the magnitude of the magnetic field on the high-field side of the configuration is $B\approx 3\,T$, which is very close to the value of the vacuum magnetic field of the W7-X device. This behavior becomes more clear on the profile of the function I associated with the helicoidal component of the magnetic field[5], presented in figure 3.5(b); note that in the static case from equation (3.70) it follows that $I=I(U)$ and thus, the current density remains on the magnetic surafces $U=$ const. In fact, the above result for the impact of pressure anisotropy also holds in the presence of equilibrium flows, since σ_d appears in the denominators of the respective flow terms in equations (3.70), (3.71). This is consistent with the result of [114] in which only the case $\sigma_d>0$ was examined and with those of [211] about the impact of pressure anisotropy on high-beta tokamak equilibria for either $P_\parallel>P_\perp$ or $P_\parallel<P_\perp$. Also the impact of pressure anisotropy for either $\sigma_d>0$ or $\sigma_d<0$ on certain equilibrium characteristics of tokamaks and stellarators were examined in [133], including the limits $P_\parallel \gg P_\perp$ and $P_\parallel \ll P_\perp$. We note that experimental observations of plasma paramagnetism in tokamaks have been reported in [214].

Furthermore, in the absence of the flow the effective pressure becomes a surface quantity, $\mathcal{P}=\mathcal{P}(U)=\mathcal{P}_s(U)$, thus remaining on the magnetic surfaces $U=$ const., as follows from equation (3.72). The static effective pressure peaks on the magnetic axis and vanishes on the boundary, while it does not depend on the pressure anisotropy parameter σ_{d_a}, in consistence with ansatz (3.1), as shown in figure 3.6. However, this result does not hold for the profiles of the scalar pressures in the directions perpendicular and parallel to $\mathbf{B}$ which have the forms

$$P_\perp(r,U) = \mathcal{P}(U) - \frac{\sigma_d}{(1-\sigma_d)}\frac{q(\mathcal{I}^2+|\nabla U|^2)}{2\mu_0}, \tag{3.76}$$

$$P_\parallel(r,U) = \mathcal{P}(U) + \frac{\sigma_d}{(1-\sigma_d)}\frac{q(\mathcal{I}^2+|\nabla U|^2)}{2\mu_0}. \tag{3.77}$$

[5]Inspection of equation (3.75) implies that B is proportional to $\sqrt{q}=1/\sqrt{k^2r^2+m^2}$

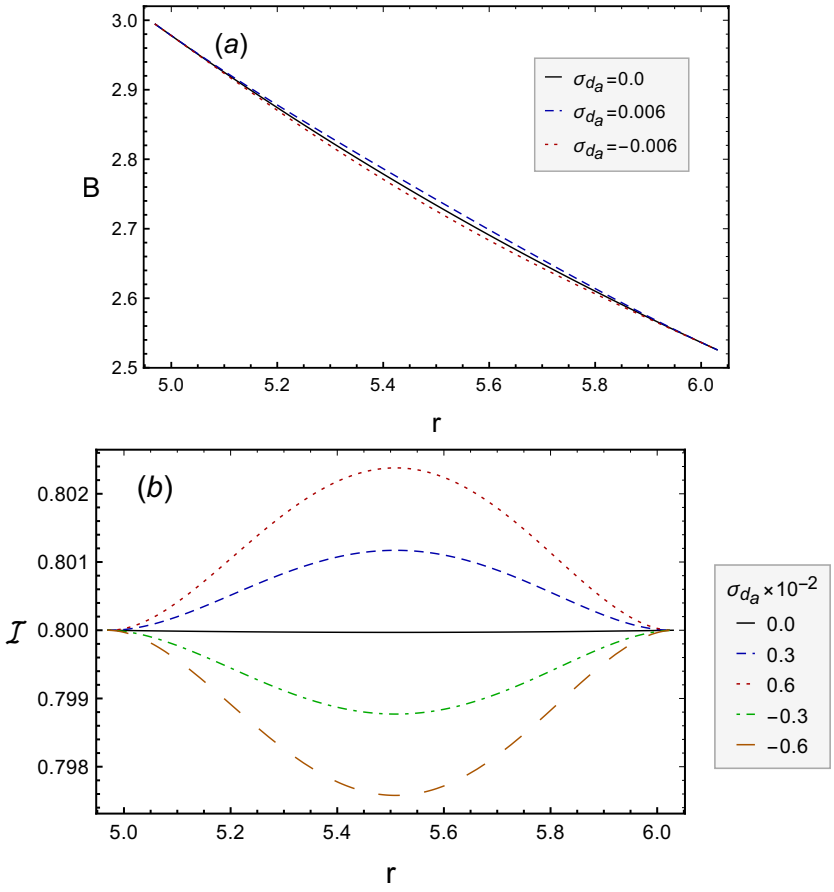

Figure 3.5: (a) The magnetic field magnitude, $B(r, u_a)$, and (b) the function $I(r, u_a)$ related to the helical component of the magnetic field, as functions of the anisotropy parameter σ_{d_a}, for $M_{p_a} = \varphi_{11} = \varphi_{22} = 0$.

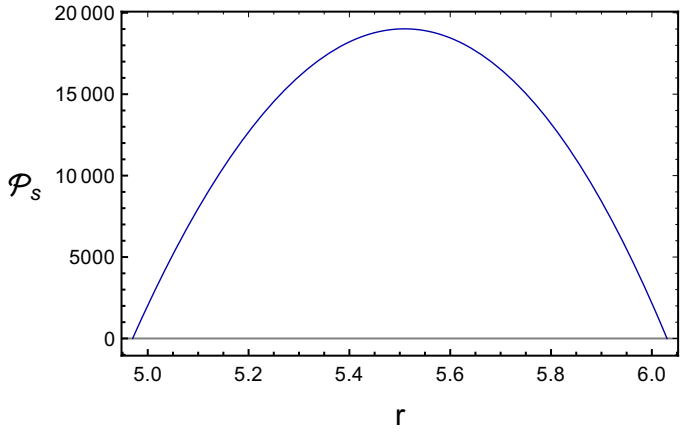

Figure 3.6: The profile of the static effective pressure, $\mathcal{P}_s(U(r, u_a))$, for the equilibrium of figure 3.2(a), in consistence with that of the flux function U shown in figure 3.3.

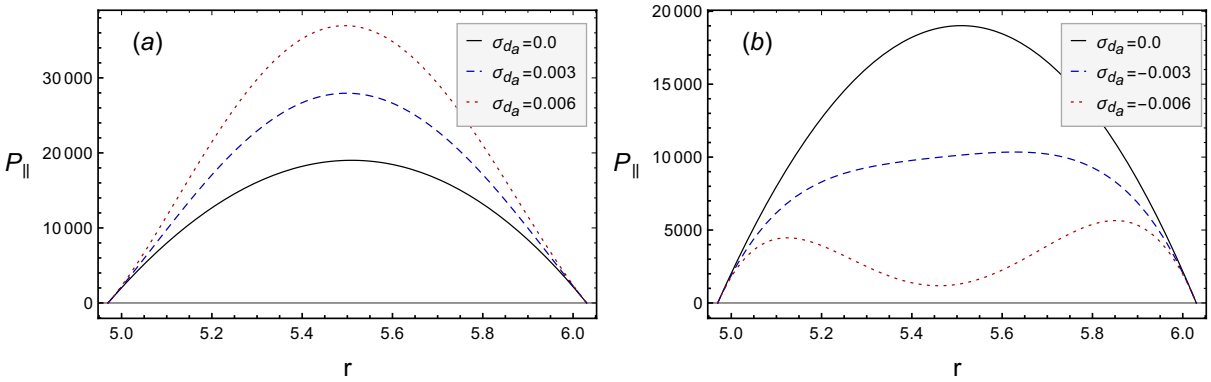

Figure 3.7: The impact of pressure anisotropy on $P_\parallel(r, u_a)$ for (a) $\sigma_{d_a} > 0$ and (b) $\sigma_{d_a} < 0$, for $M_{p_a} = \varphi_{11} = \varphi_{22} = 0$.

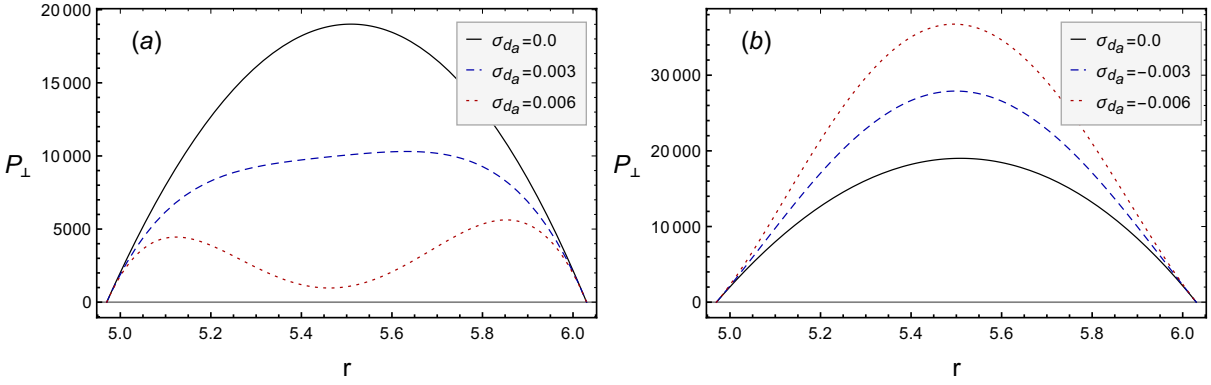

Figure 3.8: The impact of pressure anisotropy on $P_\perp(r, u_a)$ for (a) $\sigma_{d_a} > 0$ and (b) $\sigma_{d_a} < 0$, for $M_{p_a} = \varphi_{11} = \varphi_{22} = 0$.

From the above equations it follows that although for static anisotropic equilibria the effective pressure is a surface quantity, neither $P_\perp$ nor $P_\parallel$ remain constant on the magnetic surfaces; in fact the anisotropic scalar pressures never become uniform on the magnetic surfaces even in the presence of mass flows[6], as indicated by equations (3.73), (3.74). From the relations (3.76), (3.77) it follows that raise of the parameter $\sigma_{d_a} > 0$ makes $P_\parallel$ to increase and $P_\perp$ to decrease from the respective isotropic pressure, while $\sigma_{d_a} < 0$ affects the scalar pressures in just the opposite way. The impact of pressure anisotropy on $P_\parallel$ and $P_\perp$ is shown in figures 3.7 and 3.8, respectively. Therefore, the families of surfaces on which either $P_\parallel$ or $P_\perp$ are constant do not coincide with the magnetic surfaces. As indicated by figure 3.8(b), when $\sigma_d < 0$ the profiles of the perpendicular pressure peak close to the magnetic axis; in that case the topology of the $P_\perp$ surfaces does not differ from that of the magnetic surfaces, i.e. the cross-section shape of $P_\perp$ surfaces remain circular. However, when $\sigma_d > 0$ the increase of the anisotropy noticeably affects the topology of the $P_\perp$ = const. surfaces. Indeed, for $\sigma_{d_a} = 0.003$ the pertinent inner surfaces have a non-zero triangularity, thus deviating from circular. In addition, for $\sigma_{d_a} = 0.006$ it is found that the cross-sections of surfaces close to the boundary remain circular, while the ones of the inner surfaces consist of two lobes and one saddle point (X-point); the respective axes of the two lobes are located at $(r = 5.852, u = 2.94 \times 10^{-7})$ and $(r = 5.462, u = 1.46 \times 10^{-8})$, while the X-point is located at $(r = 5.123, u = -1.49 \times 10^{-7})$. These features are illustrated in figure 3.9. We note that analogous characteristics are found for the $P_\parallel$ surfaces for the opposite values of σ_d.

[6]This happens only for static, isotropic MHD equilibria ($\sigma_d = 0$) in which only a single scalar pressure is defined.

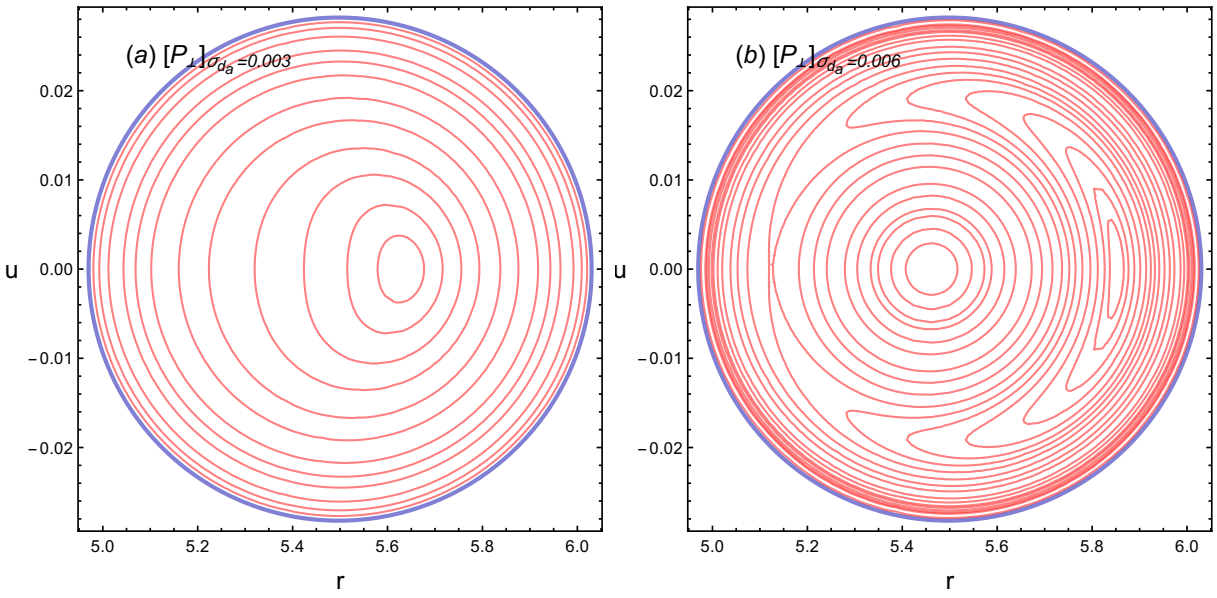

Figure 3.9: Poloidal cut of the helicoidal surfaces $P_\perp = \text{const.}$ for (a) $\sigma_{d_a} = 0.003$ and (b) $\sigma_{d_a} = 0.006$, in constistence with the respective curves of graph 3.8(a).

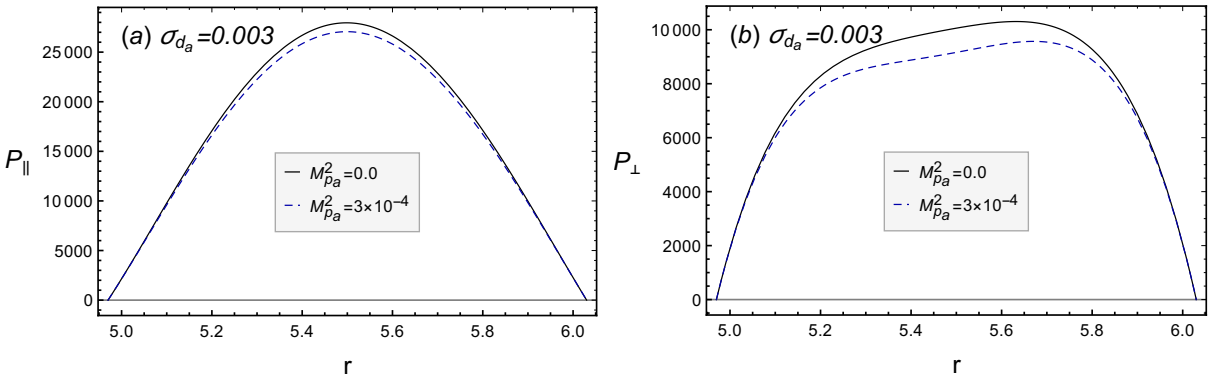

Figure 3.10: The impact of the parallel flow in connection with the parameter $M^2_{p_a}$ on (a) $P_\parallel(r, u_a)$ and (b) $P_\perp(r, u_a)$, for $\varphi_{11} = \varphi_{22} = 0$, corresponding to the cases of figures 3.7(a) and 3.8(a).

For stationary equilibria with field-aligned flows ($M_p \neq 0$, $\mathcal{F} = 0$) equations (3.70), (3.73) and (3.74) reduce to the forms

$$I(r, U) = \frac{\mathcal{I}}{(1 - \sigma_d - M_p^2)^{1/2}}, \tag{3.78}$$

$$P_\perp(r, U) = \mathcal{P}_s - \frac{(\sigma_d + M_p^2)}{(1 - \sigma_d - M_p^2)} \frac{q(\mathcal{I}^2 + |\nabla U|^2)}{2\mu_0}, \tag{3.79}$$

$$P_\parallel(r, U) = \mathcal{P}_s + \frac{(\sigma_d - M_p^2)}{(1 - \sigma_d - M_p^2)} \frac{q(\mathcal{I}^2 + |\nabla U|^2)}{2\mu_0}. \tag{3.80}$$

Inspection of the above relations implies that, in the absence of the electric field term, the parallel flow associated with M_p^2 acts additively with pressure anisotropy for $\sigma_d > 0$, with the exeption of $P_\parallel$ in which it acts additively with $\sigma_d < 0$. In fact, this also follows from the GGS equation (2.44) for $\Phi' = 0$, owing to the term $1 - \sigma_d - M_p^2$. The impact of M_p^2 on the scalar pressures parallel and perpendicular to $\mathbf{B}$ is shown in figure 3.10. Consequently, it follows that the parallel flow through the parameter $M^2_{p_a} > 0$ has a paramagnetic impact on the equilibrium

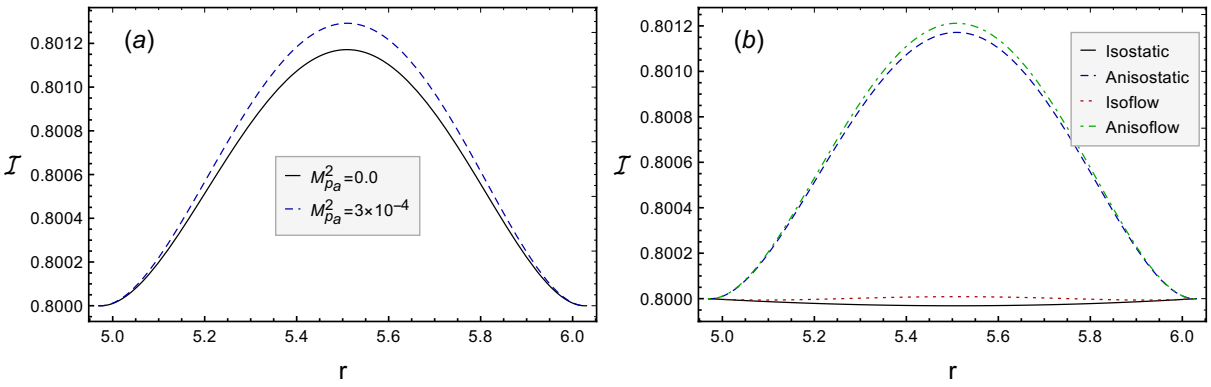

Figure 3.11: (a) The impact of $M_{p_a}^2$ on the function $I(r, u_a)$ associated with the helicoidal component of the magnetic field, for $\sigma_{d_a} = 0.003$, $\varphi_{11} = \varphi_{22} = 0$. (b) the cumulative paramagnetic impact of the pressure anisotropy and the parallel flow in the absence of the electric field term; the displayed curves correspond to the following values: Isostatic (black straight curve): $\sigma_{d_a} = M_{p_a}^2 = 0$; Anisostatic (blue dashed curve): $\sigma_{d_a} = 3 \times 10^{-3}$, $M_{p_a}^2 = 0$; Isoflow (red dotted curve): $\sigma_{d_a} = 0$, $M_{p_a}^2 = 10^{-4}$; Anisoflow (green dotdashed curve): $\sigma_{d_a} = 3 \times 10^{-3}$, $M_{p_a}^2 = 10^{-4}$.

as shown in figure 3.11(a). Although the pressure anisotropy for $P_\parallel > P_\perp$ and the parallel flow act cumulatively, the impact of the anisotropy is stronger since the maximum values of the Mach number are one order of magnitude lower than those of σ_{d_a}; it also follows that the greatest paramagnetic impact is found in the presence of both the pressure anisotropy and the parallel flow. These results are shown in figure 3.11(b). We note that for field-aligned flows the current surfaces coincide with the magnetic surfaces, $I = I(U)$ (see equation (3.78)), while the surfaces on which the effective pressure is constant deviate from the magnetic surfaces, $\mathcal{P} \neq \mathcal{P}(U)$, in connection with the second term of equation (3.72) for $\mathcal{F} = 0$.

Furthermore, for purely helicoidal flows the quantity I and the magnetic field modulus become independent on $\mathcal{F}$ (cf. equations (3.70) and (3.71) for $M_p = 0$). Therefore, it follows that the non-parallel flow affects $\mathbf{B}$ only in the presence of the parallel component of the flow, in connection with the respective flow terms in equations (3.70), (3.71). On the other hand, it is found that the non-parallel flow affects both the parallel and the perpendicular pressures in the same way, as implied by the expressions

$$P_\perp(r, U) = \mathcal{P}_s - \frac{\sigma_d}{(1-\sigma_d)} \frac{q(\mathcal{I}^2 + |\nabla U|^2)}{2\mu_0} + \frac{\mathcal{F}}{2q}, \tag{3.81}$$

$$P_\parallel(r, U) = \mathcal{P}_s + \frac{\sigma_d}{(1-\sigma_d)} \frac{q(\mathcal{I}^2 + |\nabla U|^2)}{2\mu_0} + \frac{\mathcal{F}}{2q}, \tag{3.82}$$

obtained from (3.73), (3.74) for purely helicoidal flow. In particular, it follows that the non-parallel flow has a slight positive contribution on the scalar pressures as can be seen in figure 3.12.

For equilibria with flow of arbitrary direction, that is for flow with both helicoidal and poloidal components, inspection of equations (3.70), (3.71) leads to the following conclusions.

(i) The non-parallel flow associated with the electric field related with the term $\mathcal{F}$ in (3.70) has a diamagnetic impact, in connection with a decrease of $I(r, U)$ as the parameter φ_{11} takes larger values, which can be seen in figure 3.13. Note that in that case the current density $\mathbf{J}$ does not remain on the magnetic surfaces since $I \neq I(U)$.

(ii) In contrast with the paramagnetic behavior of the parallel flow in field-aligned equilibria, in the case of mass flows of arbitrary direction the second term in equation (3.70) implies

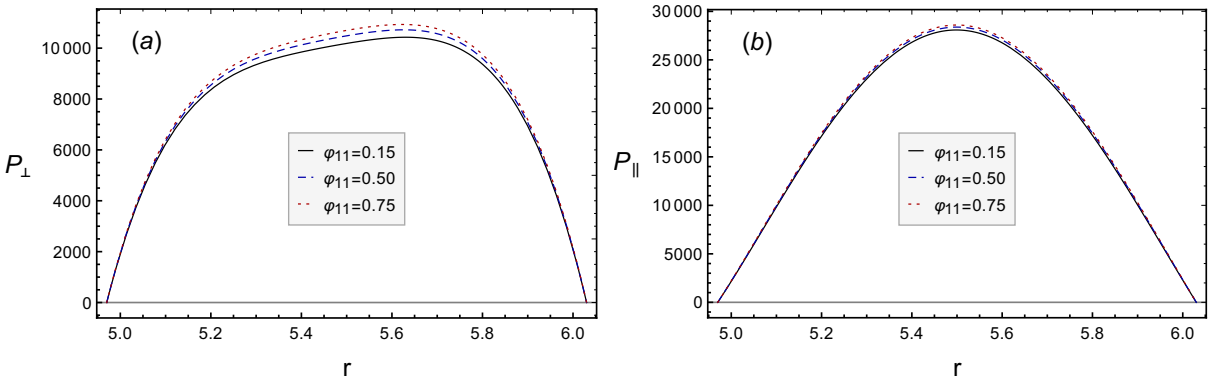

Figure 3.12: The impact of the parameter φ_{11} on (a) $P_\perp(r, u_a)$ and (b) $P_\parallel(r, u_a)$, for purely helicoidal flows: $M_p^2 = 0$, $\varphi_{22} = -0.08$ and $\sigma_{d_a} = 0.003$.

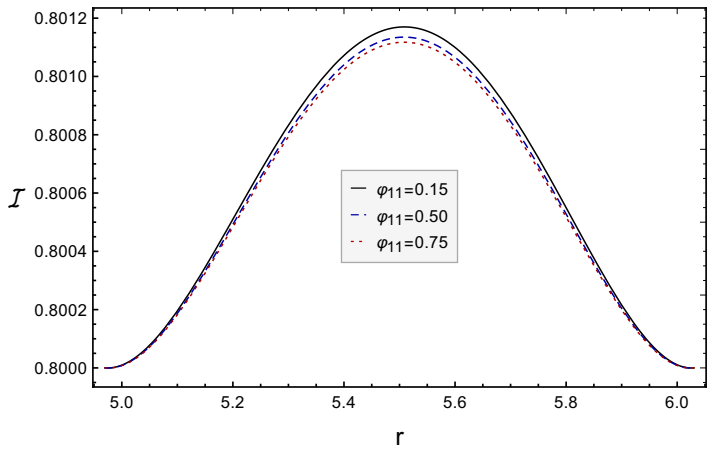

Figure 3.13: The helicoidal component of the magnetic field for the equilibrium of figure 3.2(a) for different values of the non-parallel flow parameter φ_{11}, for $\varphi_{22} = -0.08$, $M_{p_a}^2 = 10^{-4}$ and $\sigma_{d_a} = 3 \times 10^{-3}$.

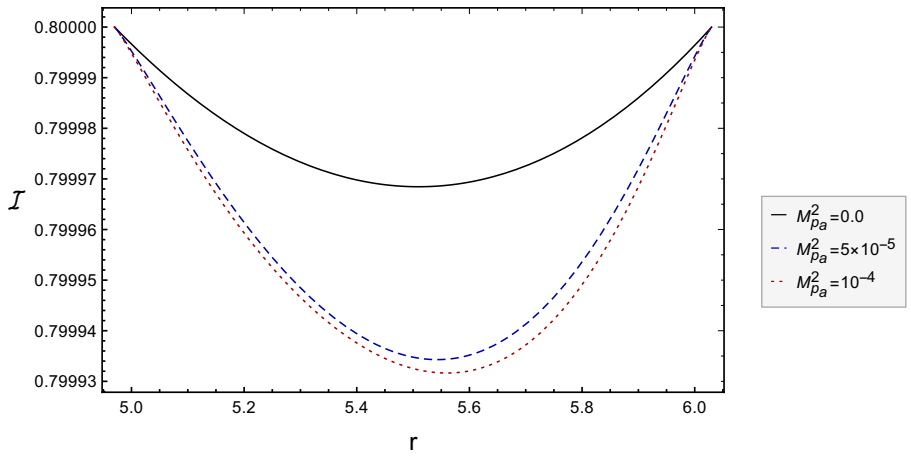

Figure 3.14: The implicit diamagnetic action of parallel flow in the presence of non-parallel one through the second term in (3.70) for $\varphi_{11} = 0.5$ and $\varphi_{22} = -0.08$. The displayed graphs correspond to $\sigma_{d_a} = 0$; however the impact of M_p^2 is similar for any $\sigma_{d_a} \neq 0$.

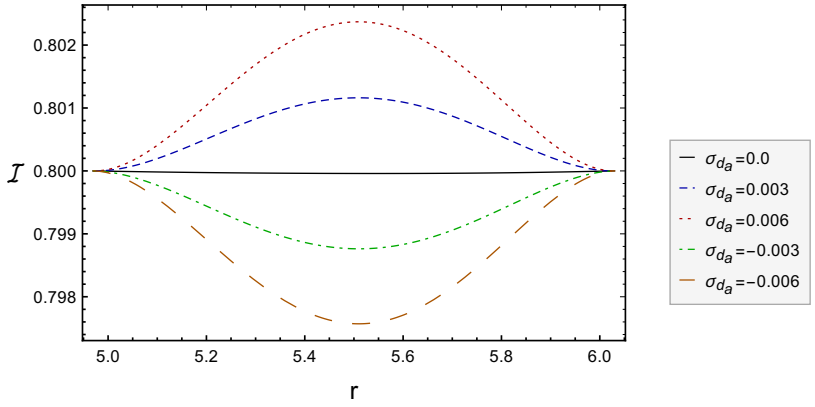

Figure 3.15: The pressure anisotropy strengthens the diamagnetic impact of the non-parallel flow for $P_\parallel < P_\perp$ and encounters that impact for $P_\parallel > P_\perp$. This figure corresponds to flows of arbitrary direction: $M^2_{p_a} = 5 \times 10^{-5}$, $\varphi_{11} = 0.5$, $\varphi_{22} = -0.08$.

that the stronger the diamagnetic effect of $\mathcal{F}$ is the higher M_p^2; that is the parallel flow enhances the diamagnetic action of the non-parallel one. This impact is shown in figure 3.14.

(iii) The second term in equation (3.70) implies that the pressure anisotropy strengthens this non-parallel flow caused diamagnetic effect for $\sigma_d < 0$ and weakens that effect for $\sigma_d > 0$, as can be seen in figure 3.15. This behavior is consistent with the diamagnetic and/or paramagnetic impact of the pressure anisotropy for $\sigma_d < 0$ and/or $\sigma_d > 0$ of figure 3.5(b) for static equilibria.

The above results for the effects of the pressure anisotropy and the flow are also consistent with their impact on the local plasma beta, which is defined as

$$\bar{\beta}_a = \left(\frac{\mathcal{P}}{B^2/2\mu_0} \right)_{|_{r=r_a, u=u_a}} \tag{3.83}$$

For field aligned flows the values of $\bar{\beta}_a$ are lower than the respective ones for static equilibria, since M_p^2 acts paramagnetically in that case. However, for purely helicoidal flows $\bar{\beta}_a$ is enhanced since the non-parallel flow term has a positive contribution to both $P_\parallel$ and $P_\perp$, though not

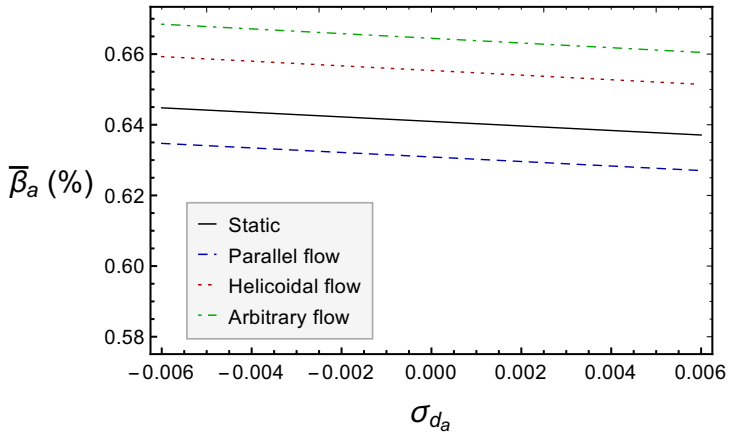

Figure 3.16: The overall impact of pressure anisotropy and flow on the local beta on the magnetic axis. The displayed curves correspond to the values: Static: $M_{p_a}^2 = \varphi_{11} = \varphi_{22} = 0$; Parallel flow: $M_{p_a}^2 = 10^{-4}$, $\varphi_{11} = \varphi_{22} = 0$; Helicoidal flow: $M_{p_a}^2 = 0$, $\varphi_{11} = 0.5$, $\varphi_{22} = -0.08$; Arbitrary flow: $M_{p_a}^2 = 10^{-4}$, $\varphi_{11} = 0.5$, $\varphi_{22} = -0.08$.

affecting the magnetic field. In addition, for flows of arbitrary direction $\bar{\beta}_a$ takes noticeably larger values when the non-parallel component of the flow has an implicit diamagnetic impact in the presence of the parallel one. In all of the above kinds of equilibria, either static or stationary, the pressure anisotropy strengthens $\bar{\beta}_a$ for $\sigma_d < 0$ and weakens it for $\sigma_d > 0$, in accordance with its diamagnetic action in the former and its paramagnetic one in the latter case. These features can be seen in figure 3.16.

Furthermore, we examine the influence of pressure anisotropy and flow on the physical components of the flow velocity and the current density along the direction of the symmetry, V_ζ and J_ζ [see equation (B.14) in Appendix B], which were calculated on the basis of equations (2.53) and (2.54) in the forms

$$V_{\bar{\zeta}} = \sqrt{\frac{qM_p^2}{\mu_0 \varrho}} \left(I - \frac{kr}{m} \frac{\partial U/\partial r}{\sqrt{1-\sigma_d - M_p^2}} \right) - \sqrt{\frac{(1-\sigma_d - M_p^2)\mathcal{F}}{q\varrho(1-\sigma_d)}}, \tag{3.84}$$

$$J_{\bar{\zeta}} = \frac{\sqrt{q}}{\mu_0} \left[\frac{\mathcal{L}U}{1-\sigma_d - M_p^2} + \frac{(1-\sigma_d - M_p^2)^{-3/2}}{2} \frac{d(\sigma_d + M_p^2)}{dU} |\nabla U|^2 \right.$$
$$\left. + 2kmqI + \frac{kr}{m} \frac{\partial I}{\partial r} \right]. \tag{3.85}$$

It turns out that the static isotropic ζ-component of the current density monotonically increases from the low to the high magnetic field side. However, in the presence of anisotropy there exists a noticeable modification of the respective profile; in that case $J_{\bar{\zeta}}$ reverses in comparison with its isotropic profile, thus exhibiting opposite behavior in the regions left and right of the magnetic axis in both cases for $\sigma_d > 0$ and $\sigma_d < 0$. The impact of pressure anisotropy on $J_{\bar{\zeta}}$ is shown in figure 3.17(a); we note that the parallel flow affects $J_{\bar{\zeta}}$ in the same way as $\sigma_d > 0$, this impact being weaker due to the lower actual values of the parameter $M_{p_a}^2$. It is also found that the increase of the non-parallel flow through φ_{11} results in a slight decrease of the values of the current density component, as may be seen in figure 3.17(b). As concerns the ζ-component of the fluid velocity, it is found that for field-aligned flows it peaks on the magnetic axis, in that case the parallel flow through M_p^2 possessing a positive contribution on $V_{\bar{\zeta}}$, as shown in figure 3.18(a). In the presence of the electric field associated with the non-parallel flow, the increase of the parameter φ_{11} weakens $V_{\bar{\zeta}}$, thus leading to a velocity reversal, presented in figure 3.18(b), in that case the parallel flow counteracting the influence

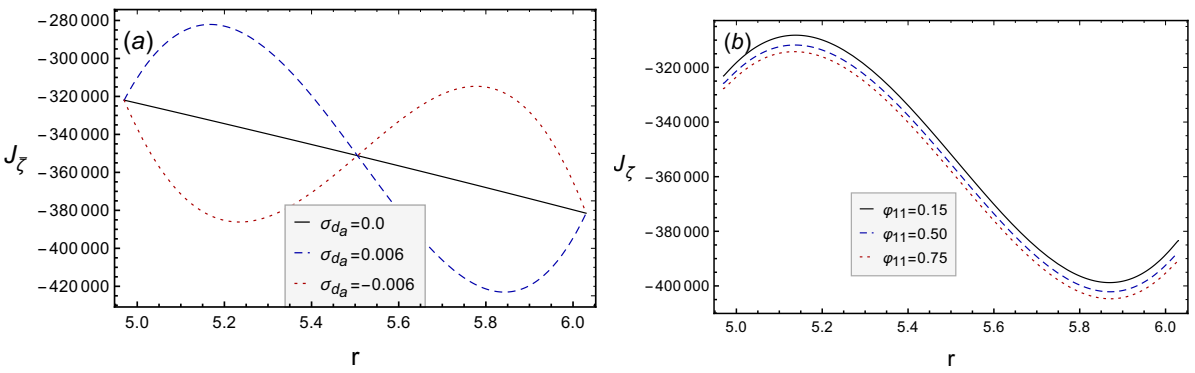

Figure 3.17: (a) The impact of pressure anisotropy on $J_{\bar{\zeta}}$ in the absence of the flow ($M_{p_a}^2 = \varphi_{11} = \varphi_{22} = 0$). (b) The impact of the non-parallel flow on $J_{\bar{\zeta}}$ through the parameter φ_{11}, for $\sigma_{d_a} = 3 \times 10^{-3}$, $M_{p_a}^2 = 10^{-4}$ and $\varphi_{22} = -0.08$.

of the non-parallel one, as can be seen in figure 3.18(c).

Finally, we examine the influence of pressure anisotropy and flow on the safety factor for the constructed equilibrium of figure 3.2(a), the profile of which is computed on the basis of equation (3.53), by using the intrinsic coordinates (ρ^*, ω) on the poloidal plane originating on the geometric center helix; it takes the form

$$\mathcal{Q}(U) = \frac{1}{2\pi r_0} \int_{\tau_0 \ell_0}^{2\pi + \tau_0 \ell_0} \mathcal{B}(U,\omega) \sqrt{\frac{\rho^{\star 2} + \left(\frac{\partial U/\partial \omega}{\partial U/\partial \rho^\star}\right)^2}{\frac{1}{m^2}\left(\frac{\partial U}{\partial r}\right)^2 + \frac{1}{r^2}\left(\frac{\partial U}{\partial u}\right)^2}} d\omega,$$

$$\mathcal{B} := mq\mathcal{I}(U) - m\sqrt{\frac{M_p^2(U)\mathcal{F}(U)}{\mu_0(1-\sigma_d(U))}} - kqr\frac{\partial U}{\partial r}. \tag{3.86}$$

This relation indicates that both the anisotropy and the flow have an impact on $\mathcal{Q}$ for flows of arbitrary direction. It is found that the safety factor monotonically decreases from the boundary to the magnetic axis, while both the parallel flow, associated with M_p^2, and the non-parallel flow, in connection with the function $\mathcal{F}$, weaken the values of $\mathcal{Q}$ and more drastically near the magnetic axis, as shown in figure 3.19. Therefore, it turns out that the rotation velocity might have unfavorable effects regarding plasma stability. We note that a similar result for the impact of the parallel flow on the safety factor was obtained in [213] for axisymmetric equilibria with toroidal mass flow (see figure 5 therein). It may be noted that pressure anisotropy for $\sigma_d > 0$ have the same effect on $\mathcal{Q}$ as M_p^2, while the opposite effect for $\sigma_d < 0$, this impact however, being negligible for the maximum permissible values of σ_{d_a} due to the factor $(1-\sigma_d)^{-1/2}$.

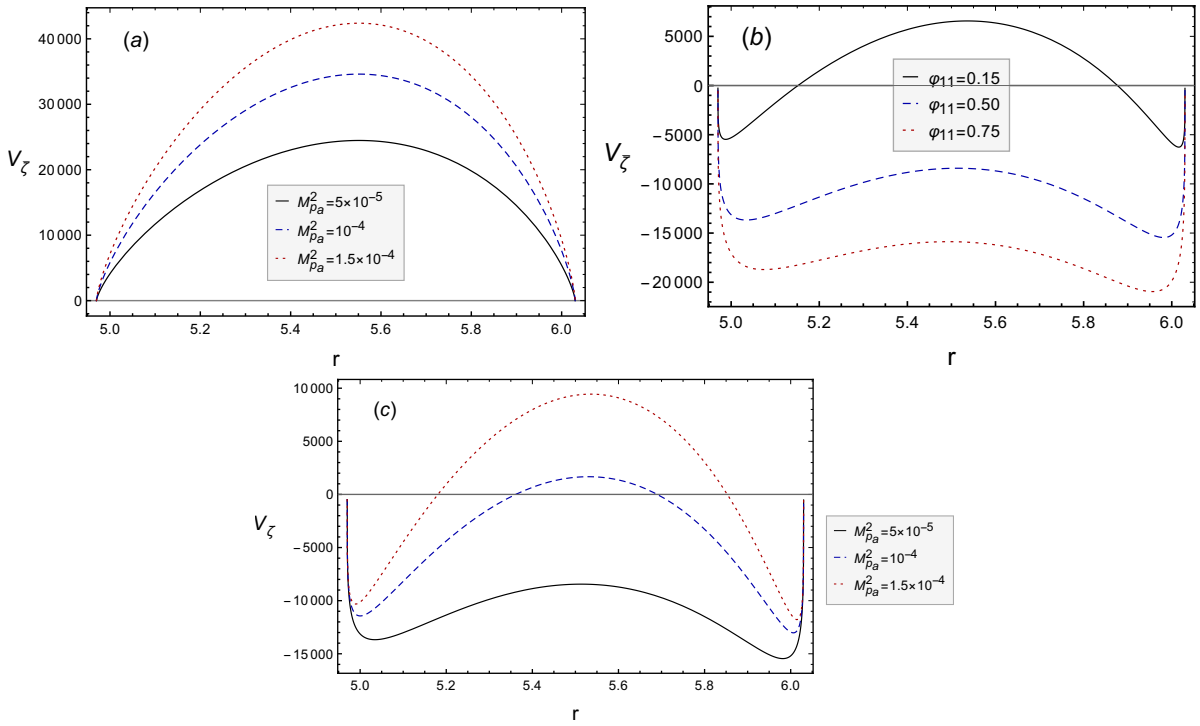

Figure 3.18: The impact on $V_{\bar{\zeta}}$ of : (a) M_p^2 for field-aligned flows and isotropic pressure, $\sigma_{d_a} = \varphi_{11} = \varphi_{22} = 0$, (b) the non-parallel flow in connection with the parameter φ_{11}, for $\sigma_{d_a} = 3 \times 10^{-3}$, $M_{p_a}^2 = 5 \times 10^{-5}$, $\varphi_{22} = -0.08$, (c) the parallel flow in the presence of the electric field term associated with non-parallel flow, for $\sigma_{d_a} = 0$, $\varphi_{11} = 0.5$, $\varphi_{22} = -0.08$.

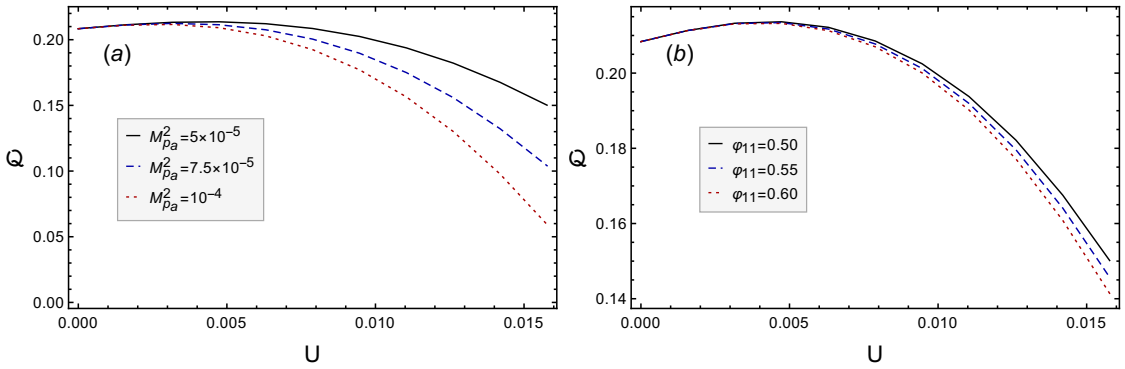

Figure 3.19: (a) The influence of the parallel flow through $M_{p_a}^2$ on the safety factor, for $\varphi_{11} = 0.5$. (b) The impact of non-parallel flow on $\mathcal{Q}$ in connection with the parameter φ_{11}, for $M_{p_a}^2 = 5 \times 10^{-5}$; Both figures correspond to the values $\varphi_{22} = -0.08$ and $\sigma_{d_a} = 0$.

4 | Symmetry Transformations for Ideal MHD and CGL Equilibria

"*On that night the sky laid bare its internal construction in many sections which, like quasi-anatomical exhibits, showed the spirals and whorls of light, the pale-green solids of darkness, the plasma of space, the tissue of dreams* ."

Bruno Schulz

4.1 Brief introduction to the symmetry transformations

As recognized earlier the establishment of a confined equilibrium is very crucial for stability and transport studies. In connection with the ideal isotropic MHD and anisotropic CGL models widely employed within the context of this thesis, one has to solve the sets of related equations (1.50)-(1.54), together with appropriate boundary conditions, in order to create pertinent equilibria. However, there do not exist any general methods for the production of exact solutions to these equations in generic 3D domains [215].

In references [73, 153, 209, 216–220] methods for constructing new continuous families of equilibria in the framework of the above mentioned models, once a given equilibrium is known, are introduced. More specifically, in references [73, 209, 216, 217] three sets of equilibrium transformations in the framework of MHD model, commonly known as 'Bogoyavlenskij transformations', were presented. The first set is applied to given equilibria with incompressible flow of arbitrary direction, while the second one to both static equilibria and stationary equilibria with field-aligned incompressible flow. The third set of transformations concerns plasma equilibria with compressible flow. In addition, in reference [153] symmetry transformations that produce an infinite class of anisotropic CGL equilibria, on the basis of prescribed CGL ones with flow of arbitrary direction are introduced; also in references [153, 218–220] symmetric transformations mapping static or stationary MHD equilibria into CGL ones are presented. All these symmetry transformations depend on a number of scalar functions which have to be constant on the magnetic field lines. This implies that the new equilibria resulting from the transformations depend on the structure of the magnetic fields of the original ones, and thus, the topology of the original equilibria is essential for these transformations.

In the present Chapter we make an extensive revision of the transformations presented previously in references [73, 153, 209, 216–220] concerning equilibria with incompressible flows, and introduce a set of transformations that can be applied to any known anisotropic CGL equilibria with field-aligned incompressible flows (or static equilibria) and anisotropy function constant on magnetic field lines, and produce an infinite family of anisotropic equilibria with collinear velocity and magnetic fields, but density and anisotropy functions that may remain arbitrary. These transformations consist of a generalization of the ones introduced in reference [216] for field-aligned MHD equilibria. We also prove that all transformations presented in references [73, 153, 209, 216–220] can break the geometrical symmetries of a known given

equilibrium, either static or with field-aligned flow, if and only if its magnetic field is purely poloidal, and construct pertinent 3D analytic equilibria related with the symmetry breaking.

4.2 Transformations for ideal MHD equilibria with field-aligned flows

In section IV of reference [216] transformations between MHD equilibria with parallel flows are presented. Specifically, it is stated therein that if $\{\mathbf{B},\, \mathbf{V},\, P,\, \varrho\}$ is a solution of the ideal MHD equilibrium system of equations with field-aligned incompressible flow ($\mathbf{V}\times\mathbf{B}=0$), which consist of the counterpart to the set (1.50)-(1.54) for $\sigma_d = 0$:

$$\begin{aligned} \varrho(\mathbf{V}\cdot\nabla)\mathbf{V} = \mathbf{J}\times\mathbf{B} - \nabla P, \quad \nabla\cdot\mathbf{B} = 0, \\ \nabla\cdot(\varrho\mathbf{V}) = 0, \quad \nabla\times\mathbf{B} = \mu_0\mathbf{J}, \end{aligned} \tag{4.1}$$

then $\{\mathbf{B}_1,\, \mathbf{V}_1,\, P_1,\, \varrho_1\}$ defined by the following symmetry transformations, that depend on the arbitrary functions $a_1(\mathbf{r})$, $b_1(\mathbf{r})$, $c_1(\mathbf{r})$, and $\lambda(\mathbf{r})$, consists of a new solution to the MHD equilibrium set of equations with field-aligned flows:

$$\begin{aligned} \mathbf{B}_1 = b_1(\mathbf{r})\mathbf{B}, \quad \mathbf{V}_1 = \frac{c_1(\mathbf{r})}{a_1(\mathbf{r})\sqrt{\mu_0\varrho}}\mathbf{B}, \\ \varrho_1(\mathbf{r}) = a_1^2(\mathbf{r})\varrho, \quad P_1 = C\left(P + \frac{\mathbf{B}^2}{2\mu_0}\right) - \frac{\mathbf{B}_1^2}{2\mu_0}, \\ C = \frac{b_1^2(\mathbf{r}) - c_1^2(\mathbf{r})}{1-\lambda^2(\mathbf{r})} = \text{const.} \neq 0. \end{aligned} \tag{4.2}$$

The above special transformations are defined only when the velocity and magnetic field of the original equilibria are related through $\mathbf{V} = (\lambda/\sqrt{\mu_0\varrho})\mathbf{B}$ [equation (2.61)], and are also valid in the static limit, $\mathbf{V} = 0$. Their reductive form for constant a_1, b_1, c_1, and λ was first derived in reference [73] from given axisymmetric equilibria found in reference [74]. According to reference [216] the functions $a_1(\mathbf{r})$, $b_1(\mathbf{r})$, $c_1(\mathbf{r})$, depending on the topology of the original equilibria may either (i) be constant on magnetic surfaces, or (ii) in case of symmetry involving two dimensional dependence, depend on two transversal variables (i.e. variables not dependent explicitly on the ignorable coordinate), or (iii) be constants in the case of force-free equilibria. Also it is claimed therein that transformations (4.2) can break the geometrical symmetry of the original equilibria (4.1) with general field-aligned incompressible flow.

4.3 Generalized symmetry transformations for anisotropic pressure

In the present Section we first generalize the transformations (4.2) introduced in reference [216] for CGL anisotropic equilibria with field-aligned incompressible flow and show that the only situation in which the symmetry of the original equiliria can be broken is that for purely poloidal magnetic fields. These considerations are summarized in the following theorem:

Theorem 1. Let $\{\mathbf{B},\, \mathbf{V},\, \varrho,\, P_\perp,\, P_\parallel\}$ be a known solution to the CGL equilibrium system of equations with field-aligned incompressible flows specially related through (2.61), and pressure anisotropy function being constant on the magnetic field lines, $\mathbf{B}\cdot\nabla\sigma_d = 0$. Then

$\{\mathbf{B}_1, \mathbf{V}_1, \varrho_1, P_{\perp_1}, P_{\parallel_1}\}$ are given by the following transformations:

$$\begin{gathered}
\mathbf{B}_1 = \frac{b_1(\mathbf{r})}{n_1(\mathbf{r})}\mathbf{B}, \quad \mathbf{V}_1 = \frac{c_1(\mathbf{r})\sqrt{1-\sigma_d}}{a_1(\mathbf{r})\sqrt{\mu_0\varrho}}\mathbf{B}, \\
\varrho_1(\mathbf{r}) = a_1^2(\mathbf{r})\varrho, \quad P_{\perp 1} = C\left(P_\perp + \frac{\mathbf{B}^2}{2\mu_0}\right) - \frac{\mathbf{B}_1^2}{2\mu_0}, \\
P_{\parallel 1} = C\left(P_\perp + \frac{\mathbf{B}^2}{2\mu_0}\right) + \left[1 - 2n_1^2(\mathbf{r})(1-\sigma_d)\right]\frac{\mathbf{B}_1^2}{2\mu_0}, \\
C = \frac{\left[b_1^2(\mathbf{r}) - c_1^2(\mathbf{r})\right](1-\sigma_d)}{1-\sigma_d-\lambda^2(\mathbf{r})} = \text{const.} \neq 0,
\end{gathered} \tag{4.3}$$

where $a_1(\mathbf{r}) \neq 0$, $b_1(\mathbf{r})$, $c_1(\mathbf{r})$, and $n_1(\mathbf{r}) \neq 0$ are arbitrary functions, define a solution to the CGL set of equilibrium equations with field-aligned flows, if and only if the functions

$$g_1(\mathbf{r}) = \frac{b_1(\mathbf{r})}{n_1(\mathbf{r})}, \quad f_1(\mathbf{r}) = a_1(\mathbf{r})c_1(\mathbf{r}), \tag{4.4}$$

are constant on the magnetic field lines of the original equilibria.

Proof. The original equilibria $\{\mathbf{B}, \mathbf{V}, \varrho, P_\perp, P_\parallel\}$ satisfy the CGL equilibrium equations with field-aligned flows ($\mathbf{V} \times \mathbf{B} = 0$):

$$\begin{gathered}
\varrho(\mathbf{V}\cdot\nabla)\mathbf{V} = \mathbf{J}\times\mathbf{B} - \nabla\cdot\mathsf{P}, \quad \nabla\cdot\mathbf{B} = 0, \\
\nabla\cdot(\varrho\mathbf{V}) = 0, \quad \nabla\times\mathbf{B} = \mu_0\mathbf{J},
\end{gathered} \tag{4.5}$$

where the CGL pressure tensor and the function σ_d measuring the pressure anisotropy are defined in (1.55). It is assumed that the flow is incompressible, $\nabla\cdot\mathbf{V} = 0$, which by the continuity equation implies that the mass density is constant on streamlines, $\mathbf{V}\cdot\nabla\varrho(\mathbf{r}) = 0$; it is also assumed that the anisotropy function is constant on the magnetic field lines, $\mathbf{B}\cdot\nabla\sigma_d(\mathbf{r}) = 0$. It may be noted that for the given field-aligned equilibria, the vectors $\mathbf{V}$ and $\mathbf{B}$ are collinear (parallel) and therefore the magnetic field lines are the same as the velocity streamlines. It follows that the function $\lambda(\mathbf{r})$ must be constant on magnetic field lines, $\mathbf{B}\cdot\nabla\lambda(\mathbf{r}) = 0$. Also, the force balance equation of the set (4.5) can be cast into the useful form

$$(1-\sigma_d-\lambda^2)\frac{1}{\mu_0}\mathbf{B}\times(\nabla\times\mathbf{B}) + (\sigma_d+\lambda^2)\nabla\left(\frac{\mathbf{B}^2}{2\mu_0}\right) + \nabla P_\perp = 0. \tag{4.6}$$

In order for the new solution (4.3) to be valid it must satisfy the following set of CGL equilibrium equations:

$$\begin{gathered}
\varrho_1(\mathbf{V}_1\cdot\nabla)\mathbf{V}_1 = \mathbf{J}_1\times\mathbf{B}_1 - \nabla\cdot\mathsf{P}_1, \quad \nabla\cdot\mathbf{B}_1 = 0, \\
\nabla\cdot(\varrho_1\mathbf{V}_1) = 0, \quad \nabla\times\mathbf{B}_1 = \mu_0\mathbf{J}_1,
\end{gathered} \tag{4.7}$$

where

$$\mathsf{P}_1 = P_{\perp_1}\mathbf{I} + \frac{\sigma_{d_1}}{\mu_0}\mathbf{B}_1\mathbf{B}_1, \quad \sigma_{d_1} = \mu_0\frac{P_{\parallel_1} - P_{\perp_1}}{\mathbf{B}_1^2} = 1 - n_1^2(\mathbf{r})(1-\sigma_d). \tag{4.8}$$

Note that systems (4.5) and (4.7) are reductions of the generic CGL equilibrium equations since for field-aligned flows it holds $\mathbf{V}\times\mathbf{B} = \mathbf{V}_1\times\mathbf{B}_1 = 0$, and therefore the electric field vanishes by Ohm's law.

Substituting (4.3) into (4.7) yields

$$\mathbf{B}\cdot\nabla\left(\frac{b_1(\mathbf{r})}{n_1(\mathbf{r})}\right)=0, \tag{4.9}$$

$$\mathbf{B}\cdot\nabla(a_1(\mathbf{r})c_1(\mathbf{r}))=0, \tag{4.10}$$

$$C\left[(1-\sigma_d-\lambda^2)\frac{1}{\mu_0}\mathbf{B}\times(\nabla\times\mathbf{B})+(\sigma_d+\lambda^2)\nabla\left(\frac{\mathbf{B}^2}{2\mu_0}\right)+\nabla P_\perp\right] -\frac{1-\sigma_d}{\mu_0}\mathbf{B}\cdot\left(b_1^2\frac{\nabla n_1}{n_1}+c^2\frac{\nabla a_1}{a_1}\right)=0. \tag{4.11}$$

With the use of equation (4.6) and assuming that $\sigma_d\neq 1$ (in which case $\mathbf{V}_1=0$, $C=0$ and the transformations (4.3) are not invertible), equation (4.11) takes the form

$$\mathbf{B}\cdot\left(b_1^2\frac{\nabla n_1}{n_1}+c_1^2\frac{\nabla a_1}{a_1}\right)=0. \tag{4.12}$$

Now with the aid of (4.4), equations (4.9), (4.10) and (4.12) assume the forms

$$\mathbf{B}\cdot\nabla g_1(\mathbf{r})=0, \tag{4.13}$$

$$\mathbf{B}\cdot\nabla f_1(\mathbf{r})=0, \tag{4.14}$$

$$\frac{C}{2}\underbrace{\mathbf{B}\cdot\nabla\left(\frac{1-\sigma_d-\lambda}{1-\sigma_d}\right)}_{0}+\frac{c_1^2(\mathbf{r})}{f_1(\mathbf{r})}\mathbf{B}\cdot\nabla f_1(\mathbf{r})-\frac{b_1^2(\mathbf{r})}{g_1(\mathbf{r})}\mathbf{B}\cdot\nabla g_1(\mathbf{r})=0. \tag{4.15}$$

Since the first term on the left hand side of (4.15) vanishes, it is apparent that if equations (4.13) and (4.14) are valid, then (4.15) is trivially satisfied. Thus, we conclude that in order for transformations (4.3) to be valid, equations (4.13) and (4.14) must be satisfied, or equivalently, both functions $g_1(\mathbf{r})$ and $f_1(\mathbf{r})$ have to be constant on the magnetic field lines of the original equilibria; quod erat demonstrandum.

Therefore, the anisotropic CGL equilibrium system (4.5) possesses a family of intrinsic symmetries since the constituent differential equations are invariant under the transformed variables (4.3).

Remark 1. The symmetry transformations (4.3) presented herein are defined only when the velocity and the magnetic field of the original equilibria are related through (2.61), and transformations (4.2) introduced in reference [216] for field-aligned MHD equilibria consist of a special case of them for $\sigma_d=0$ and $n_1(\mathbf{r})=1$. Although both sets of transformations (4.3) and (4.2) can change the magnitude of the physical equilibrium quantities or create stationary configurations from static ones, they do preserve the topology of the magnetic surfaces, $\psi=$const. (if such surfaces exist), since it holds $\mathbf{B}\cdot\nabla\psi=\mathbf{B_1}\cdot\nabla\psi=0$.

Let us now examine the structure of the arbitrary scalar functions in connection with the magnetic field by first noting that the magnetic and velocity fields of the original equilibria lie on the surfaces $\lambda(\mathbf{r})=$ const., $\mathbf{B}\cdot\nabla\lambda(\mathbf{r})=\mathbf{V}\cdot\nabla\lambda(\mathbf{r})=0$, if such surfaces exist.

If the magnetic field lines are spatially bounded closed curves, labeled by l, then the surfaces $\lambda=$ const. are defined in the neighbourhood of l, with l being itself both a magnetic field line and a streamline. In this situation, the function λ depends on two transversal variables which must define a plane normal to every point of l. If the magnetic field lines are "open", i.e. they approach infinity in one direction, defined by a variable x^3, then the magnetic field should be finite as $x^3\to\infty$. The function $\lambda(\mathbf{r})$ should depend on two transversal variables when the third one goes to infinity, $\lambda(x^1,x^2,x^3\to\infty)=\lambda(x^1,x^2)$, and thus, must depend

on these two variables in the whole plasma domain for magnetic surfaces $\lambda(x^1, x^2) = \text{const.}$ to exist. In both of the above kinds of magnetic field lines (bounded and "open"), the functions $g_1(\mathbf{r})$, $f_1(\mathbf{r})$ have to be functions of two transversal variables, i.e. x^1, x^2. One could suggest that this does not restrict the functions $a_1(\mathbf{r})$, $b_1(\mathbf{r})$, $c_1(\mathbf{r})$, $n_1(\mathbf{r})$ to have the same two-dimensional dependency (i.e. $a(\mathbf{r}) = A(x^1, x^2)D(x^3)$ and $c_1(\mathbf{r}) = K(x^1, x^2)/D(x^3)$, such that $f_1(\mathbf{r}) = A(x^1, x^2)K(x^1, x^2)$). However, equation $\nabla \cdot (\varrho_1 \mathbf{V_1}) = 0$ yields $\mathbf{B} \cdot \nabla a_1(\mathbf{r}) = 0$, which means that $a_1 = a_1(x^1, x^2)$ and consequently $c_1 = c_1(x^1, x^2)$. Then from the definition of the constant C it follows that $b_1 = b_1(x^1, x^2)$, and as a result $n_1 = n_1(x^1, x^2)$. Thus, if the magnetic field lines are finite closed loops or go to infinity in some direction, all functions of transformations must, in general, depend on two variables transversal to this direction.

If the magnetic field lines cover densely everywhere (ergodically) closed magnetic surfaces, $\lambda(\mathbf{r}) = \text{const.}$ (which are toroids), then the functions $g_1(\mathbf{r})$, $f_1(\mathbf{r})$ must be constant on them, and so must be all four functions of the transformations. In this situation, if the field possesses some geometrical symmetry, with ignorable variable x^3, the surfaces $\lambda(\mathbf{r}) = \text{const.}$ are nested, with $\lambda = \lambda(x^1, x^2)$. Then all functions $a_1(\mathbf{r})$, $b_1(\mathbf{r})$, $c_1(\mathbf{r})$, $n_1(\mathbf{r})$ have the same symmetry (i.e. are functions only of x^1, x^2). However, there exists an exception; the one when the original equilibrium has some known geometrical symmetry with purely poloidal magnetic field to be examined as follows.

Axial symmetry: Consider the case that the original equilibria are axially symmetric with field-aligned incompressible flows and anisotropy function constant on magnetic surfaces [114]. Employing cylindrical coordinates $(\rho,\, z,\, \phi)$ we have

$$\mathbf{B} = \frac{I}{\rho}\hat{\boldsymbol{\phi}} + \frac{\hat{\boldsymbol{\phi}}}{\rho} \times \nabla\psi(\rho, z), \quad \mathbf{V} = \frac{M_p}{\sqrt{\mu_0 \varrho}}\mathbf{B}, \tag{4.16}$$

where the function I relates to the toroidal magnetic field and $\psi(\rho, z) = \text{const.}$ labels the magnetic surfaces. Thus, $\lambda(\mathbf{r}) = \lambda(\psi) = M_p(\psi)$, where $M_p = (\sqrt{\mu_0 \varrho}|\mathbf{V}_{pol}|)/|\mathbf{B}_{pol}|$ is the poloidal Alfvén Mach function, which for parallel flows equals to the total Mach function ($M = \sqrt{\mu_0 \varrho}|\mathbf{V}|/|\mathbf{B}|$). To examine whether transformations (4.3) can break axisymmetry we permit the transformation functions to depend, in addition to ψ, explicitly on ϕ, i.e. $f_1 = f_1(\psi, \phi)$, $g_1 = g_1(\psi, \phi)$. Then (4.13) and (4.14) yield

$$\begin{aligned} \frac{I}{\rho^2}\left(\frac{\partial g_1}{\partial \phi}\right) &= 0, \\ \frac{I}{\rho^2}\left(\frac{\partial f_1}{\partial \phi}\right) &= 0. \end{aligned} \tag{4.17}$$

Set (4.17) is satisfied either if functions g_1, f_1 are constant on the magnetic surfaces, or $I = 0$. The latter case implies that transformations (4.3) can break the axial symmetry of field-aligned equilibria with purely poloidal magnetic field. The same statement holds for translationally symmetric equilibria with field-aligned flows [118], while the more generic case of helical symmetry will be studied separately below.

Helical symmetry: Consider now that the original equilibria are helically symmetric with field-aligned incompressible flows and anisotropy function constant on magnetic surfaces for which the following relations hold:

$$\mathbf{B} = I\mathbf{h} + \mathbf{h} \times \nabla\psi(r, u), \quad \mathbf{V} = \frac{M_p(\psi)}{\sqrt{\mu_0 \varrho}}\mathbf{B}, \tag{4.18}$$

where the function I is related to the ζ-contravariant component of $\mathbf{B}$ and the flux function ψ through (2.11), as presented in Chapter 2 and with the aid of the helical coordinates introduced

in Section 1.5. Also note that in this case the useful equations (2.7)-(2.9) hold. Now let us assume that $f_1 = f_1(\psi, \zeta)$, $g_1 = g_1(\psi, \zeta)$. Then satisfaction of equations (4.13) and (4.14) requires

$$\begin{aligned} B^\zeta \left(\frac{\partial g_1}{\partial \zeta} \right) &= 0, \\ B^\zeta \left(\frac{\partial f_1}{\partial \zeta} \right) &= 0. \end{aligned} \tag{4.19}$$

Similar to the case of (4.17), with the aid of (2.7)-(2.9), equation (4.19) leads to

$$B^\zeta = 0 \Rightarrow I = \frac{kr}{m} \frac{\partial \psi}{\partial r} \Rightarrow \mathbf{B} = \mathbf{B}_p. \tag{4.20}$$

Thus, transformations (4.3) can also break the helical symmetry of the original equilibrium with field-aligned incompressible flow and pressure anisotropy, if and only if the magnetic field is purely poloidal.

Remark 2. The flow of the transformed 3D equilibria, obtained from the application of transformations (4.3) to geometrically symmetric equilibria with purely poloidal and field-aligned incompressible flow, is indeed incompressible, $\nabla \cdot \mathbf{V_1} = 0$. However, the transformed mass density, ϱ_1, may vary on the magnetic surfaces since the continuity equation of the set (4.7) is trivially satisfied for purely poloidal velocity, $\mathbf{V_1}$.

Finally, it may happen that $\lambda =$ constant and consequently, $\nabla \lambda = 0$ in the whole plasma domain. In this situation the force balance equation (4.6) is written in the form

$$(1 - \sigma_d - \lambda^2) \mathbf{J} \times \mathbf{B} = \nabla \left(\mathcal{P} + \lambda^2 \frac{\mathbf{B}^2}{2\mu_0} \right) - \frac{\mathbf{B}^2}{2\mu_0} \nabla \sigma_d, \tag{4.21}$$

where $\mathcal{P}$ is defined through (1.60). In this case a family of magnetic surfaces $w(\mathbf{r}) =$ const., where $w \equiv \mathcal{P} + \lambda^2 \frac{\mathbf{B}^2}{2\mu_0}$ can be defined, in which both magnetic field lines and velocity streamlines lie on, $\mathbf{B} \cdot \nabla w(\mathbf{r}) = 0$. Analogous considerations can be made on the structure of these surfaces.

Now it may happen $w =$ const. with $\nabla w = 0$ if $\mathbf{J} = y(\mathbf{r}) \mathbf{B}$, that is the current density is parallel to the magnetic field, or equivalently $\nabla \times \mathbf{V} = t(\mathbf{r}) \mathbf{V}$, that is the velocity is parallel to the vorticity. This is the case of force free or Beltrami equilibria. Then magnetic surfaces $y(\mathbf{r}) =$ const. can be yet defined, $\mathbf{B} \cdot \nabla y(\mathbf{r}) = 0$. But in the particular case $y \equiv$ const. (everywhere) and therefore $\nabla y = 0$ (and then as well $t \equiv$ const., with $\nabla t = 0$), we finally escape from the topological constraint that magnetic field lines lie on surfaces. The lines of force may be chaotic (space-filling) in this case, and all functions $a_1(\mathbf{r})$, $b_1(\mathbf{r})$, $c_1(\mathbf{r})$, $n_1(\mathbf{r})$ have to be constant.

The above conclusions lead us to formulate the following corollary:

Corollary 1. Transformations (4.3) can break the geometrical symmetry, either axial or translational or helical, of the original field-aligned equilibria with incompressible flow and anisotropy function constant on magnetic surfaces, if and only if its magnetic field is purely poloidal. Otherwise, the transformed equilibria retain the original symmetry.

All conclusions derived herein concerning the validity of the transformations, the structure of the arbitrary functions and the symmetry breaking, also hold for the respective transformations (4.2) with isotropic pressure (cf Remark 1).

4.4 Construction of 3D CGL equilibria with field-aligned flows

Consider axisymmetric equilibria [114] with field-aligned incompressible flows, pressure anisotropy and purely poloidal magnetic field. In this case the equilibrium quantities are expressed as

$$\mathbf{B} = (1-\sigma_d - M_p^2)^{-1/2}\frac{\hat{\boldsymbol{\phi}}}{\rho}\times\nabla U,$$
$$\mu_0\mathbf{J} = \frac{1}{\rho}\left[(1-\sigma_d-M_p^2)^{-1/2}\Delta^* U + \frac{1}{2}\frac{\mathrm{d}(\sigma_d+M_p^2)}{\mathrm{d}U}(1-\sigma_d-M_p^2)^{-3/2}|\nabla U|^2\right]\hat{\boldsymbol{\phi}}, \quad (4.22)$$
$$\mathbf{V} = \frac{M_p}{\sqrt{\mu_0\varrho}}\mathbf{B}, \quad \mathcal{P} = \mathcal{P}_s(U) - M_p^2\frac{\mathbf{B}^2}{2\mu_0},$$

and the steady sates obey the following generalized GS equation

$$\Delta^* U + \mu_0\rho^2\frac{\mathrm{d}\mathcal{P}_s}{\mathrm{d}U} = 0, \quad \sigma_d + M_p^2 < 1. \quad (4.23)$$

Here the elliptic operator is defined as $\Delta^* = \rho^2\nabla\cdot(\nabla/\rho^2)$; $\mathcal{P}_s$ is the effective pressure in the absence of flow, and the functions ϱ, σ_d, M_p are uniform on magnetic surfaces, $U(\rho,z) =$ const. Assigning the surface function to be linear in U, $\mathcal{P}_s(U) = (p_1 U)/\mu_0$ with p_1 being free parameter, equation (4.23) takes the linearized form

$$\frac{\partial^2 U}{\partial\rho^2} + \frac{\partial^2 U}{\partial z^2} - \frac{1}{\rho}\frac{\partial U}{\partial\rho} + p_1\rho^2 = 0. \quad (4.24)$$

The partial differential equation (4.24), consisting of a reduction of the respective one found in reference [221], admits a generalized Solovev analytical solution of the form

$$U = \rho\left(\sum_j \left[w_{1_j}J_1(j\rho)\mathrm{e}^{jz} + w_{2_j}J_1(j\rho)\mathrm{e}^{-jz} + w_{3_j}Y_1(j\rho)\mathrm{e}^{jz} + w_{4_j}Y_1(j\rho)\mathrm{e}^{-jz}\right] - \frac{p_1\rho^3}{8}\right), \quad (4.25)$$

where J_1 and Y_1 are first order Bessel functions of the first and second kind, and $j = 1, 2, 3, ...$, while the coefficients w_{i_j}, $i = 1, 2, 3, 4$ can be specified by appropriate boundary conditions. To completely specify the equilibrium we choose the following peaked on-axis profiles for the following free surface functions

$$\sigma_d = \sigma_{d_a}\left(\frac{U}{U_a}\right)^2, \; M_p^2 = M_{p_a}^2\left(\frac{U}{U_a}\right)^2, \; \varrho = \varrho_a\left(\frac{U}{U_a}\right)^{1/2}, \quad (4.26)$$

where the parameters σ_{d_a}, $M_{p_a}^2$, ϱ_a, and U_a denote the values (in pertinent SI units) of the respective functions on the magnetic axis. Imposing the condition that the plasma extends up to the magnetic surface $U = 0$, such that both the pressure and the flow vanish thereon, we construct the up-down symmetric with respect to the plane $z = 0$ configuration of triangular magnetic surfaces shown in figure 4.1, the magnetic axis of which is located at the position $(\rho_a = 2.16, z_a = -6\times10^{-6})$. The cross-section of the magnetic surfaces of the above axisymmetric equilibria remain invariant along the toroidal direction, and the streamlines of its purely poloidal $\mathbf{B}$ and $\mathbf{V}$ fields lying on those surfaces are presented in figure 4.2. Furthermore, every physical quantity associated with equilibria (4.22) is ϕ-independent. Figure 4.3 shows

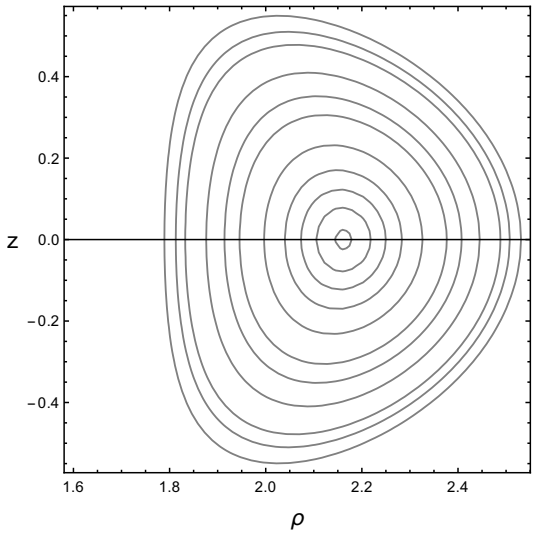

Figure 4.1: Poloidal cut of nested toiroidal magnetic surfaces $U(\rho, z)$ =const. for the axisymmetric equilibria (4.22).

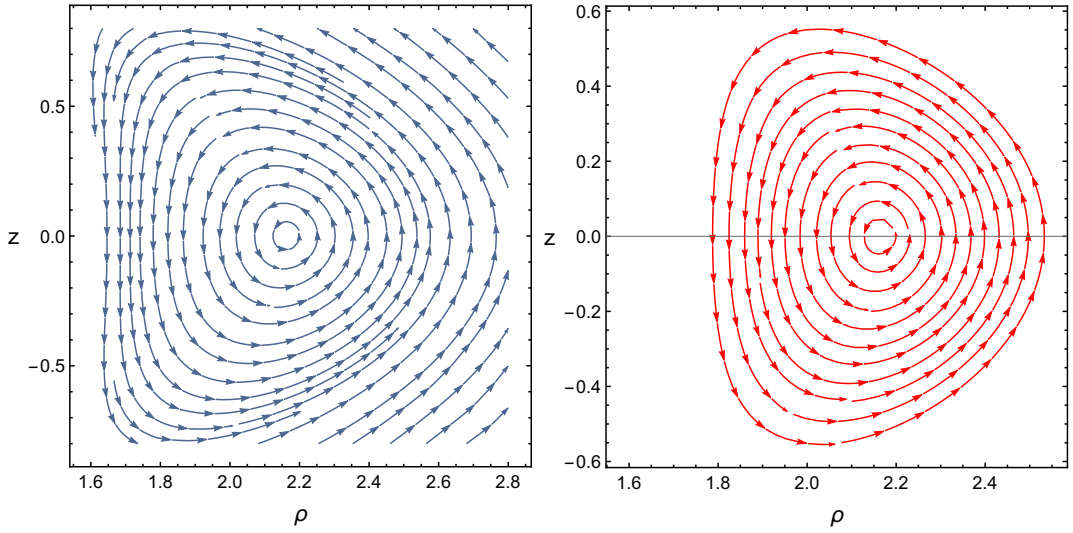

Figure 4.2: Topology of the purely poloidal magnetic field lines (left) and velocity streamlines (right) for the constructed axisymmetric equilibria (4.22).

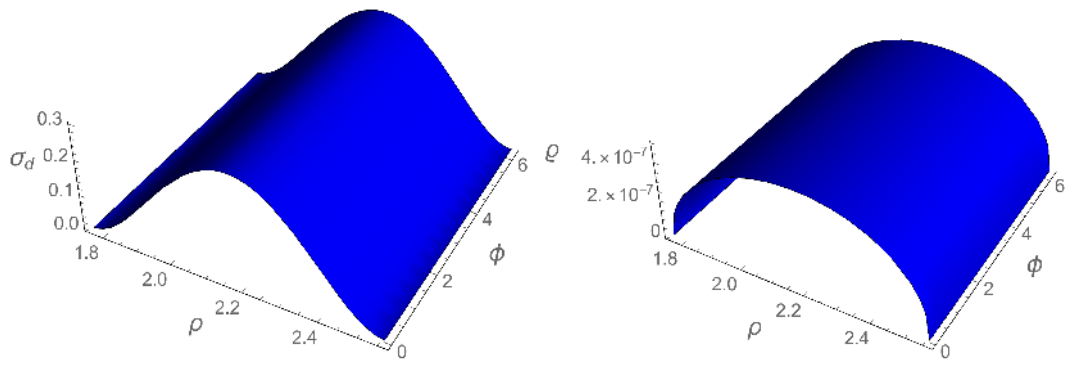

Figure 4.3: Both the pressure anisotropy function, σ_d, (left) and density, ϱ, (right) of the original equilibria peak on the magnetic axis, where $\sigma_{d_a} = 0.3$ and $\varrho_a = 5 \times 10^{-7}\,\mathrm{Kg/m^3}$, and vanish on the bounding surface $U = 0$ for any toroidal angle ϕ.

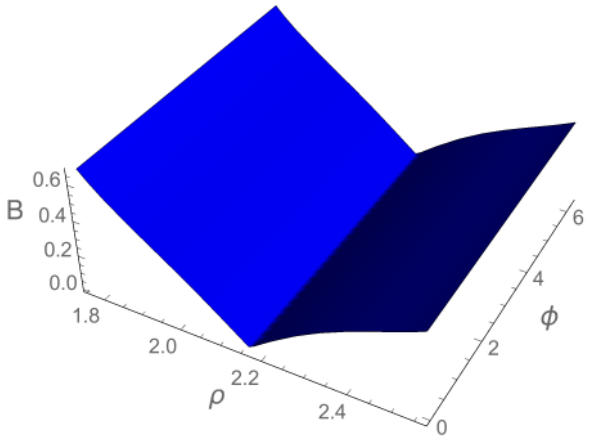

Figure 4.4: The magnetic field magnitude vanishes on the magnetic axis and varies from the high field-side ($B = 0.68\,\mathrm{T}$) to the low field-side ($B = 0.47\,\mathrm{T}$) uniformly for every any angle ϕ.

how anisotropy and density uniformly change along the radial direction for every any angle ϕ on the plane $z = z_a$, while the respective variation of the magnitude of magnetic field on the same plane is presented in figure 4.4.

Applying the symmetry transformations (4.3), with $\lambda = M_p(U)$, to (4.22) we find the following expressions for the physical quantities of the transformed equilibria:

$$\begin{aligned}
\mathbf{B}_1 &= \frac{b_1}{n_1}(1-\sigma_d-M_p^2)^{-1/2}\frac{\hat{\boldsymbol{\phi}}}{\rho}\times\nabla U, \quad \mathbf{V}_1 = \frac{c_1}{a_1}\frac{\sqrt{1-\sigma_d}}{\sqrt{\mu_0\varrho}}(1-\sigma_d-M_p^2)^{-1/2}\frac{\hat{\boldsymbol{\phi}}}{\rho}\times\nabla U,\\
\mu_0\mathbf{J}_1 &= \left[\frac{b_1}{n_1}\left((1-\sigma_d-M_p^2)^{-1/2}\Delta^* U+\frac{1}{2}\frac{\mathrm{d}(\sigma_d+M_p^2)}{\mathrm{d}U}(1-\sigma_d-M_p^2)^{-3/2}|\nabla U|^2\right)\right.\\
&\left.+(1-\sigma_d-M_p^2)^{-1/2}\frac{\partial(b_1/n_1)}{\partial U}|\nabla U|^2\right]\frac{\hat{\boldsymbol{\phi}}}{\rho}-\frac{\partial(b_1/n_1)}{\partial\phi}(1-\sigma_d-M_p^2)^{-1/2}\frac{\nabla U}{\rho^2},\\
\varrho_1 &= a_1^2\varrho, \quad \mathcal{P}_1 = C\mathcal{P}_s(U)-c_1^2(1-\sigma_d)\frac{\mathbf{B}^2}{2\mu_0}, \quad \sigma_{d_1} = 1-n_1^2(1-\sigma_d),
\end{aligned} \tag{4.27}$$

where the functions a_1, b_1, c_1, and n_1 may depend, in addition to U, on the toroidal angle ϕ. However, if either of the functions $n_1(\mathbf{r})$ or $a_1(\mathbf{r})$ remains constant on magnetic surfaces, the breaking of the geometrical symmetry of the original equilibria remains unaffected. Note that the transformed current density $\mathbf{J}_1$ has a component perpendicular to the magnetic surfaces which is undesirable for confinement but this component vanishes when the function $g_1 = b_1/n_1$ is ϕ-independent. This choice, however, yields special equilibria with purely poloidal magnetic field, $\mathbf{B}_1 = \kappa(U)\mathbf{B}$ and permits only 3D variations of velocity and pressure.

To construct a specific equilibrium let us make the following choice for the arbitrary functions:

$$\begin{aligned}
c_1(U,\phi) &= \mathsf{sinh}(\mathsf{cos}(\phi))\left(\frac{1-\sigma_d-M_p^2}{1-\sigma_d}\right)^{1/2},\\
b_1(U,\phi) &= \mathsf{cosh}(\mathsf{cos}(\phi))\left(\frac{1-\sigma_d-M_p^2}{1-\sigma_d}\right)^{1/2},\\
a_1(U,\phi) &= \mathsf{cosh}(\mathsf{cos}(\phi))(1-\sigma_d)^{-1/2}, \quad n_1(U,\phi) = [\mathsf{cosh}(\mathsf{cos}(\phi))]^{1/2}(1-\sigma_d)^{-1/2}.
\end{aligned} \tag{4.28}$$

It is apparent that (4.27) together with (4.28) define exact 3D equilibria with purely poloidal magnetic field and field-aligned flow by breaking the axisymmetry of the original equilibria (4.22). We note that the above equilibria preserve the topology of the original magnetic field

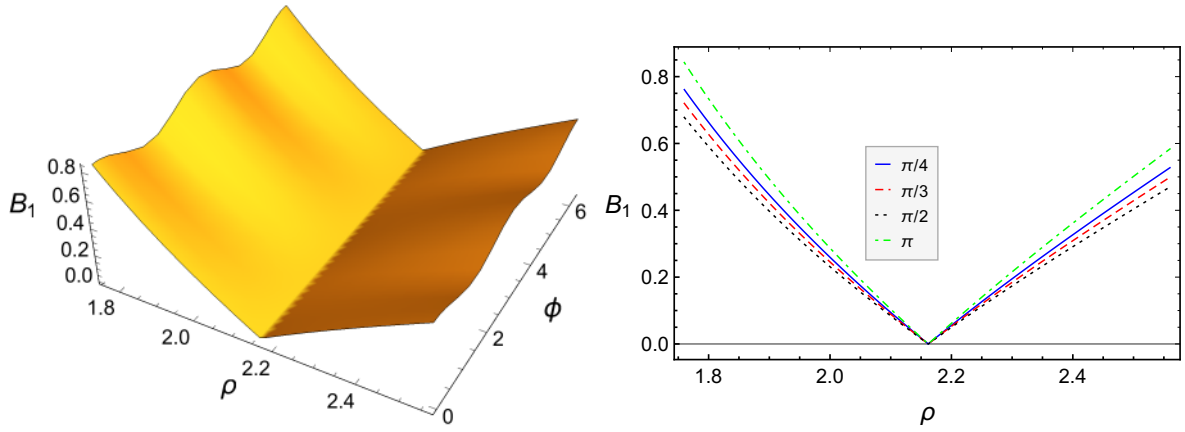

Figure 4.5: (left) The magnitude of the transformed magnetic field, B_1, does change periodically along the toroidal direction. (right) Variation of B_1 along the radial direction on the plane $z = z_a$ for different values of the toroidal angle ϕ.

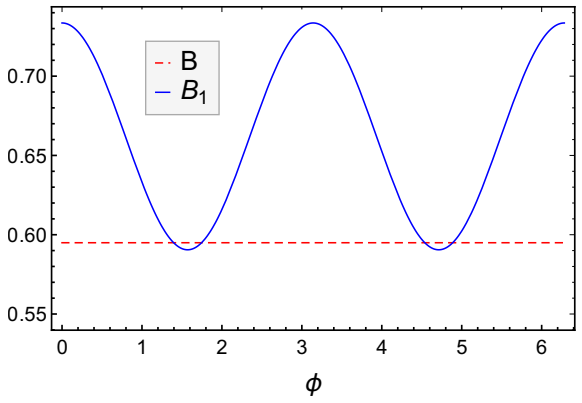

Figure 4.6: While the original B at a poloidal point (chosen as the point $(\rho = 1.8, z = z_a$ in the figure) is ϕ-independent, the respective transformed B_1 varies along the toroidal direction. The magnitude of the transformed field is in general higher than the respective original one except from some specific narrow toroidal regions.

lines and streamlines, $\mathbf{B_1} \cdot \nabla U = \mathbf{V_1} \cdot \nabla U = \mathbf{B} \cdot \nabla U = \mathbf{V} \cdot \nabla U = 0$, and do not obey a GS-like equation analogous to (4.23). Although the topology of the original field lines is preserved, the strenth of the transformed magnetic field in now dependent on the angle ϕ. The magnitude of $\mathbf{B_1}$ is not constant along a specific field-line along the toroidal direction, as shown in figure 4.5; it also differs from the magnitude of the original $\mathbf{B}$, as shown in figure 4.6.

The flow of the transformed equilibria remains incompressible (cf Remark 2). However, on account of the profile of the function $a_1(U, \phi)$ the mass density ϱ_1 is not a surface function, and its variation along the radial direction is not uniform for every toroidal angle ϕ, in contrast to the original density ϱ, as shown in figure 4.7. In addition, the anisotropy function of the transformed equilibria, σ_{d_1}, does not remain constant on the magnetic surfaces, depending on the toroidal angle ϕ, in connection with the scalar function $n_1(U, \phi)$. In contrast to σ_d which is positive and peaked on axis, meaning that $P_\parallel > P_\perp$ within the plasma region for every ϕ, the function σ_{d_1} can take negative values along the toroidal direction; for specific values of ϕ it becomes zero, and thus, $P_{\parallel_1}$ and $P_{\perp_1}$ equilibrate there. These features can be seen in figure 4.8.

Finally, on the basis of the choices for the arbitrary scalar functions (4.28) the function $g_1 = b_1/n_1$ depends in addition to U, on the toroidal angle ϕ. Owing to this dependence,

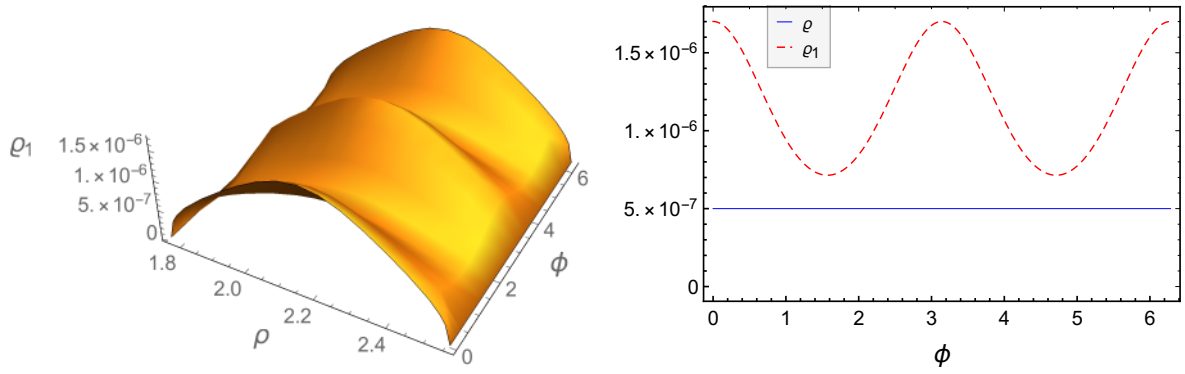

Figure 4.7: (left) The transformed density $\varrho_1(U, \phi)$ on the plane $z = z_a$ does not remain uniform on the magnetic surfaces as the toroidal angle ϕ varies. (right) The value of ϱ_1 on the magnetic axis varies along ϕ and is higher than the respective value of the original ϱ, which is constant and maximum thereon.

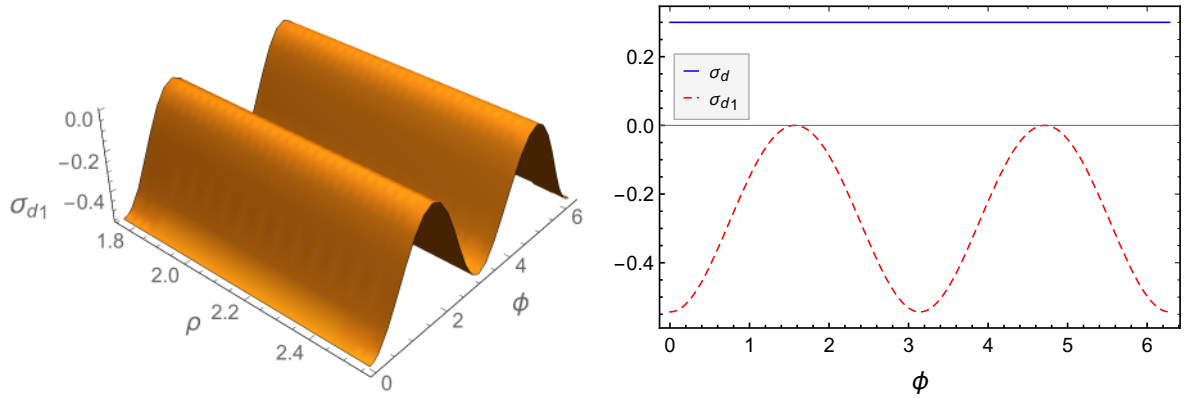

Figure 4.8: (left) The variation of the anisotropy function, σ_{d_1}, of the transformed equilibria is not uniform along the toroidal direction. (right) The perpendicular pressure of the transformed equilibria is higher than the respective parallel one, except from the toroidal angles $\pi/2$ and $3\pi/2$ for which $P_{\parallel_1} = P_{\perp_1}$, in contrast with the original σ_d which is always peaked on-axis and positive for every ϕ.

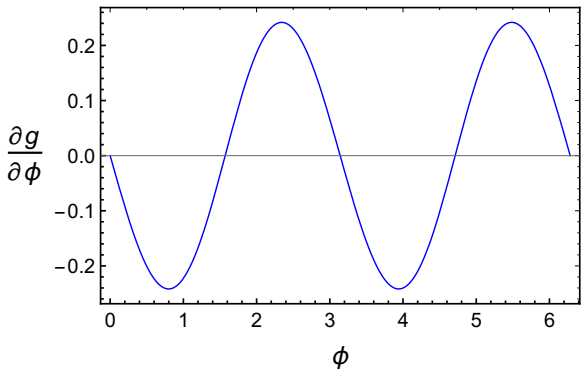

Figure 4.9: The ϕ-derivative of the function g_1 changes periodically sign with respect to ϕ at a period $\pi/2$, thus vanishing for $\phi = \delta\frac{\pi}{2}$, $\delta = 0, 1, 2, \ldots, .$ This results in a similar variation of the poloidal current density component from negative to positive values.

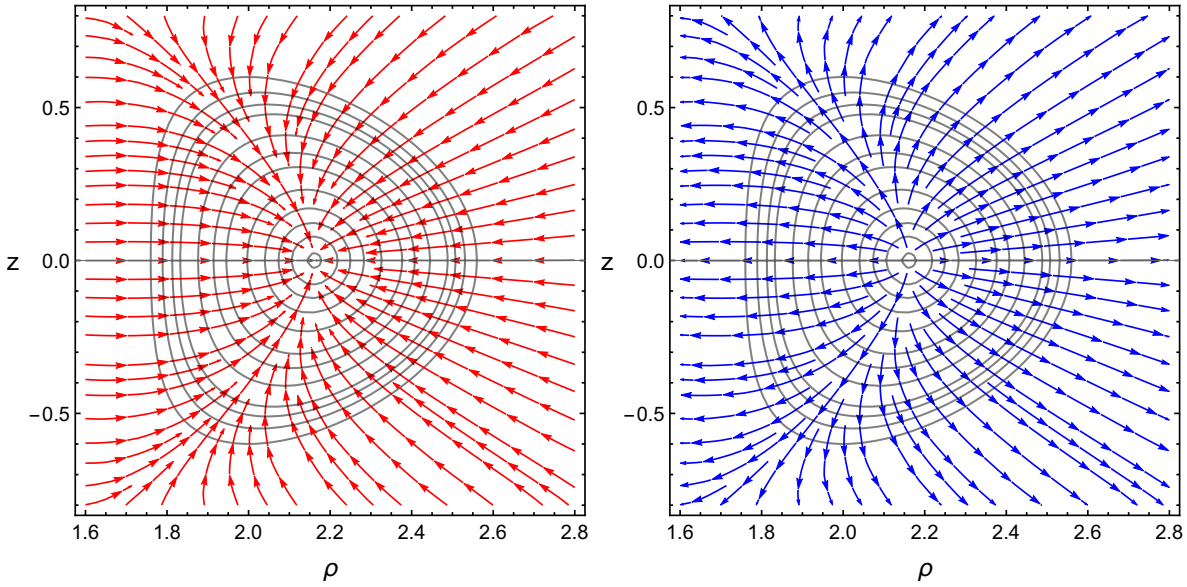

Figure 4.10: The topology of the transformed poloidal -current-density lines for the toroidal angles $\phi = \frac{\pi}{4}$ (left), and $\phi = \frac{3\pi}{4}$ (right) .

the transformed purely poloidal magnetic field is no more axisymmetric but varies periodically with ϕ; therefore, the transformed current density in (4.27) has an additional component perpendicular to the magnetic surfaces. Note that the direction of the transformed poloidal magnetic field follows the behavior of the ϕ-derivative of the function $g_1(U, \phi)$, which varying sinusoidally changes periodically sign at a period $\pi/2$ as shown in figure 4.9. As a result, as ϕ varies the direction of the poloidal current density reverses from outwards to inwards the magnetic surfaces, while it vanishes when $\phi = \delta\frac{\pi}{2}$, $\delta = 0, 1, 2, \ldots$, at which angles the transformed current density becomes purely toroidal (but not axisymmetric). The topology of the poloidal current density component for different toroidal angles is shown in figure 4.10.

Though it is well known that toroidal plasma confinement is not possible with a purely poloidal magnetic field [222], it is interesting that in that case transformations (4.3) can break the geometrical symmetry and yield 3D equilibria. These equilibria may be of astrophysical interest.

4.5 Transformations for flow of arbitrary direction

4.5.1 Review of transformations between MHD-MHD and CGL-CGL equilibria

In references [153,216,217] symmetry transformations that produce an infinite family of MHD (CGL) equilibria with arbitrary incompressible flow once a respective MHD (CGL) equilibrium with incompressible flow is given, were introduced as follows.

MHD into MHD: In the case of isotropic pressure, suppose that $\{\mathbf{B},\, \mathbf{V},\, P,\, \varrho\}$ is a known solution of the MHD equilibrium system with flow of arbitrary direction

$$\begin{aligned} &\varrho(\mathbf{V}\cdot\nabla)\mathbf{V} = \mathbf{J}\times\mathbf{B} - \nabla P, \quad \nabla\cdot(\varrho\mathbf{V}) = 0,\\ &\nabla\times\mathbf{B} = \mu_0\mathbf{J}, \quad \nabla\cdot\mathbf{B} = 0, \quad \mathbf{V}\times\mathbf{B} = \nabla\Phi, \end{aligned} \tag{4.29}$$

where Φ is the electrostatic potential. Note that the above set of equations consist of a limiting form of the set (1.50)-(1.54) for $\sigma_d = 0$. The flow is assumed to be incompressible, $\varrho = \varrho(\psi)$, and the function ψ labels the common magnetic and velocity surfaces, if such surfaces exist. Note that these two sets of surfaces should coincide for flows of arbitrary direction because of the Faraday's and Ohm's laws. Then according to references [216, 217], $\{\mathbf{B}_1,\, \mathbf{V}_1,\, P_1,\, \varrho_1\}$ defined by the following symmetry transformations (depending on the arbitrary functions $a_1(\mathbf{r})$, $b_1(\mathbf{r})$, $c_1(\mathbf{r})$)

$$\begin{aligned} \mathbf{B}_1 &= b_1(\mathbf{r})\mathbf{B} + c_1(\mathbf{r})\sqrt{\mu_0\varrho}\mathbf{V}, \quad \mathbf{V}_1 = \frac{c_1(\mathbf{r})}{a_1(\mathbf{r})\sqrt{\mu_0\varrho}}\mathbf{B} + \frac{b_1(\mathbf{r})}{a_1(\mathbf{r})}\mathbf{V},\\ \varrho_1(\mathbf{r}) &= a_1^2(\mathbf{r})\varrho, \quad P_1 = C\left(P + \frac{\mathbf{B}^2}{2\mu_0}\right) - \frac{\mathbf{B}_1^2}{2\mu_0},\\ C &\equiv b_1^2(\mathbf{r}) - c_1^2(\mathbf{r}) = \text{const.} \neq 0, \end{aligned} \tag{4.30}$$

consists of a new family of solutions to the MHD equilibrium system.

CGL into CGL: For anisotropic pressure let $\{\mathbf{B},\, \mathbf{V},\, \rho,\, P_\perp,\, P_\parallel\}$ be a given solution of the CGL equilibrium system of equations (1.50)-(1.54):

$$\begin{aligned} &\varrho(\mathbf{V}\cdot\nabla)\mathbf{V} = \mathbf{J}\times\mathbf{B} - \nabla\cdot\mathsf{P}, \quad \nabla\cdot(\varrho\mathbf{V}) = 0,\\ &\nabla\times\mathbf{B} = \mu_0\mathbf{J}, \quad \nabla\cdot\mathbf{B} = 0, \quad \mathbf{V}\times\mathbf{B} = \nabla\Phi, \end{aligned} \tag{4.31}$$

with arbitrary incompressible flow implying $\varrho = \varrho(\psi)$, and anisotropy function constant on magnetic surfaces, $\sigma_d = \sigma_d(\psi)$. Then, according to reference [153], $\{\mathbf{B}_1,\, \mathbf{V}_1,\, \varrho_1,\, P_{\perp_1},\, P_{\parallel_1}\}$ defined by the following symmetry transformations

$$\begin{aligned} \mathbf{B}_1 &= \frac{b_1(\mathbf{r})}{n_1(\mathbf{r})}\mathbf{B} + \frac{c_1(\mathbf{r})\sqrt{\mu_0\varrho}}{n_1(\mathbf{r})\sqrt{1-\sigma_d}}\mathbf{V}, \quad \mathbf{V}_1 = \frac{c_1(\mathbf{r})\sqrt{1-\sigma_d}}{a_1(\mathbf{r})\sqrt{\mu_0\varrho}}\mathbf{B} + \frac{b_1(\mathbf{r})}{a_1(\mathbf{r})}\mathbf{V}\\ \varrho_1(\mathbf{r}) &= a_1^2(\mathbf{r})\varrho, \quad P_{\perp 1} = C\left(P_\perp + \frac{\mathbf{B}^2}{2\mu_0}\right) - \frac{\mathbf{B}_1^2}{2\mu_0},\\ P_{\parallel 1} &= C\left(P_\perp + \frac{\mathbf{B}^2}{2\mu_0}\right) + \left[1 - 2n_1^2(\mathbf{r})(1-\sigma_d)\right]\frac{\mathbf{B}_1^2}{2\mu_0},\\ C &\equiv b_1^2(\mathbf{r}) - c_1^2(\mathbf{r}) = \text{const.} \neq 0, \end{aligned} \tag{4.32}$$

is also a solution. Note that transformations (4.32) depend on the arbitrary functions $a_1(\mathbf{r})$, $b_1(\mathbf{r})$, $c_1(\mathbf{r})$, $n_1(\mathbf{r})$, and reduce to the respective ones for isotropic pressure given by the set (4.30) when $\sigma_d = 0$ and $n_1(\mathbf{r}) = 1$.

As stated in reference [153] the functions $a_1(\mathbf{r})$, $b_1(\mathbf{r})$, $c_1(\mathbf{r})$, $n_1(\mathbf{r})$ have to be constant on the magnetic surfaces. Below we examine the validity of these transformations and whether they can break the geometrical symmetry of the original equilibria.

Validation of equilibrium equations for the transformed fields

In order for the new solution (4.32) to be valid it must satisfy the following set of CGL equilibrium equations

$$\begin{aligned} \nabla\cdot(\varrho_1\mathbf{V}_1) &= 0,\\ \varrho_1(\mathbf{V}_1\cdot\nabla)\mathbf{V}_1 &= \mathbf{J}_1\times\mathbf{B}_1-\nabla\cdot\mathsf{P}_1,\\ \nabla\times\mathbf{B}_1 &= \mu_0\mathbf{J}_1,\\ \nabla\times(\mathbf{V}_1\times\mathbf{B}_1) &= 0,\\ \nabla\cdot\mathbf{B}_1 &= 0,\\ \mathbf{V}_1\times\mathbf{B}_1-\nabla\Phi_1 &= 0, \end{aligned} \tag{4.33}$$

where P_1 and σ_{d_1} are given by (4.8).

Expressing in (4.33) the transformed fields in terms of the original ones by means of (4.32) leads to the following system of equations:

$$\mathbf{B}\cdot\nabla b_1+\Lambda\mathbf{V}\cdot\nabla c_1-(b_1\mathbf{B}+c_1\Lambda\mathbf{V})\cdot\frac{\nabla n_1}{n_1}=0, \tag{4.34}$$

$$\Lambda\mathbf{V}\cdot\nabla b_1+\mathbf{B}\cdot\nabla c_1+(\Lambda b_1\mathbf{V}+c_1\mathbf{B})\cdot\frac{\nabla a_1}{a_1}=0, \tag{4.35}$$

$$\mathbf{B}\cdot\left(\frac{\nabla a_1}{a_1}+\frac{\nabla n_1}{n_1}\right)=0, \tag{4.36}$$

$$\mathbf{V}\cdot\left(\frac{\nabla a_1}{a_1}+\frac{\nabla n_1}{n_1}\right)=0, \tag{4.37}$$

$$-\mathbf{B}\cdot\left(b_1^2\frac{\nabla n_1}{n_1}+c_1^2\frac{\nabla a_1}{a_1}\right)-b_1c_1\Lambda\mathbf{V}\cdot\left(\frac{\nabla n_1}{n_1}+\frac{\nabla a_1}{a_1}\right)+\Lambda\mathbf{V}\cdot(b_1\nabla c_1-c_1\nabla c_1)=0, \tag{4.38}$$

$$\Lambda\mathbf{V}\cdot\left(c_1^2\frac{\nabla n_1}{n_1}+b_1^2\frac{\nabla a_1}{a_1}\right)+b_1c_1\mathbf{B}\cdot\left(\frac{\nabla n_1}{n_1}+\frac{\nabla a_1}{a_1}\right)+\mathbf{B}\cdot(b_1\nabla c_1-c_1\nabla c_1)=0, \tag{4.39}$$

where $\Lambda\equiv\sqrt{\mu_0\varrho}/\sqrt{1-\sigma_d}$.

It is apparent that if all four functions appearing in the symmetry transformations are constant on the magnetic surfaces, equations (4.34)-(4.39) are trivially satisfied; otherwise the above system of six equations for the four functions $a_1(\mathbf{r})$, $b_1(\mathbf{r})$, $c_1(\mathbf{r})$, $n_1(\mathbf{r})$ is in general overdetermined. However, if the functions $a_1(\mathbf{r})$, $b_1(\mathbf{r})$, $c_1(\mathbf{r})$, $n_1(\mathbf{r})$ are chosen so that

$$-\frac{\nabla a_1}{a_1}=\frac{\nabla n_1}{n_1}=\frac{\nabla(b_1+c_1)}{(b_1+c_1)}, \tag{4.40}$$

being satisfied when

$$a_1=\frac{1}{n_1},\quad n_1=b_1+c_1, \tag{4.41}$$

then (4.36) and (4.37) are trivially satisfied, while (4.34), (4.35), (4.38) and (4.39) reduce to the single relationship:

$$(\mathbf{B}-\Lambda\mathbf{V})\cdot(b_1\nabla c_1-c_1\nabla b_1)=0. \tag{4.42}$$

Since $b_1\neq\pm c_1$ for the transformation to be invertible, equation (4.42) is satisfied only for parallel flows:

$$\mathbf{V}=\frac{\sqrt{1-\sigma_d}}{\sqrt{\mu_0\varrho}}\mathbf{B}. \tag{4.43}$$

Note that the field-aligned equilibria (4.43) and (2.61) differ from each other, and thus, transformations (4.32) introduced in reference [153] for flow of arbitrary direction are not

reducible into the respective transformations (4.3) for parallel flows presented herein (cf Section 4.3). This result also holds for the respective isotropic transformations (4.30) and (4.2) derived in reference [216]. For the special equilibria with field-aligned flows satisfying (4.43) and $a_1(\mathbf{r})$, $b_1(\mathbf{r})$, $c_1(\mathbf{r})$, $n_1(\mathbf{r})$ generally not constant on magnetic surfaces, transformations (4.32) reduce to

$$\begin{gathered}\mathbf{B}_1=\mathbf{B},\quad \mathbf{V}_1=(b_1+c_1)^2\mathbf{V},\quad \varrho_1=\varrho/(b_1+c_1)^2,\\ P_{\|_1}=CP_\perp+\left[C+1-2(b_1+c_1)^2(1-\sigma_d)\right]\frac{\mathbf{B}^2}{2\mu_0},\\ P_{\perp_1}=CP_\perp+(C-1)\frac{\mathbf{B}^2}{2\mu_0},\quad \sigma_{d_1}=1-(b_1+c_1)^2(1-\sigma_d),\\ C=b_1^2-c_1^2=\text{const.}\neq 0.\end{gathered}\tag{4.44}$$

For equilibria with isotropic pressure satisfying (4.30), being recovered from (4.32) for $\sigma_d=0$ and $n_1=a_1=b_1+c_1=1$, the choice (4.41) leads to

$$\begin{gathered}\mathbf{B}_1=\mathbf{B},\quad \mathbf{V}_1=\mathbf{V},\quad \varrho_1=\varrho,\\ P_1=CP+(C-1)\frac{\mathbf{B}^2}{2\mu_0},\\ C=b_1-c_1=\text{const.}\neq 0.\end{gathered}\tag{4.45}$$

With the aid of (4.44) and (4.45) we observe that in the presence of pressure anisotropy the transformed velocity and mass density differ from the respective, original ones.

Now suppose that the original equilibrium is the helically symmetric introduced in Chapter 2 for which the following relations hold

$$\mathbf{B}=I\mathbf{h}+\mathbf{h}\times\nabla\psi,\tag{4.46}$$

$$\mathbf{V}=\frac{\Theta}{\varrho}\mathbf{h}+\frac{M_p}{\sqrt{\mu_0\varrho}}\mathbf{h}\times\nabla\psi,\tag{4.47}$$

$$\frac{1}{q}\frac{\mathrm{d}\Phi}{\mathrm{d}\psi}=\frac{IM_p}{\sqrt{\mu_0\varrho}}-\frac{\Theta}{\varrho}.\tag{4.48}$$

Then, equation (4.41) implies $I=(\sqrt{1-\sigma_d}/\sqrt{\mu_0\varrho})(\Theta/\varrho)$ and $\mathrm{d}\Phi/\mathrm{d}\psi=0$, and thus, the above relations lead to the following one

$$\frac{I}{\sqrt{\mu_0\varrho}}\left(M_p-\sqrt{1-\sigma_d}\right)=0,\tag{4.49}$$

which implies either $I=0$ or $M_p^2+\sigma_d=1$. It turns out again that symmetry breaking is possible only for purely poloidal parallel flows ($I=0$). The relation $M_p^2+\sigma_d=1$ is connected to the Alfvén singularity. The same conclusion holds for axially and translationally symmetric original equilibria with or without pressure anisotropy.

Arbitrary functions constant on magnetic surfaces

In the above subsection we found that the symmetry transformations (4.32) (and the respective transformations (4.30) for isotropic pressure) are valid when the arbitrary functions are constant on magnetic surfaces, since equations (4.34)-(4.39) are trivially satisfied. Here we examine the equilibria derived from a given geometrically symmetric one of this kind.

Let the original CGL equilibria (4.31) posses magnetic surfaces $\psi=$const. which both $\mathbf{B}$ and $\mathbf{V}$ lie on. Also, suppose that respective surfaces $\psi_1=$const. are defined for the transformed equilibria (4.32) which $\mathbf{B}_1$ and $\mathbf{V}_1$ lie on. It holds that

$$\mathbf{B}_1\times\mathbf{V}_1=\frac{C}{n_1(\psi)a_1(\psi)}\mathbf{B}\times\mathbf{V},\tag{4.50}$$

and thus, the magnetic surfaces through the transformation are preserved:

$$\psi_1 = \mathsf{W}(\psi). \tag{4.51}$$

This means that all vectors $\mathbf{B}$, $\mathbf{B}_1$, $\mathbf{V}$, $\mathbf{V}_1$ lie on the surfaces ψ =const. As a result, if the original equilibria has some known geometrical symmetry, the transformed equilibria will have the same symmetry, too.

Consider now helically symmetric equilibria with incompressible flow of arbitrary direction and anisotropy function constant on magnetic surfaces presented in Chapter 2, for which the following relationships hold that we write here again for convenience:

$$\begin{aligned}
\mathbf{B} &= I\mathbf{h} + \mathbf{h}\times\nabla\psi(r,u),\\
\mathbf{V} &= \frac{\Theta}{\varrho}\mathbf{h} + \frac{M_p}{\sqrt{\mu_0\varrho}}\mathbf{h}\times\nabla\psi(r,u),\\
\mu_0\mathbf{J} &= (\mathcal{L}\psi(r,u) + 2kmqI(\psi,r))\mathbf{h} - \mathbf{h}\times\nabla I(\psi,r),\\
\mathcal{P} &= \mathcal{P}_s(\psi) - \varrho\left[\frac{\mathbf{V}^2}{2} - \frac{(1-\sigma_d)}{q(1-\sigma_d-M_p^2)}\left(\frac{\mathsf{d}\Phi}{\mathsf{d}\psi}\right)^2\right],
\end{aligned} \tag{4.52}$$

Recall that the current density lies on well defined helicoidal surfaces I =const., while the effective pressure is uniform on the surfaces defined by $\mathcal{P}$ =const., both of these two sets of surfaces not coinciding with the magnetic surfaces. By applying the symmetry transformations (4.32) with $a_1 = a_1(\psi)$, $b_1 = b_1(\psi)$, $c_1 = c_1(\psi)$, $n_1 = n_1(\psi)$, we obtain the following class of equilibria:

$$\mathbf{B}_1 = \underbrace{\frac{1}{n_1}\left(b_1 I + c\frac{\sqrt{\mu_0\varrho}}{\sqrt{1-\sigma_d}}\frac{\Theta}{\varrho}\right)}_{I_1}\mathbf{h} + \underbrace{\frac{1}{n_1}\left(b_1 + c_1\frac{M_p}{\sqrt{1-\sigma_d}}\right)}_{\mathsf{G}}\mathbf{h}\times\nabla\psi, \tag{4.53}$$

$$\mathbf{V}_1 = \frac{1}{a_1}\left(c_1\frac{\sqrt{1-\sigma_d}}{\sqrt{\mu_0\varrho}}I + b_1\frac{\Theta}{\varrho}\right)\mathbf{h} + \frac{1}{a_1\sqrt{\mu_0\varrho}}\left(c_1\frac{\sqrt{1-\sigma_d}}{\sqrt{\mu_0\varrho}} + b_1\frac{M_p}{\sqrt{1-\sigma_d}}\right)\mathbf{h}\times\nabla\psi, \tag{4.54}$$

$$\mu_0\mathbf{J}_1 = \left(G\mathcal{L}\psi + \frac{\mathsf{d}G}{\mathsf{d}\psi}|\nabla\psi|^2 + 2kmqI_1\right)\mathbf{h} - \mathbf{h}\times\nabla I_1, \tag{4.55}$$

$$\mathcal{P}_1 = C\mathcal{P} + (1-\sigma_d)\frac{(C\mathbf{B}^2 - n_1^2\mathbf{B}_1^2)}{2\mu_0}. \tag{4.56}$$

Note that although the magnetic surfaces are preserved, neither the transformed current density nor the transformed effective pressure remains on the surfaces of the respective original quantities: $\mathbf{J}_1\cdot\nabla I \neq 0$, $\mathcal{P}_1 \neq \mathcal{P}$.

Now since $\psi_1 = \mathsf{W}(\psi)$ and the original equilibria are helically symmetric the transformed ones should retain that symmetry. This means that the transformed fields can also be written in a form similar to (4.52); in particular for the transformed velocity we have:

$$\mathbf{V}_1 = \frac{\Theta_1}{\varrho_1}\mathbf{h} + \frac{M_{p1}}{\sqrt{\mu_0\varrho_1}}\mathbf{h}\times\nabla\psi_1(r,u), \tag{4.57}$$

where

$$M_{p_1}^2 = \frac{|\mathbf{V}_{p_1}|^2}{|\mathbf{B}_{p_1}|^2/\mu_0\varrho_1} = (n_1\sqrt{1-\sigma_d})\frac{c_1\sqrt{1-\sigma_d} + b_1 M_p}{b_1\sqrt{1-\sigma_d} + c_1 M_p}. \tag{4.58}$$

Equality of the poloidal velocity components in (4.54) and (4.57) yields

$$\frac{\mathsf{d}\psi_1}{\mathsf{d}\psi} = \frac{b_1\sqrt{1-\sigma_d} + c_1 M_p}{n_1\sqrt{1-\sigma_d}} \Rightarrow \psi_1(\psi) = \int_0^{\psi}\frac{b_1(\chi)\sqrt{1-\sigma_d(\chi)} + c_1(\chi)M_p(\chi)}{n_1(\chi)\sqrt{1-\sigma_d(\chi)}}\mathsf{d}\chi. \tag{4.59}$$

Adopting (2.45) both for the original and the transformed helically symmetric equilibria, equation (4.59) yields

$$\frac{\mathrm{d}U_1(U)}{\mathrm{d}U} = C^{1/2} \Rightarrow U_1 = C^{1/2}U. \tag{4.60}$$

Therefore the transformed equilibria differ from the starting ones only by a constant factor $C^{1/2}$, in agreement with the conclusions drawn in the previous Sections; the geometrical symmetry of the original equilibria can break only for purely poloidal magnetic field, otherwise the transformed equilibria retain the original symmetry.

4.5.2 Transformations between MHD-CGL equilibria

In references [153,218,219] transformations that produce CGL anisotropic equilibria from given isotropic MHD ones, are introduced as follows: If $\{\mathbf{B},\, \mathbf{V},\, P,\, \varrho\}$ is a known solution of the MHD equilibrium system (4.29), then the following symmetry transformations

$$\begin{aligned} \mathbf{B}_1 &= f_2(\mathbf{r})\mathbf{B}, \quad \mathbf{V}_1 = g_2(\mathbf{r})\mathbf{v}, \quad \varrho_1 = \frac{C_0\mu_0}{g_2^2(\mathbf{r})}\varrho, \\ P_{\perp_1} &= C_0\mu_0 P + C_1 + \left(C_0\mu_0 - f_2^2(\mathbf{r})\right)\frac{\mathbf{B}^2}{2\mu_0}, \\ P_{\parallel_1} &= C_0\mu_0 P + C_1 - \left(C_0\mu_0 - f_2^2(\mathbf{r})\right)\frac{\mathbf{B}^2}{2\mu_0}, \end{aligned} \tag{4.61}$$

where C_0 and C_1 are arbitrary constants and f_2 and g_2 are arbitrary scalar functions, produce an infinite family of CGL equilibria satisfying (4.33). Transformations (4.61) are also valid in the static limit, $\mathbf{V} = 0$. Let us examine their validity.

Substituting (4.61) into (4.33) we obtain

$$\begin{aligned} \mathbf{B}\cdot\nabla f_2(\mathbf{r}) &= 0, \\ \mathbf{V}\cdot\nabla g_2(\mathbf{r}) &= 0. \end{aligned} \tag{4.62}$$

Thus, in order for transformations (4.61) to be valid, the functions $f_2(\mathbf{r})$ and $g_2(\mathbf{r})$ must be constant on the magnetic field lines and velocity streamlines of the original equilibria, and respective considerations on their structure can be made as those in Section 4.3. Therefore it turns out again that the only way that the geometrical symmetry of the original isotropic equilibria can be broken is if and only if the magnetic and velocity fields are collinear and purely poloidal.

5 | Stability of Anisotropic Incompressible Equilibria

"There are two kinds of mistakes. There are fatal mistakes that destroy a theory, but there are also contingent ones, which are useful in testing the stability of a theory ."

Gian-Carlo Rota

5.1 Energy principle and perturbation potential energy

The Energy Principle [27, 223] is a fundamental technique in investigating ideal magnetostatic plasma stability on the basis of a variational formulation of the pertinent equations of motion. Its simpler mathematical formulation makes it advantageous over the normal mode analysis, and thus widely employed for determing whether a system is stable or not rather than precise growth rates for specific instabilities. The energy principle is based of the fact that the total perturbation energy

$$E = K + W = \frac{1}{2}\int_{\mathcal{D}} \varrho \dot{\boldsymbol{\xi}}^2 d^3r - \frac{1}{2}\int_{\mathcal{D}} \boldsymbol{\xi}\cdot\hat{\mathbf{F}}\boldsymbol{\xi} d^3r \tag{5.1}$$

is conserved, where K is the kinetic energy, W is the potential energy and $\boldsymbol{\xi}$ is a vector related to the displacement of an initial equilibrium. Stability is related to the sign of E. In fact, since, K is quadratic in velocity and therefore non negative definite, stability is related to the sign of the potential energy. More presicely, it is possible to establish instability by finding a trial function $\boldsymbol{\xi}$ for which $W < 0$ as well as to obtain sufficient conditions for the linear stability of a given equilibrium state for which it holds $W \geq 0$. It must be noted, however, that such sufficient conditions in general do depend on stringent hypothesis and their necessity remains an open problem [224, 225]. This is totally the case in the presence of equilibrium flows where, though the force operator remains Hermitian, in that case the convective flow term of the force-balance equation, $(\mathbf{V}\cdot\nabla)\mathbf{V}$, is antisymmetric (cf p.22 in [226]); as a result only a few sufficient conditions for stationary equilibria have been acquired, e.g. [145–149]. Moreover, respective stability conditions for equilibria with anisotropic pressure are also limited. In fact, the Energy Principle in [27] was extended for the case of CGL pressure anisotropy. However, that condition is applicable to static equilibrium for which no heat conduction along and across the magnetic field is assumed (double adiabatic equations of state); it may be noted that the stability of respective static CGL anisotropic equilibria is guaranteed once the respective isotropic ideal MHD (adiabatic) is found to be stable on the basis of the respective static isotropic Energy Principle [227].

Here we derive a sufficient condition for determining the linear stability of hydromagnetic equilibria with the combined effects of both mass flow, which is incompressible, and anisotropic pressure. The derivation is presented in detail bellow in this Chapter.

Consider an inviscid, perfectly conducting plasma with anisotropic pressure contained in a domain $\mathcal{D}$ surrounded by a fixed boundary $\partial\mathcal{D}$. The dynamics of such a plasma is determined by the set of equations (1.45)-(1.49) and (1.39)-(1.40), in which the quantities related with the fluid as well as with the electromagnetic field depend on both the spatial and time variables. Note that the momentum equation (1.46) can be written in the following form

$$\varrho^*(D_t\mathbf{V}^*) = (1-\sigma_d^*)\mathbf{J}^*\times\mathbf{B}^* - \nabla\mathcal{P}^* - \frac{\mathbf{B}^*}{\mu_0}(\mathbf{B}^*\cdot\nabla\sigma_d^*) + \frac{|\mathbf{B}^*|^2}{2\mu_0}\nabla\sigma_d^*, \tag{5.2}$$

in which the scalar pressures $P_\parallel^*$ and $P_\perp^*$ do not appear explicitly. This fact is very useful for the stability analysis to follow. In (5.2) the Langrangian derivative is defined as $D_t \equiv \partial_t + (\mathbf{V}^*\cdot\nabla)$ and the effective pressure $\mathcal{P}^*$ is given in (1.41). Recall that in the absence of anisotropy, owing to particle collisions, equilibration of the scalar pressures along and across $\mathbf{B}^*$ reduces $\mathcal{P}^*$ into a respective isotropic MHD pressure, P^*. The counterpart to set (1.45)-(1.49), (1.39)-(1.40) and (1.41) equilibrium equations are defined by equations (1.50)-(1.54), (1.55) and (1.60), in which all related physical equilibrium quantities (without the superscript $*$) depend only on $\mathbf{r}$. Henceforth we consider that the flow of the background equilibria is incompressible, $\nabla\cdot\mathbf{V}=0$, and thus the continuity equation (1.50) reduces to

$$\mathbf{V}\cdot\nabla\varrho = 0. \tag{5.3}$$

In order to examine the linear stability of a given equilibrium with anisotropic pressure and incompressible flows, we assume that the equilibrium position, $\mathbf{r}$, is perturbed to a position $\mathbf{r}^*(\mathbf{r},t)$, through the usual Lagrangian displacement vector $\boldsymbol{\xi}(\mathbf{r},t) \equiv \mathbf{r}^* - \mathbf{r}$, so that

$$\begin{aligned} \mathbf{B}^* &= \mathbf{B}(\mathbf{r}) + \mathbf{b}(\mathbf{r},t), \quad \mathbf{V}^* = \mathbf{V}(\mathbf{r}) + \mathbf{v}(\mathbf{r},t), \quad \mathbf{J}^* = \mathbf{J}(\mathbf{r}) + \mathbf{j}(\mathbf{r},t), \\ \mathcal{P}^* &= \mathcal{P}(\mathbf{r}) + p(\mathbf{r},t), \quad \varrho^* = \varrho(\mathbf{r}) + \delta(\mathbf{r},t), \quad {\sigma_d}^* = \sigma_d(\mathbf{r}) + \epsilon(\mathbf{r},t). \end{aligned} \tag{5.4}$$

Here, $\mathbf{b}$, $\mathbf{j}$, p, δ, ϵ, and

$$\mathbf{v} = \mathbf{u}(\mathbf{r},t) + \frac{\partial\boldsymbol{\xi}}{\partial t} \tag{5.5}$$

correspond to small perturbations of the respective equilibrium quantities. Note that we have assumed perturbations of the effective pressure, $\mathcal{P}$, and the anisotropy function, σ_d, instead of explicit perturbations of the scalar pressures $P_\parallel$ and $P_\perp$. Also, on the fixed boundary $\partial\mathcal{D}$ surrounding a plasma domain $\mathcal{D}$ of interest we adopt the following conditions:

$$\mathbf{b}\cdot\hat{\mathbf{n}} = \mathbf{u}\cdot\hat{\mathbf{n}} = 0, \tag{5.6}$$

where $\hat{\mathbf{n}}$ is the perpendicular outward unit vector on the boundary. Introducing perturbations (5.4) and employing the equilibrium equations (5.3), (1.51)-(1.54), the dynamical equations are linearized as follows. First, with the aid of (1.53) equation (1.48) yields

$$\nabla\cdot\mathbf{b} = 0. \tag{5.7}$$

Then, with the use of (5.7) together with (1.54) the linearized form of the Ampere's law (1.49) is obtained

$$\mathbf{j} = \frac{1}{\mu_0}\nabla\times\mathbf{b}. \tag{5.8}$$

In addition, by employing (5.3) the continuity equation (1.45) yields

$$\frac{\partial\delta}{\partial t} + \mathbf{V}\cdot\nabla\delta + \nabla\cdot(\varrho\mathbf{v}) = 0, \tag{5.9}$$

while with the aid of (1.51) the momentum equation (1.46) reduces into the linearized form

$$\varrho\frac{\partial \mathbf{v}}{\partial t}+\varrho\left[(\mathbf{V}\cdot\nabla)\mathbf{v}+(\mathbf{v}\cdot\nabla)\mathbf{V}\right]-(1-\sigma_d)(\mathbf{J}\times\mathbf{b}+\mathbf{j}\times\mathbf{B})+\nabla p=G(\mathbf{r},t), \tag{5.10}$$

where

$$\begin{aligned} G \;:=\; & -\delta(\mathbf{V}\cdot\nabla)\mathbf{V}-\epsilon\mathbf{J}\times\mathbf{B}+\frac{1}{\mu_0}\left[\frac{\mathbf{B}^2}{2}\nabla\epsilon-(\mathbf{B}\cdot\nabla\epsilon+\mathbf{b}\cdot\nabla\sigma_d)\mathbf{B}\right.\\ & \left.+\left(\mathbf{B}\cdot\mathbf{b}+\frac{\mathbf{b}^2}{2}\right)\nabla\sigma_d-(\mathbf{B}\cdot\nabla\epsilon)\mathbf{b}\right]. \end{aligned} \tag{5.11}$$

Finally, as concerns the linearized form of the Ohm-Faraday law (1.47), it is obtained upon the definition

$$[\mathbf{Q},\mathbf{W}]:=(\mathbf{W}\cdot\nabla)\mathbf{Q}-(\mathbf{Q}\cdot\nabla)\mathbf{W}, \tag{5.12}$$

where $\mathbf{Q}$, $\mathbf{W}$ are any two arbitrary vectors. It is found that

$$\frac{\partial \mathbf{b}}{\partial t}=[\mathbf{V},\mathbf{b}]+[\mathbf{v},\mathbf{B}], \tag{5.13}$$

where (1.52) was also employed.

At this point recall that in order that the set of dynamical equations (1.45)-(1.49) be closed one needs in connection with the pressures $P_{\parallel}^{*}$ and $P_{\perp}^{*}$ a couple of energy equations or equations of state, e.g. the double adiabatic equations [14] associated with the known CGL model. For the purposes of the present study one such equation of state corresponds to incompressibility in connection with an evolution with constant mass density; that is, we assume $\varrho^{*}=\varrho=$ const., $(\delta=0)$, which apparently implies that the fluid is incompressible. As a result, equation (5.3) is trivially satified while equation (5.9) yields

$$\nabla\cdot\mathbf{v}=0. \tag{5.14}$$

Also, the fact that the momentum equation can be cast in the form (5.2) involving the pressures $P_{\parallel}^{*}$ and $P_{\perp}^{*}$ only implicitly through the effective pressure, $\mathcal{P}^{*}$, and the anisotropy function, σ_d, motivated us to adopt as second equation of state the constrain that the latter function remains constant, $\sigma_d^{*}=\sigma_d=$ const., $(\epsilon=0)$. This implies that $P_{\parallel}^{*}$ and $P_{\perp}^{*}$ (precisely their difference) evolve in such a way that they keep proportional to the magnetic pressure $B^2/(2\mu_0)$, which on physical grounds is an acceptable approximation. Consequently, equation (5.11) implies that $G=0$, while the linearized momentum equation (5.10) reduces to

$$\varrho\frac{\partial \mathbf{v}}{\partial t}+\varrho\left[(\mathbf{V}\cdot\nabla)\mathbf{v}+(\mathbf{v}\cdot\nabla)\mathbf{V}\right]-(1-\sigma_d)(\mathbf{J}\times\mathbf{b}+\mathbf{j}\times\mathbf{B})+\nabla p=0. \tag{5.15}$$

Furthermore, in view of the relation (5.14), we consider incompressible perturbations, $\nabla\cdot\boldsymbol{\xi}=0$, which are more harsh compared to compressible ones, such that the condition $\boldsymbol{\xi}\cdot\hat{\mathbf{n}}=0$ is satisfied on the boundary. Then, equation (5.14) implies that $\nabla\cdot\mathbf{u}=0$. Subsequently, the perturbation of the velocity field can be expressed in terms of $\boldsymbol{\xi}$, as

$$\mathbf{u}=\nabla\times(\boldsymbol{\xi}\times\mathbf{V}). \tag{5.16}$$

Also, by employing the Jacobian identity, $[[\mathbf{Q},\mathbf{W}],\mathbf{S}]\equiv[\mathbf{Q},[\mathbf{W},\mathbf{S}]]-[\mathbf{W},[\mathbf{Q},\mathbf{S}]]$, in equation (5.13) for $\mathbf{Q}=\boldsymbol{\xi}$, $\mathbf{W}=\mathbf{V}$, $\mathbf{S}=\mathbf{B}$ yields

$$\frac{\partial}{\partial t}\left(\mathbf{b}-[\boldsymbol{\xi},\mathbf{B}]\right)=[\mathbf{V},\mathbf{b}-[\boldsymbol{\xi},\mathbf{B}]]. \tag{5.17}$$

Then from relation (5.17) it follows that if $\mathbf{b} = [\boldsymbol{\xi}, \mathbf{B}]$ is satisfied at $t = 0$, then it holds for any $t > 0$. Thus, we conclude that $\mathbf{b} = [\boldsymbol{\xi}, \mathbf{B}]$, or equivalently with the use of (1.53) and (1.52)

$$\mathbf{b} = \nabla \times (\boldsymbol{\xi} \times \mathbf{B}). \tag{5.18}$$

Furthermore, the linearized force balance equation (5.15) is put in the form

$$\varrho \frac{\partial^2 \boldsymbol{\xi}}{\partial t^2} + 2\varrho(\mathbf{V} \cdot \nabla)\frac{\partial \boldsymbol{\xi}}{\partial t} + \nabla f = \hat{\mathbf{F}}\boldsymbol{\xi}. \tag{5.19}$$

Here,

$$\hat{\mathbf{F}} := \varrho\mathbf{u} \times (\nabla \times \mathbf{V}) + \varrho\mathbf{V} \times (\nabla \times \mathbf{u}) + (1 - \sigma_d)\mathbf{J} \times \mathbf{b} - \frac{1}{\mu_0}\mathbf{B} \times (\nabla \times \mathbf{b}), \tag{5.20}$$

is the symmetric force operator and the scalar function f is defined as

$$f := \varrho\mathbf{V} \cdot \mathbf{u} + p. \tag{5.21}$$

So far we have succesfully linearized the dynamical equations (1.45)-(1.49) each of them being related with the displacement vector. Indeed, on account of equations (5.16)-(5.21), the potential energy $W = \frac{1}{2}\int_{\mathcal{D}} \boldsymbol{\xi} \cdot \hat{\mathbf{F}}\boldsymbol{\xi} d^3r$ is expected to depend only on the physical quantities of the background equilibrium and the displacement vector, $\boldsymbol{\xi}$, with the exception of the perturbation, p, of the effective pressure, appearing in the gradient of the quantity f. However, the contribution of the latter term to W vanishes due to the implied boundary conditions on $\partial\mathcal{D}$, (5.6). Thus, one finds for the perturbation potential energy

$$W = \frac{1}{2}\int_{\mathcal{D}} \left\{ \varrho\mathbf{u} \cdot [\boldsymbol{\xi} \times (\nabla \times \mathbf{V})] - \varrho\mathbf{u}^2 + (1 - \sigma_d)\mathbf{b} \cdot (\mathbf{J} \times \boldsymbol{\xi}) + \frac{(1 - \sigma_d)}{\mu_0}\mathbf{b}^2 \right\} d^3\mathbf{r}. \tag{5.22}$$

This is the form of the potential energy for incompressible perturbations, of an initial equilibrium with incompressible flow of arbitrary direction, of constant mass density and constant anisotropy function, the study of the sign of which may determine their stability.

5.2 Sufficient condition for linear stability of field-aligned equilibria

In connection with potential acquisition of sufficient stability conditions from the expression for the potential energy (5.22), we restrict our analysis to field-aligned flows. In other words, we henceforth consider a background equilibrium with collinear velocity and magnetic fields specially related through (2.61), as that described in Subsection 2.2.1. In fact, under the assumptions that the mass density and the anisotropy function remain constant everywhere inside a volume $\mathcal{D}$ (ϱ, σ_d = const.) it follows that the corresponding field-aligned equilibrium flow becomes incompressible and the function λ is constant on magnetic surfaces ψ = const., whenever such surfaces exist. Also, both the magnetic and velocity fields lie on those surfaces, $\mathbf{B}\cdot\nabla\lambda(\psi) = \mathbf{V}\cdot\nabla\lambda(\psi) = 0$. It is known that the existence of three-dimensional equilibria with nested toroidal magnetic surfaces is not guaranteed, and in general, irrespective of the existence of magnetic surfaces the function λ is constant on both the magnetic field lines and the velocity streamlines. Henceforth, we will presume the existence of well defined equilibrium magnetic surfaces. Such kind of field-aligned equilibria are governed by a force-balance equation of the form (2.65):

$$\mathbf{J} \times \mathbf{B} = g(\psi, \mathbf{B}^2)\nabla\psi, \tag{5.23}$$

where the exact form of the function g for $\sigma_d = \text{const.}$ is

$$g(\psi, \mathbf{B}^2) := (1 - \sigma_d - \lambda^2)^{-1} \left[\mathcal{P}_s' - (\lambda^2)' \frac{\mathbf{B}^2}{2\mu_0} \right], \tag{5.24}$$

and the static effective pressure is defined as

$$\mathcal{P}_s(\psi) := \mathcal{P} + \lambda^2 \frac{\mathbf{B}^2}{2\mu_0}. \tag{5.25}$$

Owing to equations (2.61) and (5.23)-(5.25) the potential energy of the perturbations (5.22), for equilibria with field-aligned incompressible flows, constant density and constant anisotropy function, reduces to the form

$$W = \frac{1}{2\mu_0} \int_{\mathcal{D}} \left\{ (1 - \sigma_d - \lambda^2)[\mathbf{b}^2 + \mathbf{b} \cdot (\mu_0 \mathbf{J} \times \boldsymbol{\xi})] - 2\lambda (\boldsymbol{\xi} \cdot \nabla \lambda)(\boldsymbol{\xi} \cdot [(\mathbf{B} \cdot \nabla)\mathbf{B}]) \right\} d^3\mathbf{r}. \tag{5.26}$$

In what follows we employ the form of W given in equation (5.26) to derive a sufficient condition for the linear stability of the respective kind of equilibria. To this end, we define the following quantities:

$$\mathbf{N} := \mathbf{J} \times \mathbf{B}, \quad \mathbf{M} := \nabla \times \mathbf{N} = \nabla g \times \nabla \psi, \tag{5.27}$$

from which it follows that

$$\mathbf{N} \cdot \mathbf{M} = 0. \tag{5.28}$$

As noted earlier in Subsection 2.2.1 and is also evident from equations (2.61), (5.23)-(5.25), for the equilibria with field-aligned incompressible flows, constant mass density and constant pressure anisotropy function, σ_d, the current density stays on magnetic surfaces, $\psi = \text{const.}$, and thus, the vectors $\mathbf{B}$, $\mathbf{J}$ and $\mathbf{N} = \mathbf{J} \times \mathbf{B}$, form a basis in $\mathbb{R}^3$ space. Accordingly, following references [147–149], we assume that $\mathbf{J} \times \mathbf{B} \neq 0$ and expand the displacement vector in this basis, as

$$\boldsymbol{\xi} = \alpha(\mathbf{r}, t)\mathbf{N} + \beta(\mathbf{r}, t)\mathbf{J} + \gamma(\mathbf{r}, t)\mathbf{B}, \tag{5.29}$$

where α, β, and γ are arbitrary, appropriately dimensional scalar functions. We note that in [149] a sufficient condition was derived for the linear stability of equilibria with field-aligned incompressible flows, isotropic pressure and constant density; in fact, the constant density and the vacuum magnetic permeability constant were set to unity therein. These equilibria are recovered from the respective anisotropic-pressure equilibria defined above for $\sigma_d = 0$. Also, we observe that the form (5.26) of potential energy for $\sigma_d = 0$ (and $\varrho = \mu_0 = 1$) reduces to the respective isotropic form of [149] [see equation (13) therein]. Thus, it is straightforward to derive along the same lines as in [149] a sufficient condition for the linear stability of the present anisotropic equilibria. In specific, it can be shown (see Appendix D for a detailed derivation) that W assumes the form

$$W = W_1 + W_2, \tag{5.30}$$

$$W_1 = \frac{1}{2\mu_0} \int_{\mathcal{D}} (1 - \sigma_d - \lambda^2)(\mathbf{b} + \alpha\mu_0 \mathbf{J} \times \mathbf{N})^2 d^3\mathbf{r}, \tag{5.31}$$

$$W_2 = \frac{1}{2\mu_0} \int_{\mathcal{D}} \mathcal{A}(\sqrt{2} g \alpha)^2 d^3\mathbf{r}, \tag{5.32}$$

where

$$\begin{aligned} \mathcal{A} \;:=\; & -(1 - \sigma_d - \lambda^2) \left\{ |\mu_0 \mathbf{J} \times \nabla\psi|^2 - (\mu_0 \mathbf{J} \times \nabla\psi) \cdot [(\nabla\psi \cdot \nabla)\mathbf{B}] \right\} \\ & + \frac{\mu_0}{2} [\ln(1 - \sigma_d - \lambda^2)]' |\nabla\psi|^2 \nabla\psi \cdot \nabla \left(P_\perp + \frac{\mathbf{B}^2}{2\mu_0} \right). \end{aligned} \tag{5.33}$$

Equations (5.31) and (5.32) imply that W is non-negative if both quantities $1-\sigma_d-\lambda^2$ and $\mathcal{A}$ are also non-negative definite in $\mathcal{D}$. Thus, we conclude to the following statement:

An equilibrium with anisotropic pressure with $\sigma_d = const.$, field-aligned incompressible flow in connection with constant plasma density is linearly stable if both of the following conditions are satisfied:

$$1-\sigma_d-\lambda^2 \geq 0, \tag{5.34}$$

$$\mathcal{A} \geq 0. \tag{5.35}$$

Conditions (5.34) and (5.35) can be applied to any steady state without geometrical restriction. They generalize the ones derived in [149] for isotropic pressure, since for $\sigma_d = 0$ condition (5.34) reduces to sub-Alfvénic flows, $\lambda^2 < 1$, while (5.35) reduces to the condition introduced in equation (22) of reference [149]. In fact, the expression (5.33) is more compact because it consists of three terms, instead of four terms in the respective one of [149]. The first of these terms,

$$A_1 = -(1-\sigma_d-\lambda^2)|\mu_0\mathbf{J}\times\nabla\psi|^2, \tag{5.36}$$

is negative and therefore always destabilizing, in potential connection with current-driven modes. The second term,

$$A_2 = (1-\sigma_d-\lambda^2)(\mu_0\mathbf{J}\times\nabla\psi)\cdot[(\nabla\psi\cdot\nabla)\mathbf{B}], \tag{5.37}$$

is related to the magnetic shear (i.e. it depends on the variation of $\mathbf{B}$ across the magnetic surfaces), and can be either stabilizing or destabilizing. The third term,

$$A_3 = \frac{\mu_0}{2}[\ln(1-\sigma_d-\lambda^2)]'|\nabla\psi|^2\nabla\psi\cdot\nabla\left(P_\perp+\frac{\mathbf{B}^2}{2\mu_0}\right), \tag{5.38}$$

can be regarded as flow term, though being affected by anisotropy, since it vanishes in the absence of flow ($\lambda = 0$). Note that it relates to the variation of the total pressure perpendicular to the magnetic surfaces; indeed, on account of equations (1.61) and (5.25) one finds

$$P_\perp+\frac{\mathbf{B}^2}{2\mu_0} = \underbrace{\mathcal{P}_s(\psi)}_{\text{static}} - \underbrace{\frac{1}{2}\varrho\mathbf{V}^2}_{\text{flow}} + \underbrace{(1-\sigma_d)\frac{\mathbf{B}^2}{2\mu_0}}_{\text{magnetic}}, \tag{5.39}$$

which involves all three pressures, static effective, flow and magnetic, the latter being influenced by the pressure anisotropy through the factor $(1-\sigma_d)$. In addition, satisfaction of condition (5.34) in the absence of flow, $\sigma_d \leq 1$, implies that the corresponding static anisotropic equilibria are stable under the fire-hose instability [153].

Before closing this section it is convenient to express the derived stability condition in U-space. That is, under the transformation (2.45), which implies that the condition (5.34) is always satisfied in the sub-Alfvénic region, (5.35) is written as

$$\begin{aligned}\mathcal{A} \;=\; & -|\mu_0\mathbf{J}\times\nabla U|^2 + (\mu_0\mathbf{J}\times\nabla U)\cdot[(\nabla U\cdot\nabla)\mathbf{B}] \\ & + \frac{\mu_0}{2(1-\sigma_d-\lambda^2)}\frac{d\ln(1-\sigma_d-\lambda^2)}{dU}|\nabla U|^2\nabla U\cdot\nabla\left(P_\perp+\frac{\mathbf{B}^2}{2\mu_0}\right).\end{aligned} \tag{5.40}$$

Condition $\mathcal{A}\geq 0$ in connection with form (5.40) will be employed in Section 5.4 to examine the linear stability of specific helically symmetric equilibria.

5.3 Stability under symmetry transformations

In Section 4.3 transformations that map CGL-CGL equilibria with field-aligned incompressible flows and anisotropic pressure were introduced. In this Section we examine the linear stability of the continuous families of equilibria arising from the application of those transformations to given equilibrium with field-aligned incompressible flows and constant anisotropy function, in connection with the derived sufficient stability condition as follows.

From (4.3) it readily follows that the transformed collinear velocity and magnetic fields are related through

$$\mathbf{V}_1 = \frac{\lambda_1}{\sqrt{\mu_0 \varrho_1}} \mathbf{B}_1, \quad \lambda_1 = \frac{c_1 n_1}{b_1} \sqrt{1 - \sigma_d}, \tag{5.41}$$

and thus, the trasformed equilibria satisfy a force-balance equation analogous to (2.63):

$$(1-\sigma_{d_1}-\lambda_1^2)\mathbf{J}_1 \times \mathbf{B}_1 = \nabla \left(\mathcal{P}_1 + \lambda_1^2 \frac{\mathbf{B}_1^2}{2\mu_0} \right) + \frac{\mathbf{B}_1^2}{2\mu_0} \nabla(1-\sigma_{d_1}-\lambda_1^2) - \frac{\mathbf{B}_1}{\mu_0} \left[\mathbf{B}_1 \cdot \nabla(1 - \sigma_{d_1} - \lambda_1^2) \right]. \tag{5.42}$$

With the aid of equations (4.3) and (5.41) we obtain the useful relations

$$1 - \sigma_{d_1} - \lambda_1^2 = C \left(\frac{n_1}{b_1} \right)^2 (1 - \sigma_d - \lambda^2), \tag{5.43}$$

$$\mathcal{P}_1 + \lambda_1^2 \frac{\mathbf{B}_1^2}{2\mu_0} = C \left(\mathcal{P} + \lambda^2 \frac{\mathbf{B}^2}{2\mu_0} \right) = C \mathcal{P}_s, \tag{5.44}$$

under which equation (5.42) reduces to

$$\left(\frac{n_1}{b_1} \right)^2 \mathbf{J}_1 \times \mathbf{B}_1 = \mathbf{J} \times \mathbf{B} + \frac{\mathbf{B}_1^2}{2\mu_0} \nabla \left(\frac{n_1}{b_1} \right)^2. \tag{5.45}$$

Now, presume that the original equilibrium belongs to the family described in Section 5.2 for which equations (2.61) and (5.23)-(5.25) hold; then equation (5.45) becomes

$$\left(\frac{n_1}{b_1} \right)^2 \mathbf{J}_1 \times \mathbf{B}_1 = g(\psi, \mathbf{B}^2) \nabla \psi + \frac{\mathbf{B}_1^2}{2\mu_0} \nabla \left(\frac{n_1}{b_1} \right)^2. \tag{5.46}$$

Projection of equation (5.46) along $\mathbf{J}_1$ yields

$$\mathbf{J}_1 \cdot \nabla \psi = -\frac{\mathbf{B}_1^2}{2\mu_0} \left[\mathbf{J}_1 \cdot \nabla \left(\frac{n_1}{b_1} \right)^2 \right], \tag{5.47}$$

and thus, it turns out that the transformed current density, $\mathbf{J}_1$, remains on the magnetic surfaces if and only if the ratio n_1/b_1 is uniform on those surfaces

$$\frac{n_1}{b_1} := y_1(\psi). \tag{5.48}$$

In this case, the transformed vectors, $\mathbf{J}_1$, $\mathbf{B}_1$, and $\mathbf{N}_1 \equiv \mathbf{J}_1 \times \mathbf{B}_1$, form a basis in $\mathbb{R}^3$, and thus, for constant ϱ_1 and σ_{d_1}, sufficient conditions for the linear stability of the transformed equilibria, satisfying (4.3), (5.41) and (5.48), analogous to (5.34) and (5.35) can be derived:

$$1 - \sigma_{d_1} - \lambda_1^2 \geq 0, \tag{5.49}$$

$$\mathcal{A}_1 \geq 0, \tag{5.50}$$

where

$$\begin{aligned}\mathcal{A}_1 &= -(1-\sigma_{d_1}-\lambda_1^2)\{|\mu_0\mathbf{J}_1\times\nabla\psi|^2+(\mu_0\mathbf{J}_1\times\nabla\psi)\cdot[(\nabla\psi\cdot\nabla)\mathbf{B}_1]\}\\ &\quad+\frac{\mu_0}{2}[\ln(1-\sigma_{d_1}-\lambda_1^2)]'|\nabla\psi|^2\nabla\psi\cdot\nabla\left(\mathcal{P}_{\perp_1}+\frac{\mathbf{B}_1^2}{2\mu_0}\right).\end{aligned}\tag{5.51}$$

In order to investigate the stability of an aforementioned transformed equilibrium, we presume that the original equilibrium has constant density and anisotropy functions ($\varrho=$ const., $\sigma_d=$ const.) and is stable under small three-dimensional perturbations; therefore, conditions (5.34) and (5.35) are satisfied in $\mathcal{D}$. Note that in this case the scalar functions of transformation (4.3) must have a structrure of the form: $a_1=$ const., $n_1=$ const., $b_1=b_1(\psi)$, $c_1=c_1(\psi)$; as a result, breaking potential geometrical symmetry of the original equilibrium is not possible by the transformation even for purely poloidal $\mathbf{B}$ and $\mathbf{V}$ fields. In [148] the stability of respective isotropic equilibria was examined; in particular, it was stated therein that all equilibrium families resulting from the application of the respective isotropic transformations introduced by Bogoyavlenskij to given equilibria of field-aligned incompressible flows, isotropic pressure and constant mass density, are linearly stable, if either the original equilibria is stable and $C>0$, or the original equilibria is unstable and $C<0$. A straightforward calculation shows that

$$\mathcal{A}_1=C\mathcal{A},\tag{5.52}$$

so that conditions (5.49) and (5.50) assume the form

$$C\left(\frac{n_1}{b_1}\right)^2(1-\sigma_d-\lambda^2)\geq 0,\tag{5.53}$$

$$C\mathcal{A}\geq 0.\tag{5.54}$$

By inspection of the latter relations we come to the conclusion that the transformed equilibrium is linearly stable if, either (i) the original one is linearly stable and $C>0$, or (ii) neither of the conditions (5.34), (5.35) are satisfied and $C<0$. However, when C is negative equation (5.44) in the absence of flow ($\lambda=0$) yields the physically unacceptable relation

$$\frac{\mathcal{P}_1}{\mathcal{P}}<0.\tag{5.55}$$

Thus, we finally conclude to the formulation of the following statement:

The infinite class of equilibria, obtained from the application of the symmetry transformations (4.3) for the case $\varrho_1=$ const. and $\sigma_{d_1}=$ const. to given respective equilibria which are linearly stable (by satisfying the sufficient conditions (5.34)-(5.35)), are also linearly stable if the transformation constant C is positive definite.

This statement corrects and generalises the respective statement in [148] for isotropic equilibria ($\sigma_d=\sigma_{d_1}=0$, $n_1=1$).

5.4 Linear stability of helically symmetric equilibria

Consider helically symmetric equilibria of astrophysical jets with field-aligned incompressible flows and anisotropic pressure defined by equations (3.65)-(3.68), derived in [209]. In order to construct specific equilibria, we restict our analysis to solution (3.67) for $\delta=2$, $\mu=1$, $\nu=0$, and $\chi_{11}=7/(6m)$, which assumes the simpler form [see equation (4.2) in [209]]:

$$U(r,u)=e^{-wr^2}[1-10wr^2+8w^2r^4+c_{10}\cos(u/m)].\tag{5.56}$$

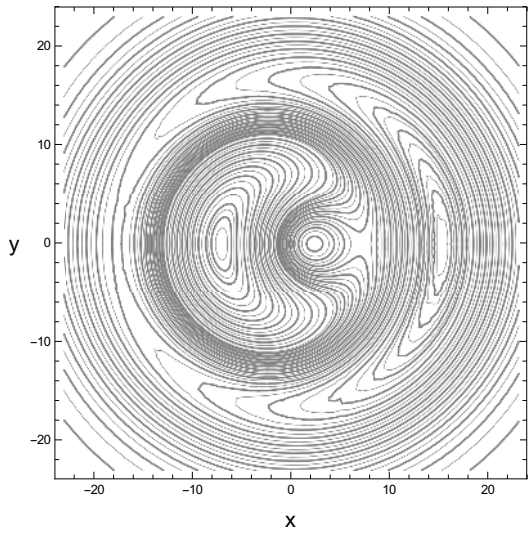

Figure 5.1: Poloidal cut of helicoidal magnetic surfaces $U(x, y, z = 0)$ =const. for the helically symmetric equilibrium solution (5.56).

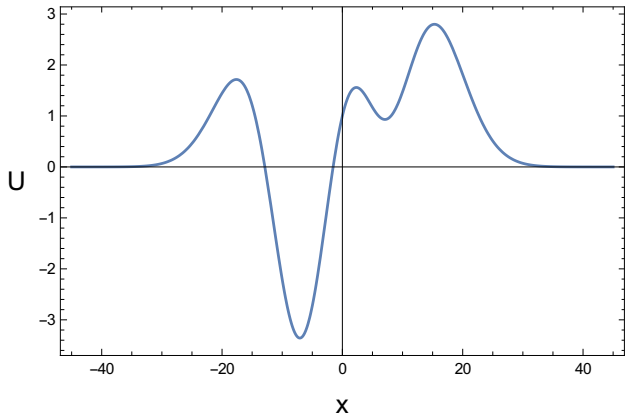

Figure 5.2: Profile of the function $U(x, y = 0, z = 0)$ =const. for the helically symmetric equilibrium solution (5.56).

Solution (5.56) of the GGS equation (2.46) associated with the profiles (3.65) defines a special class of exact helically symmetric equilibria with field-aligned incompressible flows and anisotropic pressure, valid for any functional dependence of $M_p^2(U)$, $\varrho(U)$ and $\sigma_d(U)$. In connection with the present Chapter, in order to completely determine an equilibrium we assume that both the mass density and pressure anisotropy functions are constant everywhere inside the plasma volume $\mathcal{D}$: $\varrho = \sigma_d =$ const.; also we employ the following profile for the Mach function

$$M_p^2(U) = M_{p_0}^2 U^2, \tag{5.57}$$

where M_{p_0} is an arbitrary parameter. The magnetic surfaces of the above constructed equilibria on the Cartesian plane $z = 0$, for $w = 0.01$, $c_{10} = 0.5$, $\pi_{00} = 2\mu_0$, and $m = 2.318$, are shown in figure 5.1; all dimensional quantities present in this section are measured in appropriate SI units. Also, the profile of the flux function U along the x-axis is given in figure 5.2. In figures 5.1 and 5.2 it can be seen that the plasma domain consists of two sub-domains: an outer one consisting of magnetic surfaces with circular poloidal cross-sections extending up to infinity ($r \to \infty$), and an inner sub-domain containing three lobes and a couple of saddle points (X-points). The inner X-point, corresponding to a maximum of U is located at $x = -17.6$. Then on the right hand side of this first X-point are located successively two lobes, then the second X point and farther outwards the third lob. The respective magnetic axes of the lobes

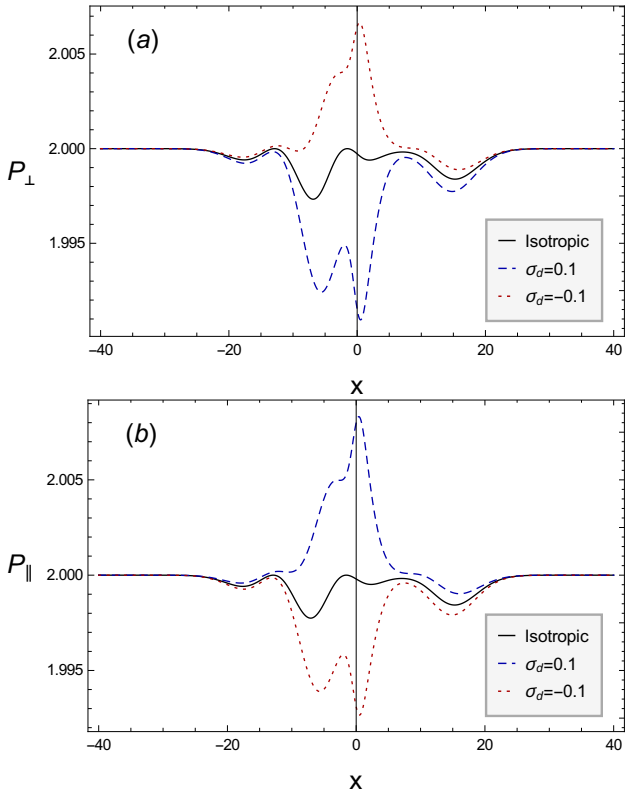

Figure 5.3: The profiles of the scalar pressures (a) $P_\perp(x, y = 0, z = 0)$ and (b) $P_\parallel(x, y = 0, z = 0)$ for the constructed stationary equilibria, for $M^2_{p_0} = 10^{-3}$. The blue dashed curve correspond to $\sigma_d = 0.1$, while the red dotted one to $\sigma_d = -0.1$.

are located at $x = -7.07$, $x = 2.31$ and $x = 15.3$ while the second X-point is located at $x = 7.07$. Each helix composing such a helically symmetric configuration is characterized by a pitch, η, and a torsion, τ, given by

$$\eta = 2\pi m, \qquad \tau = \frac{m}{r^2 + m^2}. \tag{5.58}$$

The above equilibrium can model helically symmetric jets with anisotropic pressure, tending to become isotropic at very long distances ($r \to \infty$). In more detail, for any $\sigma_d = \text{const.} \neq 0$ inside $\mathcal{D}$, the scalar pressures parallel and perpendicular to $\mathbf{B}$ are given by the relations (1.61) indicating that when $\sigma_d > 0$, its increase results in an enhancement of $P_\perp$ while $P_\parallel$ decreases, and vice versa for $\sigma_d < 0$, as can be seen at the profiles of $P_\parallel$ and $P_\perp$ shown in figure 5.3. In the limit of $r \to \infty$ the magnetic field, current density and velocity vanish and therefore the scalar pressures become equal each other, i.e. $P_\perp = P_\parallel = \pi_{00}/\mu_0 = \text{const.}$ because of the second of (3.65) and (1.61). Thus the configuration becomes in this limit isotropic. Note that this is compatible with a non zero value of σ_d on account of the definition (1.55), which makes σ_d indefinite in the limit of $r \to \infty$. Profiles of the magnetic field magnitude, B, and the helicoidal component of the current density, J_h, are shown in figure 5.4. The values of B becomes greater (lower) for $\sigma_d > 0$ ($\sigma_d < 0$), in connection with a diamagnetic (paramagnetic) behavior. The helicoidal current density, J_h, reverses near the origin and becomes more peaked (hollow) for $\sigma_d > 0$ ($\sigma_d < 0$). In addition profiles of the helicoidal velocity component, V_h and the Mach function, M^2_p, are provided in figure 5.5. It is noted that V_h reverses in the region of the left-lobe, where U becomes negative, and that the flow in terms of the Mach function, M^2_p, strengthens the impact of pressure anisotropy for $\sigma_d > 0$, due to the factor $1 - \sigma_d - M^2_p$. In this respect, it is expected that the increase of the parameter $M^2_{p_0}$ has the same impact on V_h as that shown in figure 5.5(a) for $\sigma_d > 0$.

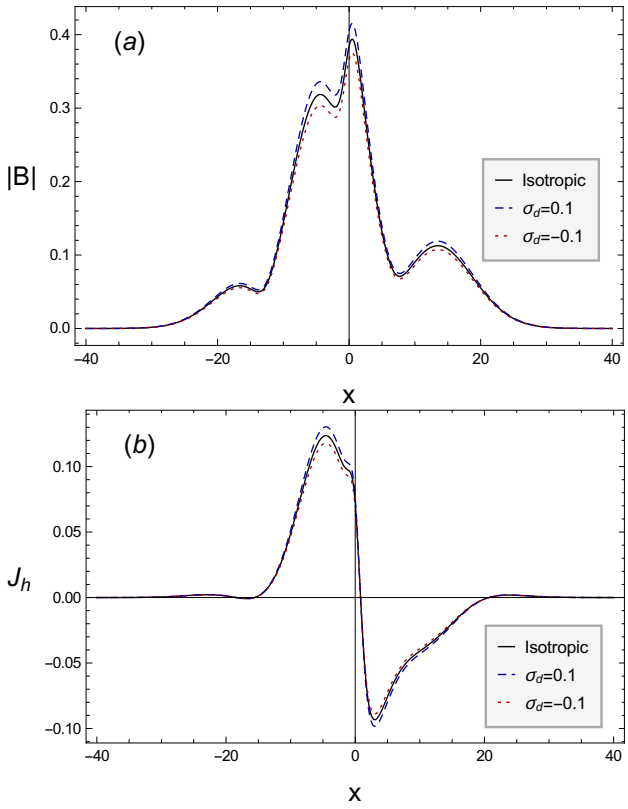

Figure 5.4: Variation of (a) $|\mathbf{B}(x, y = 0, z = 0)|$ and (b) $J_h(x, y = 0, z = 0)$, for the stationary equilibria constructed here, for $M^2_{p_0} = 10^{-3}$ and the impact of pressure anisotropy on them for positive and negative values of σ_d.

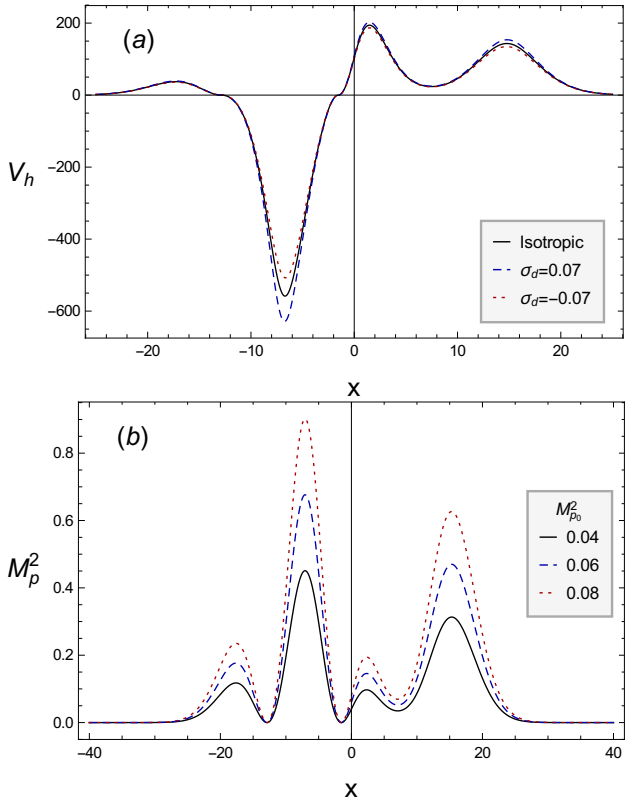

Figure 5.5: Profiles of (a) the helicoidal velocity component for $M^2_{p_0} = 0.06$, and the impact of pressure anisotropy through σ_d, and (b) the Mach function along the x-axis for different values of the flow parameter $M^2_{p_0}$.

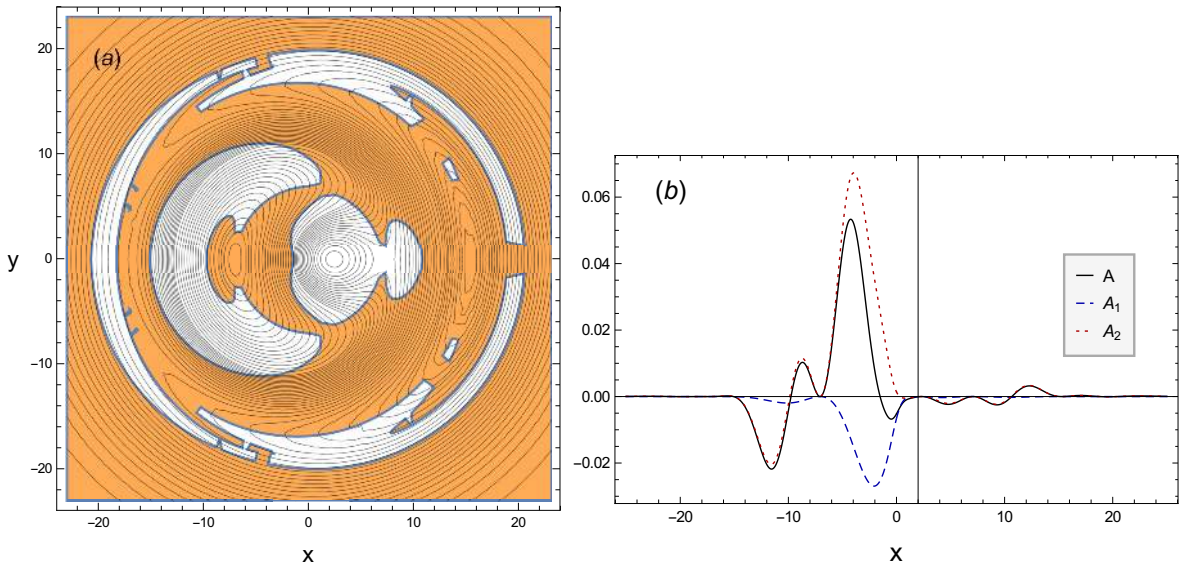

Figure 5.6: (a): For the static anisotropic helically symmetric equilibrium ($\sigma_d = M_{p_0}^2 = 0$) the stability condition $\mathcal{A} \geq 0$ is satisfied in the orange coloured regions. (b): The term A_2 has a stabilizing effect (red-dotted curve) which counteracts the destabilizing one of A_1 (blue-dashed curve), so that the quantity $\mathcal{A} = A_1 + A_2$ indicated by the black-straight curve becomes positive in the aforementioned orange coloured regions.

In what follows, we employ the derived suffiecient condition by calculating the quantity $\mathcal{A} = A_1 + A_2 + A_3$ of equation (5.40) (in connection with equations (5.33), (5.36)-(5.38) in the ψ-space) for the helically symmetric equilibria under consideration, in order to examine the impact of the pressure anisotropy, flow and torsion on their linear stability, through the variation of the parameters σ_d, M_{p_0}, and η, respectively. We recall that the aforementioned relations were obtained by applying the integral transformation (2.45); in this respect the condition (5.34) is trivially satisfied. Figure 5.6(a) shows that the condition $\mathcal{A} \geq 0$ in the absence of pressure anisotropy and flow, $\sigma_d = M_{p_0}^2 = 0$, is satisfied in a broad region including the outer domain and the two magnetic axes located on the left and right side of the origin $(x = y = 0)$. In these regions, the term A_2 being stabilising surpasses the destabilising term A_1 as shown in figure 5.6(b) (while in this case the flow term A_3 vanishes). However, the condition is satisfied neither near the central magnetic axis, where J_h reverses and U is negative, nor in a small region located at the left side of the magnetic axis of the left lobe, in which V_h reverses; in this respect it should be noted that since the condition is only sufficient, the white colored regions in figure 5.6(a) and in the figures to follow, where $\mathcal{A} < 0$, do not necessarily imply instability. Thus we will consider only regions in which the condition $\mathcal{A} \geq 0$ is satisfied.

The presence of pressure anisotropy does not affect the isotropic stability map of figure 5.6(a), as it is clearly indicated in the profiles of figure 5.7. However, it affects the values of A. Specifically, in the regions where $\mathcal{A} \geq 0$, for $P_{\|} > P_{\perp}$ ($\sigma_d > 0$) the anisotropy has a stabilizing impact, in the sense that the maximum values of $\mathcal{A}$ become larger than the respective isotropic ones, and a destabilizing effect for $\sigma_d < 0$. These characteristics are illustrated in figure 5.7. In addition, it is found that the flow in terms of M_p^2 has a peculiar effect on stability. Specifically, on the one hand it results in shrinking the orange colored area located on the left hand side of the first lobe, where the helicoidal velocity reverses, as it can be seen in figure 5.8(a),(b). This shrinking is connected with a destabilizing effect of $M_{p_0}^2$ on both terms A_1 and A_2 as shown in figure 5.9(a),(b). On the other hand the flow has a stabilizing effect, similar to that of $\sigma_d > 0$, because the respective maximum values of $\mathcal{A}$ get larger in this area as M_p^2 increases, as it can be seen in figure 5.8(c). Also, the flow gives rise to a stabilizing contribution via the

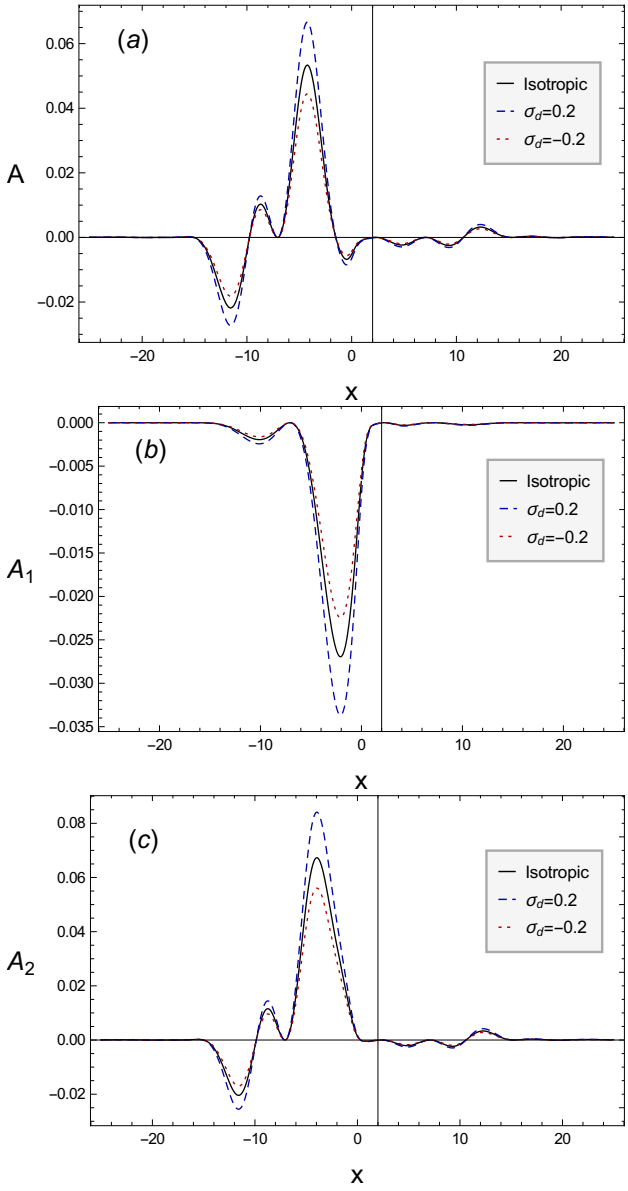

Figure 5.7: The impact of pressure anisotropy on the quantities (a) $\mathcal{A}$, (b) A_1 and (c) A_2 in the absence of flow ($M_{p_0} = 0$) for $\sigma_d = 0.2$ (blue-dashed curves) and $\sigma_d = -0.2$ (red-dotted curve). For comparison are also given the respective isotropic black continuous curves. In the regions where $\mathcal{A} \geq 0$ this impact is stabilizing for $\sigma_d > 0$ and destabilizing for $\sigma_d < 0$.

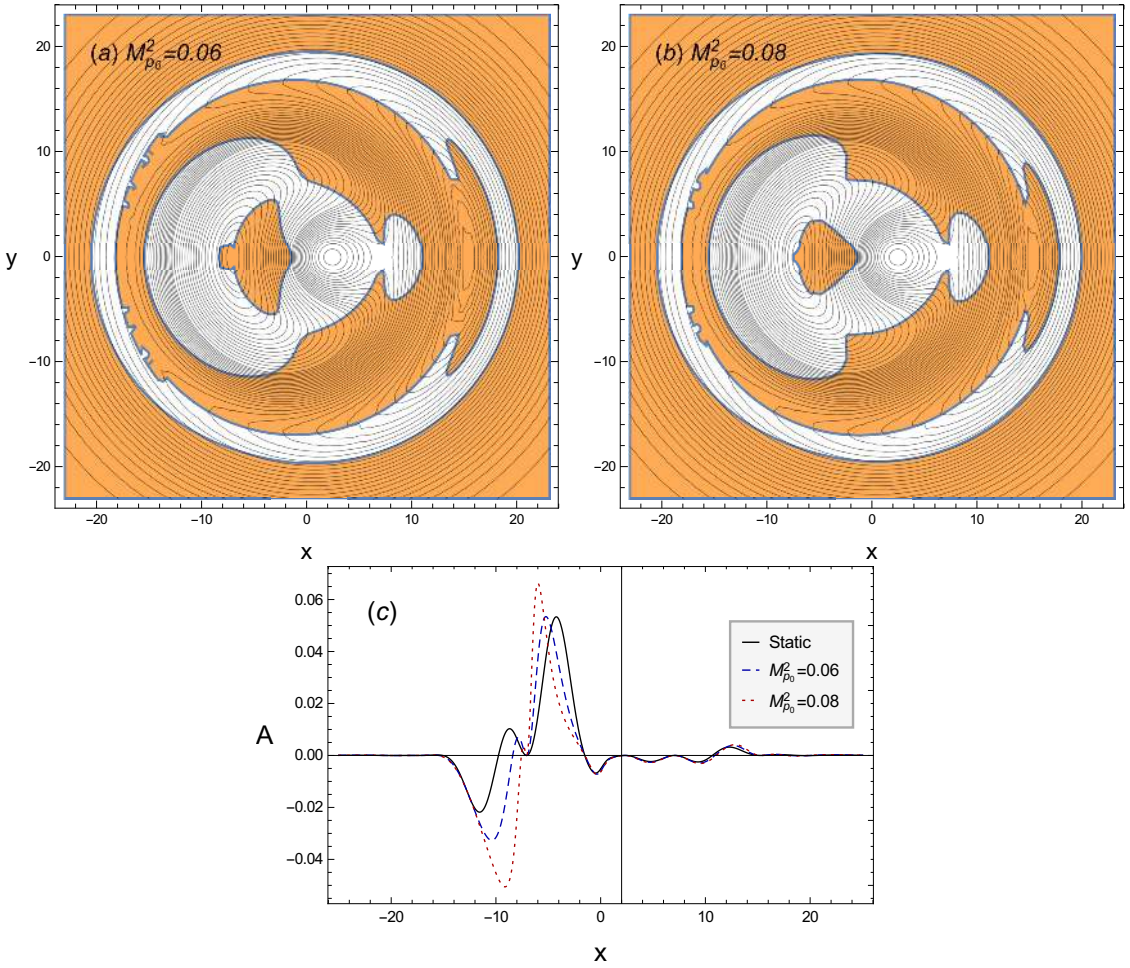

Figure 5.8: Impact of the flow through $M^2_{p_0}$ in the central orange colored region where the stability condition $\mathcal{A} \geq 0$ is satisfied in comparison with the respective static isotropic equilibrium. The maximum used value of the parameter M_{p_0} for which all the pressures remain positive is 0.08.

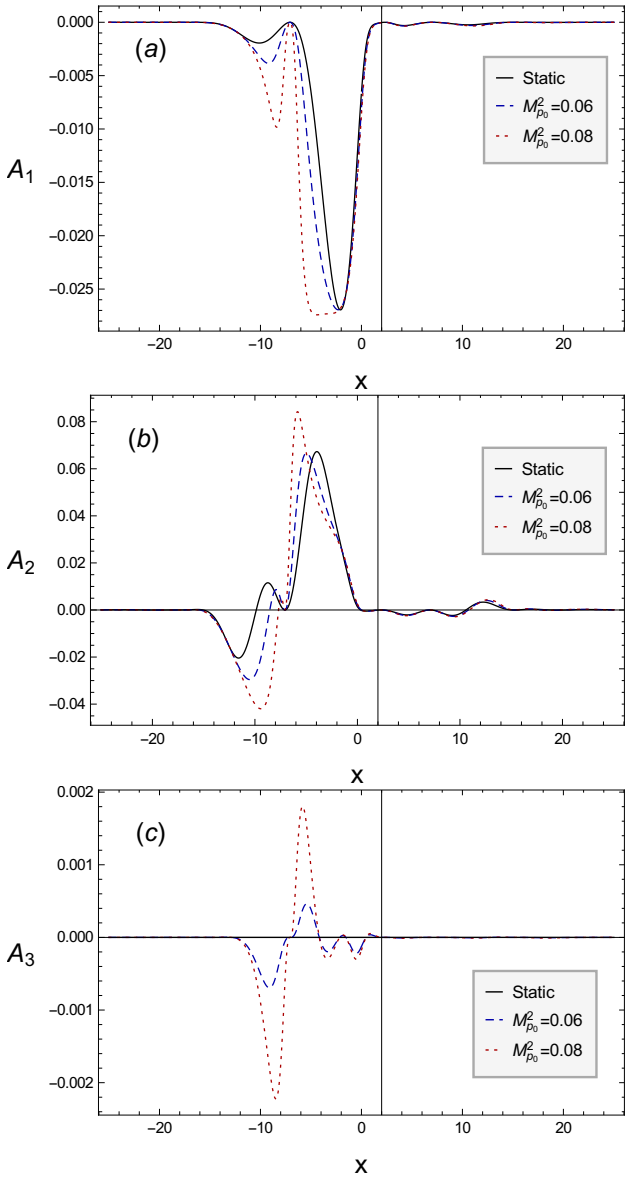

Figure 5.9: The impact of the flow parameter M_{p0}^2 on the terms: (a) A_1, (b) A_2, and (c) A_3, for $\sigma_d = 0$.

term A_3. However, this contribution in the region of interest is an order of magnitude lower than the destabilizing impact of M_p^2 on A_1 and A_2, as can be seen in figure 5.9(c). Because of the stronger impact of the pressure anisotropy on $\mathcal{A}$ than the destabilizing effect of the flow, the presence of both anisotropy and flow has an overall stabilizing effect in terms of the region where the condition $\mathcal{A} \geq 0$ is satisfied and the maximum values of $\mathcal{A}$. This is shown in figure 5.10.

Finally, as concerns the impact of the torsion, τ, on the quantity $\mathcal{A}$, for a specific helix, defined by the equations $r = r_c = \text{const.}$, $u = u_c = \text{const.}$ (in helical coordinates), equation (5.58) implies that τ depends only on the parameter η, which characterises the pitch of that helix. Inspection of equation (5.58) implies that τ has an extremum for $m = r_c$, corresponding to the maximum torsion, $\tau_{max} = 1/2r_c$. For example, for the static, isotropic equilibrium of figure 5.1 the helical magnetic axis of the central lobe intersects the plane $z = 0$ at the position $x_c = 2.318$, $y_c = 0$, corresponding to $r_c = 2.318$, and has maximum torsion, $\tau_{max} = 0.2157$. Therefore, there can exist two different helically symmetric configurations with the same torsion but different values of m one for $m < r_c$ and the other $m > r_c$, corresponding to different pitches η. However, the same torsion does not imply that these configurations have necessarily

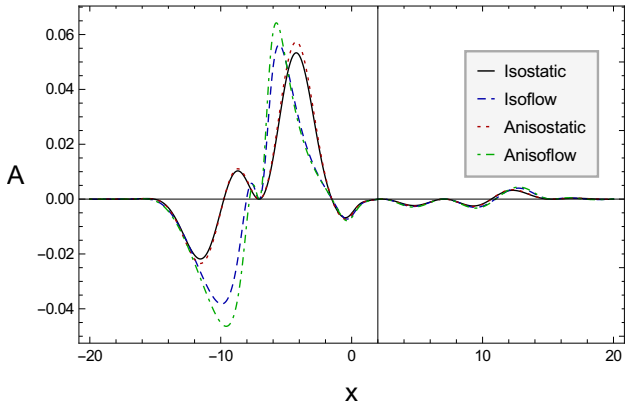

Figure 5.10: The overall stabilizing impact of pressure anisotropy in combination with flow on the stability of the constructed helically symmetric equilibria. The pertinent parametric values employed are as follows: (straight black curve) $\sigma_d = M_{p_0}^2 = 0$, (blue dashed curve) $\sigma_d = 0$, $M_{p_0}^2 = 0.07$, (red dotted curve) $\sigma_d = 0.07$, $M_{p_0}^2 = 0$, and (green dot-dashed curve) $\sigma_d = M_{p_0}^2 = 0.07$.

the same stability properties. The regions in which the condition $\mathcal{A} \geq 0$ is satisfied for the equilibrium of figure 5.1 is shown in figure 5.6. We found the respective stability maps for three pairs of equilibria, shown in figure 5.11. Each pair corresponds to the same torsion, $\tau < \tau_{max}$ but different pitch lengths, $\eta < 2\pi r_c$ and $\eta > 2\pi r_c$. Specifically, the torsion and pitch values we employed in connection with these equilibrium pairs are the following: (upper pair consisting of the figures 5.11(a),(b)) $\tau_{(a),(b)} = 0.207$, $\eta_{(a)} = 10.10$, $\eta_{(b)} = 19.29$, (middle pair consisting of the figures 5.11(c),(d)) $\tau_{(c),(d)} = 0.157$, $\eta_{(c)} = 2\pi$, $\eta_{(d)} = 33.76$, and (lower pair consisting of the figures 5.11(e),(f)) $\tau_{(e),(f)} = 0.089$, $\eta_{(e)} = \pi$, $\eta_{(f)} = 67.52$. The stability maps indicate that the condition $\mathcal{A} \geq 0$ is satisfied in a wider region as the torsion decreases from its maximum value and for a given torsion $\mathcal{A}$ it gets larger as the pitch length $\eta > 2\pi r_c$ increases. Thus, we conclude that helical configurations with smaller torsion and bigger pitch lengths may have improved stability characteristics. This result is reasonable if one considers the limit of zero torsion and infinite pitch length in which a helically symmetric plasma column degenerates into an one dimensional, cylindrical θ-pinch. It is well known that such a configuration has favorable stability properties, since the safety factor approaches infinity. However, confinement in a θ-pinch is not possible in the presence of toroidicity because the axial magnetic field becomes purely toroidal.

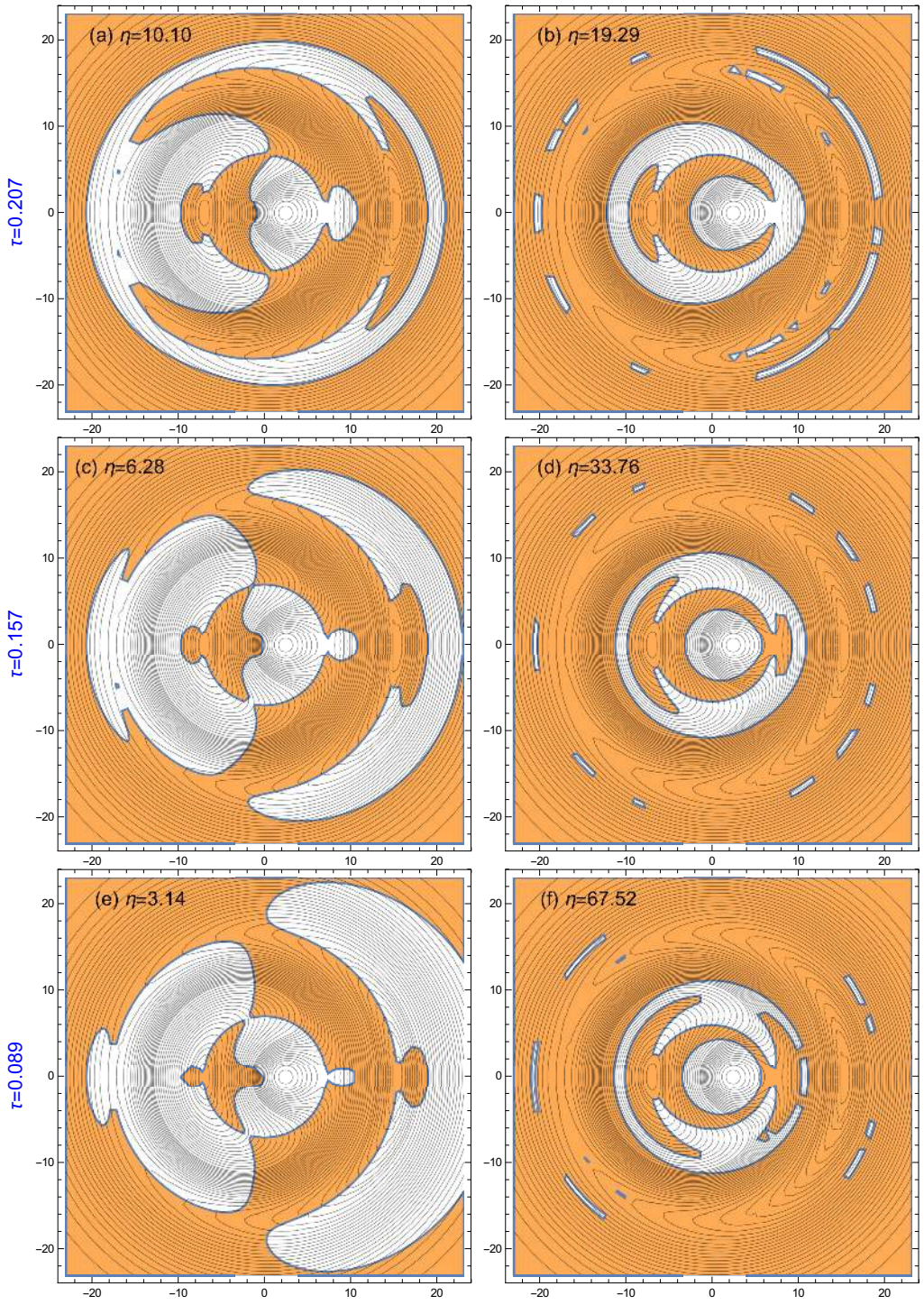

Figure 5.11: The impact of the torsion of the magnetic axis and of the picth on the linear stability of helically symmetric equilibria. Each pair of figures illustrate configurations that have same torsion, but different pitch values as explained in the text.

6 | Conclusions and potential future work

> "*We're always, by the way, in fundamental physics, always trying to investigate those things in which we don't understand the conclusions. After we've checked them enough, we're okay.*"
>
> Richard P. Feynman

6.1 Summary and main conclusions

Equilibrium and stability are important disciplines of magnetic confinement fusion science and engineering in connection with the outstanding challenge of controlled thermonuclear fusion, the successful implementation of which would open up the possibility of completely worldwide solving the energy problem. In the present thesis we investigated the equilibrium and stability properties of a helically symmetric magnetized plasma with pressure anisotropy and incompressible mass flow of arbitrary direction. The main conclusions are summarized as follows.

I. *Helically symmetric equilibria with pressure anisotropy and incompressible flow*

   (a) In Chapter 2 we derived a generalized Grad-Shafranov equation [equation (2.46)] which governs the equilibrium of helically symmetric magnetized plasmas in the presence of pressure anisotropy and incompressible flow. That equation recovers the respective GS-like ones that govern both isotropic helically symmetric equilibria, either static or stationary, and axisymmetric as well as translationally symmetric equilibria either with pressure anisotropy and/or mass flow or not. Also, it contains six free surface quantities, as functions of the poloidal magnetic flux. The derivation was based on the adoption of a diagonal pressure tensor, known as CGL pressure tensor, with one element parallel to the magnetic field, $P_{\parallel}$, and two equal perpendicular ones, $P_{\perp}$. As a measure of the pressure anisotropy we introduced the function σ_d [see equation (1.55)], assumed to be uniform on magnetic surfaces, while the parallel component of the flow was expressed by the poloidal Alfvénic Mach function M_p [see equation (2.32)]. The form of the GGS equation containing the sum $\sigma_d + M_p^2$ indicates that pressure anisotropy and flow act additively in the absence of the electric field term, associated with the non-parallel component of the flow. Furthermore, we derived a generalized Bernoulli equation [equation (2.43)] involving the effective isotropic pressure $\mathcal{P}$ [see equation (1.60)].

   (b) In addition, under the assumption of the existence of well defined 3D magnetic surfaces we examined the properties of special ideal, anisotropic MHD equilibria with incompressible flow such that any two of the vectors of flow velocity, $\mathbf{V}$, vorticity, $\mathbf{\Omega}$,

magnetic field, $\mathbf{B}$, and current density, $\mathbf{J}$, are parallel one another including the cases of magnetic-field-aligned flows, force-free, in the sense that the magnetic force vanishes, and Beltrami. It turns out that the vorticity and the current density share the same surfaces with the magnetic field and velocity. In many of the cases considered it is shown that the only possible isodynamic state is the axisymmetric Palumbo one. Also, we examined the respective helically symmetric equilibria for which the specific forms of the GGS equations were obtained. For these equilibria it was proved that the flow should be parallel to the magnetic field with the exception of equilibria with $\mathbf{V}$ parallel to $\mathbf{J}$. Furthermore, we examined axisymmetric and helically symmetric equilibria with either complex lamellar flow or complex lamellar magnetic field. In these cases it turns out that the electric field results in non-isodynamic equilibria governed by a couple of differential equations [equations (2.101)-(2.103)].

(c) In Chapter 3 the GGS equation was solved by adopting the most generic linearizing choices for the arbitrary function terms contained in it, and a new class of exact helically symmetric equlibria with pressure anisotropy and flow of arbitrary direction was obtained. This analytic class recovers known solutions as particular cases, e.g. solutions describing equilibria of helically symmetric astrophysical jets. On the basis of those generic analytical considerations we constructed equilibria describing configurations pertinent to 'straight stellarators', consisting of a helicoidal tude of nested magnetic surfaces, with poloidal cross-section shape invariant along the helical direction. That tube was considered to be surrounded by a fixed helicoidal boundary, of finite length and non-zero torsion, in connection with appropriate boundary/ shaping conditions.

(d) In addition, we examined the impact of pressure anisotropy and flow on the properties of the equilibrium constructed, through physical quantities, and came to the following conclusions. As concerns the plasma magnetic properties, it turns out that anisotropy acts paramagnetically for $P_{\parallel} > P_{\perp}$ and diamagnetically for $P_{\parallel} < P_{\perp}$, irrespective of the presence of flow. The non-parallel component of the flow decreases the magnetic field from its static value, thus inducing diamagnetism. Also, in the absence of the electric field term, associated with non-parallel flow, the component of the flow parallel to $\mathbf{B}$, in connection with M_p^2, has a paramagnetic impact due to the cumulative effect with anisotropy for $\sigma_d > 0$. However, for flows of arbitrary direction the parallel flow enhances the diamagnetic effect of the non-parallel one. Moreover, both the flow and anisotropy have a noticeable influence on the scalar pressures along and across $\mathbf{B}$ and consequently on the plasma beta; specifically, the local beta on the magnetic axis takes its largest values in the presence of both mass flows of arbitrary direction and pressure anisotropy for $\sigma_d < 0$, indicating more favorable confinement properties in that case. At last, it is found that both anisotropy and flow have a significant impact on the components of the current density and velocity along the direction of symmetry, while it turns out that the flow weakens the safety factor near the magnetic axis, which might be disadvantageous regarding stability.

II. *Symmetry transformations for ideal MHD and CGL equilibria*

(a) In Chapter 4 we presented a new set of symmetry transformations [transformations (4.3)] that can be applied to any known CGL equilibrium with special field-aligned incompressible flow and pressure anisotropy function, σ_d, constant on the magnetic field lines, to produce an infinite new continuous families of respective equilibria with collinear velocity and magnetic fields, and with arbitrary mass density and pressure anisotropy functions. They contain four arbitrary scalar functions, the structure of which depends on the topology of the magnetic field of the given equilibria; also,

they can be used for changing the magnitude of the equilibrium quantities or create stationary configurations from static ones without changing the solutions' magnetic surfaces. These transformations consist of a generalization of the ones introduced in reference [216] for the same kind of field-aligned incompressible flow and isotropic pressure, known as 'Bogoyavlenskij transformations'.

(b) In addition, we examined the structure of the arbitrary scalar functions included in the symmetry transformations in relation to the topology of the magnetic field of the original equilibrium and the existence of magnetic surfaces, and proved that if the original equilibrium possesses some known continuous geometrical symmetry, either helical or axial or translational, this can be broken by the transformations if and only if the magnetic field is purely poloidal. In this respect, we applied the aforementioned symmetry transformations to specifically prescibed axisymmetric CGL equilibria with collinear and purely poloidal $\mathbf{V}$ and $\mathbf{B}$ fields, incompressible flow, and σ_d uniform on the magnetic surfaces; we constructed 3D equilibria with collinear and purely poloidal velocity and magnetic fields, but with mass density and anisotropy function varying on the magnetic surfaces, all physical quantities of which depending on all three spatial variables not being invariant along the toroidal direction.

(c) Furthermore, we extensively studied the symmetry transformations previously introduced in a series of papers in references [73, 153, 209, 216–220] applied to given equilibria with incompressible flow of arbitrary direction. We examined several transformations that map MHD into MHD, CGL into CGL and MHD into CGL equilibria, with $\mathbf{V}$ non-collinear to $\mathbf{B}$. We showed that these transformations are valid if the arbitrary scalar functions included therein are either constant on the magnetic surfaces, if such surfaces exist, or if they are related by a special relationship; in the latter case it turns out that the velocity and magnetic fields of the original equilibria are restricted to be collinear. If the original equilibria have certain geometrical symmetry, in the former case they differ from the transformed ones only by a constant factor, while in the latter case this symmetry can be broken only for purely poloidal magnetic fields.

The generic conclusion of the study presented in the fourth Chapter is that all aforementioned sets of symmetry transformations can break the geometrical symmetry of the original equilibria, if and only if the magnetic field is purely poloidal. Otherwise the transformed equilibria retain the geometrical symmetry of the original ones.

III. *Linear stability of anisotropic pressure equilibria with field-aligned incompressible flow*

(a) At the end, in Chapter 5 we derived a sufficient condition for the linear stability of plasma equilibria for field-aligned incompressible flows, and plasmas of constant density, and pressure anisotropy such that the difference between the pressures along and across $\mathbf{B}$ be proportional to the magnetic pressure, by employing an Energy Principle. Specifically, we have shown that the linear stability of such kind of equilibria, being guaranteed when the functional of the perturbation potential energy is positive definite, relates to the sign of a function $\mathcal{A}$ [equation (5.33)] which depends only on equilibrium quantities. According to that condition, any equilibrium is linearly stable to small three-dimensional perturbations whenever (i) the sum of the anisotropy function plus the Mach function of the equilibrium velocity collinear with the magnetic field lower than unity [equation (5.34)] and (ii) $\mathcal{A}$ is non-negative [equation (5.35)]. This condition generalizes the sufficient condition derived in [149] for respective equilibria with isotropic pressure.

(b) The aforementioned condition can be applied to any plasma state without geometrical restriction, that is, it can be employed for three-dimensional equilibria. The quantity $\mathcal{A}$ involved consists of three physically interpretable terms. The first of these terms, being always negative and therefore destabilizing, may relate to current driven instabilities. The other two terms may have either positive or negative contributions to $\mathcal{A}$ depending on the characteristics of the background equilibria. The second term relates to the magnetic shear, while the third term relates to the velocity shear and to the variation of the total pressure perpendicular to the magnetic surfaces; the latter term vanishes for static equilibria.

(c) In addition, we have shown that if a given equilibrium with field-aligned incompressible flows of constant mass density and constant pressure anisotropy function fulfills the aforementioned condition, and therefore is linearly stable, then all the families of equilibria obtained by the application of the symmetry transformations (4.2) and/or (4.3) on the original equilibrium, are also linearly stable, provided that a parameter, C, appearing in these transformations, is positive definite.

(d) At last, we applied the derived sufficient condition to a special class of helically symmetric analytic equilibria describing astrophysical jets in order to examine the impact of flow, pressure anisotropy as well as of the torsion and pitch of certain equilibrium helices on stability. For this class of equilibria we have found that both the flow and the anisotropy can have noticeable impact on stability, which in different plasma regions can be either stabilizing or destabilizing; the impact of pressure anisotropy is in general stronger than that of the flow. Specifically, in the regions where the stability condition $\mathcal{A} \geq 0$ is satisfied the combined effect of flow and anisotropy is stabilizing when $P_{\parallel} > P_{\perp}$. Finally, the results indicate that helically symmetric equilibria with smaller torsion and larger pitch length are favored in terms of stability.

6.2 Future directions

In the framework of the present thesis we employed the ideal MHD and CGL single fluid models, to study the equilibrium and stability properties of helically symmetric incompressible plasmas with uniform pressure anisotropy. However, complete understanding of the equilibrium and stability properties of magnetized plasmas in the presence of mass flows and pressure anisotropy requires substantial additional work in connection with the actual physical mechanisms by exploiting advanced computational techniques. To this end, below are presented some ideas that may constitute the objectives of future studies.

I. The exact class of helically symmetric equlibria obtained in this thesis as solution of the GGS equation derived recovers known solutions as particular cases. As an example, in the limiting case of axisymmetric equilibria with incompressible flow of arbitrary direction and anisotropic pressure, it recovers a respective solution obtained in [114] (equation (50) therein) consistining of an extension of the well known Solovév solution widely employed to validate numerical codes. In this respect the new analytic solutions constructed here can be employed for alternative or additional validation of equilibrium codes. In this view the development of a flexible code solving the GGS equation, as HELENA [228, 229] in the axisymmetric case, could be established.

II. The results of the study on the different reduced kinds of the equilibria, in which two out of the magnetic field, velocity, current density and vorticity vectors are specially related, performed in Chapter 2 indicate a preference of the ideal steady states to involve either parallel flows or isodynamicity. Moreover, the current density lies on the magnetic

surfaces, a property which played an important role in deriving the sufficient condition for linear stability for 3D equilibria with parallel incompressible flows and constant anisotropy function [condition (5.34), (5.35)]. Therefore, we conjecture that the aforementioned condition might be extended to other cases of special equilibria, such as equilibria with velocity parallel to the current density, thus contributing to the elimination of the tough problem of stability with equilibrium flows.

III. Incompressibility together with the condition of anisotropy function being uniform on magnetic surfaces where key assumptions along the lines of the present thesis that played an important role in deriving the GGS equilibrium equation in Chapter 2 as well as the sufficient stability condition in Chapter 5. It is interesting to pursue additional extensions on the equilibrium and stability concerning compressible flows or/and more physically relevant pressure anisotropy which may represent better the actual experimental situations. This requires replacing incompressibility and the assumption of uniform pressure anisotropy function by alternative equations of state on the understanding that finding self consistently more appropriate equations of state (or energy equations) associated with the pressure tensor elements $P_{\|}$ and $P_{\perp}$ relates to the tough closure problem of a hybrid kinetic-fluid model, e.g. [230, 231].

IV. The results of the analytic studies presented in this dissertation were performed self consistently within the frameworks of the ideal MHD and CGL fluid models under the condition of helical symmetry, and though toroidicity is absent they may contribute to better understanding the physics of confinement in tokamaks and stellarators. In this respect it should be noted that, although a (non trivial) analytic study has its own value, 3D equilibrium codes permitting arbitrary toroidicity and connecting the parallel pressure with kinetic theory provide a more realistic description. However, since these codes are based on a hybrid model, i.e. a fluid model perpendicularly and a kinetic one parallel to the magnetic field, lack complete self-consistency. In this view the construction of 3D equilibria or quasi-symmetric equilibria with toroidicity in the framework of full kinetic models, e.g. gyrokinetic or more ambitiously Maxwell-Vlasov ones, would be not only advantageous as concerns self-consistency but in the prospect that it might provide more fundamental additional information.

Appendices

A | General curvilinear coordinates for magnetic confinement geometries

We suppose that we have three level surfaces $x^i = x^i(x, y, z) = c^i$ for each i and that $[\nabla x^1, \nabla x^2, \nabla x^3] > 0$, where the bracket denotes the triple scalar product. These are coordinate surfaces. Any two coordinate surfaces intersect in a coordinate curve. All three coordinate curves intersect in a single point P. Since P is uniquely specified by (c^1, c^2, c^3), then a point P is uniquely specified by prescribing values for (x^1, x^2, x^3). Thus, (x^1, x^2, x^3) represent P in curvilinear coordinates. We also assume that each function can be inverted to the cartesian basis (x_1, x_2, x_3). Hence we can write:

$$x^i = f^i(x_1, x_2, x_3) \quad \longleftrightarrow \quad x_i = \bar{f}^i(x^1, x^2, x^3).$$

Then we can write the vector field of position in curvilinear coordinates

$$\mathbf{r} = \sum_{i=1}^{3} \bar{f}^i(x^1, x^2, x^3)\hat{\mathbf{e}}_i, \tag{A.1}$$

where $\hat{\mathbf{e}}_i$ are the cartesian base vectors.

A.1 Covariant and contravariant basis vectors

The covariant basis vectors $\mathbf{g}_i$ are defined as

$$\mathbf{g}_i \equiv \frac{\partial \mathbf{r}}{\partial x^i}. \tag{A.2}$$

Since the derivative is taken along the x^i curve (i.e., with x^j and x^k held fixed), $\mathbf{g}_i$ is the tangent vector to the x^i curve through P. Note that $\mathbf{g}_i$ and $\mathbf{g}_j$ are generally not orthogonal vectors (i.e., for $i \neq j$, $\mathbf{g}_i \cdot \mathbf{g}_j \neq 0$) nor they are unit vectors (i.e., $\mathbf{g}_i \cdot \mathbf{g}_j \neq 1$). The contravariant basis vectors $\mathbf{g}^i$ are defined as the vectors normal to the x^i coordinate surfaces

$$\mathbf{g}^i \equiv \nabla x^i. \tag{A.3}$$

In general, $\mathbf{g}^i$ is not proportional to $\mathbf{g}_i$. In the orthogonal case, these vectors coincide up to scaling, but this does not hold in general. We can expand both sets of vectors in the Cartesian basis. We end up with the following:

$$\mathbf{g}_i = \sum_j \frac{\partial x_j}{\partial x^i}\hat{\mathbf{e}}_j, \qquad \mathbf{g}^i = \sum_j \frac{\partial x^i}{\partial x_j}\hat{\mathbf{e}}_j. \tag{A.4}$$

It turns out that each triplet of vectors is linearly independent and hence at each point P forms a basis for $\mathbb{R}^3$ footed at P. Since $(\mathbf{g}^1, \mathbf{g}^2, \mathbf{g}^3)$ form a basis for $\mathbb{R}^3$, we can expand any vector $\mathbf{v}$ in this basis. Hence we can write:

$$\mathbf{v} = \sum_i v_i \mathbf{g}^i \tag{A.5}$$

and therefore $v_i = \mathbf{v} \cdot \mathbf{g}_i$. Since the vectors $\mathbf{g}^i$ are not unit vectors, the numbers v_i are not physical components of the vector. They are called the covariant components of $\mathbf{v}$. Similarly we can expand $\mathbf{v}$ in the basis $(\mathbf{g}_1, \mathbf{g}_2, \mathbf{g}_3)$ to wrtite

$$\mathbf{v} = \sum_i v^i \mathbf{g}_i. \tag{A.6}$$

It also turns out that $v^i = \mathbf{v} \cdot \mathbf{g}^i$. Since the vectors $\mathbf{g}_i$ do not have unit length, the real numbers v^i are not physical components of $\mathbf{v}$ too. They are called the contravariant components of $\mathbf{v}$. The sets of vectors $(\mathbf{g}_1, \mathbf{g}_2, \mathbf{g}_3)$ and $(\mathbf{g}^1, \mathbf{g}^2, \mathbf{g}^3)$ are reciprocal, or adjoint, sets of vectors; this means that for all i and j

$$\mathbf{g}_i \cdot \mathbf{g}^j = \delta_i{}^j. \tag{A.7}$$

Since these reciprocal sets of vectors are both bases for $\mathbb{R}^3$, we say that the sets are dual bases. If we define A to be the matrix whose rows are the vectors $\mathbf{g}^i$ and B to be the matrix whose columns are the vectors $\mathbf{g}_i$, it follows that A and B are inverse. Since the determinant of A is the triple scalar product $[\mathbf{g}^1, \mathbf{g}^2, \mathbf{g}^3]$ we get the relation

$$detB = (detA)^{-1} \tag{A.8}$$

and the metric coefficients g_{ij} (for $i, j = 1, 2, 3$) are defined by

$$g_{ij} = \mathbf{g}_i \cdot \mathbf{g}_j. \tag{A.9}$$

Note that if the curvilinear coordinates are orthogonal, the metric coefficients are zero unless $i = j$, in which case the metric coefficient is the square of the i^{th} Lamé coefficient. We can also define reciprocal metric coefficients g^{ij} as

$$g^{ij} = \mathbf{g}^i \cdot \mathbf{g}^j. \tag{A.10}$$

The commutativity of the dot product implies that

$$g_{ij} = g_{ji}, \qquad g^{ij} = g^{ji} \qquad \forall \ \ i, j. \tag{A.11}$$

Using the metric coefficients and the reciprocal metric coefficients, we can determine the contravariant components of $\mathbf{g}^i$ and the covariant components of $\mathbf{g}_i$. Specifically:

$$\mathbf{g}^i = \sum_j g^{ij} \mathbf{g}_j, \qquad \mathbf{g}_i = \sum_j g_{ij} \mathbf{g}^j. \tag{A.12}$$

We can use these relations to determine how to transform between covariant and contravariant components of a vector as:

$$v_i = \sum_j g_{ij} v^j, \qquad v^i = \sum_j g^{ij} v_j. \tag{A.13}$$

A.2 Integration in general curvilinear coordinates

Let G be a matrix with elements g_{ij} (metric coefficients), and

$$g = detG. \tag{A.14}$$

It will be shown that g is related with the Jacobian of the transformation from Cartesian to curvilinear coordinates (x^i). We can similarly arrange the reciprocal coefficients in a matrix and the result is the inverse G^{-1}. To integrate in general curvilinear coordinates the integrand must be multiplied by $\sqrt{g}$. For any cyclic permutation of i, j, k equation (A.7) implies that

$$\mathbf{g}_i = \sqrt{g}(\mathbf{g}^j \times \mathbf{g}^k), \tag{A.15}$$

where

$$\sqrt{g} = \frac{1}{\mathbf{g}^1 \cdot (\mathbf{g}^2 \times \mathbf{g}^3)}. \tag{A.16}$$

Taking the cross product of $\mathbf{g}_i$ and $\mathbf{g}_j$ and using equation (A.15) yields

$$\mathbf{g}^i = \frac{\mathbf{g}_j \times \mathbf{g}_k}{\sqrt{g}}. \tag{A.17}$$

Thus, from equations (A.7) and (A.17) it follows

$$\sqrt{g} = (\mathbf{g}_1 \times \mathbf{g}_2) \cdot \mathbf{g}_3 = \left(\frac{\partial \mathbf{r}}{\partial x^1} \times \frac{\partial \mathbf{r}}{\partial x^2}\right) \cdot \frac{\partial \mathbf{r}}{\partial x^3}, \tag{A.18}$$

implying that $\sqrt{g}$ is the Jacobian. In addition, equations (A.15) and (A.17) give us the cross-product relationships:

$$\mathbf{g}_i \times \mathbf{g}_j = \sum_k \epsilon_{ijk}\sqrt{g}\mathbf{g}^k \tag{A.19}$$

and

$$\mathbf{g}^i \times \mathbf{g}^j = \sum_k \epsilon^{ijk}\frac{1}{\sqrt{g}}\mathbf{g}_k. \tag{A.20}$$

Also, with the aid of equations (A.5)-(A.7) the dot-product of two vectors $\mathbf{v}$ and $\mathbf{u}$ is written as

$$\mathbf{v} \cdot \mathbf{u} = v_i u^j \delta_i^j, \tag{A.21}$$

while, considering equations (A.19) and (A.20), their cross-product is written as

$$\mathbf{v} \times \mathbf{u} = \sqrt{g}\epsilon_{ijk}v^i u^j \mathbf{g}^k = \frac{1}{\sqrt{g}}\epsilon^{ijk}v_i u_j \mathbf{g}_k. \tag{A.22}$$

A.3 Vector operators in curvilinear coordinates

For any scalar function Φ the gradient operator $\nabla\Phi$ is defined as

$$d\Phi \equiv \frac{\partial \Phi}{\partial x^i}dx^i = \nabla\Phi \cdot d\mathbf{r}, \tag{A.23}$$

where

$$d\mathbf{r} = \frac{\partial \mathbf{r}}{\partial x^i}dx^i = \mathbf{g}_i dx^i. \tag{A.24}$$

Equating coefficients of dx^i in equation (A.23) yields the covariant components of $\nabla\Phi$: $\mathbf{g}_i \cdot \nabla\Phi = \frac{\partial\Phi}{\partial x^i}$, and thus, using equations (A.5)-(A.6) yields

$$\nabla\Phi = \frac{\partial\Phi}{\partial x^i}\mathbf{g}^i. \tag{A.25}$$

Now, consider the vector identities:

$$\nabla\cdot\left(\frac{\mathbf{g}_i}{\sqrt{g}}\right) = \nabla\cdot\left(\mathbf{g}^j\times\mathbf{g}^k\right) = \nabla\cdot\left(\nabla x^j\times\nabla x^k\right) = 0, \tag{A.26}$$

and

$$\nabla\times\mathbf{g}^i = \nabla\times\left(\nabla x^i\right) = 0. \tag{A.27}$$

Then using equations (A.5)-(A.6) in the form $\mathbf{v} = (g^{1/2}v^i)(g^{-1/2}\mathbf{g}_i)$, together with (A.26) yields the curvilinear formula for the divergence operator:

$$\nabla\cdot\mathbf{v} = \frac{1}{\sqrt{g}}\frac{\partial}{\partial x^i}(\sqrt{g}v^i). \tag{A.28}$$

Also, using equations (A.5)-(A.6) and (A.27) yields the curl operator

$$\nabla\times\mathbf{v} = \frac{\partial v_j}{\partial x^i}(\mathbf{g}^\mathbf{i}\times\mathbf{g}^j) \tag{A.29}$$

or, with the aid of (A.20):

$$\nabla\times\mathbf{v} = \frac{1}{\sqrt{g}}\epsilon_{ijk}\frac{\partial v_j}{\partial x^i}\mathbf{g}_k. \tag{A.30}$$

Furthermore, the Laplacian operator $\nabla^2\Phi \equiv \nabla\cdot(\nabla\Phi)$ can be obtained by using equation (A.28) with $v^i = (\partial\Phi/\partial x^j)\mathbf{g}^i\cdot\mathbf{g}^j$:

$$\nabla^2\Phi = \frac{1}{\sqrt{g}}\frac{\partial}{\partial x^i}\left(\sqrt{g}g^{ij}\frac{\partial\Phi}{\partial x^j}\right). \tag{A.31}$$

The differential arclength $d\ell^2 \equiv d\mathbf{r}\cdot d\mathbf{r}$ can be written

$$d\ell^2 = g_{ij}dx^i dx^j. \tag{A.32}$$

The element of the line segment $d\mathbf{l}_i$ along the coordinate curve x^i is also given by

$$d\mathbf{l}_i = \mathbf{g}_i dx^i \tag{A.33}$$

with no implied summation. Also, as concerns the element of surface area $d\mathbf{s}_i$ directed normal to the coordinate surface x^i =constant, this is

$$d\mathbf{s}_i = \sqrt{g}dx^j dx^k\mathbf{g}^i. \tag{A.34}$$

Note that it holds

$$|d\mathbf{s}_i| = \sqrt{g_{jj}g_{kk} - g_{jk}^2}dx^j dx^k. \tag{A.35}$$

Finally, the element of volume is given by the following expression

$$dV = \sqrt{g}dx^1dx^2dx^3. \tag{A.36}$$

A.4 Physical components of a vector

The physical components $v_{\bar{i}}$ of a vector $\mathbf{v}$ in general curvilinear coordinates is related with its covariant and contravariant components as

$$v_{\bar{i}} = \sqrt{g_{ii}}v^i = \sqrt{g_{ii}}g^{ij}v_j. \tag{A.37}$$

B | Helical coordinate system

B.1 Vector representation and differential operators

We introduce helical coordinates $(x^1, x^2, x^3) = (r, u, \zeta)$ related with the Cartesian (x, y, z) and the cylindrical (ρ, ϕ, z) ones as

$$\begin{aligned} r &= \sqrt{x^2 + y^2} = \rho, \\ u &= m \arccos\left(\frac{x}{\sqrt{x^2 + y^2}}\right) - kz = m\phi - kz, \\ \zeta &= z. \end{aligned} \tag{B.1}$$

The inverse transformations are given by

$$\begin{aligned} x &= r\cos\left(\frac{u + k\zeta}{m}\right), \qquad \rho = r, \\ y &= r\sin\left(\frac{u + k\zeta}{m}\right), \qquad \phi = \frac{u + k\zeta}{m}, \\ z &= \zeta, \end{aligned} \tag{B.2}$$

where m and k are real constant parameters. The vector field of position can be written

$$\mathbf{r}(r, u, \zeta) = r\hat{\boldsymbol{\rho}}(u, \zeta) + \zeta\hat{\mathbf{z}}, \tag{B.3}$$

where the cylindrical unit vectors are expressed in terms of the helical coordinates as

$$\begin{aligned} \hat{\boldsymbol{\rho}}(u, \zeta) &= \cos\left(\frac{u + k\zeta}{m}\right)\hat{\mathbf{x}} + \sin\left(\frac{u + k\zeta}{m}\right)\hat{\mathbf{y}}, \\ \hat{\boldsymbol{\phi}}(u, \zeta) &= -\sin\left(\frac{u + k\zeta}{m}\right)\hat{\mathbf{x}} + \cos\left(\frac{u + k\zeta}{m}\right)\hat{\mathbf{y}}. \end{aligned} \tag{B.4}$$

Using equations (A.2), (A.3) we find the tangent vectors to the (r, u, ζ) curves and the vectors normal to the helical coordinate surfaces as:

$$\begin{aligned} \mathbf{g}_1 := \mathbf{g}_r = \hat{\boldsymbol{\rho}}, \qquad & \mathbf{g}^1 \equiv \mathbf{g}^r = \hat{\boldsymbol{\rho}}, \\ \mathbf{g}_2 := \mathbf{g}_u = \frac{r}{m}\hat{\boldsymbol{\phi}}, \qquad & \mathbf{g}^2 := \mathbf{g}^u = \frac{m}{r}\hat{\boldsymbol{\phi}} - k\hat{\mathbf{z}}, \\ \mathbf{g}_3 := \mathbf{g}_\zeta = \frac{rk}{m}\hat{\boldsymbol{\phi}} + \hat{\mathbf{z}}, \qquad & \mathbf{g}^3 := \mathbf{g}^\zeta = \hat{\mathbf{z}}. \end{aligned} \tag{B.5}$$

Also, with the aid of equation (A.9) we find the following metric coefficients:

$$g_{rr} = 1,\ g_{uu} = \frac{r^2}{m^2},\ g_{\zeta\zeta} = \frac{1}{qm^2},\ g_{u\zeta} = g_{\zeta u} = \frac{kr^2}{m^2},\ g_{ru} = g_{ur} = g_{r\zeta} = g_{\zeta r} = 0. \tag{B.6}$$

Then, the matrix of the metric coefficients is obtained

$$G = \begin{pmatrix} 1 & 0 & 0 \\ 0 & \frac{r^2}{m^2} & \frac{kr^2}{m^2} \\ 0 & \frac{kr^2}{m^2} & \frac{1}{qm^2} \end{pmatrix} \tag{B.7}$$

and thus, we find that

$$g = \frac{r^2}{m^2}. \tag{B.8}$$

In addition, using equation (A.10) we find the reciprocal metric coefficients as:

$$g^{rr} = 1,\ g^{uu} = \frac{1}{qr^2},\ g^{\zeta\zeta} = 1,\ g^{u\zeta} = g^{\zeta u} = -k,\ g^{ru} = g^{ur} = g^{r\zeta} = g^{\zeta r} = 0. \tag{B.9}$$

Any vector $\mathbf{v}$ can be expanded both in contravariant (covariant) basis as:

$$\mathbf{v} = v_r\mathbf{g}^r + v_u\mathbf{g}^u + v_\zeta\mathbf{g}^\zeta = v^r\mathbf{g}_r + v^u\mathbf{g}_u + v^\zeta\mathbf{g}_\zeta, \tag{B.10}$$

where (v_r, v_u, v_ζ) are the covariant and (v^r, v^u, v^ζ) the contravariant components of $\mathbf{v}$. The transformations between the covariant and contravariant components of $\mathbf{v}$ are:

$$\begin{aligned} v_r &= v^r \\ v_u = \frac{r^2}{m^2}v^u + \frac{kr^2}{m^2}v^\zeta, &\qquad v^u = \frac{1}{qr^2}v_u - kv_\zeta, \\ v_\zeta = \frac{kr^2}{m^2}v^u + \frac{1}{qm^2}v^\zeta, &\qquad v^\zeta = -kv_u + v_\zeta, \end{aligned} \tag{B.11}$$

while the vectors of the two bases are related as:

$$\begin{aligned} \mathbf{g}_r &= \mathbf{g}^r \\ \mathbf{g}_u = \frac{r^2}{m^2}\mathbf{g}^u + \frac{kr^2}{m^2}\mathbf{g}^\zeta, &\qquad \mathbf{g}^u = \frac{1}{qr^2}\mathbf{g}_u - k\mathbf{g}_\zeta, \\ \mathbf{g}_\zeta = \frac{kr^2}{m^2}\mathbf{g}^u + \frac{1}{qm^2}\mathbf{g}^\zeta, &\qquad \mathbf{g}^\zeta = -k\mathbf{g}_u + \mathbf{g}_\zeta. \end{aligned} \tag{B.12}$$

Furthermore, under equations (A.15) and (A.17) the following relations for the cross-products arise:

$$\begin{aligned} \mathbf{g}_r \times \mathbf{g}_u = \frac{r}{m}\mathbf{g}^\zeta, &\qquad \mathbf{g}^r \times \mathbf{g}^u = \frac{m}{r}\mathbf{g}_\zeta, \\ \mathbf{g}_r \times \mathbf{g}_\zeta = -\frac{r}{m}\mathbf{g}^u, &\qquad \mathbf{g}^r \times \mathbf{g}^\zeta = -\frac{m}{r}\mathbf{g}_u, \\ \mathbf{g}_u \times \mathbf{g}_\zeta = \frac{r}{m}\mathbf{g}^r, &\qquad \mathbf{g}^u \times \mathbf{g}^\zeta = \frac{m}{r}\mathbf{g}_r. \end{aligned} \tag{B.13}$$

The physical components of a vector in helical coordinates are related with its contravariant and covariant components as:

$$\begin{aligned} v_{\bar{r}} &= v^r = v_r \\ v_{\bar{u}} = \frac{r}{m}v^u &= \frac{1}{qrm}v_u - \frac{kr}{m}v_\zeta \\ v_{\bar{\zeta}} = \frac{1}{mq^{1/2}}v^\zeta &= -\frac{k}{mq^{1/2}}v_u + \frac{1}{mq^{1/2}}v_\zeta. \end{aligned} \tag{B.14}$$

Now, using equations (A.23)-(A.36) we find for the differential elements and operators in the helical coordinate system the following relationships:

$$d\mathbf{r} = \mathbf{g}_r dr + \mathbf{g}_u du + \mathbf{g}_\zeta d\zeta, \tag{B.15}$$

$$d\ell^2 = dr^2 + \frac{r^2}{m^2} du^2 + \frac{1}{qm^2} d\zeta^2 + \frac{2kr^2}{m^2} du d\zeta, \tag{B.16}$$

$$d\mathbf{l}_1 = \mathbf{g}_r dr, \qquad d\mathbf{l}_2 = \mathbf{g}_u du, \qquad d\mathbf{l}_3 = \mathbf{g}_\zeta d\zeta, \tag{B.17}$$

$$d\mathbf{s}_1 = \frac{r}{m} du d\zeta \mathbf{g}^r, \qquad d\mathbf{s}_2 = -\frac{r}{m} dr d\zeta \mathbf{g}^u, \qquad d\mathbf{s}_3 = \frac{r}{m} dr du \mathbf{g}^\zeta, \tag{B.18}$$

$$dV = \frac{r}{m} dr du d\zeta, \tag{B.19}$$

$$\nabla\Phi = \mathbf{g}^r \frac{\partial\Phi}{\partial r} + \mathbf{g}^u \frac{\partial\Phi}{\partial u} + \mathbf{g}^\zeta \frac{\partial\Phi}{\partial\zeta}, \tag{B.20}$$

$$\nabla \cdot \mathbf{v} = \frac{1}{r}\frac{\partial}{\partial r}(r v^r) + \frac{\partial v^u}{\partial u} + \frac{\partial v^\zeta}{\partial\zeta}, \tag{B.21}$$

$$\nabla \times \mathbf{v} = \frac{m}{r}\left[\left(\frac{\partial v_\zeta}{\partial u} - \frac{\partial v_u}{\partial\zeta}\right)\mathbf{g}_r + \left(\frac{\partial v_r}{\partial\zeta} - \frac{\partial v_\zeta}{\partial r}\right)\mathbf{g}_u + \left(\frac{\partial v_u}{\partial r} - \frac{\partial v_r}{\partial u}\right)\mathbf{g}_\zeta\right], \tag{B.22}$$

$$\nabla^2\Phi = \frac{1}{r}\frac{\partial}{\partial r}\left(r\frac{\partial\Phi}{\partial r}\right) + \frac{1}{qr^2}\frac{\partial^2\Phi}{\partial u^2} + \frac{\partial^2\Phi}{\partial\zeta^2} - 2k\frac{\partial^2\Phi}{\partial u\partial\zeta}. \tag{B.23}$$

The covariant, contravariant and physical components of a vector in helical coordinates are related with its components in the cylindrical system as follows:

$$\begin{aligned} v_\rho = v_r = v^r, \qquad & v_\rho = v_{\bar{r}} \\ v_\phi = \frac{m}{r}v_u = \frac{r}{m}v^u + \frac{rk}{m}v^\zeta, \qquad & v_\phi = v_{\bar{u}} + rkq^{1/2}v_{\bar{\zeta}} \\ v_z = v_\zeta - kv_u = v^\zeta, \qquad & v_z = mq^{1/2}v_{\bar{\zeta}}. \end{aligned} \tag{B.24}$$

B.2 Helix parametrization

In the helical system introduced in section B.1 of the present Appendix, a helix is characterized by the equations: r = constant, u = constant. Consider a helix of reference defined by the following equations

$$\begin{aligned} r &= r_0 = \text{const.}, \\ u &= u_0 = \text{const.}. \end{aligned} \tag{B.25}$$

Then the coordinate ζ is related to the differential arc-length, ℓ, along this helix as

$$\zeta(\ell) = mq_0^{1/2}\int_{\ell_0}^{\ell} d\ell, \tag{B.26}$$

where $q_0 = q(r = r_0) = (k^2r_0^2 + m^2)^{-1}$. Setting $\ell_0 = 0$ and $u_0 = 0$ for simplicity we obtain

$$\begin{aligned} \zeta(\ell) &= mq_0^{1/2}\ell, \\ \phi(\ell) &= kq_0^{1/2}\ell. \end{aligned} \tag{B.27}$$

The position of every point of this helix is then described by the vector

$$\mathbf{r}_0 = r_0\mathbf{g}^r(\ell) + mq_0^{1/2}\ell\mathbf{g}^\zeta. \tag{B.28}$$

Once the above relation is put in the form

$$\mathbf{r}_a(\phi) = r_a \cos\phi\hat{\mathbf{x}} + r_a \sin\phi\hat{\mathbf{y}} + \frac{m}{k}\phi\hat{\mathbf{z}}, \tag{B.29}$$

it is obvious that the helix has a pitch

$$\eta_0 = 2\pi\frac{m}{k}. \tag{B.30}$$

Also for a finite helix we may choose for the parameter ℓ the interval

$$0 \leq \ell \leq N\sqrt{(2\pi r_0)^2 + \eta_0^2}, \tag{B.31}$$

and thus, in this case

$$0 \leq \zeta \leq L, \tag{B.32}$$

where $L = N\eta_0$ is denoted as the heigth of the helix, with N equals to the number of its spirals (how many times the helix turns around the axis of symmetry, $0 \leq \phi \leq N2\pi$). In fact, the restrictions for the arc-length of the relations (B.31) and (B.32) are pertinent for describing the limiting case of a helix of finite height; however, formally, helical symmetry corresponds to infinite helical length $(-\infty < \ell, \zeta < \infty)$.

The covariant and contravariant helical basis vectors are found to relate with the parameter ℓ as:

$$\begin{aligned}
\mathbf{g}_r(\ell) = \mathbf{g}^r(\ell) &= \cos(kq_0^{1/2}\ell)\hat{\mathbf{x}} + \sin(kq_0^{1/2}\ell)\hat{\mathbf{y}},\\
\mathbf{g}_u(\ell) &= -\frac{r_0}{m}\sin(kq_0^{1/2}\ell)\hat{\mathbf{x}} + \frac{r_0}{m}\cos(kq_0^{1/2}\ell)\hat{\mathbf{y}},\\
\mathbf{g}^u(\ell) &= -\frac{m}{r_0}\sin(kq_0^{1/2}\ell)\hat{\mathbf{x}} + \frac{m}{r_0}\cos(kq_0^{1/2}\ell)\hat{\mathbf{y}} - k\hat{\mathbf{z}},\\
\mathbf{g}_\zeta(\ell) = -\frac{r_0 k}{m}\sin(kq_0^{1/2}\ell)\hat{\mathbf{x}} &+ \frac{r_0 k}{m}\cos(kq_0^{1/2}\ell)\hat{\mathbf{y}} + \hat{\mathbf{z}}, \qquad \mathbf{g}^\zeta = \hat{\mathbf{z}}.
\end{aligned} \tag{B.33}$$

B.2.1 Frenet-Serret Formulas

Employing the Frenet-Serret formulas for the helix curve the tangent vector to this helix, defined as $\mathbf{t} \equiv (d\mathbf{r}_0/d\ell)/|d\mathbf{r}_0/d\ell|$, is found to be

$$\mathbf{t}(\ell) = mq_0^{1/2}\mathbf{g}_\zeta(\ell) = \frac{\mathbf{h}_0(\ell)}{|\mathbf{h}_0|}, \tag{B.34}$$

where $\mathbf{h}_0 = \mathbf{h}(r = r_0, u = u_0)$. Then, the vector of curvature, $\boldsymbol{\kappa} = d\mathbf{t}/d\ell$, is obtained

$$\boldsymbol{\kappa}(\ell) = -r_0 k^2 q_0 \mathbf{g}_r(\ell). \tag{B.35}$$

and thus, the curvature of the helix equals

$$\kappa(\ell) = |\boldsymbol{\kappa}(\ell)| = r_0 k^2 q_0, \tag{B.36}$$

while the curvature radius is

$$R = \frac{1}{\kappa} = \frac{1}{r_0}\sqrt{r_0^2 + (\frac{\eta_0}{2\pi})^2}. \tag{B.37}$$

In addition, the first and second normal vectors to that helix defined as: $\mathbf{n} \equiv \boldsymbol{\kappa}/\kappa$, and $\mathbf{b} \equiv \mathbf{t} \times \mathbf{n}$, are found to be

$$\begin{aligned}
\mathbf{n}(\ell) &= -\mathbf{g}_r(\ell),\\
\mathbf{b}(\ell) &= -r_0 q_0^{1/2}\mathbf{g}^u(\ell).
\end{aligned} \tag{B.38}$$

Then, the torsion of this helix, defined as $\tau_0 \equiv -\mathbf{n} \cdot (d\mathbf{b}/d\ell)$ is independent on ℓ:

$$\tau = kmq_0. \tag{B.39}$$

B.3 Intrinsic coordinates - Poloidal cross-section modeling

We now introduce a coordinate system associated with the special curve $\mathbf{r} = \mathbf{r}_0(\ell)$, which we will take to be the axis of the coordinate system. Let x_n, x_b be "cartesian" coordinates with rerspect to the axis of the system, and ℓ is the arc-length along the axis computed from the fixed point $\ell_0 = 0$. This system is defined from the Frenet triad, $\mathbf{t}\,,\mathbf{n}\,,\mathbf{b}$ in the sence that x_n is the distance from the helix in the direction $\mathbf{n}$ and x_b measures the distance from that helix in the direction $\mathbf{b}$. The position of every point M of the poloidal plane with origin at any point ℓ of the helix of reference is described by the vector

$$\mathbf{r}_{cs} = x_n\mathbf{n}(\ell) + x_b\mathbf{b}(\ell). \tag{B.40}$$

Since the plane $(\mathbf{n}, \mathbf{b})$ is normal to the helix, the coordinates (x_n, x_b) denote the position of the points on this plane, henceforth called poloidal plane, for every ℓ. This is because the system is co-moving with the helix.

With respect to the origin of the Cartesian system (fixed point $O(x = 0, y = 0, z = 0)$) the position of the points of the poloidal plane are defined by the vector

$$\mathbf{r} = \mathbf{r}_0(\ell) + \mathbf{r}_{cs}. \tag{B.41}$$

Thus, the intrinsic coordinates $(x_n\,, x_b\,, \ell)$ are related with the Cartesian coordinates $(x\,, y\,, z)$ as

$$\begin{aligned} x(x_n, x_b, \ell) &= (r_0 - x_n)\cos(kq_0^{1/2}\ell) + mq_0^{1/2}x_b\sin(kq_0^{1/2}\ell), \\ y(x_n, x_b, \ell) &= (r_0 - x_n)\sin(kq_0^{1/2}\ell) - mq_0^{1/2}x_b\cos(kq_0^{1/2}\ell), \\ z(x_n, x_b, \ell) &= q_0^{1/2}(m\ell + kr_0x_b), \end{aligned} \tag{B.42}$$

and as a result with the helical coordinates (r, u, ζ) as

$$\begin{aligned} u(x_n, x_b, \ell) &= m\arccos\left(\frac{(r_0 - x_n)\cos(kq_0^{1/2}\ell) + mq_0^{1/2}x_b\sin(kq_0^{1/2}\ell)}{\sqrt{(r_0 - x_n)^2 + m^2q_0x_b^2}}\right) \\ &\quad -kq_0^{1/2}(m\ell + kr_0x_b), \\ r(x_n, x_b) &= \sqrt{(r_0 - x_n)^2 + m^2q_0x_b^2}, \\ \zeta(x_b, \ell) &= q_0^{1/2}(m\ell + kr_0x_b). \end{aligned} \tag{B.43}$$

Then one finds the transformations between the covariant and contravariant basis vectors with the vectors of the Frenet triad

$$\begin{aligned} \mathbf{g}_r &= \mathbf{g}^r = -\mathbf{n}(\ell), \\ \mathbf{g}_u &= \frac{kr_0^2q_0^{1/2}}{m}\mathbf{t}(\ell) - r_0q_0^{1/2}\mathbf{b}(\ell), \\ \mathbf{g}^u &= -\frac{1}{r_0q_0^{1/2}}\mathbf{b}(\ell), \qquad \mathbf{g}_\zeta = \frac{1}{mq_0^{1/2}}\mathbf{t}(\ell), \\ \mathbf{g}^\zeta &= mq_0^{1/2}\mathbf{t}(\ell) + kr_0q_0^{1/2}\mathbf{b}(\ell), \end{aligned} \tag{B.44}$$

and the inverse transformations as

$$\begin{aligned} \mathbf{t}(\ell) &= \frac{kr_0^2q_0^{1/2}}{m}\mathbf{g}^u + \frac{1}{mq_0^{1/2}}\mathbf{g}^\zeta, \\ \mathbf{n}(\ell) &= -\mathbf{g}^r, \\ \mathbf{b}(\ell) &= -\frac{1}{r_0q_0^{1/2}}\mathbf{g}_u + kr_0q_0^{1/2}\mathbf{g}_\zeta, \end{aligned} \tag{B.45}$$

together with equations (B.34) and (B.38). Then the vector of position (B.41) can be cast into the form

$$\mathbf{r} = m^2 q_0 \ell \mathbf{t}(\ell) + (x_n - r_0)\mathbf{n}(\ell) + (x_b + kmr_0 q_0 \ell)\mathbf{b}(\ell). \tag{B.46}$$

Taking into account the Frenet formulas

$$\begin{aligned} \frac{d\mathbf{b}(\ell)}{d\ell} &= -\tau \mathbf{n}(\ell), \\ \frac{d\mathbf{t}(\ell)}{d\ell} &= \kappa \mathbf{n}(\ell), \\ \frac{d\mathbf{n}(\ell)}{d\ell} &= -\kappa \mathbf{t}(\ell) + \tau \mathbf{b}(\ell), \end{aligned} \tag{B.47}$$

one finds

$$\begin{aligned} d\mathbf{r} \cdot d\mathbf{r} = \Big(\big[m^2 q_0 - \kappa(x_n - r_0) \big]^2 + \tau_0^2 (x_n^2 + x_b^2) \Big) d\ell^2 + \\ + dx_n^2 + dx_b^2 + 2\tau (x_n d\ell dx_b - x_b d\ell dx_n) \end{aligned} \tag{B.48}$$

which means that the coordinate system (x_n, x_b, ℓ) is not orthogonal in the sence that its metric is not diagonal. We have to note that there is a flexibility in connecting "cartesian intrinsic" coordinates (x_n, x_b) with various other coordinates in order to obtain desirable cross-section shapes. Here we present a generalized set of intrinsic coordinates related with x_n, x_b as

$$\begin{aligned} x_n &= \rho^* (1 + \delta(\rho^*) \cos\theta) \cos\theta, \\ x_b &= e_1 \rho^* \sin\theta, \end{aligned} \tag{B.49}$$

with

$$\delta(\rho^*) = \gamma_1 + \gamma_2 \rho^{*\beta_1}, \tag{B.50}$$

where the parameters e_1, γ_1, γ_2, β_1 determine the shaping of the magnetic surfaces (i.e. elongation, triangularity).

B.3.1 Circular cross-section

We introduce intrinsic-polar coordinates $(\rho^\star, \theta)$ in the plane $(\mathbf{n}, \mathbf{b})$ related with the intrinsic-cartesian ones as

$$x_n = \rho^\star \cos\theta, \qquad x_b = \rho^\star \sin\theta. \tag{B.51}$$

These coordinates are recovered from the ones defined in equations (B.49)-(B.50) for $\gamma_1 = \gamma_2 = 0$ and $e_1 = 1$. Then coordinates $(\rho^\star, \theta, \ell)$ are related with helical ones as

$$\begin{aligned} r(\rho^\star, \theta) &= \sqrt{(r_0 - \rho^\star \cos\theta)^2 + m^2 q_0 \rho^{\star 2} \sin^2\theta}, \\ u(\rho^\star, \theta, \ell) &= m \arccos\left(\frac{(r_0 - \rho^\star \cos\theta)\cos(k q_0^{1/2} \ell) + m q_0^{1/2} \rho^\star \sin\theta \sin(k q_0^{1/2} \ell)}{\sqrt{(r_0 - \rho^\star \cos\theta)^2 + m^2 q_0 \rho^{\star 2} \sin^2\theta}} \right) \\ &\quad - k q_0^{1/2} (m\ell + k r_0 \rho^\star \sin\theta), \\ \zeta(\rho^\star, \theta, \ell) &= q_0^{1/2} (m\ell + k r_0 \rho^\star \sin\theta). \end{aligned} \tag{B.52}$$

The vector of position can be written in the form

$$\mathbf{r} = (m^2 q_0 \ell)\mathbf{t}(\ell) + (\rho^\star \cos\theta - r_0)\mathbf{n}(\ell) + (\rho^\star \sin\theta + \tau_0 r_0 \ell)\mathbf{b}(\ell), \tag{B.53}$$

to find that that the coordinates $(\rho^\star, \theta, \ell)$ are indeed not orthogonal:

$$d\mathbf{r}\cdot d\mathbf{r} = \left(\left[m^2 q_0 - \kappa(\rho^\star\cos\theta - r_0)\right]^2 + \tau_0^2\rho^{\star 2}\right) d\ell^2 + d\rho^{\star 2} + \rho^{\star 2} d\theta^2 + 2\tau_0\rho^{\star 2} d\ell d\theta. \quad \text{(B.54)}$$

The unit vectors along the coordinate lines are:

$$\begin{aligned} \hat{\mathbf{e}}_{\rho^\star} &= \cos\theta\mathbf{n} + \sin\theta\mathbf{b}, \\ \hat{\mathbf{e}}_{\theta} &= -\sin\theta\mathbf{n} + \cos\theta\mathbf{b} = \frac{\partial\hat{\mathbf{e}}_{\rho^\star}}{\partial\theta}, \\ \hat{\mathbf{e}}_{\ell} &= \mathbf{t}. \end{aligned} \quad \text{(B.55)}$$

The above system can easily be made orthogonal if the variable θ is replaced by the new angle variable [62, 199, 200]:

$$\omega := \theta + \alpha(\ell), \qquad \alpha(\ell) := \int_{\ell_0=0}^{\ell} \tau_0 d\ell = \tau_0\ell. \quad \text{(B.56)}$$

The metric for this orthogonal coordinate system is now

$$d\mathbf{r}\cdot d\mathbf{r} = d\rho^{\star 2} + \rho^{\star 2} d\omega^2 + \left[1 - \kappa\rho^\star\cos\theta(\omega,\ell)\right]^2 d\ell^2. \quad \text{(B.57)}$$

If the coordinate axis is a closed line, the coordinate surfaces $\omega =$ const. (surface curvature strips) do not close upon themselves in a complete circuit along the axis. The ambiguity in the coordinate ω that arises under these conditions is easily circumvented by requiring that all physical quantities depend on the angle variable ω in combination with the function $\alpha(\ell)$:

$$f = f(\rho^\star, \theta, \ell), \qquad \theta = \omega - \alpha(\ell) = \omega - \tau_0\ell. \quad \text{(B.58)}$$

The lines $\omega =$ const. on the surface $\rho^\star =$ const. are orthogonal (by definition) to the cross section $\ell =$ const. and follow the ℓ axis continuously. The surface $\theta =$ const. (asymptotic surface strip) closes upon itself since it forms a fixed angle with the closed surface $\theta = 0$ that extends along the principal normal $\mathbf{n}(\ell)$. The principal normal to the $\mathbf{n}$ axis is rotaded with respect to the surface $\omega = 0$ by an angle $\alpha(\ell)$, so that $\theta = \omega - \alpha(\ell)$; the angle $\alpha(\ell)$ can change discontinuously [200].

In the case of smooth rotation, the rate of change of the angle $\alpha(\ell)$ along ℓ, which gives the angle of rotation of the binormal $\mathbf{b}$ in space, is the torsion of the axis, $\tau_0 = d\alpha(\ell)/d\ell$. If $\mathbf{n}_R$ and $\mathbf{b}_R$ are two orthonormal vectors related by $\alpha(\ell)$ with respect to $\mathbf{n}$ and $\mathbf{b}$ such that

$$\begin{aligned} \mathbf{n}_R &= \cos\alpha(\ell)\mathbf{n} - \sin\alpha(\ell)\mathbf{b}, \\ \mathbf{b}_R &= \sin\alpha(\ell)\mathbf{n} + \cos\alpha(\ell)\mathbf{b}, \end{aligned} \quad \text{(B.59)}$$

then:

$$\begin{aligned} \hat{\mathbf{e}}_{\rho^\star} &= \cos\omega\mathbf{n}_R + \sin\omega\mathbf{b}_R = \cos\theta\mathbf{n} + \sin\theta\mathbf{b}, \\ \hat{\mathbf{e}}_{\omega} &= -\sin\omega\mathbf{n}_R + \cos\omega\mathbf{b}_R = -\sin\theta\mathbf{n} + \cos\theta\mathbf{b}. \end{aligned} \quad \text{(B.60)}$$

A geometrical representation of the coordinate system (ρ^*, ω, ℓ) is given in figure B.1. For this orthogonal system we obtain the following relationships:

$$d\mathbf{r}\cdot\mathbf{r} = h_{\rho^\star} d\rho^\star \hat{\mathbf{e}}_{\rho^\star} + h_\omega d\omega\hat{\mathbf{e}}_\omega + h_\ell d\ell\hat{\mathbf{e}}_\ell, \quad \text{(B.61)}$$

with $h_{\rho^\star} = 1\,, h_\omega = \rho^\star\,, h_\ell = 1 - \kappa\rho^\star\cos(\omega - \tau_0\ell)$ and $\hat{\mathbf{e}}_{\rho^\star}\times\hat{\mathbf{e}}_\omega = \hat{\mathbf{e}}_\ell\,, \hat{\mathbf{e}}_{\rho^\star}\times\hat{\mathbf{e}}_\ell = -\hat{\mathbf{e}}_\omega\,, \hat{\mathbf{e}}_\omega = \times\hat{\mathbf{e}}_\ell = \hat{\mathbf{e}}_{\rho^\star}$. Also we obtain:

$$\begin{aligned} d\mathbf{s}_1 &= h_\omega h_\ell d\omega d\ell\hat{e}_{\rho^\star} \\ d\mathbf{s}_2 &= h_{\rho^\star} h_\ell d\rho^\star d\ell\hat{e}_\omega \\ d\mathbf{s}_3 &= h_\omega h_{\rho^\star} d\omega d\rho^\star\hat{e}_\ell \\ dV &= h_{\rho^\star} h_\omega h_\ell d\rho^\star d\omega d\ell. \end{aligned} \quad \text{(B.62)}$$

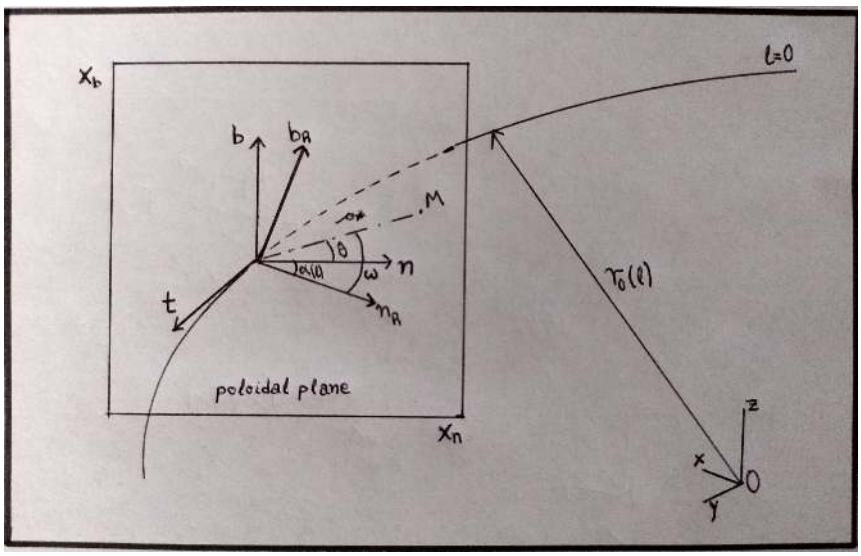

Figure B.1: The coordinates of any point M on the poloidal plane: ρ^*, θ coordinates refer to the natural axes $\mathbf{n}, \mathbf{b}$; ρ^*, ω coordinates refer to the rotated axes $\mathbf{n}_R, \mathbf{b}_R$.

As for the differential operators:

$$\begin{aligned}
\nabla f &= \frac{1}{h_{\rho^\star}}\frac{\partial f}{\partial \rho^\star}\hat{\mathbf{e}}_{\rho^\star} + \frac{1}{h_\omega}\frac{\partial f}{\partial \omega}\hat{\mathbf{e}}_\omega + \frac{1}{h_\ell}\frac{\partial f}{\partial \ell}\hat{\mathbf{e}}_\ell,\\
\nabla^2 f &= \frac{1}{h_{\rho^\star}h_\omega h_\ell}\left[\frac{\partial}{\partial \rho^\star}\left(\frac{h_\omega h_\ell}{h_{\rho^\star}}\frac{\partial f}{\partial \rho^\star}\right) + \frac{\partial}{\partial \omega}\left(\frac{h_{\rho^\star}h_\ell}{h_\omega}\frac{\partial f}{\partial \omega}\right) + \frac{\partial}{\partial \ell}\left(\frac{h_\omega h_{\rho^\star}}{h_\ell}\frac{\partial f}{\partial \ell}\right)\right],\\
\nabla\cdot\mathbf{B} &= \frac{1}{h_{\rho^\star}h_\omega h_\ell}\left[\frac{\partial}{\partial \rho^\star}(h_\omega h_\ell B_{\rho^\star}) + \frac{\partial}{\partial \omega}(h_{\rho^\star}h_\ell B_\omega) + \frac{\partial}{\partial \ell}(h_{\rho^\star}h_\omega B_\ell)\right],\\
\nabla\times\mathbf{B} &= \frac{1}{h_\ell h_\omega}\left[\frac{\partial}{\partial \omega}(h_\ell B_\ell) - \frac{\partial}{\partial \ell}(h_\omega B_\omega)\right]\hat{\mathbf{e}}_{\rho^\star} +\\
&\quad \frac{1}{h_\ell}\left[\frac{\partial B_{\rho^\star}}{\partial \ell} - \frac{\partial}{\partial \rho^\star}(h_\ell B_\ell)\right]\hat{\mathbf{e}}_\omega + \frac{1}{h_\omega}\left[\frac{\partial}{\partial \rho^\star}(h_\omega B_\omega) - \frac{\partial B_{\rho^\star}}{\partial \omega}\right]\hat{\mathbf{e}}_\ell.
\end{aligned} \tag{B.63}$$

The coordinates $(\rho^\star, \omega, \ell)$ are related with the helical coordinates (r, u, ζ) as:

$$\begin{aligned}
r(\rho^\star,\omega,\ell) &= \sqrt{(r_0 - \rho^\star\cos\theta(\omega,\ell))^2 + \rho^{\star 2}\sin^2\theta(\omega,\ell)m^2 q_0},\\
u(\rho^\star,\omega,\ell) &= m\arccos\left(\frac{(r_0 - \rho^\star\cos\theta(\omega,\ell))\cos(kq_0^{1/2}\ell) + \rho^\star\sin\theta(\omega,\ell)mq_0^{1/2}\sin(kq_0^{1/2}\ell)}{r(\rho^\star,\omega,\ell)}\right)\\
&\quad - kq_0^{1/2}(m\ell + kr_0\rho^\star\sin\theta(\omega,\ell)),\\
\zeta(\rho^\star,\omega,\ell) &= q_0^{1/2}(m\ell + kr_0\rho^\star\sin\theta(\omega,\ell)).
\end{aligned} \tag{B.64}$$

Each vector can be expanded in the polar-intrisic coordinate basis as:

$$\mathbf{v} = v_{\rho^\star}\hat{\mathbf{e}}_{\rho^\star} + v_\omega\hat{\mathbf{e}}_\omega + v_\ell\hat{\mathbf{e}}_\ell. \tag{B.65}$$

Then the transformations between the components $(v_{\rho^\star}, v_\omega, v_\ell)$ and the respective ones in the helical sytem are:

$$\begin{aligned}
v_{\rho^\star} &= -\cos\theta v^r - r_0 q_0^{1/2}\sin\theta v^u = -\cos\theta v_{\bar{r}} - r_0 q_0^{1/2}\sin\theta\frac{m}{r}v_{\bar{u}},\\
v_\omega &= \sin\theta v^r - r_0 q_0^{1/2}\cos\theta v^u = \sin\theta v_{\bar{r}} - r_0 q_0^{1/2}\cos\theta\frac{m}{r}v_{\bar{u}},\\
v_\ell &= \frac{kr_0^2 q_0^{1/2}}{m}v^u + \frac{1}{mq_0^{1/2}}v^\zeta = \frac{kr_0^2 q_0^{1/2}}{r}v_{\bar{u}} + \left(\frac{q}{q_0}\right)^{1/2}v_{\bar{\zeta}}.
\end{aligned} \tag{B.66}$$

As for the transformations between the basis $(\hat{\mathbf{e}}_{\rho^\star}, \hat{\mathbf{e}}_\omega, \hat{\mathbf{e}}_\ell)$ and the covariant, contravariant and Frenet triad bases we obtain:

$$\begin{aligned}
\begin{pmatrix} \hat{\mathbf{e}}_{\rho^\star} \\ \hat{\mathbf{e}}_\omega \\ \hat{\mathbf{e}}_\ell \end{pmatrix} &= \begin{pmatrix} 0 & \cos\theta & \sin\theta \\ 0 & -\sin\theta & \cos\theta \\ 1 & 0 & 0 \end{pmatrix} \begin{pmatrix} \mathbf{t} \\ \mathbf{n} \\ \mathbf{b} \end{pmatrix} \\
&= \begin{pmatrix} -\cos\theta & -\frac{\sin\theta}{r_0 q_0^{1/2}} & kr_0 q_0^{1/2} \sin\theta \\ \sin\theta & -\frac{\cos\theta}{r_0 q_0^{1/2}} & kr_0 q_0^{1/2} \cos\theta \\ 0 & 0 & m q_0^{1/2} \end{pmatrix} \begin{pmatrix} \mathbf{g}_r \\ \mathbf{g}_u \\ \mathbf{g}_\zeta \end{pmatrix} \\
&= \begin{pmatrix} -\cos\theta & -r_0 q_0^{1/2} \sin\theta & 0 \\ \sin\theta & -r_0 q_0^{1/2} \cos\theta & 0 \\ 0 & \frac{k r_0^2 q_0^{1/2}}{m} & \frac{1}{m q_0^{1/2}} \end{pmatrix} \begin{pmatrix} \mathbf{g}^r \\ \mathbf{g}^u \\ \mathbf{g}^\zeta \end{pmatrix}.
\end{aligned} \tag{B.67}$$

Finally, the inverse transformations are:

$$\begin{pmatrix} \mathbf{t} \\ \mathbf{n} \\ \mathbf{b} \end{pmatrix} = \begin{pmatrix} 0 & 0 & 1 \\ \cos\theta & -\sin\theta & 0 \\ \sin\theta & \cos\theta & 0 \end{pmatrix} \begin{pmatrix} \hat{\mathbf{e}}_{\rho^\star} \\ \hat{\mathbf{e}}_\omega \\ \hat{\mathbf{e}}_\ell \end{pmatrix},$$

$$\begin{pmatrix} \mathbf{g}_r \\ \mathbf{g}_u \\ \mathbf{g}_\zeta \end{pmatrix} = \begin{pmatrix} -\cos\theta & \sin\theta & 0 \\ -r_0 q_0^{1/2} \sin\theta & -r_0 q_0^{1/2} \cos\theta & \frac{k r_0^2 q_0^{1/2}}{m} \\ 0 & 0 & \frac{1}{m q_0^{1/2}} \end{pmatrix} \begin{pmatrix} \hat{\mathbf{e}}_{\rho^\star} \\ \hat{\mathbf{e}}_\omega \\ \hat{\mathbf{e}}_\ell \end{pmatrix},$$

$$\begin{pmatrix} \mathbf{g}^r \\ \mathbf{g}^u \\ \mathbf{g}^\zeta \end{pmatrix} = \begin{pmatrix} -\cos\theta & \sin\theta & 0 \\ -\frac{\sin\theta}{r_0 q_0^{1/2}} & -\frac{\cos\theta}{r_0 q_0^{1/2}} & 0 \\ kr_0 q_0^{1/2} \sin\theta & kr_0 q_0^{1/2} \cos\theta & m q_0^{1/2} \end{pmatrix} \begin{pmatrix} \hat{\mathbf{e}}_\rho \\ \hat{\mathbf{e}}_\omega \\ \hat{\mathbf{e}}_\ell \end{pmatrix}. \tag{B.68}$$

C | Solution of ODE (3.18) in the neighborhood of a regular singular point

We present an alternative analytical solution for (3.18) by first writting this ODE in canonical form as

$$R''(s) + P(s)R'(s) + Q(s)R(s) = 0, \qquad s \geq 0, \tag{C.1}$$

where $P(s) = (\varepsilon_{00} + \varepsilon_{11}s + \varepsilon_{22}s^2)/s(1+s)$, $Q(s) = (\varepsilon_{33} + \varepsilon_{44}s + \Upsilon_4 s^3)/s(1+s)$ and the prime denotes differentiation with respect to s. It is apparent that the point $s = 0$ consists of a regular singular point of ODE (C.1). Since both functions $sP(s)$ and $s^2Q(s)$ are analytic at $s = 0$ we can expand them as

$$sP(s) = \sum_{j=0}^{\infty} a_j s^j, \qquad s^2Q(s) = \sum_{j=0}^{\infty} b_j s^j, \tag{C.2}$$

assuming that each of these series have a radius of convergence, e.g. $\bar{\rho}_1$ and $\bar{\rho}_2$, respectively. In order to solve ODE (C.1) we employ the Frobenius method applying a series expandion for the solution around the regular singular point of the form

$$R(s) = \sum_{j=0}^{\infty} B_j s^{j+r}, \qquad s < \bar{\rho}, \tag{C.3}$$

where $\bar{\rho} = \min(\bar{\rho}_1, \bar{\rho}_2)$ denotes its convergence radius and the index r should not be confused with the radial helical coordinate. Then substitution of (C.3), together with its first and second derivatives with respect to s, into (C.1) using the expansions (C.2) yields

$$\begin{aligned}[r(r-1) + ra_0 \quad + \quad b_0]B_0 s^{r-2} + \sum_{j=1}^{\infty} \Big[\{(j+r)(j+r-1+a_0) + b_0\} B_j \\ + \sum_{l=0}^{j-1} \{(l+r)a_{j-l} + b_{j-l}\} B_l \Big] s^{j+r-2} = 0,\end{aligned} \tag{C.4}$$

which in order to be satisfied the coefficients of both s^{r-2} and s^{j+r-2} must vanish:

$$[r(r-1) + ra_0 + b_0]B_0 = 0, \tag{C.5}$$

$$\{(j+r)(j+r-1+a_0) + b_0\} B_j + \sum_{l=0}^{j-1} \{(l+r)a_{j-l} + b_{j-l}\} B_l = 0, \qquad j = 1, 2, \ldots \tag{C.6}$$

We assume $B_0 \neq 0$ and consequently from (C.5) we obtain the indicial equation

$$r(r-1) + ra_0 + b_0 = 0, \tag{C.7}$$

which has the following roots

$$r_{1,2} = \frac{1}{2}\left(1 - a_0 \pm \sqrt{(a_0-1)^2 - 4b_0}\right). \tag{C.8}$$

Also note that by comparing the coefficients of the powers of s in (C.2) we find the following specific expressions for a_j and b_j

$$a_j = \begin{cases} a_0 = 1 + 2n, \\ a_1 = -(1 + 2\varkappa), \\ a_2 = 1, \\ a_j = -a_{j-1},\ j \geq 3, \end{cases} \tag{C.9}$$

and

$$b_j = \begin{cases} b_0 = 0, \\ b_1 = \varepsilon_{33}, \\ b_2 = \varepsilon_{44} - b_1, \\ b_3 = -b_2, \\ b_4 = \Upsilon_4 - b_3, \\ b_j = -b_{j-1},\ j \geq 5. \end{cases} \tag{C.10}$$

As a result, we find that the roots of the indicial equation are

$$r_1 = 0 \qquad \text{and} \qquad r_2 = -2n. \tag{C.11}$$

By noticing that the difference between these two roots are $r_1 - r_2 = 2n$, equation (C.6) is simplieifed as

$$R_j(r)B_j + \sum_{l=0}^{j-1}\left\{(l+r)a_{j-l} + b_{j-l}\right\}B_l = 0, \qquad j = 1, 2, ..., \tag{C.12}$$

where

$$R_j(r) = (j + r)(j + r + r_1 - r_2). \tag{C.13}$$

In order for a solution to ODE (C.1) to exist it must hold for both roots that $\forall j \neq 0$: $R_j(r_1) = j(j + 2n) \neq 0$ and $R_j(r_2) = j(j - 2n) \neq 0$. Thus, we conclude that different families of solutions may be found dependent on the specific value of the separation constant n. Each of those cases are separately examined below.

C.1 n>0

In this case it follows that $\Re(r_1) > \Re(r_2)$ so we first proceed into finding a solution for $r_1 = 0$; note that it holds $R_j(0) \neq 0 \forall\, j \neq 0$ (recall that $j \geq 0$). Depending on whether the difference of the roots of the indicial equation is an integer or not we examine these two cases separately as follows.

$\mathbf{r_1 - r_2 = 2n \neq}$integer

In this case, equation (C.12) for $j = 1$ yields $B_1 = 0$ which is unacceptable, while it also implies that

$$B_j = -\frac{\sum_{l=0}^{j-1}(la_{j-l} + b_{j-l})B_l}{j(j+2n)}, \qquad j \geq 1. \tag{C.14}$$

Thus, a first series solution is the following:

$$R_1(s;n)=\sum_{j=0}^{\infty}B_j s^j, \qquad B_j=\begin{cases} B_0\,(\text{arbitrary}), \\ -\frac{\sum_{l=0}^{j-1}(la_{j-l}+b_{j-l})B_l}{j(j+2n)}, \qquad j\geq 1. \end{cases} \tag{C.15}$$

Furthermore, since $j=1,2,...$ and $2n\neq$integer, it holds $R_j(r_2)\neq 0\,\forall\, j\neq 0$, and thus a second solution can be constructed along the same lines. That is

$$R_2(s;n)=s^{-2n}\sum_{j=0}^{\infty}C_j s^j, \qquad C_j=\begin{cases} C_0\,(\text{arbitrary}), \\ -\frac{\sum_{l=0}^{j-1}[(l-2n)a_{j-l}+b_{j-l}]C_l}{j(j+2n)}, \qquad j\geq 1. \end{cases} \tag{C.16}$$

Thus, the general solution of the radial ODE (C.1) when the separation constant n is not a positive integer reads

$$R(s)=w_1R_1(s;n)+w_2R_2(s;n), \qquad \{n>0\,|\,n\notin\ \mathbb{Z}_+\,|n\neq+\frac{1}{2}\}, \tag{C.17}$$

where R_1, R_2 are two linearly independent solutions given by equations (C.15)-(C.16).

$\mathbf{r_1-r_2=2n}$ =integer

This is equivalent to the case $n\in\mathbb{Z}_+$ or $n=1/2$, respectively. We observe that $R_j(r_1=0)\neq 0\,\forall\, j\neq 0$ and thus a first solution can be constructed again having the exact form (C.15).

In this case we observe that $R_j(r_2)=0$ when $j=2n$ and as result all coefficients C_j with $j\geq 2n$ cannot be determined. Therefore, a second solution cannot be constructed by applying an analogous procedure. However, the method of the differentiation of coefficients guarantees that a second linearly independent solution can be yet constructed of the form

$$R_2(s)=cR_1(s)\log s+\sum_{j=0}^{\infty}C_j(r_2)s^{j-2n}, \tag{C.18}$$

where c is a constant which may be zero and the coefficients C_j can be calculated through

$$C_j(r_2=-2n)=\left\{\frac{\partial}{\partial r}\left[(r+2n)B_j(r)\right]\right\}_{|r=r_2}, \qquad j=1,2,..., \tag{C.19}$$

with

$$B_j(r)=-\frac{\sum_{l=0}^{j-1}[(l-2n)a_{j-l}+b_{j-l}]B_l}{(j+r)(j+r+2n)}. \tag{C.20}$$

In order to formally determine the constant c and the coefficients C_j we substitute (C.18) into the ODE (C.1); after some algebraic calculations be find the following

$$c=-\frac{\sum_{l=0}^{2n-1}[(l-2n)a_{2n-l}+b_{2n-l}]C_l}{2nB_0}, \tag{C.21}$$

and

$$C_j = \begin{cases} C_0 \,(\text{arbitrary}), \\ -\frac{\sum_{l=0}^{j-1}[(l-2n)a_{j-l}+b_{j-l}]C_l}{j(j-2n)}, \qquad 1 \le j \le 2n-1, \\ C_{2n} \,(\text{arbitrary}), \\ -\frac{\sum_{l=0}^{j-1}[(l-2n)a_{j-l}+b_{j-l}]C_l + c\left(2(j-n)B_{j-2n} + \sum_{l=0}^{j-2n-1} a_{j-2n-l}B_l\right)}{j(j-2n)}, \qquad j \ge 2n+1. \end{cases} \tag{C.22}$$

Thus, the general solution of the radial ODE (C.1) when the separation constant n equals a positive integer reads

$$R(s;n) = w_1 R_1(s;n) + w_2 R_2(s;n), \qquad \{n \in \mathbb{Z}_+ \,|\, n = +\frac{1}{2}\}, \tag{C.23}$$

where R_1, R_2 are two linearly independent solutions given by equations [(C.15), (C.18)] and [(C.21), (C.22)] respectively.

C.2 n<0

In this case it follows that $\Re(r_2) > \Re(r_1)$. By following in detail the same procedure as that in Section C.1 for the case $n > 0$, we find that for $n < 0$ in all cases there exists a symmetry between the solutions for $n \leftrightarrow -n$. Below we present all the resulting forms for the solutions.

When $r_2 - r_1 = -2n \neq$ integer, or equivalently $\{n \notin \mathbb{Z}_- \,|\, n \neq -1/2\}$, we obtain two linearly independent solutions $R_1(s;n)$ and $R_2(s;n)$ of the forms:

$$R_1(s;n) = s^{-2n}\sum_{j=0}^{\infty} B_j s^j, \qquad B_j = \begin{cases} B_0 \,(\text{arbitrary}), \\ -\frac{\sum_{l=0}^{j-1}[(l-2n)a_{j-l}+b_{j-l}]B_l}{j(j-2n)}, \qquad j \ge 1, \end{cases} \tag{C.24}$$

and

$$R_2(s;n) = \sum_{j=0}^{\infty} C_j s^j, \qquad C_j = \begin{cases} C_0 \,(\text{arbitrary}), \\ -\frac{\sum_{l=0}^{j-1}(la_{j-l}+b_{j-l})C_l}{j(j-2n)}, \qquad j \ge 1. \end{cases} \tag{C.25}$$

On the other hand, when $r_2 - r_1 = -2n =$ integer, or equivalently $\{n \in \mathbb{Z}_- \,|\, n = -1/2\}$, we obtain two linearly independent solutions, from which $R_1(s;n)$ has the form (C.24) and $R_2(s;n)$ is of the form:

$$R_2(s;n) = cR_1(s;n)\log s + \sum_{j=0}^{\infty} C_j s^j, \tag{C.26}$$

where

$$C_j = \begin{cases} C_0 \,(\text{arbitrary}), \\ -\frac{\sum_{l=0}^{j-1}[la_{j-l}+b_{j-l}]C_l}{j(j+2n)}, \qquad 1 \le j \le -2n-1, \\ C_{-2n} \,(\text{arbitrary}), \\ -\frac{\sum_{l=0}^{j-1}[la_{j-l}+b_{j-l}]C_l + c\left(2(j+n)B_{j+2n} + \sum_{l=0}^{j+2n-1} a_{j+2n-l}B_l\right)}{j(j+2n)}, \qquad j \ge -2n+1, \end{cases} \tag{C.27}$$

and with

$$c = \frac{\sum_{l=0}^{-2n-1}[la_{-(2n+l)} + b_{-(2n+l)}]C_l}{2nB_0}. \tag{C.28}$$

C.3 n=0

Finally we examine the special case when the separation constant is zero. In this case the two roots of the indicial equation are equal, $r_1 = r_2 = 0$. Thus, it holds $R_j(r_1) = R_j(r_2) = j^2 \,\forall\, j \neq 0$. Then ODE (C.1) yields

$$j^2 B_j + \sum_{l=0}^{j-1}[la_{j-l} + b_{j-l}]B_l = 0, \qquad j = 0, 1, 2, ... \tag{C.29}$$

which implies that B_0 may remain arbitrary. Therefore, a first independent solution is the following:

$$R_1(s;n) = \sum_{j=0}^{\infty} B_j s^j, \qquad B_j = \begin{cases} B_0 \,(\text{arbitrary}), \\ -\frac{\sum_{l=0}^{j-1}[la_{j-l}+b_{j-l}]B_l}{j^2}, \qquad j \ge 1. \end{cases} \tag{C.30}$$

Finally, in order to construct a second linearly independent solution we assume that

$$R_2(s;n) = R_1(s;n)\log s + \sum_{j=0}^{\infty} C_j s^j, \tag{C.31}$$

and find that this indeed is a solution once the following relationships for the coefficients C_j are satisfied:

$$C_j = \begin{cases} C_0 \,(\text{arbitrary}), \\ -\frac{1}{j^2}\left\{2jB_j + \sum_{l=0}^{j-1}[(la_{j-l} + b_{j-l})C_l + a_{j-l}B_l]\right\}, \qquad j \ge 1. \end{cases} \tag{C.32}$$

D | Proof of the relations (5.30)-(5.33)

Preliminarily, we present the useful vector identities

$$\nabla\cdot(\mathbf{Q}\times\mathbf{W})\equiv\mathbf{W}\cdot(\nabla\times\mathbf{Q})-\mathbf{Q}\cdot(\nabla\times\mathbf{W}), \tag{D.1}$$
$$\nabla\times(\mathbf{Q}\times\mathbf{W})\equiv(\mathbf{W}\cdot\nabla)\mathbf{Q}-\mathbf{W}(\nabla\cdot\mathbf{Q})-(\mathbf{Q}\cdot\nabla)\mathbf{W}+\mathbf{Q}(\nabla\cdot\mathbf{W}), \tag{D.2}$$
$$\nabla(\mathbf{Q}\cdot\mathbf{W})\equiv(\mathbf{W}\cdot\nabla)\mathbf{Q}+(\mathbf{Q}\cdot\nabla)\mathbf{W}+\mathbf{W}\times(\nabla\times\mathbf{Q})+\mathbf{Q}\times(\nabla\times\mathbf{W}), \tag{D.3}$$

as well as the useful following relations

$$\nabla\cdot(\alpha\mathbf{N})+\mathbf{J}\cdot\nabla\beta+\mathbf{B}\cdot\nabla\gamma=0, \tag{D.4}$$
$$\boldsymbol{\xi}\times\mathbf{B}=\alpha\mathbf{N}\times\mathbf{B}+\beta\mathbf{N}, \tag{D.5}$$
$$\mathbf{J}\times\boldsymbol{\xi}=\alpha\mathbf{J}\times\mathbf{N}+\gamma\mathbf{N}, \tag{D.6}$$
$$\mathbf{b}=\nabla\times(\alpha\mathbf{N}\times\mathbf{B}+\beta\mathbf{N}), \tag{D.7}$$

which are obtained on the basis of representation (5.29) and the condition $\nabla\cdot\boldsymbol{\xi}=0$.

To begin with, we decompose the potential energy of equation (5.26) into two integrals as

$$W=\frac{1}{2\mu_0}\left(\underbrace{\int_{\mathcal{D}}(1-\sigma_d-\lambda^2)[\mathbf{b}^2+\mathbf{b}\cdot(\mu_0\mathbf{J}\times\boldsymbol{\xi})]d^3\mathbf{r}}_{S_1}-2\underbrace{\int_{\mathcal{D}}\lambda(\boldsymbol{\xi}\cdot\nabla\lambda)\{\boldsymbol{\xi}\cdot[(\mathbf{B}\cdot\nabla)\mathbf{B}]\}d^3\mathbf{r}}_{S_2}\right). \tag{D.8}$$

The rest of the present Appendix is dedicated in calculating these integrals in order to derive the exact expressions (5.30)-(5.33) as follows.

Calculation of S_1: By employing equation (D.6) we obtain

$$\begin{aligned}\mathbf{b}^2+\mathbf{b}\cdot(\mu_0\mathbf{J}\times\boldsymbol{\xi}) &= \mathbf{b}^2+\alpha\mathbf{b}\cdot(\mu_0\mathbf{J}\times\mathbf{N})+\mu_0\gamma\mathbf{b}\cdot\mathbf{N}\\ &= (\mathbf{b}+\alpha\mu_0\mathbf{J}\times\mathbf{N})^2-\alpha\mathbf{b}\cdot(\mu_0\mathbf{J}\times\mathbf{N})\\ &\quad -\alpha^2(\mu_0\mathbf{J}\times\mathbf{N})^2+\mu_0\gamma\mathbf{b}\cdot\mathbf{N}.\end{aligned} \tag{D.9}$$

Also, with the aid of the identity (D.1) we find that

$$\begin{aligned}\mu_0\gamma\mathbf{b}\cdot\mathbf{N} &= \mu_0\gamma\mathbf{N}\cdot[\nabla\times(\alpha\mathbf{N}\times\mathbf{B}+\beta\mathbf{N})]\\ &= \mu_0(\alpha\mathbf{N}\times\mathbf{B}+\beta\mathbf{N})\cdot[\nabla\times(\gamma\mathbf{N})]+\nabla\cdot(\mu_0\gamma\alpha\mathbf{N}^2\mathbf{B}),\end{aligned} \tag{D.10}$$

and therefore

$$\begin{aligned}(1-\sigma_d-\lambda^2)\mu_0\gamma\mathbf{b}\cdot\mathbf{N} &= (1-\sigma_d-\lambda^2)\mu_0(\alpha\mathbf{N}\times\mathbf{B}+\beta\mathbf{N})\cdot[\nabla\times(\gamma\mathbf{N})]\\ &\quad +\nabla\cdot[(1-\sigma_d-\lambda^2)\mu_0\alpha\gamma\mathbf{N}^2\mathbf{B}].\end{aligned} \tag{D.11}$$

Then owing to (D.9) together with (D.11) and the fact that $\int_{\mathcal{D}} \nabla\cdot[(1-\sigma_d-\lambda^2)\mu_0\alpha\gamma\mathbf{N}^2\mathbf{B}]d^3\mathbf{r}$ vanishes due to the boundary conditions, the integral S_1 can be written in the form

$$\begin{aligned} S_1 &= \int_{\mathcal{D}}(1-\sigma_d-\lambda^2)\{(\mathbf{b}+\alpha\mu_0\mathbf{J}\times\mathbf{N})^2-\alpha^2(\mu_0\mathbf{J}\times\mathbf{N})^2 \\ &\quad \underbrace{-\alpha\mathbf{b}\cdot(\mu_0\mathbf{J}\times\mathbf{N})+\mu_0(\alpha\mathbf{N}\times\mathbf{B}+\beta\mathbf{N})\cdot[\nabla\times(\gamma\mathbf{N})]}_{\Lambda_1}\}d^3\mathbf{r}. \end{aligned} \tag{D.12}$$

In order to obtain a more useful form for S_1, we further proceed as below.

For the third and fourth term of the integral in (D.12) we find

$$\begin{aligned} -\alpha\mathbf{b}\cdot(\mu_0\mathbf{J}\times\mathbf{N}) &= -\alpha(\mu_0\mathbf{J}\times\mathbf{N})\cdot[\nabla\times(\alpha\mathbf{N}\times\mathbf{B}+\beta\mathbf{N})] \\ &= -\alpha(\mu_0\mathbf{J}\times\mathbf{N})\cdot[\alpha\nabla\times(\mathbf{N}\times\mathbf{B})+\nabla\alpha\times(\mathbf{N}\times\mathbf{B})+\beta\mathbf{M}+\nabla\beta\times\mathbf{N}] \\ &= -\mu_0\alpha\mathbf{N}^2(\mathbf{J}\cdot\nabla\beta+\mathbf{N}\cdot\nabla\alpha)-\mu_0\alpha\beta\mathbf{M}\cdot(\mathbf{J}\times\mathbf{N}) \\ &\quad -\mu_0\alpha^2(\mathbf{J}\times\mathbf{N})\cdot[\nabla\times(\mathbf{N}\times\mathbf{B})], \end{aligned} \tag{D.13}$$

and

$$\begin{aligned} \mu_0(\alpha\mathbf{N}\times\mathbf{B}+\beta\mathbf{N})\cdot[\nabla\times(\gamma\mathbf{N})] &= \mu_0(\alpha\mathbf{N}\times\mathbf{B}+\beta\mathbf{N})\cdot(\gamma\mathbf{M}+\nabla\gamma\times\mathbf{N}) \\ &= \mu_0\alpha\gamma\mathbf{M}\cdot(\mathbf{N}\times\mathbf{B})-\mu_0\alpha\mathbf{N}^2\mathbf{B}\cdot\nabla\gamma. \end{aligned} \tag{D.14}$$

Also, employing the identities (D.2) and (D.3) for $\mathbf{Q}=\mathbf{N}$ and $\mathbf{W}=\mathbf{B}$ yields

$$\begin{aligned} \mu_0(\mathbf{J}\times\mathbf{N})\cdot[\nabla\times(\mathbf{N}\times\mathbf{B})] &= \mu_0(\mathbf{J}\times\mathbf{N})\cdot[2(\mathbf{B}\cdot\nabla)\mathbf{N}+\mathbf{B}\times\mathbf{M}] \\ &\quad -(\mu_0\mathbf{J}\times\mathbf{N})^2+\mu_0\mathbf{N}^2(\nabla\cdot\mathbf{N}). \end{aligned} \tag{D.15}$$

Therefore, with the use of relations (D.13)-(D.15), we find in a straightforward way that the quantity Λ_1 reads

$$\Lambda_1=\alpha^2(\mu_0\mathbf{J}\times\mathbf{N})^2-\mu_0\alpha(\beta\mathbf{J}+\gamma\mathbf{B})\cdot(\mathbf{N}\times\mathbf{M})-2\alpha^2(\mu_0\mathbf{J}\times\mathbf{N})\cdot[(\mathbf{B}\cdot\nabla)\mathbf{N}]. \tag{D.16}$$

Afterall, substitution of the later relation into (D.12) results into the following useful form for the integral S_1

$$\begin{aligned} S_1 &= \int_{\mathcal{D}}(1-\sigma_d-\lambda^2)\{(\mathbf{b}+\alpha\mu_0\mathbf{J}\times\mathbf{N})^2-\mu_0\alpha(\beta\mathbf{J}+\gamma\mathbf{B})\cdot(\mathbf{N}\times\mathbf{M}) \\ &\quad -2\alpha^2(\mu_0\mathbf{J}\times\mathbf{N})\cdot[(\mathbf{B}\cdot\nabla)\mathbf{N}]\}d^3\mathbf{r}. \end{aligned} \tag{D.17}$$

Calculation of S_2: We now consider the second integral of W in equation (D.8) as follows. Using the relations

$$\boldsymbol{\xi}\cdot\nabla\lambda=\alpha\mathbf{N}\cdot\nabla\lambda, \tag{D.18}$$

and

$$\boldsymbol{\xi}\cdot[(\mathbf{B}\cdot\nabla)\mathbf{B}]=(\alpha\mathbf{N}+\beta\mathbf{J}+\gamma\mathbf{B})\cdot\nabla\left(\frac{\mathbf{B}^2}{2}\right)+\mu_0\alpha\mathbf{N}^2, \tag{D.19}$$

the later obtained with the aid of identity (D.3) for $\mathbf{Q}=\mathbf{W}=\mathbf{B}$, the integral S_2 is written in the useful form

$$S_2=\mu_0\int_{\mathcal{D}}\left\{\lambda\alpha^2(\mathbf{N}\cdot\nabla\lambda)\left[\mathbf{N}\cdot\nabla\left(\frac{\mathbf{B}^2}{2\mu_0}\right)+\mathbf{N}^2\right]+\alpha(\beta\mathbf{J}+\gamma\mathbf{B})\cdot\nabla\left(\frac{\mathbf{B}^2}{2\mu_0}\right)\right\}d^3\mathbf{r}. \tag{D.20}$$

To continue with, we plug the expressions (D.17) and (D.20) back into the relation for the potential energy (D.8); then if we further rearrange the containing terms and integrate by parts, W is put in the following form

$$W = \frac{1}{2\mu_0}\left[\int_{\mathcal{D}}(1-\sigma_d-\lambda^2)(\mathbf{b}+\alpha\mu_0\mathbf{J}\times\mathbf{N})^2 d^3\mathbf{r} + \int_{\mathcal{D}}\mathfrak{A}\alpha^2 d^3\mathbf{r} \right. \\ \left. -\mu_0\int_{\mathcal{D}}\alpha\beta(\mathbf{J}\cdot\mathbf{L})d^3\mathbf{r} - \mu_0\int_{\mathcal{D}}\alpha\gamma(\mathbf{B}\cdot\mathbf{L})d^3\mathbf{r}\right], \tag{D.21}$$

where

$$\mathbf{L} := (1-\sigma_d-\lambda^2)(\mathbf{N}\times\mathbf{M}) + 2\lambda(\mathbf{N}\cdot\nabla\lambda)\nabla\left(\frac{\mathbf{B}^2}{2\mu_0}\right), \tag{D.22}$$

and

$$\mathfrak{A} := -2\Big\{(1-\sigma_d-\lambda^2)(\mu_0\mathbf{J}\times\mathbf{N})\cdot[(\mathbf{B}\cdot\nabla)\mathbf{N}] + \mu_0\lambda(\mathbf{N}\cdot\nabla\lambda)\times \\ \left[\mathbf{N}\cdot\nabla\left(\frac{\mathbf{B}^2}{2\mu_0}\right)+\mathbf{N}^2\right]\Big\}. \tag{D.23}$$

Then we can show that the coefficients of $\alpha\beta$ and $\alpha\gamma$ in the third and fourth integrals of (D.21) vanish identically. Indeed, with the aid of the equilibrium equations (5.23)-(5.25), (5.27), the fact that $\lambda = \lambda(\psi)$, $\mathcal{P}_s = \mathcal{P}_s(\psi)$, and the identity $\nabla(qw) \equiv q\nabla w + w\nabla q$ for arbitrary scalar functions q, w, equation (D.22) yields

$$\mathbf{L} = g|\nabla\psi|^2\left[(\mathcal{P}_s)'' + (\lambda^2)'g - (\lambda^2)''\frac{\mathbf{B}^2}{2\mu_0}\right]\nabla\psi. \tag{D.24}$$

Thus, it follows that

$$\mathbf{J}\cdot\mathbf{L} = \mathbf{B}\cdot\mathbf{L} = 0, \tag{D.25}$$

since for the field-aligned incompressible equilibria under consideration, it holds $\mathbf{J}\cdot\nabla\psi = \mathbf{B}\cdot\nabla\psi = 0$.

Finally, as concerns the quantity $\mathfrak{A}$ given in (D.23), it can be written in a more useful form as follows. Recall that $\mathbf{N} = g\nabla\psi$, as implied from the equilibrium equations (5.23), (5.24) and (5.27). On account of this relation, and with the use of the identity (D.3) for $\mathbf{Q} = \nabla\psi$, $\mathbf{W} = \mathbf{B}$, as well as of the identity $(\mathbf{B}\cdot\nabla)(g\nabla\psi) \equiv \nabla\psi(\mathbf{B}\cdot\nabla g) + g(\mathbf{B}\cdot\nabla)\nabla\psi$, we obtain from (D.23)

$$\mathcal{A} := \frac{\mathfrak{A}}{2g^2} = -(1-\sigma_d-\lambda^2)\left\{|\mu_0\mathbf{J}\times\nabla\psi|^2 - (\mu_0\mathbf{J}\times\nabla\psi)\cdot[(\nabla\psi\cdot\nabla)\mathbf{B}]\right\} \\ +\frac{\mu_0}{2}[\ln(1-\sigma_d-\lambda^2)]'|\nabla\psi|^2\nabla\psi\cdot\nabla\left(\mathcal{P}+(1-\sigma_d)\frac{\mathbf{B}^2}{2\mu_0}\right), \tag{D.26}$$

or equivalently, with the use of (1.61)

$$\mathcal{A} = -(1-\sigma_d-\lambda^2)\left\{|\mu_0\mathbf{J}\times\nabla\psi|^2 - (\mu_0\mathbf{J}\times\nabla\psi)\cdot[(\nabla\psi\cdot\nabla)\mathbf{B}]\right\} \\ +\frac{\mu_0}{2}[\ln(1-\sigma_d-\lambda^2)]'|\nabla\psi|^2\nabla\psi\cdot\nabla\left(P_\perp+\frac{\mathbf{B}^2}{2\mu_0}\right), \tag{D.27}$$

the later relation having the exact form (5.33). Thus, substitution of the relations (D.25) and (D.26) into (D.21) yields for the exact expressions (5.30)-(5.32) for the potential energy:

$$W = \underbrace{\frac{1}{2\mu_0}\int_{\mathcal{D}}(1-\sigma_d-\lambda^2)(\mathbf{b}+\alpha\mu_0\mathbf{J}\times\mathbf{N})^2 d^3\mathbf{r}}_{W_1} + \underbrace{\frac{1}{2\mu_0}\int_{\mathcal{D}}\mathcal{A}(\sqrt{2}g\alpha)^2 d^3\mathbf{r}}_{W_2}. \tag{D.28}$$

Bibliography

[1] M. N. Saha, "LIII. Ionization in the solar chromosphere," *The London, Edinburgh, and Dublin Philosophical Magazine and Journal of Science*, vol. 40, no. 238, pp. 472–488, 1920. [Online]. Available: https://doi.org/10.1080/14786441008636148

[2] M. N. Saha, "Versuch einer theorie der physikalischen erscheinungen bei hohen temperaturen mit anwendungen auf die astrophysik," *Zeitschrift für Physik*, vol. 6, p. 40–55, 1921. [Online]. Available: https://doi.org/10.1007/BF01327962

[3] R. S. Cohen, L. Spitzer, and P. M. Routly, "The electrical conductivity of an ionized gas," *Phys. Rev.*, vol. 80, pp. 230–238, Oct 1950. [Online]. Available: https://link.aps.org/doi/10.1103/PhysRev.80.230

[4] L. Spitzer and R. Härm, "Transport phenomena in a completely ionized gas," *Phys. Rev.*, vol. 89, pp. 977–981, Mar 1953. [Online]. Available: https://link.aps.org/doi/10.1103/PhysRev.89.977

[5] J. D. Lawson, "Some criteria for a power producing thermonuclear reactor," *Proceedings of the Physical Society. Section B*, vol. 70, no. 1, pp. 6–10, jan 1957. [Online]. Available: https://doi.org/10.1088%2F0370-1301%2F70%2F1%2F303

[6] P. Helander, C. D. Beidler, T. M. Bird, M. Drevlak, Y. Feng, R. Hatzky, F. Jenko, R. Kleiber, J. H. E. Proll, Y. Turkin, and P. Xanthopoulos, "Stellarator and tokamak plasmas: a comparison," *Plasma Physics and Controlled Fusion*, vol. 54, no. 12, p. 124009, nov 2012. [Online]. Available: https://doi.org/10.1088%2F0741-3335%2F54%2F12%2F124009

[7] Y. Xu, "A general comparison between tokamak and stellarator plasmas," *Matter and Radiation at Extremes*, vol. 1, no. 4, pp. 192–200, 2016. [Online]. Available: https://aip.scitation.org/doi/abs/10.1016/j.mre.2016.07.001

[8] "24 - The transport equation in the case of Coulomb interactions," in *Collected Papers of L.D. Landau*, D. T. HAAR, Ed. Pergamon, 1965, pp. 163 – 170. [Online]. Available: http://www.sciencedirect.com/science/article/pii/B9780080105864500298

[9] A. Lenard, "On Bogoliubov's kinetic equation for a spatially homogeneous plasma," *Annals of Physics*, vol. 10, no. 3, pp. 390 – 400, 1960. [Online]. Available: http://www.sciencedirect.com/science/article/pii/0003491660900038

[10] R. Balescu, "Irreversible processes in ionized gases," *The Physics of Fluids*, vol. 3, no. 1, pp. 52–63, 1960. [Online]. Available: https://aip.scitation.org/doi/abs/10.1063/1.1706002

[11] P. L. Bhatnagar, E. P. Gross, and M. Krook, "A model for collision processes in gases. I. Small amplitude processes in charged and neutral one-component

systems," *Phys. Rev.*, vol. 94, pp. 511–525, May 1954. [Online]. Available: https://link.aps.org/doi/10.1103/PhysRev.94.511

[12] S. Chapman and T. G. Cowling, *The Mathematical Theory of Non-uniform Gases*, 3rd ed., ser. Cambridge Mathematical Library. Cambridge University Press, 1991.

[13] J. P. Freidberg, "Ideal magnetohydrodynamic theory of magnetic fusion systems," *Rev. Mod. Phys.*, vol. 54, pp. 801–902, Jul 1982. [Online]. Available: https://link.aps.org/doi/10.1103/RevModPhys.54.801

[14] G. F. Chew, M. L. Goldberger, and F. E. Low, "The Boltzmann equation and the one-fluid hydromagnetic equations in the absence of particle collisions," *Proc. R. Soc. Lond. A*, vol. 236, pp. 112–118, Jul 1956. [Online]. Available: https://royalsocietypublishing.org/doi/abs/10.1098/rspa.1956.0116

[15] S. I. Braginskii, *Transport processes in a plasma*, ser. in Reviews of Plasma Physics Vol: 1. Consultants Bureau, 1965.

[16] D. Biskamp, *Nonlinear Magnetohydrodynamics*, ser. Cambridge Monographs on Plasma Physics. Cambridge University Press, 1993.

[17] D. Biskamp, *Magnetic Reconnection in Plasmas*, ser. Cambridge Monographs on Plasma Physics. Cambridge University Press, 2000.

[18] R. M. Kulsrud, "MHD description of plasma," in *Basic Plasma Physics: Selected Chapters, Handbook of Plasma Physics, Volume 1*, Jan. 1983, p. 1.

[19] P. Hunana, A. Tenerani, G. P. Zank, E. Khomenko, M. L. Goldstein, G. M. Webb, P. S. Cally, M. Collados, M. Velli, L. Adhikari, and et al., "An introductory guide to fluid models with anisotropic temperatures. Part 1. CGL description and collisionless fluid hierarchy," *Journal of Plasma Physics*, vol. 85, no. 6, p. 205850602, 2019.

[20] H. de Blank, "MHD instabilities in tokamaks," *Fusion Science and Technology*, vol. 53, no. 2T, pp. 122–134, 2008. [Online]. Available: https://doi.org/10.13182/FST08-A1698

[21] M. D. Kruskal and R. M. Kulsrud, "Equilibrium of a magnetically confined plasma in a toroid," *The Physics of Fluids*, vol. 1, no. 4, pp. 265–274, 1958. [Online]. Available: https://aip.scitation.org/doi/abs/10.1063/1.1705884

[22] P. Alexandroff and H. Hopf, *Topologie*. Springer, 1935.

[23] A. I. Morozov and L. S. Solovev, "Typical structure of a toroidal magnetic field," *Journal of Experimental and Theoretical Physics*, vol. 18, no. 3, p. 955, 1964. [Online]. Available: http://www.jetp.ac.ru/cgi-bin/e/index/e/18/3/p660?a=list

[24] H. Grad, "Toroidal containment of a plasma," *The Physics of Fluids*, vol. 10, no. 1, pp. 137–154, 1967. [Online]. Available: https://aip.scitation.org/doi/abs/10.1063/1.1761965

[25] H. K. Moffatt, *On the existence, structure and stability of MHD equilibrium states, in: Turbulence and Nonlinear Dynamics in MHD Flows*. North-Holland, 1989.

[26] S. M. Moawad and D. A. Ibrahim, "Three-dimensional nonlinear ideal MHD equilibria with field-aligned incompressible and compressible flows," *Physics of Plasmas*, vol. 23, no. 8, p. 082502, 2016. [Online]. Available: https://doi.org/10.1063/1.4960043

[27] I. B. Bernstein, E. A. Frieman, M. D. Kruskal, and R. M. Kulsrud, "An energy principle for hydromagnetic stability problems," *Quarterly Journal of Mechanics and Applied Mathematics*, vol. 244, no. 1236, pp. 17 – 40, 1958. [Online]. Available: https://royalsocietypublishing.org/doi/abs/10.1098/rspa.1958.0023

[28] J. P. H. Goedbloed and S. Poedts, *Principles of Magnetohydrodynamics: With Applications to Laboratory and Astrophysical Plasmas*. Cambridge University Press, 2004.

[29] R. H. A. IJzermans, R. Hagmeijer, and P. J. van Langen, "Accumulation of heavy particles around a helical vortex filament," *Physics of Fluids*, vol. 19, no. 10, p. 107102, 2007. [Online]. Available: https://doi.org/10.1063/1.2771658

[30] D. Lucas and D. G. Dritschel, "A family of helically symmetric vortex equilibria," *Journal of Fluid Mechanics*, vol. 634, p. 245–268, 2009.

[31] O. Kelbin, A. F. Cheviakov, and M. Oberlack, "New conservation laws of helically symmetric, plane and rotationally symmetric viscous and inviscid flows," *Journal of Fluid Mechanics*, vol. 721, p. 340–366, 2013.

[32] S. N. Aristov and D. V. Knyazev, "Localized helically symmetric flows of an ideal fluid," *Journal of Applied Mechanics and Technical Physics*, vol. 51, no. 6, pp. 815 – 818, 2010. [Online]. Available: https://link.springer.com/article/10.1007/s10808-010-0102-2#article-info

[33] M. Germano, "The Dean equations extended to a helical pipe flow," *Journal of Fluid Mechanics*, vol. 203, p. 289–305, 1989.

[34] D. L. Thomson, Y. Bayazitoglu, and A. J. Meade, "Series solution of low Dean and Germano number flows in helical rectangular ducts," *International Journal of Thermal Sciences*, vol. 40, no. 11, pp. 937 – 948, 2001. [Online]. Available: http://www.sciencedirect.com/science/article/pii/S1290072901012807

[35] K. Yamamoto, A. Aribowo, Y. Hayamizu, T. Hirose, and K. Kawahara, "Visualization of the flow in a helical pipe," *Fluid Dynamics Research*, vol. 30, no. 4, pp. 251 – 267, 2002. [Online]. Available: http://www.sciencedirect.com/science/article/pii/S0169598302000436

[36] P. Verma and P. Ram, "On the low-Reynolds number magnetic fluid flow in a helical pipe," *International Journal of Engineering Science*, vol. 31, no. 2, pp. 229 – 239, 1993. [Online]. Available: http://www.sciencedirect.com/science/article/pii/002072259390036T

[37] M. Alam, D. Begum, and K. Yamamoto, "Flow through a helical pipe with rectangular cross-section," *Journal of Naval Architecture and Marine Engineering*, vol. 4, no. 2, pp. 99–110, 1 1. [Online]. Available: https://www.banglajol.info/index.php/JNAME/article/view/991

[38] M. J. Landman, "Time-dependent helical waves in rotating pipe flow," *Journal of Fluid Mechanics*, vol. 221, p. 289–310, 1990.

[39] E. Marušić-Paloka and I. Pazanin, "Fluid flow through a helical pipe," *Zeitschrift für angewandte Mathematik und Physik*, vol. 58, pp. 81 – 99, 2007. [Online]. Available: https://link.springer.com/article/10.1007/s00033-006-0073-6#article-info

[40] Z. Jinsuo and Z. Benzhao, "Fluid flow in a helical pipe," *Acta Mechanica Sinica*, vol. 15, no. 4, pp. 299 – 312, 1999. [Online]. Available: https://link.springer.com/article/10.1007/BF02487928

[41] M. Germano and M. S. Oggiano, "Potential flow in helical pipes," *Meccanica*, vol. 22, pp. 8 – 13, 1987. [Online]. Available: https://link.springer.com/article/10.1007/BF01560119

[42] E. K. Vachagina and A. I. Kadyirov, "The use of helical coordinate systems," *Proceedings of the Royal Society A*, vol. 67, no. 4, pp. 553 – 566, 2014. [Online]. Available: https://ieeexplore.ieee.org/abstract/document/8152924/citations#citations

[43] L. Zovatto and G. Pedrizzetti, "Fluid flow in a helical vessel in presence of a stenosis," *Meccanica*, vol. 52, pp. 545 – 553, 2017. [Online]. Available: https://link.springer.com/article/10.1007/s11012-015-0297-7

[44] L. Zabielski and A. J. Mestel, "Steady flow in a helically symmetric pipe," *Journal of Fluid Mechanics*, vol. 370, p. 297–320, 1998.

[45] L. Zabielski and A. J. Mestel, "Unsteady blood flow in a helically symmetric pipe," *Journal of Fluid Mechanics*, vol. 370, p. 321–345, 1998.

[46] T. Shimanouchi and S. Mizushima, "On the helical configuration of a polymer chain," *The Journal of Chemical Physics*, vol. 23, no. 4, pp. 707–711, 1955. [Online]. Available: https://doi.org/10.1063/1.1742083

[47] L. Pauling and R. Corey, "Compound helical configurations of polypeptide chains: Structure of proteins of the a-keratin type," *Nature*, vol. 171, pp. 59–61, 1953. [Online]. Available: https://www.nature.com/articles/171059a0

[48] J. E. Magee, V. R. Vasquez, and L. Lue, "Helical structures from an isotropic homopolymer model," *Phys. Rev. Lett.*, vol. 96, p. 207802, May 2006. [Online]. Available: https://link.aps.org/doi/10.1103/PhysRevLett.96.207802

[49] E. M. de Gouveia Dal Pino, "Astrophysical jets and outflows," *Advances in Space Research*, vol. 35, no. 5, pp. 908 – 924, 2005, fundamentals of Space Environment Science. [Online]. Available: http://www.sciencedirect.com/science/article/pii/S0273117705004916

[50] R. E. Pudritz, M. J. Hardcastle, and D. C. Gabuzda, "Magnetic fields in astrophysical jets: From launch to termination," *Space Science Reviews*, vol. 169, pp. 27 – 72, 2012. [Online]. Available: https://link.springer.com/article/10.1007/s11214-012-9895-z

[51] O. I. Bogoyavlenskij, "Helically symmetric astrophysical jets," *Phys. Rev. E*, vol. 62, pp. 8616–8627, Dec 2000. [Online]. Available: https://link.aps.org/doi/10.1103/PhysRevE.62.8616

[52] O. I. Bogoyavlenskij, "Exact helically symmetric plasma equilibria," *Letters in Mathematical Physics*, vol. 51, pp. 235–247, Mar 2000. [Online]. Available: https://link.springer.com/article/10.1023/A:1007620802075

[53] F. Paresce and A. Nota, "Dust in the circumstellar environment of AG Carinae - Evidence for a bipolar and helical structure," *Astrophysical Journal, Part 2 - Letters*, vol. 341, pp. L83 – L85, 1989. [Online]. Available: http://adsabs.harvard.edu/full/1989ApJ...341L..83P

[54] F. Macchetto *et al.*, "HST observations of 3C 66B - A double-stranded optical jet," *Astrophysical Journal, Part 2 - Letters*, vol. 373, pp. L55 – L58, 1991. [Online]. Available: http://adsabs.harvard.edu/full/1991ApJ...373L..55M

[55] D. C. Barnes and J. R. Cary, "Free boundary stability of straight stellarators," *The Physics of Fluids*, vol. 27, no. 10, pp. 2522–2534, 1984. [Online]. Available: https://aip.scitation.org/doi/abs/10.1063/1.864534

[56] A. Bhattacharjee, J. E. Sedlak, P. L. Similon, M. N. Rosenbluth, and D. W. Ross, "Drift waves in a straight stellarator," *The Physics of Fluids*, vol. 26, no. 4, pp. 880–882, 1983. [Online]. Available: https://aip.scitation.org/doi/abs/10.1063/1.864229

[57] I. A. Girka and P. K. Kovtun, "Effect of the helical nonuniformity of the confining magnetic field on the MHD eigenmodes in straight stellarators," *Plasma Physics Reports*, vol. 26, pp. 33–40, 2000. [Online]. Available: https://link.springer.com/article/10.1134/1.952819

[58] A. E. Koniges and J. L. Johnson, "A helical axis stellarator equilibrium model," *The Physics of Fluids*, vol. 28, no. 10, pp. 3127–3135, 1985. [Online]. Available: https://aip.scitation.org/doi/abs/10.1063/1.865354

[59] Y. Hamada, Y. Suzuki, K. Ohasa, M. Fujiwara, and K. Miyamoto, "Study of helical plasma equilibria," *Plasma Physics*, vol. 18, no. 12, pp. 889–896, dec 1976. [Online]. Available: https://doi.org/10.1088%2F0032-1028%2F18%2F12%2F002

[60] H. Gardner, R. Dewar, and W.-C. Sy, "The free-boundary equilibrium problem for helically symmetric plasmas," *Journal of Computational Physics*, vol. 74, no. 2, pp. 477 – 487, 1988. [Online]. Available: http://www.sciencedirect.com/science/article/pii/0021999188900897

[61] M. Andersen and M. Brons, "Topology of helical fluid flow," *European Journal of Applied Mathematics*, vol. 25, no. 3, p. 375–396, 2014.

[62] M. Germano, "On the effect of torsion on a helical pipe flow," *Journal of Fluid Mechanics*, vol. 125, p. 1–8, 1982.

[63] M. Nobari and A. Malvandi, "Torsion and curvature effects on fluid flow in a helical annulus," *International Journal of Non-Linear Mechanics*, vol. 57, pp. 90 – 101, 2013. [Online]. Available: http://www.sciencedirect.com/science/article/pii/S0020746213001297

[64] D. G. Xie, "Torsion effect on secondary flow in a helical pipe," *International Journal of Heat and Fluid Flow*, vol. 11, no. 2, pp. 114 – 119, 1990. [Online]. Available: http://www.sciencedirect.com/science/article/pii/0142727X9090004U

[65] K. Yamamoto, S. Yanase, and T. Yoshida, "Torsion effect on the flow in a helical pipe," *Fluid Dynamics Research*, vol. 14, no. 5, pp. 259 – 273, 1994. [Online]. Available: http://www.sciencedirect.com/science/article/pii/0169598394900353

[66] M. Vasudevaiah and R. Ratturaj, "Effect of torsion in a helical pipe flow," *International Journal of Mathematics and Mathematical Sciences*, vol. 17, pp. 553 – 560, 1993. [Online]. Available: https://www.hindawi.com/journals/ijmms/1994/802837/

[67] W. D'haeseleer, W. Hitchon, J. Callen, and J. Shohet, *Flux Coordinates and Magnetic Field Structure: A Guide to a Fundamental Tool of Plasma Theory*, ser. Scientific Computation. Springer-Verlag Berlin Heidelberg, 1991.

[68] H. Grad and H. Rubin, "Hydromagnetic equilibria and force-free fields," in *Proceedings of the 2nd UN Conf. on the Peaceful Uses of Atomic Energy, Vol. 31*, Geneva: IAEA, 1958, p. 190.

[69] V. D. Shafranov, *Plasma equilibrium in a magnetic field*, ser. Reviews of Plasma Physics, Vol. 2. Consultants Bureau, 1966.

[70] L. S. Solovev, "The theory of hydromagnetic stability of toroidal plasma configurations," *Journal of Experimental and Theoretical Physics*, vol. 53, no. 2, p. 626, 1968. [Online]. Available: http://www.jetp.ac.ru/cgi-bin/e/index/e/26/2/p400?a=list

[71] F. Hernegger, in *E. Canobbio et al., Proceedings of the 5th Conference on Control. Fusion, Vol. I Commissariat a l' Energie Atomique*, Grenoble, 1972, p. 26.

[72] E. K. Maschke, "Exact solutions of the MHD equilibrium equation for a toroidal plasma," *Plasma Physics*, vol. 15, no. 6, pp. 535–541, jun 1973. [Online]. Available: https://doi.org/10.1088%2F0032-1028%2F15%2F6%2F006

[73] O. I. Bogoyavlenskij, "MHD model of astrophysical jets," *Physics Letters A*, vol. 276, no. 5, pp. 257 – 266, 2000. [Online]. Available: http://www.sciencedirect.com/science/article/pii/S0375960100006289

[74] O. I. Bogoyavlenskij, "Astrophysical jets as exact plasma equilibria," *Phys. Rev. Lett.*, vol. 84, pp. 1914–1917, Feb 2000. [Online]. Available: https://link.aps.org/doi/10.1103/PhysRevLett.84.1914

[75] J. L. Johnson, C. R. Oberman, R. M. Kulsrud, and E. A. Frieman, "Some stable hydromagnetic equilibria," *The Physics of Fluids*, vol. 1, no. 4, pp. 281–296, 1958. [Online]. Available: https://aip.scitation.org/doi/abs/10.1063/1.1705886

[76] D. Correa and D. Lortz, "A class of helically symmetric MHD-equilibria," *Nuclear Fusion*, vol. 13, no. 1, pp. 127–129, jan 1973. [Online]. Available: https://doi.org/10.1088%2F0029-5515%2F13%2F1%2F016

[77] D. Correa, "Untersuchungen der Stabilitat von magnetohydrodynamischen Gleichgewichten mit helikaler Symmetrie." Ph.D. dissertation, Max-Planck-Institute fur Plasmaphysik, Garching, 1973.

[78] D. R. Smith and A. H. Reiman, "Analytic, high beta solutions of the helical Grad–Shafranov equation," *Physics of Plasmas*, vol. 11, no. 8, pp. 3752–3757, 2004. [Online]. Available: https://doi.org/10.1063/1.1763576

[79] K. Ohasa, Y. Hamada, M. Fujiwara, and K. Miyamoto, "Helically symmetric equilibrium of current-carrying finite beta plasma," *Japanese Journal of Applied Physics*, vol. 16, no. 4, pp. 617–621, apr 1977. [Online]. Available: https://doi.org/10.1143%2Fjjap.16.617

[80] G. Cattanei *et al.*, "Neutral-Injection Heating in the Wendelstein VII-A Stellarator," in *Proceedings of the 9th International Conference on Plasma Physics and Controlled Fusion, Vol. 2*, Baltimore, IAEA, 1982, p. 241.

[81] F. Wagner, "A quarter-century of H-mode studies," *Plasma Physics and Controlled Fusion*, vol. 49, no. 12B, pp. B1–B33, nov 2007. [Online]. Available: https://doi.org/10.1088%2F0741-3335%2F49%2F12b%2Fs01

[82] R. C. Wolf, "Internal transport barriers in tokamak plasmas," *Plasma Physics and Controlled Fusion*, vol. 45, no. 1, pp. R1–R91, nov 2002. [Online]. Available: https://doi.org/10.1088%2F0741-3335%2F45%2F1%2F201

[83] P. H. Diamond, S.-I. Itoh, K. Itoh, and T. S. Hahm, "Zonal flows in plasma—a review," *Plasma Physics and Controlled Fusion*, vol. 47, no. 5, pp. R35–R161, apr 2005. [Online]. Available: https://doi.org/10.1088%2F0741-3335%2F47%2F5%2Fr01

[84] C. D. Challis, "The use of internal transport barriers in tokamak plasmas," *Plasma Physics and Controlled Fusion*, vol. 46, no. 12B, pp. B23–B40, nov 2004. [Online]. Available: https://doi.org/10.1088%2F0741-3335%2F46%2F12b%2F003

[85] K. G. McClements and M. J. Hole, "On steady poloidal and toroidal flows in tokamak plasmas," *Physics of Plasmas*, vol. 17, no. 8, p. 082509, 2010. [Online]. Available: https://doi.org/10.1063/1.3469580

[86] A. Fasoli, C. Gormenzano, H. Berk, B. Breizman, S. Briguglio, D. Darrow, N. Gorelenkov, W. Heidbrink, A. Jaun, S. Konovalov, R. Nazikian, J.-M. Noterdaeme, S. Sharapov, K. Shinohara, D. Testa, K. Tobita, Y. Todo, G. Vlad, and F. Zonca, "Chapter 5: Physics of energetic ions," *Nuclear Fusion*, vol. 47, no. 6, pp. S264–S284, jun 2007. [Online]. Available: https://doi.org/10.1088%2F0029-5515%2F47%2F6%2Fs05

[87] G. Cottrell and D. Start, "A large-orbit model of fast ion slowing down during ICRH: Comparison with JET data," *Nuclear Fusion*, vol. 31, no. 1, pp. 61–71, jan 1991. [Online]. Available: https://doi.org/10.1088%2F0029-5515%2F31%2F1%2F006

[88] H. Yamada, K. Ida, H. Iguchi, S. Morita, O. Kaneko, H. Arimoto, M. Hosokawa, H. Idei, S. Kubo, K. Matsuoka, K. Nishimura, S. Okamura, Y. Takeiri, Y. Takita, C. Takahashi, K. Hanatani, H. Howe, S. Hirshman, and D. Lee, "Shafranov shift in the low aspect ratio heliotron/torsatron Compact Helical System," *Nuclear Fusion*, vol. 32, no. 1, pp. 25–32, jan 1992. [Online]. Available: https://doi.org/10.1088%2F0029-5515%2F32%2F1%2Fi03

[89] T. Yamaguchi, K. Watanabe, S. Sakakibara, Y. Narushima, K. Narihara, T. Tokuzawa, K. Tanaka, I. Yamada, M. Osakabe, H. Yamada, K. Kawahata, K. Yamazaki, and L. E. Group, "Measurement of anisotropic pressure using magnetic measurements in LHD," *Nuclear Fusion*, vol. 45, no. 11, pp. L33–L36, oct 2005. [Online]. Available: https://doi.org/10.1088%2F0029-5515%2F45%2F11%2Fl01

[90] K. Y. Watanabe, Y. Suzuki, S. Sakakibara, T. Yamaguchi, Y. Narushima, Y. Nakamura, K. Ida, N. Nakajima, H. Yamada, and L. E. Group, "Characteristics of MHD Equilibrium and Related Issues on LHD," *Fusion Science and Technology*, vol. 58, no. 1, pp. 160–175, 2010. [Online]. Available: https://doi.org/10.13182/FST10-A10803

[91] S. Cowley, "The effect of pressure anisotropy on the equilibrium structure of magnetic current sheets," *Planetary and Space Science*, vol. 26, no. 11, pp. 1037 – 1061, 1978. [Online]. Available: http://www.sciencedirect.com/science/article/pii/0032063378900284

[92] A. Nötzel, K. Schindler, and J. Birn, "On the cause of approximate pressure isotropy in the quiet near-earth plasma sheet," *Journal of Geophysical Research: Space Physics*, vol. 90, no. A9, pp. 8293–8300, 1985. [Online]. Available: https://agupubs.onlinelibrary.wiley.com/doi/abs/10.1029/JA090iA09p08293

[93] M. Hesse and J. Birn, "MHD modeling of magnetotail instability for anisotropic pressure," *Journal of Geophysical Research: Space Physics*, vol. 97, no. A7, pp. 10 643–10 654, 1992. [Online]. Available: https://agupubs.onlinelibrary.wiley.com/doi/abs/10.1029/92JA00793

[94] L. N. Hau, "Anisotropic magnetotail equilibrium and convection," *Geophysical Research Letters*, vol. 20, no. 7, pp. 555–558, 1993. [Online]. Available: https://agupubs.onlinelibrary.wiley.com/doi/abs/10.1029/93GL00243

[95] V. S. Beskin and I. V. Kuznetsova, "Grad-Shafranov equation with anisotropic pressure," *The Astrophysical Journal*, vol. 541, no. 1, pp. 257–260, sep 2000. [Online]. Available: https://doi.org/10.1086%2F309438

[96] I. V. Kuznetsova, "Relativistic Grad-Shafranov equation with anisotropic pressure," *The Astrophysical Journal*, vol. 618, no. 1, pp. 432–437, jan 2005. [Online]. Available: https://doi.org/10.1086%2F425065

[97] C. Z. Cheng, "Magnetospheric equilibrium with anisotropic pressure," *Journal of Geophysical Research: Space Physics*, vol. 97, no. A2, pp. 1497–1510, 1992. [Online]. Available: https://agupubs.onlinelibrary.wiley.com/doi/abs/10.1029/91JA02433

[98] S. I. Krasheninnikov and P. J. Catto, "Effects of pressure anisotropy on plasma equilibrium in the magnetic field of a point dipole," *Physics of Plasmas*, vol. 7, no. 2, pp. 626–628, 2000. [Online]. Available: https://doi.org/10.1063/1.873848

[99] S. Zaharia and C. Z. Cheng, "Can an isotropic plasma pressure distribution be in force balance with the t96 model field?" *Journal of Geophysical Research: Space Physics*, vol. 108, no. A11, 2003. [Online]. Available: https://agupubs.onlinelibrary.wiley.com/doi/abs/10.1029/2002JA009501

[100] L. Wu, F. Toffoletto, R. A. Wolf, and C. Lemon, "Computing magnetospheric equilibria with anisotropic pressures," *Journal of Geophysical Research: Space Physics*, vol. 114, no. A5, 2009. [Online]. Available: https://agupubs.onlinelibrary.wiley.com/doi/abs/10.1029/2008JA013556

[101] I. Calvo, F. I. Parra, J. L. Velasco, and J. M. García-Regaña, "Impact of main ion pressure anisotropy on stellarator impurity transport," *Nuclear Fusion*, vol. 60, no. 1, p. 016035, dec 2019. [Online]. Available: https://doi.org/10.1088%2F1741-4326%2Fab581f

[102] V. D. Pustovitov, "Anisotropic pressure effects on plasma equilibrium in toroidal systems," *Plasma Physics and Controlled Fusion*, vol. 52, no. 6, p. 065001, apr 2010. [Online]. Available: https://doi.org/10.1088%2F0741-3335%2F52%2F6%2F065001

[103] R. Iacono, A. Bondeson, F. Troyon, and R. Gruber, "Axisymmetric toroidal equilibrium with flow and anisotropic pressure," *Physics of Fluids B: Plasma Physics*, vol. 2, no. 8, pp. 1794–1803, 1990. [Online]. Available: https://doi.org/10.1063/1.859451

[104] V. I. Ilgisonis, "Anisotropic plasma with flows in tokamak: Steady state and stability," *Physics of Plasmas*, vol. 3, no. 12, pp. 4577–4582, 1996. [Online]. Available: https://doi.org/10.1063/1.872074

[105] Z. S. Qu, M. Fitzgerald, and M. J. Hole, "Analysing the impact of anisotropy pressure on tokamak equilibria," *Plasma Physics and Controlled Fusion*, vol. 56, no. 7, p. 075007, may 2014. [Online]. Available: https://doi.org/10.1088%2F0741-3335%2F56%2F7%2F075007

[106] N. D. Lepikhin and V. D. Pustovitov, "Analytical modeling of equilibrium of strongly anisotropic plasma in tokamaks and stellarators," *Plasma Physics Reports*, vol. 39, pp. 605–614, 2013. [Online]. Available: https://link.springer.com/article/10.1134/S1063780X13080059

[107] A. A. Ivanov, A. A. Martynov, S. Y. Medvedev, and Y. Y. Poshekhonov, "Tokamak plasma equilibrium problems with anisotropic pressure and rotation and their numerical solution," *Plasma Physics Reports*, vol. 41, no. 3, pp. 203–211, 2015. [Online]. Available: https://link.springer.com/article/10.1134/S1063780X15030046

[108] W. Hitchon, "Anisotropic pressure equilibrium in a toroidal stellarator," *Nuclear Fusion*, vol. 23, no. 3, pp. 383–386, mar 1983. [Online]. Available: https://doi.org/10.1088%2F0029-5515%2F23%2F3%2F009

[109] N. Madden and R. Hastie, "Tokamak equilibrium with anisotropic pressure," *Nuclear Fusion*, vol. 34, no. 4, pp. 519–526, apr 1994. [Online]. Available: https://doi.org/10.1088%2F0029-5515%2F34%2F4%2Fi05

[110] E. R. Salberta, R. C. Grimm, J. L. Johnson, J. Manickam, and W. M. Tang, "Anisotropic pressure tokamak equilibrium and stability considerations," *The Physics of Fluids*, vol. 30, no. 9, pp. 2796–2805, 1987. [Online]. Available: https://aip.scitation.org/doi/abs/10.1063/1.866505

[111] J. W. Connor and R. J. Hastie, "Effect of anisotropic pressure on the localized magnetohydrodynamic interchange modes in an axisymmetric torus," *The Physics of Fluids*, vol. 19, no. 11, pp. 1727–1732, 1976. [Online]. Available: https://aip.scitation.org/doi/abs/10.1063/1.861389

[112] Y. Asahi, Y. Suzuki, K. Watanabe, and W. A. Cooper, "MHD equilibrium analysis with anisotropic pressure in LHD," *Plasma and Fusion Research*, vol. 6, pp. 2 403 123–2 403 123, 2011.

[113] A. Sestero and A. Taroni, "Numerical computation of toroidal equilibria with anisotropic pressure in the presence of a dominant vacuum toroidal field," *Nuclear Fusion*, vol. 16, pp. 164–167, Feb 1976.

[114] A. Evangelias and G. N. Throumoulopoulos, "Axisymmetric equilibria with pressure anisotropy and plasma flow," *Plasma Physics and Controlled Fusion*, vol. 58, no. 4, p. 045022, feb 2016. [Online]. Available: https://doi.org/10.1088%2F0741-3335%2F58%2F4%2F045022

[115] G. N. Throumoulopoulos and H. Tasso, "Ideal magnetohydrodynamic equilibria with helical symmetry and incompressible flows," *Journal of Plasma Physics*, vol. 62, no. 4, p. 449–459, 1999.

[116] A. Kuiroukidis, A. Evangelias, and G. N. Throumoulopoulos, "Analytic axisymmetric equilibria with pressure anisotropy and non-parallel flow," *Plasma Physics and Controlled Fusion*, vol. 59, no. 10, p. 102001, aug 2017. [Online]. Available: https://doi.org/10.1088%2F1361-6587%2Faa7c8d

[117] H. Tasso and G. N. Throumoulopoulos, "Axisymmetric ideal magnetohydrodynamic equilibria with incompressible flows," *Physics of Plasmas*, vol. 5, no. 6, pp. 2378–2383, 1998. [Online]. Available: https://doi.org/10.1063/1.872912

[118] G. N. Throumoulopoulos and H. Tasso, "Cylindrical ideal magnetohydrodynamic equilibria with incompressible flows," *Physics of Plasmas*, vol. 4, no. 5, pp. 1492–1494, 1997. [Online]. Available: https://doi.org/10.1063/1.872322

[119] G. N. Throumoulopoulos and H. Tasso, "Axisymmetric equilibria of a gravitating plasma with incompressible flows," *Geophysical & Astrophysical Fluid Dynamics*, vol. 94, no. 3-4, pp. 249–262, 2001. [Online]. Available: https://doi.org/10.1080/03091920108203409

[120] L. J. Palumbo and A. M. Platzeck, "Magnetically confined plasma flows with helical symmetry," *Journal of Plasma Physics*, vol. 60, no. 3, p. 449–467, 1998.

[121] Y. Z. Agim and J. A. Tataronis, "General two-dimensional magnetohydrodynamic equilibria with mass flow," *Journal of Plasma Physics*, vol. 34, no. 3, p. 337–360, 1985.

[122] J. Hodgson and T. Neukirch, "On the theory of translationally invariant magnetohydrodynamic equilibria with anisotropic pressure and magnetic shear," *Geophysical & Astrophysical Fluid Dynamics*, vol. 109, no. 5, pp. 524–537, 2015. [Online]. Available: https://doi.org/10.1080/03091929.2015.1081188

[123] A. Sestero and A. Taroni, "Large aspect ratio expansion of toroidal magnetofluid equilibria with anisotropic pressure," *Nuovo Cimento Lettere*, vol. 20, pp. 537–545, Dec 1977.

[124] C. Mercier and M. Cotsaftis, "Equilibrium and stability of an axially symmetric plasma with anisotropic pressure," *Nuclear Fusion*, vol. 1, no. 2, pp. 121–124, mar 1961. [Online]. Available: https://doi.org/10.1088%2F0029-5515%2F1%2F2%2F005

[125] R. Clemente, "Anisotropic axisymmetric equilibria via an analytic method," *Nuclear Fusion*, vol. 33, no. 6, pp. 963–965, jun 1993. [Online]. Available: https://doi.org/10.1088%2F0029-5515%2F33%2F6%2Fi12

[126] R. A. Clemente, "A method for obtaining rotating anisotropic toroidal equilibria," *Plasma Physics and Controlled Fusion*, vol. 36, no. 4, pp. 707–710, apr 1994. [Online]. Available: https://doi.org/10.1088%2F0741-3335%2F36%2F4%2F011

[127] R. A. Clemente and R. L. Viana, "On axisymmetric double adiabatic MHD equilibria with plasma flow," *Plasma Physics and Controlled Fusion*, vol. 41, no. 4, pp. 567–573, jan 1999. [Online]. Available: https://doi.org/10.1088%2F0741-3335%2F41%2F4%2F008

[128] R. A. Clemente and D. Sterzo, "Anisotropic ideal magnetohydrodynamic cylindrical equilibria with incompressible adiabatic flow," *Plasma Physics and Controlled Fusion*, vol. 51, no. 8, p. 085011, jul 2009. [Online]. Available: https://doi.org/10.1088%2F0741-3335%2F51%2F8%2F085011

[129] W. Zwingmann, L.-G. Eriksson, and P. Stubberfield, "Equilibrium analysis of tokamak discharges with anisotropic pressure," *Plasma Physics and Controlled Fusion*, vol. 43, no. 11, pp. 1441–1456, oct 2001. [Online]. Available: https://doi.org/10.1088%2F0741-3335%2F43%2F11%2F302

[130] L. Guazzotto, R. Betti, J. Manickam, and S. Kaye, "Numerical study of tokamak equilibria with arbitrary flow," *Physics of Plasmas*, vol. 11, no. 2, pp. 604–614, 2004. [Online]. Available: https://doi.org/10.1063/1.1637918

[131] T. Andreussi, P. J. Morrison, and F. Pegoraro, "MHD equilibrium variational principles with symmetry," *Plasma Physics and Controlled Fusion*, vol. 52, no. 5, p. 055001, mar 2010. [Online]. Available: https://doi.org/10.1088%2F0741-3335%2F52%2F5%2F055001

[132] T. Andreussi, P. J. Morrison, and F. Pegoraro, "Hamiltonian magnetohydrodynamics: Helically symmetric formulation, casimir invariants, and equilibrium variational principles," *Physics of Plasmas*, vol. 19, no. 5, p. 052102, 2012. [Online]. Available: https://doi.org/10.1063/1.4714761

[133] V. D. Pustovitov, "Extension of conventional mhd equilibrium theory to model the fast particle effects," *AIP Conference Proceedings*, vol. 1478, no. 1, pp. 50–64, 2012. [Online]. Available: https://aip.scitation.org/doi/abs/10.1063/1.4751639

[134] M. Fitzgerald, L. Appel, and M. Hole, "EFIT tokamak equilibria with toroidal flow and anisotropic pressure using the two-temperature guiding-centre plasma," *Nuclear Fusion*, vol. 53, no. 11, p. 113040, oct 2013. [Online]. Available: https://doi.org/10.1088%2F0029-5515%2F53%2F11%2F113040

[135] K. C. Tsinganos, "Magnetohydrodynamic equilibrium. iii - helically symmetric fields," *Astrophysical Journal*, vol. 259, pp. 820–831, aug 1982. [Online]. Available: http://adsabs.harvard.edu/full/1982ApJ...259..820T

[136] M. Villata and A. Ferrari, "Exact solutions for helical magnetohydrodynamic equilibria. ii. nonstatic and nonbarotropic solutions," *Physics of Plasmas*, vol. 1, no. 7, pp. 2200–2206, 1994. [Online]. Available: https://doi.org/10.1063/1.870619

[137] M. Villata and K. Tsinganos, "Exact solutions for helical magnetohydrodynamic equilibria," *Physics of Fluids B: Plasma Physics*, vol. 5, no. 7, pp. 2153–2164, 1993. [Online]. Available: https://doi.org/10.1063/1.860750

[138] S. T. da Silva, F. F. de Carvalho, P. T. E. Marroquin, and R. L. Viana, "Adiabatic plasma rotations and symmetric magnetohydrodynamical stationary equilibria: analytical and semi-numerical solutions," *Journal of Physics Communications*, vol. 2, no. 3, p. 035011, mar 2018. [Online]. Available: https://doi.org/10.1088%2F2399-6528%2Faab10a

[139] E. Hameiri, "The equilibrium and stability of rotating plasmas," *The Physics of Fluids*, vol. 26, no. 1, pp. 230–237, 1983. [Online]. Available: https://aip.scitation.org/doi/abs/10.1063/1.864012

[140] A. I. Morozov and L. S. Solovev, *In:Leontovich M.A. (eds) Reviews of Plasma Physics*. Boston, MA: Springer, 1980, ch. Steady-State Plasma Flow in a Magnetic Field, pp. 1–103.

[141] R. Courant and D. Hilbert, *Methods of Mathematical Physics, Vol. 2*. Interscience Publishers, 1966.

[142] E. A. Kuznetsov, T. Passot, V. P. Ruban, and P. L. Sulem, "Variational approach for static mirror structures," *Physics of Plasmas*, vol. 22, no. 4, p. 042114, 2015. [Online]. Available: https://doi.org/10.1063/1.4919027

[143] M. Furukawa, "Effects of pressure anisotropy on magnetospheric magnetohydrodynamics equilibrium of an internal ring current system," *Physics of Plasmas*, vol. 21, no. 1, p. 012511, 2014. [Online]. Available: https://doi.org/10.1063/1.4862037

[144] J. W. Edenstrasser, "Stability criterion for symmetric mhd equilibria by minimizing the potential energy," *Journal of Plasma Physics*, vol. 20, no. 3, p. 503–520, 1978.

[145] E. Frieman and M. Rotenberg, "On hydromagnetic stability of stationary equilibria," *Rev. Mod. Phys.*, vol. 32, pp. 898–902, Oct 1960. [Online]. Available: https://link.aps.org/doi/10.1103/RevModPhys.32.898

[146] E. Hameiri, "Variational principles for equilibrium states with plasma flow," *Physics of Plasmas*, vol. 5, no. 9, pp. 3270–3281, 1998. [Online]. Available: https://doi.org/10.1063/1.872995

[147] V. A. Vladimirov and K. I. Ilin, "The three-dimensional stability of steady magnetohydrodynamic flows of an ideal fluid," *Physics of Plasmas*, vol. 5, no. 12, pp. 4199–4204, 1998. [Online]. Available: https://doi.org/10.1063/1.873154

[148] K. I. Ilin and V. A. Vladimirov, "Energy principle for magnetohydrodynamic flows and Bogoyavlenskij's transformation," *Physics of Plasmas*, vol. 11, no. 7, pp. 3586–3594, 2004. [Online]. Available: https://doi.org/10.1063/1.1759337

[149] G. N. Throumoulopoulos and H. Tasso, "A sufficient condition for the linear stability of magnetohydrodynamic equilibria with field aligned incompressible flows," *Physics of Plasmas*, vol. 14, no. 12, p. 122104, 2007. [Online]. Available: https://doi.org/10.1063/1.2817957

[150] D. J. Southwood and M. G. Kivelson, "Mirror instability: 1. Physical mechanism of linear instability," *Journal of Geophysical Research: Space Physics*, vol. 98, no. A6, pp. 9181–9187, 1993. [Online]. Available: https://agupubs.onlinelibrary.wiley.com/doi/abs/10.1029/92JA02837

[151] B. J. Wang and L. N. Hau, "MHD aspects of fire-hose type instabilities," *Journal of Geophysical Research: Space Physics*, vol. 108, no. A12, 2003. [Online]. Available: https://agupubs.onlinelibrary.wiley.com/doi/abs/10.1029/2003JA009986

[152] L.-N. Hau and B.-J. Wang, "On MHD waves, fire-hose and mirror instabilities in anisotropic plasmas," *Nonlinear Processes in Geophysics*, vol. 14, no. 5, pp. 557–568, Sep. 2007. [Online]. Available: https://hal.archives-ouvertes.fr/hal-00302903

[153] A. F. Cheviakov and O. I. Bogoyavlenskij, "Exact anisotropic MHD equilibria," *Journal of Physics A: Mathematical and General*, vol. 37, no. 30, pp. 7593–7607, jul 2004. [Online]. Available: https://doi.org/10.1088%2F0305-4470%2F37%2F30%2F014

[154] A. A. Schekochihin, S. C. Cowley, F. Rincon, and M. S. Rosin, "Magnetofluid dynamics of magnetized cosmic plasma: firehose and gyrothermal instabilities," *Monthly Notices of the Royal Astronomical Society*, vol. 405, no. 1, pp. 291–300, 06 2010. [Online]. Available: https://doi.org/10.1111/j.1365-2966.2010.16493.x

[155] P. Hellinger, "Comment on the linear mirror instability near the threshold," *Physics of Plasmas*, vol. 14, no. 8, p. 082105, 2007. [Online]. Available: https://doi.org/10.1063/1.2768318

[156] R. L. Miller, "Hot electron stabilization of a helically symmetric plasma," *The Physics of Fluids*, vol. 29, no. 4, pp. 1176–1180, 1986. [Online]. Available: https://aip.scitation.org/doi/abs/10.1063/1.865865

[157] W. A. Cooper, S. P. Hirshman, and M. C. Depassier, "Inverse moments equilibria for helical anisotropic systems," *The Physics of Fluids*, vol. 30, no. 11, pp. 3532–3539, 1987. [Online]. Available: https://aip.scitation.org/doi/abs/10.1063/1.866435

[158] S. Hirshman, W. van RIJ, and P. Merkel, "Three-dimensional free boundary calculations using a spectral Green's function method," *Computer Physics Communications*, vol. 43, no. 1, pp. 143 – 155, 1986. [Online]. Available: http://www.sciencedirect.com/science/article/pii/0010465586900585

[159] R. Wilcox, J. Talmadge, D. Anderson, F. Anderson, and J. Lore, "Intrinsic plasma rotation and reynolds stress at the plasma edge in the HSX stellarator," *Nuclear Fusion*, vol. 56, no. 3, p. 036002, feb 2016. [Online]. Available: https://doi.org/10.1088%2F0029-5515%2F56%2F3%2F036002

[160] W. Cooper, J. Graves, S. Hirshman, T. Yamaguchi, Y. Narushima, S. Okamura, S. Sakakibara, C. Suzuki, K. Watanabe, H. Yamada, and K. Yamazaki, "Anisotropic pressure bi-maxwellian distribution function model for three-dimensional equilibria," *Nuclear Fusion*, vol. 46, no. 7, pp. 683–698, may 2006. [Online]. Available: https://doi.org/10.1088%2F0029-5515%2F46%2F7%2F001

[161] W. A. Cooper, J. P. Graves, M. Jucker, K. Y. Watanabe, Y. Narushima, and T. Yamaguchi, "Fluid magnetohydrodynamic stability in a heliotron with anisotropic fast particle species," *Plasma Physics and Controlled Fusion*, vol. 49, no. 8, pp. 1177–1191, jul 2007. [Online]. Available: https://doi.org/10.1088%2F0741-3335%2F49%2F8%2F006

[162] J. M. Faustin, W. A. Cooper, J. P. Graves, and D. Pfefferlé, "Modeling of ion-cyclotron resonant heating in Wendelstein 7-X equilibrium," *Journal of Physics: Conference Series*, vol. 561, p. 012006, nov 2014. [Online]. Available: https://doi.org/10.1088%2F1742-6596%2F561%2F1%2F012006

[163] S. Hirshman and O. Betancourt, "Preconditioned descent algorithm for rapid calculations of magnetohydrodynamic equilibria," *Journal of Computational Physics*, vol. 96, no. 1, pp. 99 – 109, 1991. [Online]. Available: http://www.sciencedirect.com/science/article/pii/002199919190267O

[164] W. Cooper, S. Hirshman, P. Merkel, J. Graves, J. Kisslinger, H. Wobig, Y. Narushima, S. Okamura, and K. Watanabe, "Three-dimensional anisotropic pressure free boundary equilibria," *Computer Physics Communications*, vol. 180, no. 9, pp. 1524 – 1533, 2009. [Online]. Available: http://www.sciencedirect.com/science/article/pii/S0010465509001179

[165] A. Evangelias, A. Kuiroukidis, and G. N. Throumoulopoulos, "Helically symmetric equilibria with pressure anisotropy and incompressible plasma flow," *Plasma Physics and Controlled Fusion*, vol. 60, no. 2, p. 025005, dec 2017. [Online]. Available: https://doi.org/10.1088%2F1361-6587%2Faa93a7

[166] A. Evangelias *et al.*, "Certain developments on the equilibrium of magnetized plasmas," in *Proceedings of the 45th EPS Conference on Plasma Physics, Vol. 42A*, Prague, ECA, July 2018, p. P1.1048.

[167] G. Throumoulopoulos, D. Kaltsas, A. Evangelias, and A. Kuiroukidis, "Special ideal MHD equilibria with incompressible flow," *Physics Letters A*, vol. 382, no. 5, pp. 321 – 326, 2018. [Online]. Available: http://www.sciencedirect.com/science/article/pii/S0375960117311519

[168] A. Evangelias and G. N. Throumoulopoulos, "Symmetry transformations for magnetohydrodynamics and Chew–Goldberger–Low equilibria revisited," *Plasma Science and Technology*, vol. 21, no. 9, p. 095102, jul 2019. [Online]. Available: https://doi.org/10.1088%2F2058-6272%2Fab2136

[169] A. Evangelias and G. N. Throumoulopoulos, "On the linear stability of anisotropic pressure equilibria with field-aligned incompressible flow," *Journal of Plasma Physics*, vol. 86, no. 3, p. 905860312, 2020.

[170] J. P. Goedbloed and A. Lifschitz, "Stationary symmetric magnetohydrodynamic flows," *Physics of Plasmas*, vol. 4, no. 10, pp. 3544–3564, 1997. [Online]. Available: https://doi.org/10.1063/1.872251

[171] J.-Y. Shiraishi, S. Ohsaki, and Z. Yoshida, "Regularization of the Alfvén singularity by the Hall effect," *Physics of Plasmas*, vol. 12, no. 9, p. 092308, 2005. [Online]. Available: https://doi.org/10.1063/1.2042948

[172] K. Elsässer and A. Heimsoth, "Axisymmetric plasma equilibria with incompressible flow," *Zeitschrift für Naturforschung A*, vol. 41, no. 7, 1986.

[173] V. P. Lakhin and E. A. Sorokina, "Low-Frequency Continuous MHD Spectrum of Toroidally Rotating Tokamak Plasmas with Anisotropic Pressure," *Plasma Physics Reports*, vol. 45, no. 3, pp. 179–194, 2019. [Online]. Available: https://link.springer.com/article/10.1134/S1063780X19020065

[174] C. Simintzis, G. N. Throumoulopoulos, G. Pantis, and H. Tasso, "Analytic magnetohydrodynamic equilibria of a magnetically confined plasma with sheared flows," *Physics of Plasmas*, vol. 8, no. 6, pp. 2641–2648, 2001. [Online]. Available: https://doi.org/10.1063/1.1371768

[175] G. N. Throumoulopoulos and H. Tasso, "Cylindrical ideal magnetohydrodynamic equilibria with incompressible flows," *Physics of Plasmas*, vol. 4, no. 5, pp. 1492–1494, 1997. [Online]. Available: https://doi.org/10.1063/1.872322

[176] T. H. Stix, "Magnetic braiding in a toroidal plasma," *Phys. Rev. Lett.*, vol. 30, pp. 833–835, Apr 1973. [Online]. Available: https://link.aps.org/doi/10.1103/PhysRevLett.30.833

[177] G. Miller and L. Turner, "Force free equilibria in toroidal geometry," *The Physics of Fluids*, vol. 24, no. 2, pp. 363–365, 1981. [Online]. Available: https://aip.scitation.org/doi/abs/10.1063/1.863351

[178] P. Barberio-Corsetti, "Force-free helical equilibria," *Plasma Physics*, vol. 15, no. 11, pp. 1131–1139, nov 1973. [Online]. Available: https://doi.org/10.1088%2F0032-1028%2F15%2F11%2F007

[179] A. A. Martynov and S. Y. Medvedev, "Analytic examples of force-free toroidal MHD equilibria," *Plasma Physics Reports*, vol. 28, pp. 259–267, 2002. [Online]. Available: https://link.springer.com/article/10.1134/1.1469166

[180] D. Lortz, W. Lotz, and J. Nührenberg, "Three-dimensional analytical force-free MHD equilibria," *Zeitschrift für Naturforschung A*, vol. 36, pp. 144–149, 2014. [Online]. Available: https://www.degruyter.com/view/j/zna.1981.36.issue-2/zna-1981-0206/zna-1981-0206.xml

[181] R. Paccagnella and L. Guazzotto, "Analytical and numerical solutions of force-free equilibria with flow," *Plasma Physics and Controlled Fusion*, vol. 53, no. 9, p. 095013, aug 2011. [Online]. Available: https://doi.org/10.1088%2F0741-3335%2F53%2F9%2F095013

[182] D. G. Dritschel, "Generalized helical beltrami flows in hydrodynamics and magnetohydrodynamics," *Journal of Fluid Mechanics*, vol. 222, p. 525–541, 1991.

[183] F. Qingzeng, "On force-free magnetic fields and beltrami flows," *Applied Mathematics and Mechanics*, vol. 18, pp. 997–1002, 1997. [Online]. Available: https://link.springer.com/article/10.1007/BF00189291

[184] Z. Yoshida, S. M. Mahajan, S. Ohsaki, M. Iqbal, and N. Shatashvili, "Beltrami fields in plasmas: High-confinement mode boundary layers and high beta equilibria," *Physics of Plasmas*, vol. 8, no. 5, pp. 2125–2131, 2001. [Online]. Available: https://doi.org/10.1063/1.1354149

[185] Z. Yoshida, S. Ohsaki, A. Ito, and S. M. Mahajan, "Stability of beltrami flows," *Journal of Mathematical Physics*, vol. 44, no. 5, pp. 2168–2178, 2003. [Online]. Available: https://doi.org/10.1063/1.1567798

[186] R. González, A. Costa, and E. S. Santini, "On a variational principle for beltrami flows," *Physics of Fluids*, vol. 22, no. 7, p. 074102, 2010. [Online]. Available: https://doi.org/10.1063/1.3460297

[187] D. Palumbo, "Some considerations on closed configurations of magnetohydrostatic equilibrium," *Nuovo Cimento B*, vol. 53, pp. 507–511, Febr 1968. [Online]. Available: https://link.springer.com/article/10.1007/BF02710251

[188] C. M. Bishop and J. B. Taylor, "Degenerate toroidal magnetohydrodynamic equilibria and minimum b," *The Physics of Fluids*, vol. 29, no. 4, pp. 1144–1148, 1986. [Online]. Available: https://aip.scitation.org/doi/abs/10.1063/1.865913

[189] D. Palumbo and M. Balzano, *Atti della accademia di scienze lettere earti di Palermo, serie quinta*, vol. IV, p. 497, anno accademico 1983-84, part prima: scienze.

[190] J. B. Taylor, "Relaxation of toroidal plasma and generation of reverse magnetic fields," *Phys. Rev. Lett.*, vol. 33, pp. 1139–1141, Nov 1974. [Online]. Available: https://link.aps.org/doi/10.1103/PhysRevLett.33.1139

[191] J. B. Taylor, "Relaxation revisited," *Physics of Plasmas*, vol. 7, no. 5, pp. 1623–1629, 2000. [Online]. Available: https://doi.org/10.1063/1.873984

[192] W. K. Schief, "Hidden integrability in ideal magnetohydrodynamics: The pohlmeyer–lund–regge model," *Physics of Plasmas*, vol. 10, no. 7, pp. 2677–2685, 2003. [Online]. Available: https://doi.org/10.1063/1.1577347

[193] G. N. Throumoulopoulos, H. Tasso, and G. Poulipoulis, "Side-conditioned axisymmetric equilibria with incompressible flows," *Journal of Plasma Physics*, vol. 74, no. 3, p. 327–344, 2008.

[194] J. W. Yokota, "Potential/complex-lamellar descriptions of incompressible viscous flow," *Physics of Fluids*, vol. 9, no. 8, pp. 2264–2272, 1997. [Online]. Available: https://doi.org/10.1063/1.869348

[195] X. Hu, Y. Huang, and Y. Zeng, "A method for exploring some new solutions of complex lamellar flow," *Communications in Nonlinear Science and Numerical Simulation*, vol. 5, no. 1, pp. 17 – 20, 2000. [Online]. Available: http://www.sciencedirect.com/science/article/pii/S1007570400900170

[196] I. Dimitriou, "Geometrical interpretations of continuous and complex-lamellar steady flows," *European Journal of Mechanics - B/Fluids*, vol. 61, pp. 86 – 99, 2017. [Online]. Available: http://www.sciencedirect.com/science/article/pii/S0997754615301485

[197] R. L. Panton, "Potential/complex-lamellar velocity decomposition and its relevance to turbulence," *Journal of Fluid Mechanics*, vol. 88, no. 1, p. 97–114, 1978.

[198] C. Mercier and H. Luc, "Lectures in plasma physics: The magnetohydrodynamic approach to the problem of plasma confinement in closed magnetic configurations," Commission of the European Communities, Tech. Rep., 1974.

[199] C. Mercier, "On a representation of toroidal surfaces. Applications to magnetohydrodynamic equilibria," *Nuclear Fusion*, vol. 3, no. 2, pp. 89–98, jun 1963. [Online]. Available: https://doi.org/10.1088%2F0029-5515%2F3%2F2%2F006

[200] L. S. Solovev and V. D. Shafranov, *Plasma Confinement in Closed Magnetic Systems. In:Leontovich M.A. (eds) Reviews of Plasma Physics*. Boston, MA: Springer, 1970, ch. Orthogonal coordinate system with spatial axis, pp. 28–37.

[201] T. Sunn Pedersen, A. Dinklage, Y. Turkin, R. Wolf, S. Bozhenkov, J. Geiger, G. Fuchert, H.-S. Bosch, K. Rahbarnia, H. Thomsen, U. Neuner, T. Klinger, A. Langenberg, H. Trimiño Mora, P. Kornejew, J. Knauer, M. Hirsch, and N. Pablant, "Key results from the first plasma operation phase and outlook for future performance in Wendelstein 7-X," *Physics of Plasmas*, vol. 24, no. 5, p. 055503, 2017. [Online]. Available: https://doi.org/10.1063/1.4983629

[202] J. P. Freidberg, *Ideal Magnetohydrodynamics.*, ser. Modern perspectives in energy. New York : Plenum Press, p 108, 1987.

[203] R. L. Miller, M. S. Chu, J. M. Greene, Y. R. Lin-Liu, and R. E. Waltz, "Noncircular, finite aspect ratio, local equilibrium model," *Physics of Plasmas*, vol. 5, no. 4, pp. 973–978, 1998. [Online]. Available: https://doi.org/10.1063/1.872666

[204] T. G. Collart and W. M. Stacey, "Improved analytical flux surface representation and calculation models for poloidal asymmetries," *Physics of Plasmas*, vol. 23, no. 5, p. 052505, 2016. [Online]. Available: https://doi.org/10.1063/1.4948552

[205] U. Stroth, M. Murakami, R. Dory, H. Yamada, S. Okamura, F. Sano, and T. Obiki, "Energy confinement scaling from the international stellarator database," *Nuclear Fusion*, vol. 36, no. 8, pp. 1063–1077, aug 1996. [Online]. Available: https://doi.org/10.1088%2F0029-5515%2F36%2F8%2Fi11

[206] S. P. Hirshman, D. A. Spong, J. C. Whitson, B. Nelson, D. B. Batchelor, J. F. Lyon, R. Sanchez, A. Brooks, G. Y.-Fu, R. J. Goldston, L.-P. Ku, D. A. Monticello, H. Mynick, G. H. Neilson, N. Pomphrey, M. Redi, W. Reiersen, A. H. Reiman, J. Schmidt, R. White, M. C. Zarnstorff, W. H. Miner, P. M. Valanju, and A. Boozer, "Physics of compact stellarators," *Physics of Plasmas*, vol. 6, no. 5, pp. 1858–1864, 1999. [Online]. Available: https://doi.org/10.1063/1.873489

[207] A. Kuiroukidis and G. Throumoulopoulos, "Tokamak equilibria with non-parallel flow in a triangularity-deformed axisymmetric toroidal coordinate system," *Heliyon*, vol. 4, no. 1, p. e00499, 2018. [Online]. Available: http://www.sciencedirect.com/science/article/pii/S2405844017315050

[208] M. Drevlak, D. Monticello, and A. Reiman, "PIES free boundary stellarator equilibria with improved initial conditions," *Nuclear Fusion*, vol. 45, no. 7, pp. 731–740, jul 2005. [Online]. Available: https://doi.org/10.1088%2F0029-5515%2F45%2F7%2F022

[209] O. I. Bogoyavlenskij, "Helically symmetric astrophysical jets," *Phys. Rev. E*, vol. 62, pp. 8616–8627, Dec 2000. [Online]. Available: https://link.aps.org/doi/10.1103/PhysRevE.62.8616

[210] M. Jucker, J. P. Graves, W. A. Cooper, and T. Johnson, "Ion cyclotron resonance heating with consistent finite orbit widths and anisotropic equilibria," *Plasma Physics and Controlled Fusion*, vol. 53, no. 5, p. 054010, apr 2011. [Online]. Available: https://doi.org/10.1088%2F0741-3335%2F53%2F5%2F054010

[211] B. Layden, M. J. Hole, and R. Ridden-Harper, "High-beta equilibria in tokamaks with pressure anisotropy and toroidal flow," *Physics of Plasmas*, vol. 22, no. 12, p. 122513, 2015. [Online]. Available: https://doi.org/10.1063/1.4939026

[212] K. Brau, M. Bitter, R. Goldston, D. Manos, K. McGuire, and S. Suckewer, "Plasma rotation in the PDX tokamak," *Nuclear Fusion*, vol. 23, no. 12, pp. 1643–1655, dec 1983. [Online]. Available: https://doi.org/10.1088%2F0029-5515%2F23%2F12%2F008

[213] G. N. Throumoulopoulos and G. Pantis, "Analytic axisymmetric magnetohydrodynamic equilibria of a plasma torus with toroidal mass flow," *Physics of Fluids B: Plasma Physics*, vol. 1, no. 9, pp. 1827–1833, 1989. [Online]. Available: https://doi.org/10.1063/1.858914

[214] D. J. Holly, S. C. Prager, M. W. Phillips, and J. C. Sprott, "Experimental observation of plasma paramagnetism in a tokamak," *The Physics of Fluids*, vol. 23, no. 2, pp. 417–418, 1980. [Online]. Available: https://aip.scitation.org/doi/abs/10.1063/1.862991

[215] A. F. Cheviakov, "Exact plasma equilibria from symmetries and transformations of MHD and CGL equilibrium equations," 2004.

[216] O. I. Bogoyavlenskij, "Symmetry transforms for ideal magnetohydrodynamics equilibria," *Phys. Rev. E*, vol. 66, p. 056410, Nov 2002. [Online]. Available: https://link.aps.org/doi/10.1103/PhysRevE.66.056410

[217] O. I. Bogoyavlenskij, "Infinite symmetries of the ideal MHD equilibrium equations," *Physics Letters A*, vol. 291, no. 4, pp. 256 – 264, 2001. [Online]. Available: http://www.sciencedirect.com/science/article/pii/S0375960101006508

[218] A. F. Cheviakov, "Construction of exact plasma equilibrium solutions with different geometries," *Phys. Rev. Lett.*, vol. 94, p. 165001, Apr 2005. [Online]. Available: https://link.aps.org/doi/10.1103/PhysRevLett.94.165001

[219] A. F. Cheviakov, "Analytical 3-dimensional anisotropic plasma equilibria," *Topology and its Applications*, vol. 152, no. 1, pp. 157 – 173, 2005, proceedings of the Dynamical Systems Conference. [Online]. Available: http://www.sciencedirect.com/science/article/pii/S0166864104002706

[220] A. F. Cheviakov and S. C. Anco, "Analytical properties and exact solutions of static plasma equilibrium systems in three dimensions," *Physics Letters A*, vol. 372, no. 9, pp. 1363 – 1373, 2008. [Online]. Available: http://www.sciencedirect.com/science/article/pii/S0375960107014211

[221] D. A. Kaltsas and G. N. Throumoulopoulos, "Generalized Solovev equilibrium with sheared flow of arbitrary direction and stability consideration," *Physics of Plasmas*, vol. 21, no. 8, p. 084502, 2014. [Online]. Available: https://doi.org/10.1063/1.4892380

[222] G. N. Throumoulopoulos, H. Weitzner, and H. Tasso, "On nonexistence of tokamak equilibria with purely poloidal flow," *Physics of Plasmas*, vol. 13, no. 12, p. 122501, 2006. [Online]. Available: https://doi.org/10.1063/1.2397042

[223] K. Hain, R. Lüst, and A. Schlüter, "Zur Stabilität eines Plasmas," *Zeitschrift Naturforschung Teil A*, vol. 12, no. 10, pp. 833–841, Oct. 1957. [Online]. Available: https://ui.adsabs.harvard.edu/abs/1957ZNatA..12..833H

[224] G. Laval, C. Mercier, and R. Pellat, "Necessity of the energy principles for magnetostatic stability," *Nuclear Fusion*, vol. 5, no. 2, pp. 156–158, jun 1965. [Online]. Available: https://doi.org/10.1088%2F0029-5515%2F5%2F2%2F007

[225] G. Spies, "Magnetohydrodynamic stability theory with closed magnetic field lines," *The Physics of Fluids*, vol. 17, no. 2, pp. 400–408, 1974. [Online]. Available: https://aip.scitation.org/doi/abs/10.1063/1.1694729

[226] J. P. Goedbloed, R. Keppens, and S. Poedts, *Advanced Magnetohydrodynamics: With Applications to Laboratory and Astrophysical Plasmas*. Cambridge University Press, 2010.

[227] S. B. White, *Theory of Toroidally Confined Plasmas*, 3rd ed. Imperial College Press, 2014.

[228] G. Huysmans, J. Goedbloed, and W. Kerner, "Isoparametric bicubic Hermite elements for solution of the Grad-Shafranov equation," *International Journal of Modern Physics C*, vol. 02, no. 01, pp. 371–376, 1991. [Online]. Available: https://doi.org/10.1142/S0129183191000512

[229] G. Poulipoulis, G. N. Throumoulopoulos, and C. Konz, "Remapping HELENA to incompressible plasma rotation parallel to the magnetic field," *Physics of Plasmas*, vol. 23, no. 7, p. 072507, 2016. [Online]. Available: https://doi.org/10.1063/1.4955326

[230] P. B. Snyder, G. W. Hammett, and W. Dorland, "Landau fluid models of collisionless magnetohydrodynamics," *Physics of Plasmas*, vol. 4, no. 11, pp. 3974–3985, 1997. [Online]. Available: https://doi.org/10.1063/1.872517

[231] J. J. Ramos, "Quasineutrality and parallel force balance in kinetic magnetohydrodynamics," *Journal of Plasma Physics*, vol. 81, no. 1, p. 905810111, 2015.